UNIVERSITY OF KWAZULU-NATAL

INYUVESI YAKWAZULU-NATALI

Autonomous Sea Craft for Search and Rescue Operations: Marine Vehicle Modelling and Analysis

Chiemela Onunka

205512204

In fulfilment of the degree of Master of Science in Mechanical Engineering at the school of Mechanical Engineering, University of KwaZulu-Natal, Howard College, Durban.

June 2011

As the candidate's Supervisor I agree to the submission of this dissertation.

Supervisor: Prof Glen Bright

Co-Supervisor: Dr Riaan Stopforth

Declaration

I, Chiemela Onunka, do hereby declare that

I. The work reported in this dissertation, except where otherwise indicated, is my original work.

II. This dissertation has not been submitted for any examination or degree at any other university.

III. This dissertation does not contain other person's information, pictures, graphs or any other data, unless where specifically referenced and acknowledged as being sourced from other persons.

IV. This dissertation does not contain other person's writings, unless specifically acknowledged as being sourced from other research writings and publications. Where other written sources have been quoted then:

   a. Their words have been re-written and the overall data attributed to them has been referenced;
   b. Where their exact words have been used, their writings has been placed inside quotation marks and referenced

V. Where I have reproduced publications of which I am an author, co-author or editor, I have indicated in detail the part of the publication which was actually written by myself alone and have fully referenced such publications

VI. This dissertation does not contain text, tables, or graphics copied and pasted from the internet unless specifically acknowledged with the source being detailed in the dissertation and in the reference sections.

Signed: _____

_____ _____

Prof. Glen Bright Dr. Riaan Stopforth

Acknowledgments

The work presented in this dissertation was done under the supervision of Prof. Glen Bright and co-supervision of Dr. Riaan Stopforth of the School of Mechanical Engineering, University of KwaZulu-Natal Howard College. I wish to thank Prof. Glen Bright for his immense support, advice and dedicated supervision in the completion of this study. My gratitude is also extended to the University of KwaZulu-Natal Innovation Company for sponsoring the project.

Dedication

This dissertation is dedicated my parents, Mr. and Mrs. C.O. Onunka for their care and immense support throughout the program and to my brothers and my sisters with whom am also indebted to for their love and care. To God be the Glory for his mercies.

Abstract

Marine search and rescue activities have been plagued with the problem of risking the lives of rescuers in rescue operations. With increasing developments in sensor technologies, it became a necessity in the marine search and rescue community to develop an autonomous marine craft to assist in rescue operations. Autonomy of marine craft requires a robust localization technique and process. To apply robust localization to marine craft, GPS technology was used to determine the position of the marine craft at any given point in time. Given that the operational environment of the marine was at open air, river, sea etc. GPS signal was always available to the marine craft as there are no obstructions to GPS signal. Adequate cognizance of the current position and states of an unmanned marine craft was a critical requirement for navigation of an unmanned surface vehicle (USV). The unmanned surface vehicle uses GPS in conjunction with state estimated solution provided by inertial sensors. In the absence of the GPS signal, navigation is resumed with a digital compass and inertial sensors to such a time when the GPS signal becomes accessible.

GPS based navigation can be used for an unmanned marine craft with the mathematical modelling of the craft meeting the functional requirements of an unmanned marine craft. A low cost GPS unit was used in conjunction with a low cost inertial measurement unit (IMU) with sonar for obstacle detection. The use of sonar in navigation algorithm of marine craft was aimed at surveillance of the operational environment of the marine craft to detect obstacles on its path of motion. Inertial sensors were used to determine the attitude of the marine craft in motion.

Table of Contents

List of Acronyms

ADC	Analog to Digital Converter
AHRS	Attitude Heading and Reference System
CAD	Computer Aided Design
COG	Course on Ground
DC	Direct Current
DCM	Direction Cosine Matrix
DOF	Degrees of Freedom
DP	Dynamic Position
EKF	Extended Kalman Filter
FLIR	Forward Looking Infrared
GBP	Generic Bayesian Program
GPC	Generalized Predictive Control
GPS	Global Positioning System
IO	Input Output
I^2C	Inter-Integrated Circuit
IMC	Internal Model Control
IMTS	Intelligent Marine Transport System
IMU	Inertia Measurement Unit
INS	Inertia Navigation System
ISR	Intelligence Surveillance and Reconnaissance
KF	Kalman Filter

LOS	Line of Sight
LQG	Linear Quadratic Gaussian
MR^2G	Mechatronics and Robotics Research Group
PD	Proportional Derivative
PIC	Peripheral Interface Controller
PID	Proportional Integral Derivative
PVC	Polyvinyl Chloride
PWM	Pulse Width Modulation
RADAR	Radio Detection and Ranging
RC	Radio Control
RIB	Rigid Inflatable Boat
SISO	Single Input Single Output
SNAME	The Society of Naval Architects and Marine Engineers
SONAR	Sound Navigation and Ranging
TWI	Two Wire Interface
USA	United States of America
UGMV	Unmanned Guided Marine Vehicle
USV	Unmanned Surface Vehicle
VGS	Visual Guidance System

List of Figures

List of Tables

Chapter 1

General Introduction

1.0 Introduction

Seacat is an autonomous unmanned marine craft under development at the Mechatronics and Robotics Research Group (MR^2G), University of KwaZulu-Natal, Howard College, Durban. Seacat's primary developmental purpose was to assist marine search and rescue organisations in rescuing survivors at the river, sea etc. Its operational environments are environments and environmental conditions which are deemed dangerous to send in rescuers. The knowledge of the immediate global positioning of the craft, attitudes and other navigational properties of the marine craft are of paramount importance to search and rescue exercise more especially as there are other users of the environment. The marine craft has a rigid inflatable structure and is limited to carry a maximum of two persons at a time. This limitation was as a result of using a pleasure rigid inflatable marine craft for simulation purposes. The marine craft is specified to have a semi- autonomous mode of operation. By semi- autonomous, it has to be controlled via a remote control. Should there be a scenario when there is no GPS signal; the semi- autonomous mode of navigation can be activated. Should there be a scenario when the remote control signals are out of reach; navigation protocol of the marine craft returns the craft to its starting point. In subsequent sections of this dissertation, Seacat shall be referred to as an autonomous marine craft, unmanned surface vehicle, or marine vehicle.

The changing environment of the world reflects an ever increasing uncertainty in the behaviour of weather patterns, about the origins of forces of nature impacting on human activities at sea at different water bodies. These uncertainties increase threats in coastal waters and in the open sea which may be a result of bad weather, rising coastal waters, changes in sea temperature, global warming effects and attacks by marine mammals on humans have prompted uncertainties in the modes in which these uncertainties might be delivered. Emphasis has been placed alongside with these changes in the search for suitable marine crafts having new capabilities which are required for surveillance of coastal waters and search and rescue operations. These operations and missions have in their requirements for a comprehensive system an integrated persistent Intelligence, Surveillance and Reconnaissance (ISR), system command, control and communication and distribution and transmission of real time data. The

increasing quest for an efficient search and rescue operations may be alleviated to a substantial extent by exploiting the benefits of unmanned systems leveraged by sensor fusion and networking, data fusion techniques and real time communication technologies to the most possible advantage that can be gained while using unmanned surface vehicles as nodes in sensor and communication network. The use of sonar in navigation algorithm of marine craft was aimed at surveillance of the operational environment of the marine craft to detect obstacles on its path of motion. Inertial sensors were used to determine the attitude of the marine craft in motion [1].

1.1 Objectives

In as much as the research involved working with electronic equipments, the motive which has been included in the idea behind this research was to develop an autonomous marine craft which has the capability of serving different functions to the society we live in, more especially in search and rescue missions so as to develop a field cost effective marine craft.

The specific objectives of this research include:

- A survey of USVs and existing guidance and navigation algorithms that can be used to develop unmanned search rescue marine craft.
- An investigation into the characteristics of a GPS based navigation and attitude determination for autonomous marine craft navigation.
- The development an algorithm and mathematical model(s) of an autonomous marine craft with decision making models and algorithms which can be implemented in autonomous systems and intelligent systems.
- The development of a suitable platform for sensor and data fusion for use in autonomous navigation, guidance and control of marine crafts.
- To model the different aspects of the marine craft system dynamics, motion and intelligent reasoning functions.

1.2 Specifications and Requirements

The specifications and requirements of the USV include the functional characteristics of the marine vehicle that will enable it be to be classified as a USV. The specifications also include the control modes of the craft. These include:

- Full enhancement of a functional marine vehicle with adequate sensors and electronics for semi-autonomous and autonomous motion.

- Remote controlled mode: This involved USV motion within the distance of less than 300m, docking and agile manoeuvring of the marine craft using a radio- control module.
- Semi-autonomous mode: This involved the marine craft being controlled from a radio-control module, with the heading and speed kept as constant as possible while using visuals from camera to aid manoeuvring and exercising some form of autonomy using the GPS module.
- Autonomous mode: This involved the marine craft moving through pre-programmed routes or waypoints.

1.3 Marine Craft Testing

The following testing procedures will be carried out on the USV. They include:

- The turning, manoeuvring and straight line stability test of the marine vehicle.
- The testing of the marine vehicle is to be done in calm waters.

1.4 Marine Craft Type and Missions

For this research purposes, the type of marine craft considered as a test bed was the Rigid Inflatable Boat (RIB), considering the constraints faced in the design and the interfacing of the unmanned marine vehicle with the sea surface. The choice of marine craft gave possibilities to the type of mission which could be conducted using RIB USV. The missions included maritime security and surveillance, search and rescue and also maritime interdiction operations support.

1.5 Software and Hardware

The software used in the development of the autonomous marine craft was based on an open source development board, known as Arduino. Arduino programming environment and language uses the Wiring language which is another open source development and programming language. Wiring is considered as a big brother to Arduino. Arduino and Wiring developmental boards make use of Atmel chips. To visualise results and data from the Arduino and Wiring boards, the results and data are sent through to Processing. Processing is an open source programming environment based on Java to create visual representation of data.

1.6 Platform Description

The marine craft used for this research has a length of 2.5m and 1.5m in width and shown in Figure 2-1(a). It has been enhanced for full or semi autonomous mode of operation. It has two 90 Amps, 12 volts battery to provide power for the craft. It has an appreciable size for testing purposes and it's easily carried out to the river with a trailer or four men. These characteristics that are associated with the

physical appearance and size of the craft helped to facilitate the process of converting it into a fully or semi autonomous marine craft.

1.7 The Motivation for a Search and Rescue USV

Search and rescue robots have been in service as an additional response unit in a disaster situation, providing sensory information and real time video of the disaster environment. The response to any disaster has always been a race against time to move as fast as possible, in order to reach potential survivors while ensuring that further disaster has not been caused in the process, or the lives of rescuers and victims of disaster are not jeopardised in the process. The primary objective of search and rescue activity has been to save lives. An unmanned surface vehicle can assist in this activity and has the potential of achieving this goal either by direct interaction with the victims, or automation of support activities that facilitate rescue operation [2]. The technological advancements that were made in robotics and intelligent systems supported the moral obligation to save lives. The impacts of natural disasters such as Tsunamis, Cyclones and torrential rain, which causes flooding, have been devastating to an extent that the use of robots to reach out to victims have been encouraged tremendously, as this will increase the percentage of survivors in such disasters. As much as it has been the primary motive of using search and rescue robots to save lives, specific functionalities, tasks and designs depend largely on the potential assignment of the robot [2].

1.8 Unmanned Surface Vehicle Tasks

The unmanned search and rescue marine vehicle has the sole prerogative to locate, assess and recover disaster victims in situations which cannot allow rescue personnel to be at the scene of the disaster. The functionality and specification of the unmanned surface vehicle increases the rescue personnel's ability to see and act accordingly, in search and rescue activities. The tasks for the unmanned surface vehicle can be categorised based on the size of the craft and functionality amongst other criteria. The specification and tasks for the unmanned search and rescue surface vehicle are described below:

- Search: This has to be a concentrated activity on sections of a river bank, coastal areas with objectives of locating victims, survivors and potential hazards in the disaster or search environment. The search task has to be conducted as quickly as possible and in completeness without increasing risk to survivors or rescuers.
- Reconnaissance and Mapping: The mapping of the search area can be done using GPS coordinates and radar system to map out the search area. This allows for speedy coverage of a large search area with the appropriate resolution [2].

- Medical Assessment and Intervention on the Site: This functionality allows medical personnel to interact with survivors on how to use onboard medical equipment and visually inspect the victims before they get back to shore.
- Mobile Beacon or Repeater Functionality: This functionality enables the unmanned surface vehicle to extend wireless communication ranges, enabling appropriate localization of radio signal transmission by providing more receivers. This enables rescuers to localize themselves during search and rescue operation.
- Logistic Support: This functionality enables the marine craft to provide the necessary logistic support through automation of onboard equipments and assisting both victims and rescuers to get onboard the craft.

1.9 Research Publications

The following publications were research results by the author as primary author or as co-author.

- Onunka C., Bright G. "On The Implementation of Quaternion in Direction Cosine Matrix for Marine Craft Navigation" Submitted to AUTOMATIKA-The Journal for Control, Measurements, Electronics, Computing and Communication, September 2010.
- Onunka C., Bright G. "Autonomous Marine Craft Navigation: On the Study of Radar Obstacle Detection"; 11th International Conference on Control, Automation, Robotics and Vision, ICARCV2010, Singapore, December 2010.
- Onunka C.,Bright G. *"A Study on Direction Cosine Matrix(DCM) for Autonomous Navigation"*; 25th ISPE International Conference on CAD/CAM Robotics & Factories of the Future,CARs&FOF2010, CSIR, Pretoria, South Africa, July 2010.
- R. Stopforth, Onunka C., Bright G. "*Robots for Search and Rescue Purposes in Urban and Water Environments – A Survey and Comparison"*; International Conference on Competitive Manufacturing COMA'10, Cape Town, South Africa, February 2010.
- Onunka C., Bright G. "*The Dynamics of An Autonomous Sea Craft for Deep Sea Rescue Operation*" 3rd Symposium in Robotics and Mechatronics (RobMech) 2009, CSIR, Pretoria, South Africa, November 2009.

1.10 Dissertation Outline and Chapter Overviews

1.10.1 USV System Dynamics and Kinematics

This section of the dissertation will discuss the primary literature studied for this research project. It will also identify the system dynamic modelling, mathematical and analytical models and the autopilot system modelling for the unmanned surface vehicle.

1.10.2 Mechanical Design

This chapter will show the various mechanical modifications, which were carried on a commercially available pleasure craft so as to convert it and make a USV. It also featured the various future designs models which were patented, which at a later stage will be commercialised.

1.10.3 Sensory architecture

This chapter will discuss the various sensory integrations which were carried out during the course of the research. It also showed the various electronic interfaces, power supply architectures and sensor fusion in the USV.

1.10.4 Marine Craft Autonomous Motion and Uncertainty

This chapter will discuss the secondary literature studied during the course of the research. It showcases and demonstrates how probability theory, Bayesian inference and uncertainty are part of autonomous motion of the USV as a robotic, mechatronic and autonomous system

1.10.5 Sensor Fusion and Software Design Implementation

This chapter will discuss the identification and modelling of the sensors integrated in the USV within a dynamic environment and also will discuss the software implementation in the USV to monitor and control the autonomous marine vehicle. It also discussed the firmware integration used in IO board and also low-level interfaces for the sensors.

1.10.6 Results and Discussion

This chapter will discuss the various results achieved and attained during the course of the research as well as various qualitative analysis results. The results are evaluated against achievable performances and specifications given in the introductory part of the dissertation. A summary of contributions made towards the development of a USV is also discussed and finally this section of the dissertation will end the thesis.

1.10.7 Conclusions

This chapter will summarize the contributions made in the research and also highlight suggestions for further research

1.11 Summary

The chapter made introductions to the reasons why the research into an autonomous marine craft was carried out. It also discussed the expected functions and tasks of the autonomous marine vehicle as well as the control modes of the autonomous marine craft. The chapter also discussed the expected aims of the research and ended with an introduction to the various chapters in the dissertation.

Chapter 2

USV System Dynamics and Kinematics

2.0 Introduction

This chapter starts with the review on the various technological advancements that have been made at different mechatronic laboratories and advancements made in USV autopilot development. The chapter also discussed the mathematical and analytical models in relation to the system dynamics of the marine craft. The models discussed in this chapter are implemented in the MSS [3] and results from the models are discussed further in chapter seven. The system model described the dynamic motion of the craft as a rigid structure. The model was developed from previous work done by Fossen [4]. The hydrodynamic coefficients of the test platform were assumed to be constant in some cases due to the complicated nature of non-linear fluid dynamic modelling and computation. The modelling of the marine craft took into consideration the kinetics and the kinematics aspects of the system dynamics. The kinetics of the marine craft involves the analysis of the forces which caused the marine craft to be in motion. The kinematics of the craft explains the geometric relations of marine craft motion. The chapter also discusses various literatures reviewed and studied during the course of the research. The chapter begins with a broad view of marine vehicle modelling. The different section of the chapter provides insights in detail, into the various aspects of marine craft modelling and analysis required for a marine craft to be autonomous. Also discussed in the chapter is the marine vehicle autopilot system.

2.1 Review on USV Technological Development

With increasing demand from US navy and other naval forces in various countries [5], there have been agreements that USVs form an integral part of a more responsive naval force. The advancement in USV technology led to its application in search and rescue activities thereby providing a more agile search and rescue community and organisations. The following advantages were identified in the development and usage of USV in search and rescue activities [6].

- Minimal risk to personnel in bad weather and conditions deemed unsafe for rescue personnel.
- The USV has the ability to send information to personnel who are on the shore or at safety.
- Limitation to USV outclasses limitations for human beings.
- USV can be developed at a considerable minimal cost.

In much debated cases for USV acceptance in environments where human beings operate, it has been widely accepted that technical advancements and improvements are to be made in the areas of USV autonomy. The development of USVs can be dated as far back as 1940s used for target training purposes [7]. The recent focus of USV has been the different applications in commercially viable markets, search and rescue operations and also surveillance of coastal waters. Typical developmental sizes of USVs are usually from 2.5m long as shown in Figures 2-1(a) and Figure 2-1(b).

(a) MR^{2}G USV

(b) Roboski USV [8]

Figure 2-1: Different Sizes of Marine Craft USVs

More advanced USVs have been developed over the years and these developments have been going on for quite a considerable amount of time at various research centers around the world. Such research centers include the Defense Advanced Research Projects Agency (DARPA), Systems Center San Diego (SPAWAR), Elbit Systems which developed Stingray, and Protector which is developed by REFAEL Armament Development Authority. Marine and Industrial Analysis Research Group (MIDAS) developed Springer and General Dynamics Robotic Systems, The Odyssey and SPARTAN developed by Radix marine, Navetec Inc. developed Owl MK II, ECA Group developed JETSTAR and INSPECTOR, AOS unmanned surface vehicle from Atmospheric Observing Systems Inc. The advancement of autonomous marine craft into rescue operations has been a test of the various autonomous technologies that have been developed over the years [6]. These are capable of carrying out different missions at sea.

2.2 Review on Autopilot Developments, Course Keeping and Tracking

Course keeping marine craft autopilots are designed from feedback information coming in through a gyrocompass measuring the heading. Rate measuring device, gyro and numerical differentiation of heading measurement provided information on heading rate measurement. The influence of autopilots on control design is discussed in this section of the chapter. The difficulties and challenges affecting control design are reviewed. The section discusses intelligent autopilot for controlling yaw dynamics of an autonomous sea craft with roll stabilization. A proposed solution for autopilot control problem was stated with the performance checked through numerical simulation. The use of rudder to stabilize marine craft started through observing autopilot performance under the unusual ship roll behaviour. Taggart [9] observed and tested the characteristics of autopilot under different sea conditions. His observation showed that under certain conditions, significant amount of roll motion is induced by the rudder [9]. Van Gunsteren [10] conducted full range of tests using rudder as a stabiliser in the Netherlands. Cowley and Lambert in 1972 [11], presented a study which postulated that a rudder can be used as a stabilising tool. The controller design used in study is made up of an autopilot and roll feedback. The autopilot has a phase-lead compensator which considered not the roll motion effect on the system. Presented in the study, is the roll loop which was made up of a simple feedback loop [11]. This was added after the autopilot is designed. Carley and Duberley [12] after reviewing the results of Cowley and Lambert, recommended that integrated rudder and fin control system will improve fin performance with rudder stabilisation [12]. Carley [13] in his study presented a practicability investigation on the use of rudder as a stabilising tool. Carley [13] investigated the potential roll motion induced by the rudder and the effects of steering characteristics on marine craft. In Carley's theoretical study, system identification was used to estimate the transfer function from rudder to roll and to heading $G_{\phi\alpha}(s)$ and $G_{\psi\alpha}(s)$ and the following controllers were a consequence of that estimation [13].

$$C_{\psi}(s) = K_1 \frac{1+aT_1 s}{1+T_1} + \frac{1}{T_3 s}; \quad C_{\phi}(s) = K_2 \frac{s(1+T_1 s)}{s^2 + 2\xi\omega_{\phi} s + \omega_{\phi}^2}, \tag{2.1}$$

where ω_{ϕ} is the natural roll frequency of the marine craft and the last term of the autopilot (heading controller) is an optional weather-helm term [14-15]. Carley studied stability of closed-loop system and coupling between roll and heading with frequency reduction under which roll reduction was achieved and recognised the limitations imposed on control system design. These limitations were as a result of non-minimum phase properties of rudder to roll response having the possibility of roll amplification at low encounter frequencies with trade off between roll reductions and heading interference. Lloryd [16] demonstrated from trial data simulated in calm water, that forced roll induced by rudder has a comparable magnitude to that induced by fins [16]. van der Klugt in his doctoral thesis [17] and van Amerongen et al

[18] simulated rudder control design using Linear Quadratic Gaussian (LQG) methods. The methods used did not consider the constraints imposed by actuators and was modified to accommodate the nonlinearities which were inherent in the differential equations. In their findings the state vector presented in the study was $x = [v', p, r, \phi, \psi]^T$ where v' is the sway velocity due to rudder action only. Their method investigated the following properties of autopilot control system design:

- Automatic Gain Control (AGC)
- Gain Scheduling
- Adaptive criterion

The investigation of the above characteristics was to avoid saturation of the steering mechanism of the marine craft. Gain scheduling was done using gain sets which were changed from disturbance characteristics estimated using Kalman filter. Automatic gain control in their study was used to reduce the control command which was necessary to avoid saturation of steering mechanism [17-18].

Blanke et al [19] in his study designed a single multi-variable controller system using linear quadratic techniques. The study investigated the possibility of decoupling roll from yaw in controller design for vessels with different configurations. Blanke et al [19] made an adjustment to his findings and introduced an option in which an operator is able to choose either to reduce roll or heading interference. After much assessment of the controller, the desired rudder angle was divided into two parts $\alpha_d = \alpha_\phi + \alpha_\psi$ where $\alpha_\phi = k_r u_{rel} \frac{s^2+2\xi_z\omega_z s+\omega_z^2}{s^2+2\xi_p\omega_p s+\omega_p^2} \left(\tau_p p(s) + \hat{\phi}(s)\right)$ and $\alpha_\psi = f(r, \delta\psi, u)$. $\hat{\phi}$ is the high pass filtered roll angle [20]. For this type of system, the resulting autopilot was non-linear having the appropriate gains scheduled according to the speed of the craft and propulsion mechanisms administered by α_ψ [21]. Källström et al implemented straight course autopilot systems, which also made use of linear quadratic Gaussian techniques in its execution with different adaptation mechanisms incorporated [22]. The autopilot was turned off during a major manoeuvring as needed by the craft and resumed back when the craft is in steady course. Blanke and Christensen [23] investigated the sensitivity of linear quadratic control performance to variations in the coupling coefficients of equations of motion. The study was based on a linear model developed from hydrodynamic data, estimated at design stage of SF300 vessels. The model was modelled using a multi-variable linear quadratic controller whose change in performance was analysed from changes in the following variables [23]: U- speed; K_p- roll moment due to roll rate; N_p- yaw moment due to roll rate and VCG – vertical centre of gravity. Blanke et al [24] discovered that the linear roll damping coefficient, $N_{p,}$ had a significant effect on the results. Zhou et al [25] in his study suggested that recursive method be used in error prediction methods, used in identifying rudder to motion

response and combine the result with a linear quadratic Gaussian controller [26]. The use of linear quadratic Gaussian controller was also proposed by Katebi and Grimble [27]. The use of Quantitative Feedback theory was suggested by Blanke and Hearns [24], for use in cascade SISO controllers design for roll and yaw and this was used to resolve the problem of uncertainty in the resulting model [24, 28]. The control systems specifications in frequency domain were specified in Stroustrup et al [29], and adopted the optimization of $\mathcal{H}_\infty$. The performance of $\mathcal{H}_\infty$ controller was investigated and evaluated against the linear quadratic controller and it was found that the roll angle amplification in $\mathcal{H}_\infty$ controller at low frequencies was less than that of linear quadratic controller [29-30]. The uncertainty models suggested by Blanke in [31], were incorporated by Blanke and Yang [19] to form a robust control design framework and used μ - synthesis [19]. The linear systems discussed so far were used mostly in course keeping activities and hence only small deviations from the steady state course models were anticipated. Laudval and Fossen [32], proposed a non-linear technique and made use of sliding mode control. Oda et al [33] and Sasaki et al [34] proposed a stochastic technique, based on autoregressive models and full scale implementations [34-36]. Identification of a multi-variable autoregressive model was initially done in calm water, thereafter the problem of optimal control of linear quadratic models were resolved to obtain control gains. This technique of modelling and designing controllers describes the Generalized Predictive Control (GPC) framework and this can be reduced to a Linear Quadratic Gaussian (LQG) model [37].

The use of constrained model predictive control was suggested by Perez et al [38], to be used as a natural extension for successful applications and implementations of earlier autopilot designs [17-18, 20, 39]. In this particular technique, the constraints on rudder rate were incorporated right at the beginning of the design process. The performance of the system in terms of yaw, rudder angle and roll were preserved by implementing linear quadratic control into system. The technique also made use of an optimal predictor which denoted wave induced model and performed as a shaping filter. Future roll angles and future roll rates were predicted, using the shaping filter and may be used as a feed forward control mechanism, if the control decision made is based on current and predicted disturbance data. In Perez [15], the properties of the shaping filter were assumed to be known and this assumption was later discarded in [38], where a quasi-adaptive technique was proposed. Estimation of properties of the predictor was done in an open loop, prior to switching the controller to quasi-adaptive method while implementing this approach. The method made provision for the control technique to be adaptive with respect to speed, heading and changes in sea state [38-40]. The use of Internal Model Control (IMC) was proposed by Perez et al [39] . With this method, the desired profile of the roll sensitivity transfer function is selected and approximated with a controller designed using Youla parameterization of controllers [41-42].

2.3 System Dynamics and Kinematics

The modelling of the autonomous sea craft required the understanding and the study of the statics and dynamics of marine vehicles. Marine craft statics dealt with the equilibrium of marine vehicles at rest or in situations when they are moving with constant velocity, while marine craft dynamics involved the analysis of marine craft in accelerated motion. Six independent coordinates were used to express the motion of marine craft in six degrees of freedom (6-DOF). The first three coordinates and their time derivatives are used to represent the position and translational motion of marine craft along the *x, y,* and *z* axes, while the last three coordinates and their time derivatives were used to represent the orientation and rotational motion of the marine craft [43-44]. The six components of the coordinate system were defined as: surge, sway, heave, roll, pitch and yaw [4]. The kinematics of the marine craft expressed the coordinate system in terms of the different notations used in describing the geometrical orientation of the marine vehicle. The crucial aspect of this process required the positioning of the coordinate system. To minimize complications which might arise and for all practical purposes, the coordinate system was placed in such a way that it coincided with the centre of gravity of the craft [45]. The centre of gravity for the marine vehicle in this case was in principle at the plane of symmetry on the craft or any point on the craft for convenience. In the marine vehicle computations, it was assumed that acceleration of particles or bodies on the surface of the earth can be ignored and this led to a proposition which suggested that the position and orientation of the marine craft should be expressed relative to inertial reference frame, while the linear and angular velocities can be described using the body-fixed coordinate system [4, 43]. The notations and symbols used in describing and expressing the kinematics of the marine craft were defined by the Society of Naval Architects and Marine Engineers (SNAME) [46-48] and based on these definitions, the 6-DOF general marine craft motion were expressed using the following vectors:

$$\eta = [\eta_1^T, \eta_2^T]^T \qquad V = [V_1^T, V_2^T]^T \qquad \tau = [\tau_1^T, \tau_2^T]^T \tag{2.2}$$

$$\eta_1 = [x, y, z]^T \qquad V_1 = [u, v, w]^T \qquad \tau_1 = [X, Y, Z]^T \tag{2.3}$$

$$\eta_2 = [\phi, \theta, \psi]^T \qquad V_2 = [p, q, r]^T \qquad \tau_2 = [K, M, N]^T \tag{2.4}$$

where the position η_1 and orientation η_2 of the marine vehicle are represented in the earth fixed frame using the notation η. The linear velocity V_1 and angular velocity V_2 are represented using V while τ was used to express the forces τ_1 and moments $\tau_2$experienced by the marine vehicle [49].

2.4 The Euler Angles and the Quaternion

The flight path of the marine craft relative to earth-fixed coordinate system was represented by the velocity transformation in equation (2.5). This provided a complete representation of the mathematical

model of the autonomous marine craft in relation to the vector of linear and angular velocities in body-fixed coordinate system υ with vector of position and orientation in Earth-fixed coordinate system η.

$$\dot{\eta}_1 = J_1(\eta_2)\upsilon_1 \tag{2.5}$$

$J_1(\eta_2)$ described the transformation matrix which has direct relationship with Euler angles: roll (ϕ), pitch (θ), and yaw (ψ). $\upsilon = [u\ v\ w\ ]^T$ described the linear velocity of the craft in body fixed frame. $\eta_2 = [\theta\ \phi\ \psi\ ]^T$ described the orientation vector and $\eta_1 = [\ x\ y\ z]^T$ described the position vector. With the above representation of Euler angles in *xyz* orientation convention, the linear velocity transformation of the marine vehicle was expressed as a rotation matrix, whose translation in the earth-fixed coordinate system coincided with the origin of the body-fixed coordinate system. Equation (2.6) expressed the linear transformation as:

$$J_1(\eta_2) = \begin{bmatrix} c\psi c\theta & -s\psi c\phi + c\psi s\theta s\phi & s\psi s\phi + c\psi c\phi s\theta \\ s\psi c\theta & c\psi c\phi + s\phi s\theta s\psi & -c\psi s\phi + s\theta s\psi c\phi \\ -s\theta & c\theta s\phi & c\theta c\phi \end{bmatrix}, \tag{2.6}$$

where *c = cos, s = sin.*

The angular velocity vector $V_2 = [p, q, r]^T$ and the Euler rate $\dot{\eta_2} = \left[\dot{\phi}, \dot{\theta}, \dot{\psi}\right]^T$ were related through the transformation matrix $J_2\ (\eta_2)$ [4] and expressed as

$$\dot{\eta}_2 = J_2(\eta_2)V_2 \tag{2.7}$$

This yielded the following angular velocity transformation matrix:

$$J_2(\eta_2) = \begin{bmatrix} 1 & s\phi t\theta & c\phi t\theta \\ 0 & c\phi & -s\phi \\ 0 & s\phi/c\theta & c\phi/c\theta \end{bmatrix} \qquad J_2^{-1}(\eta_2) = \begin{bmatrix} 1 & 0 & -s\theta \\ 0 & c\phi & c\theta s\phi \\ 0 & -s\phi & c\theta c\phi \end{bmatrix} \tag{2.8}$$

The quaternion was also used in the representation of the marine craft rotation matrix, to resolve issues with singularities that existed in using Euler angles in representing the rotation matrix. The quaternion having Euler parameters as its components were expressed as:

$$e = \begin{bmatrix} \varepsilon_1 \\ \varepsilon_2 \\ \varepsilon_3 \\ \eta \end{bmatrix} \tag{2.9}$$

with the linear velocity transformation matrix expressed as:

$$\dot{\eta}_1 = E_1(e)V_1 \tag{2.10}$$

where

$$E_1(e) = \begin{bmatrix} 1-2(\varepsilon_2^2+\varepsilon_3^2) & 2(\varepsilon_1\varepsilon_2-\varepsilon_3\eta) & 2(\varepsilon_1\varepsilon_3+\varepsilon_2\eta) \\ 2(\varepsilon_1\varepsilon_2+\varepsilon_3\eta) & 1-2(\varepsilon_1^2+\varepsilon_3^2) & 2(\varepsilon_2\varepsilon_3-\varepsilon_1\eta) \\ 2(\varepsilon_1\varepsilon_3-\varepsilon_2\eta) & 2(\varepsilon_2\varepsilon_3+\varepsilon_1\eta) & 1-2(\varepsilon_1^2+\varepsilon_2^2) \end{bmatrix} \tag{2.11}$$

$$J_1 = \begin{bmatrix} J_{11} & J_{12} & J_{13} \\ J_{21} & J_{22} & J_{23} \\ J_{31} & J_{32} & J_{33} \end{bmatrix} \quad \triangleq \quad E_1 = \begin{bmatrix} E_{11} & E_{12} & E_{13} \\ E_{21} & E_{22} & E_{23} \\ E_{31} & E_{32} & E_{33} \end{bmatrix} \tag{2.12}$$

Equation (2.11) represents a new rotation matrix which can be used to replace equation (2.6) so as to resolve the singularity issues that exist in using Euler angles in rotation matrix.

2.5 System State Estimation and Impact of Kalman Filter

System State estimation and Kalman filter Estimation of instantaneous state of the dynamic system perturbed by white noise, has been a statistical problem in modern control engineering [50]. The use of measurements which are linearly related to the state of a system but corrupted by white noise has resulted in the estimator being statistically optimal in accordance to any quadratic function describing the estimation error. Kalman filter in dynamic state estimation has provided the means of attributing the missing data from indirect and noisy measurements. In modern navigation algorithms, Kalman filter has played a major role in predictions, estimations of future paths of dynamic systems and motion planning algorithms. The applications involving the use of Kalman filter have gone across many fields, more especially its application as a tool in control engineering and have almost exclusively been used for estimation and performance analysis of estimators [51]. Modern control problems and stochastic estimation analysis have been considered as one of the achievements in using estimation theory in robotics, state estimation, and guidance and navigations problems. Many of the problems that were solved using Kalman filter would have not been possible without it [52]. The progresses made in different research areas using Kalman filter have provided technologies for space exploration and in the development of accurate and efficient navigation technology for spacecrafts. The principle is being used in modern control systems and this involves tracking, guidance and navigation of different kinds of vehicles and crafts, as well as in predictive design of control and estimation systems [53-54]. The implementation form for the Kalman filter took the form of a digital computer algorithm, which replaced other forms of analog circuitry for estimation and control which could have been used. The deterministic

dynamics of the craft or random processes which have stationary properties representing the craft were not a requirement for a functional Kalman filter algorithm and stochastic processes. The state space formulation of the marine craft dynamic controller was compatible with Kalman filter algorithm for optimal property estimation and control of the dynamic system of the craft. The necessary information for mathematically and statistically based decision methods for detecting and rejecting anomalous data, whose implications determined the effectiveness of the autopilot algorithm, was provided by the Kalman filter.

2.6 USV Speed Model

For adequate approach to the modelling of the rigid structure of the marine craft, the coordinate system origin was chosen to coincide with the centre line of the craft. In addition to this condition, the following assumptions were made and incorporated into the marine craft speed and steering equations of motion. The assumptions were;

- The marine craft has homogenous mass distribution and there exists *xz*-plane symmetry i.e. ($I_{xy} = I_{yz} = 0$).
- The heave, roll and pitch motion and modes are neglected.
  i.e. ($w = p = q = \dot{w} = \dot{p} = \dot{q} = 0$).

These two assumptions applied to the general 6-DOF rigid-body equation for marine vehicles, led to the following result:

$$m(\dot{u} - vr - x_G r^2) = X \tag{2.13}$$

$$m(\dot{v} + ur + x_G \dot{r}) = Y \tag{2.14}$$

$$I_z \dot{r} + m x_G (\dot{v} + ur) = N \tag{2.15}$$

where *m* represents the mass of the marine vehicle, *X* and *Y* are the forces causing the marine craft motion in Cartesian coordinates and *N* denotes the moments experienced by the marine vehicle. Equation (2.13) represents surge motion, equation (2.14) represents sway motion and equation (2.15) represents yaw motion. The perturbed marine craft equations of motion were derived from considering an additional assumption, which stated that the sway velocity v, the yaw rate r and the rudder angle δ are small. With this assumption in place, surge mode can be decoupled from sway and yaw motion while assuming that the mean forward speed u_0 of the marine craft remained constant for constant thrust from the propeller. In addition to that, it was assumed that the mean velocities in sway and yaw are $v_0 = r_0 = 0$. The application of these assumptions yielded the following result, valid for only small rudder angles

$$m\dot{u} = X \tag{2.16}$$

$$m(\dot{v} + u_0 r + x_G \dot{r}) = Y \tag{2.17}$$

$$I_z \dot{r} + m x_G (\dot{v} + u_0 r) = N \tag{2.18}$$

The importance of marine craft speed model lied on its relation of propeller thrust *T*, to forward speed *u*. Equation (2.19) described the non-linear speed equation of the marine craft for surge motion. The model took into account the hydrodynamics forces and moments [55].

$$m(\dot{u} - vr - x_G r^2) = X(u, v, r, \dot{u}, \delta, T) \tag{2.19}$$

where *X* represented the non-linear hydrodynamic surge force function [56] given by

$$X = X_{\dot{u}}\dot{u} + X_{vr}vr + X_{|u|u}|u|u + X_{rr}r^2 + (1-t)T + X_{cc\delta\delta}c^2\delta^2 + X_{ext} \tag{2.20}$$

The hydrodynamic derivatives for the craft were presented as [57]:

$$(m - X_{\dot{u}})\dot{u} = X_{|u|u}|u|u + (1-t)T + T_{loss} \tag{2.21}$$

and

$$T_{loss} = (m + X_{vr})vr + X_{cc\delta\delta}c^2\delta^2 + (X_{rr} + mx_G)r^2 + X_{ext} \tag{2.22}$$

van Berlekom [58] suggested that the square velocity of the flow past the rudder be modelled as:

$$c^2 = V_a^2 + C_T^2 T \tag{2.23}$$

with an average C_T-value for the rudder as:

$$C_T \approx 0.8\,\alpha\,\frac{8}{\pi\rho D^2} \tag{2.24}$$

with α, as the ratio between the screw diameter and the height of the rudder. V_a represented the speed of water going through the propeller and *D* represented propeller diameter [58]. The introduction of small perturbations to equation (2.19), through linear approximations yielded the following results:

$$u = u_0 + \Delta u\,;\, T = T_0 + \Delta T\;;\; T_{loss} = (T_{loss})_0 + \Delta T_{loss} \tag{2.25}$$

with $\Delta u, \Delta T$ and ΔT_{loss} representing the small perturbation from nominal values u_0, T_0 and $(T_{loss})_0$. This brought about a linear representation of the speed equation as:

$$(m - X_{\dot{u}})\Delta\dot{u} = X_u \Delta u + (1-t)\Delta T + \Delta T_{loss} \tag{2.26}$$

where $X_u = 2u_0X_{u|u|}$ represented the linear damping derivative in surge motion and the balance condition equivalent to the steady state yielded the following result:

$$|u_0|u_0 = \frac{1}{-X_{|u|u}}[(1-t)T_0 + (T_{loss})_0] \tag{2.27}$$

2.7 USV Steering Model

The linear marine craft steering equations were modelled under certain assumptions, which include state variables υ, r, ψ and the control input δ. With these state variables in place, the Davidson and Schiff [59] as well as Nomoto et al [60] models were used in modelling the steering equation of the marine craft [4]. Figure 2-2 shows the convention for positive control input δ measurement and angular velocity r [25]. From the non-linear model of marine craft equation in equation (2.19), in sway and yaw motion,

$$m(\dot{\upsilon} + ur + x_G\dot{r}) = Y \tag{2.28}$$

$$I_z\dot{r} + mx_G(\dot{\upsilon} + ur) = N \tag{2.29}$$

The hydrodynamic force and moment on the marine craft are modelled as in equation (2.30) and (2.31), using Davidson and Schiff [59] perspective.

$$Y_{\dot{\upsilon}}\dot{\upsilon} + Y_{\dot{r}}\dot{r} + Y_{\upsilon}\upsilon + Y_r r + Y_\delta\delta_R = Y \tag{2.30}$$

$$N_{\dot{\upsilon}}\dot{\upsilon} + N_{\dot{r}}\dot{r} + N_{\upsilon}\upsilon + N_r r + N_\delta\delta_R = N \tag{2.31}$$

This gave rise to the equation of motion being rewritten as:

$$M\dot{\upsilon} + N(u_0)\upsilon = w\delta_R \tag{2.32}$$

with $\upsilon = [v, r]^T$ as the state vector and δ_R as the rudder angle. The full representation of equation of motion is shown below

$$M = \begin{bmatrix} m - Y_{\dot{\upsilon}} & mx_G - Y_{\dot{r}} \\ mx_G - N_{\dot{\upsilon}} & I_z - N_{\dot{r}} \end{bmatrix} \quad N(u_0) = \begin{bmatrix} -Y_{\upsilon} & mu_0 - Y_r \\ -N_{\upsilon} & mx_G - N_r \end{bmatrix} \quad w = \begin{bmatrix} Y_\delta \\ N_\delta \end{bmatrix} \tag{2.33}$$

where $N(u_0)$ was obtained from the summation of the linear damping D with coriolis and centripetal terms $C(u_0)$ [59, 61]

$$N(u_0) = C(u_0) + D \tag{2.34}$$

The state space model for steering equation was obtained by setting $x = [v, r]^T$ and $u = \delta_R$. Hence

$$\dot{x} = Ax + w_1 u \tag{2.35}$$

$$A = -M^{-1}N = \begin{bmatrix} a_{11} & a_{12} \\ a_{21} & a_{22} \end{bmatrix} \qquad w_1 = M^{-1}w = \begin{bmatrix} w_1 \\ w_2 \end{bmatrix} \tag{2.36}$$

The coefficients in the matrix are defined as:

$$a_{11} = \frac{(I_z - N_{\dot{r}})Y_v - (mx_G - Y_{\dot{r}})N_v}{\det(M)}$$

$$a_{12} = \frac{(I_z - N_{\dot{r}})(Y_r - mu_0) - (mx_G - Y_{\dot{r}})(N_{\dot{r}} - mx_G u_0)}{\det(M)}$$

$$a_{21} = \frac{(m - Y_{\dot{v}})N_v - (mx_G - N_{\dot{v}})Y_v}{\det(M)}$$

$$a_{22} = \frac{(m - Y_{\dot{v}})(N_r - mx_G u_0) - (mx_G - N_{\dot{v}})(Y_r - mu_0)}{\det(M)} \tag{2.37}$$

$$w_1 = \frac{(I_z - N_{\dot{r}})Y_\delta - (mx_G - Y_{\dot{r}})N_\delta}{\det(M)}$$

$$w_2 = \frac{(m - Y_{\dot{v}})N_\delta - (mx_G - N_{\dot{v}})Y_\delta}{\det(M)}$$

$$\det(M) = (m - Y_{\dot{v}})(I_z - N_{\dot{r}}) - (mx_G - N_{\dot{v}})(mx_G - Y_{\dot{r}})$$

$$\det(N) = Y_v(N_r - mx_G u_0) - N_v(Y_r - mu_0)$$

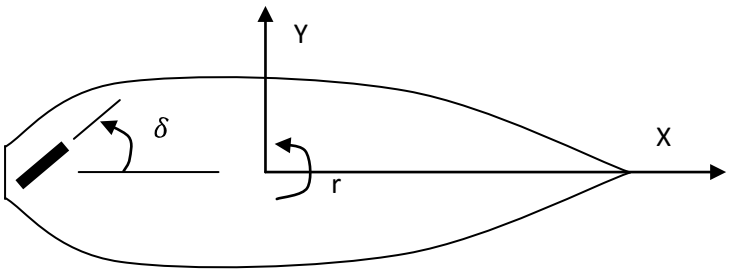

Figure 2-2: The Convention For Positive Rudder Angle In Marine Vehicle Reference System [62]

The Nomoto steering model for marine craft was derived from eliminating the sway velocity v from equation (2.15). These were suggested by Nomoto, Taguchi, Honda and Hirano [60]. The steering model presented an alternative representation to the steering model of Davidson and Schiff [59]. Hence equation (2.38) showed the transfer function of the steering model as a function of r and δ_R.

$$\frac{r}{\delta_R}(s) = \frac{K_R(1+T_3 s)}{(1+T_1 s)(1+T_2 s)} \tag{2.38}$$

The components of the transfer function were derived from the hydrodynamic derivatives using the following method:

$$T_1 T_2 = \frac{\det(M)}{\det(N)}$$

$$T_1 + T_2 = \frac{n_{11}m_{22} + n_{22}m_{11} - n_{12}m_{21} - n_{21}m_{12}}{\det(N)} \tag{2.39}$$

$$K_R = \frac{n_{21}w_1 - n_{11}w_2}{\det(N)}$$

$$T_3 = \frac{1}{K_R}\ \frac{m_{21}w_1 - m_{11}w_2}{\det(N)}$$

Nomoto's first order model was derived through making a first order approximation. This was done by equating the time constant as follows:

$$T = T_1 + T_2 - T_3 \tag{2.40}$$

with the transfer function as:

$$\frac{\psi}{\delta}(s) = \frac{K}{s(1+Ts)} \tag{2.41}$$

This model worked well for low frequencies. For higher frequencies, the Nomoto's second order model became a more adequate model and has the following form:

$$\frac{\psi}{\delta}(s) = \frac{K(1+T_3 s)}{s(1+T_1 s)(1+T_2 s)} \tag{2.42}$$

2.8 USV Stability and Dead Reckoning

Linear and nonlinear modelling methods were considered in the modelling of the dynamics and stability of the marine craft. These included the use of standard ship steering equations of motion, modelling of the speed system and the sensor system and environmental disturbances, which are consequences from wind,

ocean current and ocean wave. The computation of heading and longitudinal speed of the craft from GPS data provided the dead reckoning characteristic of the marine craft, which was used for navigation of the craft. Given that U denoted the estimated longitudinal speed over ground and ψ denoted the estimated heading, while ignoring lateral velocity, yields the Cartesian coordinates for computation of the marine craft position. The position of the marine vehicle can be computed using equation (2.43) and equation (2.44) using data from GPS as inputs

$$\dot{x} = U\cos\psi \tag{2.43}$$

$$\dot{y} = U\sin\psi \tag{2.44}$$

Considering the mathematical formulation of the marine craft rigid body dynamics derived from equation (2.36) and equation (2.37) as a homogenous system, where

$$\dot{s_1} = a_{11}s_1 + a_{12}s_2 \tag{2.45}$$

$$\dot{s_2} = a_{21}s_1 + a_{22}s_2 \tag{2.46}$$

Rewriting equation (2.46) as:

$$s_2 = \left(\frac{d(\cdot)}{dt} - a_{22}\right)^{-1} a_{21}s_1 \tag{2.47}$$

And substitute in equation (2.45) to yield,

$$\ddot{s_1} + (-a_{11} - a_{22})\dot{s_1} + (a_{11}a_{22} - a_{12}a_{21})s_1 = 0 \tag{2.48}$$

The necessary and sufficient condition for stability, for the ODE lied in the capacity of having each coefficient to be greater than zero:

$$-a_{11} - a_{22} > 0 \tag{2.49}$$

$$a_{11}a_{22} - a_{12}a_{21} > 0 \tag{2.50}$$

Taking the origin of the coordinate system at the centre of mass of the marine craft, coinciding at the geometric centre, the value of x_G was approximated as:

$$x_G = 0 \tag{2.51}$$

Since the marine craft has a reasonable balanced structure, the values of $N_{\dot{v}}, Y_{\dot{r}}, N_v, Y_r$ were assumed to be very small, compared to other terms in the formulation. The added mass term equation (2.33) took the order of the marine craft material mass m and $N_{\dot{r}} \cong -I_{zz}$. $Y_{\dot{v}}$ *and* $N_{\dot{r}}$ took on large negative values, as well as the linear and rotational drag Y_v and N_r This enabled the determinant of the mass matrix, det (M), to be reduced to $(m - Y_{\dot{v}})(I_{zz} - N_{\dot{r}})$ and

$$a_{11} = \frac{Y_v}{m - Y_{\dot{v}}} < 0 \tag{2.52}$$

$$a_{22} = \frac{N_r}{I_{zz} - N_{\dot{r}}} < 0 \tag{2.53}$$

This satisfied and met the first condition for stability,

$$-a_{11} - a_{22} > 0 \tag{2.54}$$

The second condition required that

$$(I_{zz} - N_{\dot{r}})Y_v(m - Y_{\dot{v}})N_r - [N_{\dot{v}}Y_v + (m - Y_{\dot{v}})N_v][-(I_{zz} - N_{\dot{r}})(mU - Y_r) + Y_{\dot{r}}N_r] > 0 \tag{2.55}$$

The first term contained the product of two large positive and negative values and the second term had a large positive value, mU. This made stability of the craft critical on the negative term N_v. A simpler form of the second condition provided a way of stabilizing the craft, using the largest terms. Equation (2.56) showed the simple form as:

$$C = Y_v N_r + N_v(mU - Y_r) > 0 \tag{2.56}$$

where C denoted the crafts stability parameter. The yaw/sway stability depended largely on the magnitude and sign of N_v and this was made more positive by adding additional surface area to the marine craft, thereby, making the craft more stable as expected. Stability was also be achieved by and improved by shifting the centre of gravity forward, thereby making x_G nonzero

$$C = Y_v(N_r - mx_G U) + N_v(mU - Y_r) > 0 \tag{2.57}$$

Since N_r and Y_v are both negative, positive value of x_G increased the positive influence of $C's$ first term.

2.9 Position and Velocity State Estimator Design

The modelling of the Dynamic Position (DP) of the marine vehicle required the filtering and the state estimation of marine vehicle model, as they formed an integral part of dynamic positioning of the marine vehicle [63-64]. The main objective of the state estimator was to predict unmeasured signals and filter the

signals, before they are implemented in a feedback control system for dynamic positioning. The inputs to the state estimator were from the sensory data associated with the IMU. Another function of the estimator was to estimate velocities from position measurements. The design of the state estimator has been an important aspect of the control system of the marine vehicle, because in situations involving temporary loss of heading and position measurements, the estimator should be able to function in dead reckoning mode. This implied that the predicted position and velocity data were used for feedback control. Temporary loss of position and velocity data does not affect the positioning accuracy of the marine vehicle, as the state estimator provided a smooth transition to the true position of the craft when signals reappear. The position and heading measurements were affected by coloured noise, induced by wind, waves, and currents and can only be counteracted by the propeller if their motion properties are slow and varying. If the motion of the craft became oscillatory as a result of wave action, wave filtering techniques were employed to identify and separate the position and heading measurements into, low-frequency and wave frequency position and heading data [65]. In the estimation of the marine vehicle state properties, it was assumed that the craft was meta-centric stable. This implied that, there were restoring forces in roll, pitch and heave motions. This required that these motions be modelled as damped oscillators, with zero mean and limited amplitude. This made provisions for the surge, sway, and yaw motions to be modelled alongside the state estimator [64].

2.9.1 Functions of the State Estimator

The state estimator was to provide reconstructed data from IMU at low speeds. The functions are elaborated as follows:

- Velocity estimation: It was assumed that only position and heading measurements were available to facilitate velocity estimates for feedback control [66].
- Bias estimation: Estimating the bias component of the system took into account slowly varying environmental effects and un-modelled effects, hence there were no steady states offsets in the velocity estimates. The advantage of having bias estimates was that they were used for feed forward control in position control [66].
- Wave filtering: The use of a synthetic wave-induced motion model in the estimator provided the required wave filtering model as the wave frequency element of motion was not required in the position and heading data used in the feedback control of the system.

2.10 Nonlinear Low-Frequency Marine Vehicle Model

The modelling of the marine craft for position and velocity estimates was done in 3-DOF used for simulation in the Marine Systems Simulator (MSS) [3]. The position (x, y) and the heading ψ of the

marine vehicle were represented by the vector $\eta = [x, y, \psi]^T$. The velocity components in the body-fixed frame of reference were represented by the vector $\nu = [u, v, r]^T$where u represented the surge motion, v represented sway motion and r represented the yaw motion of the marine vehicle. The modelling was separated into low frequency model and wave frequency model [63]. The mathematical model derived from these two models was used to express the physical properties of the marine vehicle dynamic system.

The low frequency model in surge, sway and yaw motion was derived from the following expression:

$$\dot{\eta} = R(\psi)\upsilon \tag{2.58}$$

$$M\dot{\upsilon} + D\upsilon + R^T(\psi)G\eta = \tau + R^T(\psi)b \tag{2.59}$$

where the rotation matrix in yaw has the characteristics of special orthogonal group, SO (3) and defined as:

$$R(\psi) = \begin{bmatrix} \cos(\psi) & -\sin(\psi) & 0 \\ \sin(\psi) & \cos(\psi) & 0 \\ 0 & 0 & 1 \end{bmatrix} \tag{2.60}$$

$M \in R^{3\times3}$represented the inertia matrix with the added hydrodynamic inertia for the marine craft, $D \in R^{3\times3}$ represented the damping matrix, $G \in R^{3\times3}$represented the stiffness/restoring forces matrix and $b \in R^3$ represented the bias term which accounts for the external forces and moments acting on the marine craft. These forces and moments were a consequence of the actions of waves, wind and current. The matrixes were defined as follows with $G \in R^{3\times3}$assumed to be constant diagonal matrix [63]:

$$M = \begin{bmatrix} m - X_{\dot{u}} & 0 & 0 \\ 0 & m - Y_{\dot{v}} & mx_G - Y_{\dot{r}} \\ 0 & mx_G - N_{\dot{v}} & I_z - N_{\dot{r}} \end{bmatrix}, \; D = \begin{bmatrix} -X_u & 0 & 0 \\ 0 & -Y_v & -Y_r \\ 0 & -N_v & -N_r \end{bmatrix}, G = \begin{bmatrix} -X_x & 0 & 0 \\ 0 & -Y_y & 0 \\ 0 & 0 & -N_\psi \end{bmatrix} \tag{2.61}$$

2.11 Linear Wave Marine Vehicle Model

To represent wave induced motions on the marine, a linear second order wave frequency model was used to model the wave induced motions in the following way:

$$\dot{\xi} = A\omega\xi + E_w w_w \tag{2.62}$$

$$\eta_w = C\omega\xi \tag{2.63}$$

where $\eta_w = [x_w, y_w, \psi_w]^T$, $\xi \in \Re^6$ and $w_w \in \Re^3$ denoted the zero- mean Gaussian white noise vector.

$$A_w = \begin{bmatrix} \begin{matrix} 0 & 0 & 0 \\ 0 & 0 & 0 \\ 0 & 0 & 0 \end{matrix} & \begin{matrix} I_{xx} & 0 & 0 \\ 0 & I_{yy} & 0 \\ 0 & 0 & I_{zz} \end{matrix} \\ -\begin{pmatrix} \omega_1 & 0 & 0 \\ 0 & \omega_2 & 0 \\ 0 & 0 & \omega_3 \end{pmatrix}^2 & -2\begin{pmatrix} \zeta_1 & 0 & 0 \\ 0 & \zeta_2 & 0 \\ 0 & 0 & \zeta_3 \end{pmatrix}\begin{pmatrix} \omega_1 & 0 & 0 \\ 0 & \omega_2 & 0 \\ 0 & 0 & \omega_3 \end{pmatrix} \end{bmatrix} \tag{2.64}$$

$$C_w = \begin{bmatrix} 0 & 0 & 0 & I_{xx} & 0 & 0 \\ 0 & 0 & 0 & 0 & I_{yy} & 0 \\ 0 & 0 & 0 & 0 & 0 & I_{zz} \end{bmatrix} \quad , \quad E_w = \begin{bmatrix} 0 & 0 & 0 \\ 0 & 0 & 0 \\ 0 & 0 & 0 \\ K_{w1} & 0 & 0 \\ 0 & K_{w2} & 0 \\ 0 & 0 & K_{w2} \end{bmatrix} \tag{2.65}$$

The corresponding decoupled wave frequency model was given as:

$$\frac{\eta_{w_i}}{w_{w_i}} = \frac{K_{w_i} s}{s^2 + 2\zeta_i \omega_i s + \omega_i^2} \quad for\ i = 1,2,3 \tag{2.66}$$

Equation (2.66), represented the first-order wave-induced disturbances on the marine vehicle. The wave frequencies model parameters are slowly varying quantities which were dependent on the state of the aquatic environment. The relative damping ratio ζ_i was usually within the range of 0.05 to 0.10 and the corresponding wave frequency $\omega_i = 2\pi/T_i$ having T_i within the range of 5 to 20 seconds [65].

2.12 Normalization of Matrix Components

The Prime-system of SNAME [48] formed the standard for the normalization form used for steering equations. Under this system, the marine craft's length L, instantaneous speed U, time unit L/U and the mass unit $0.5\rho L^3$ *or* $0.5L^2T$ were used as normalization variables. Equation (2.67) showed the normalized model of Davidson and Schiff [59]

$$M' = \begin{bmatrix} m' - Y_{\dot{v}}' & m'x_G' - Y_{\dot{r}}' \\ m'x_G' - N_{\dot{v}}' & I_z' - N_{\dot{r}}' \end{bmatrix} \quad N'(u_0') = \begin{bmatrix} -Y_v' & m'u_0' - Y_r' \\ -N_v' & m'x_G' - N_r' \end{bmatrix} \quad w' = \begin{bmatrix} Y_\delta' \\ N_\delta' \end{bmatrix} \quad u_0' \approx 1 \tag{2.67}$$

The principle of strip theory required that the underwater part of the marine craft be divided into strips. The theory allowed for computation of a two-dimensional hydrodynamic coefficient for added mass and damping. The application of strip theory to the steering model allowed for an estimate of the hydrodynamic derivatives in the model [67]. The approximations of the hydrodynamic derivatives are shown below:

$$Y_v' = -\left(\frac{\pi T}{L} - C_{D0}\right)$$

$$Y_r' = X_{\dot{u}}' + \frac{x_P}{L} Y_v'$$

$$N_v' = -(X_u' - Y_{\dot{v}}') + \frac{x_P}{L} Y_v' \tag{2.68}$$

$$N_r' = 0.25\, Y_v'$$

$$Y_\delta' = 0.25\, \pi\rho\, \frac{A_\delta}{LT}$$

$$N_\delta' = -0.5\, Y_\delta'$$

$$I_z = m x_G^2 + I_r \quad ; \quad I_r = m r^2$$

$$x_P = x_G \pm 0.1L$$

where m (kg) represented the mass of the marine craft, r represented the radius of gyration and $0.15L < r < 0.3\,L$. x_P *(m)* represented the distance between the centre of gravity and the centre of pressure, with $I_z(kgm^2)$ denoting the moment of inertia of the marine craft. $A_\delta(m^2)$ denoted the rudder area, $U(m/s)$ denoted the speed of the marine craft, $T\,(m)$ represented the draft depth, $L(m)$ represented the hull length, $\rho\,(kg/m^3)$ represented the sea water density and C_{D0} represented the drag coefficient of the marine craft at zero angle of attack.

2.13 Autopilot Course Keeping and Tracking

The course-keeping functionality of the autonomous marine craft was investigated through the use of an autopilot. The course-keeping functionality of the autopilot is based on the feedback from the digital compass measuring the heading of the marine vehicle. The heading rate is measured from the gyro readings representing the yaw axis. This can also be obtained from the numerical differentiation of the heading measurement or the heading state estimator. The autopilot used in controlling the marine craft was based on a simple PD control. The rudder motions of the marine craft were suppressed in order to maintain the integrity and performance of the autopilot especially as the speed of the marine craft changes. This was done through gain scheduling which was applied to eliminate the effects of the marine craft speed on the hydrodynamic properties of the craft. The low-frequency motion model of the marine craft is described by Nomoto's 1st order model [60] as:

$$T\ddot{\psi} + \dot{\psi} = K\delta \tag{2.69}$$

Based on the low-frequency model, the P and PD control of the marine craft was investigated. In P-control,

$$\delta = K_p(\psi_d - \psi) \tag{2.70}$$

with $K_p > 0$ as the regulatory design parameter. The closed-loop dynamics is expressed as:

$$T\ddot{\psi} + \dot{\psi} + KK_p\psi = KK_p\psi_d \tag{2.71}$$

With the marine craft having open-loop unstable properties ($T < 0$), the P-controller will not be able to stabilize the marine craft once it is unstable. The critically damped design parameter is obtained from:

$$K_p = \frac{1}{4TK} \tag{2.72}$$

Therefore the P-controller is restricted to only open-loop stable marine craft control.

The PD-control is used when the marine craft is unstable and marginally stable. The control model is expressed as:

$$\delta = K_p(\psi_d - \psi) - K_d\dot{\psi} \tag{2.73}$$

The controller design parameters are K_p and K_d. The closed-loop of the resulting marine craft dynamics is given by:

$$T\ddot{\psi} + (1 + KK_d)\dot{\psi} + KK_p\psi = KK_pK_d \tag{2.75}$$

And this is equivalent to the 2nd second order system

$$\ddot{\psi} + 2\zeta\omega_n\dot{\psi} + \omega_n^2\psi = \omega_n^2\psi_d \tag{2.76}$$

with

$$K_p = \frac{T\omega_n^2}{K} \text{ and } K_d = \frac{2T\zeta\omega_n - 1}{K}. \tag{2.77}$$

Conventional autopilot design involves the filtering of the measured yaw angle and yaw rate to discard wave frequency elements and retain only low frequency components for use, as feedback signal for autopilot to make necessary corrections. The control of the marine vehicle involved controlling the yaw angle or course angle ψ. The inclusion of a control-loop with position feedback in the control program provides a tracking system for guidance and control of the marine vehicle. The system is designed such that, the marine vehicle moves with a constant speed U which can be set using the remote control module

and at the same time controlling the sway position of the vehicle. The marine vehicle is made to follow a predefined path generated by the path management system. The desired path is easily specified using way points. The system is combined with the low-gain PD controller cascaded with the autopilot. The output from the autopilot then represents the desired course angle.

The non linear kinematics for the track controller is represented as:

$$\dot{x} = ucos\psi - vsin\psi \tag{2.78}$$

$$\dot{y} = usin\psi + vcos\psi \tag{2.79}$$

$$\dot{\psi} = r \tag{2.80}$$

Linear approximations of the track kinematics controller, are derived under the assumption that the earth-fixed reference frame can be rotated, such that the desired heading is zero and also the origin can be moved to coincide with the body-fixed coordinate system. This will allow the heading angle to be very small during tracking and control such that $sin\psi \approx \psi$; $cos\,\psi \approx 1$ and $u \approx U$.

The linearized kinematics equations are represented as:

$$\dot{x} = U + d_x \tag{2.81}$$

$$\dot{y} = U\psi + v + d_y \tag{2.82}$$

where d_x and d_y are errors due to linearization and drift from environmental disturbances. The coordinate system for the marine vehicle tracking system is shown in Figure 2-3. The autopilot tracking system is shown in Figure 2-4.

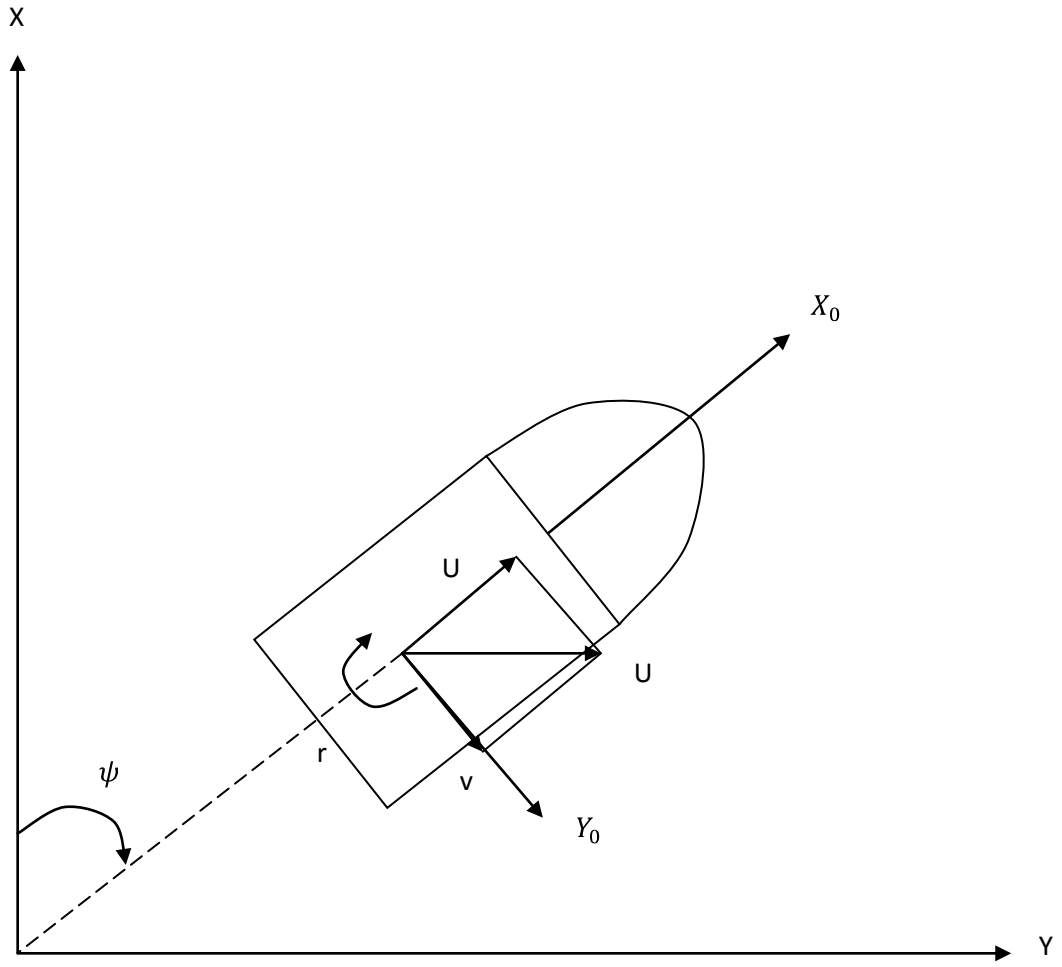

Figure 2-3: Coordinate System for Marine Vehicle Tracking System [4]

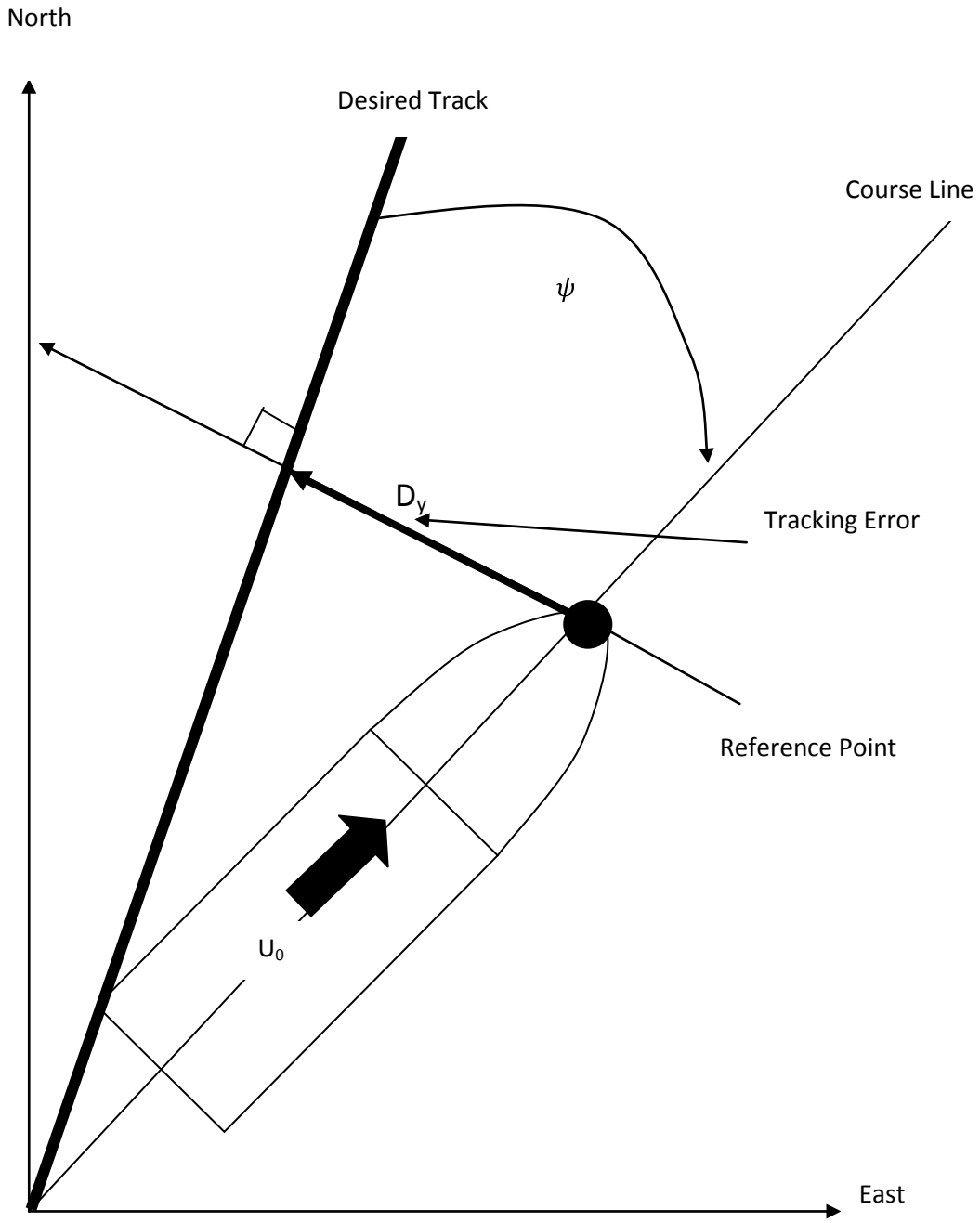

Figure 2-4: Autopilot Tracking System [68]

2.14 Waypoint Guidance System

The guidance of the marine vehicle between two waypoints at any given time, with a forward speed U, approach time, $t_{f,s}$ was used to obtain the desired heading angle

$$\psi_d = tan^{-1}\left(\frac{y_d(t_f)-y_d(t_0)}{x_d(t_f)-x_d(t_0)}\right) \tag{2.83}$$

where $[x_d(t_f), y_d(t_f)]$ and $[x_d(t_0), y_d(t_0)]$ are the coordinates of the waypoints. The model allows the heading angle to change at each waypoint. To obtain a smoother trajectory, the guidance of the marine vehicle was done using Line of Sight (LOS) way point guidance system. The desired angle in terms of LOS is given as:

$$\psi_d(t) = tan^{-1}\left(\frac{y_d(k)-y(t)}{x_d(k)-(t)}\right) \tag{2.84}$$

The waypoints are then chosen provided that they fall within the circle of acceptance with radius ρ_0 and also if the marine vehicle position$[x(t), y(t)]$, at time, t, meets the following requirements:

$$[x_d(k) - x(t)]^2 + [y_d(k) - y(t)]^2 \leq \rho_0^2 \; ; \rho_0 = 2L \tag{2.85}$$

where L is the length of the marine vehicle.

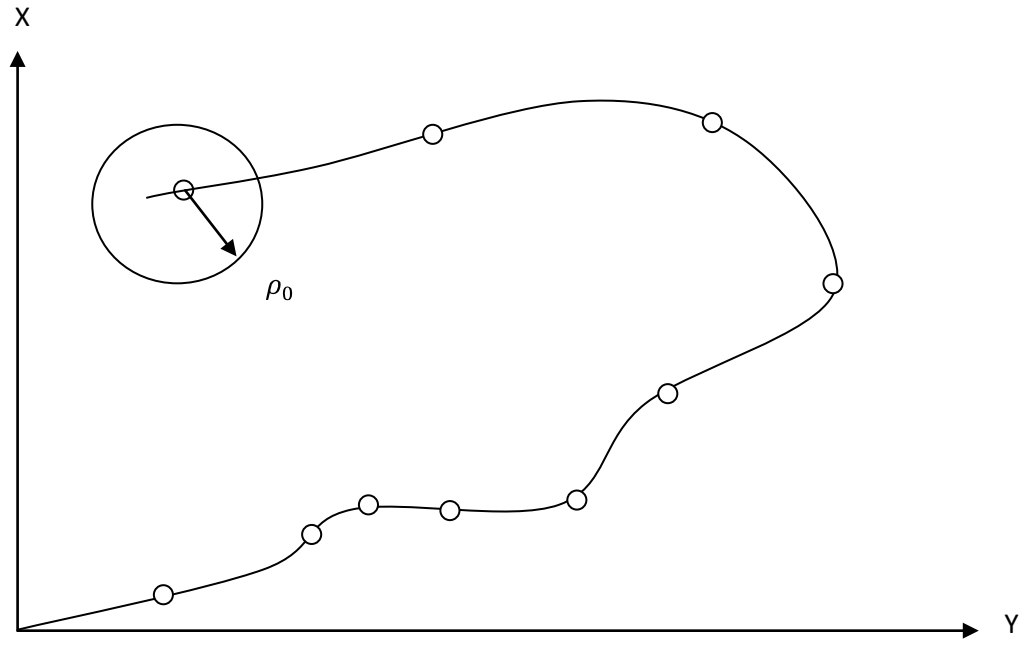

Figure 2-5: Waypoint Guidance by Line of Sight (LOS) [4]

2.15 Performance Evaluation

The autonomous marine craft performance evaluation, robustness and limitations of the onboard control system were investigated using standard steering manoeuvring characteristics. This was done by prior definition of conditions in terms of manoeuvring characteristics or manoeuvring index and the performance compared against the objectives and specifications set in sections 1.1 and 1.2. The following standard manoeuvring trials were investigated:

2.15.1 Turning Circle

This trial was used to compute the marine craft steady turning radius and to evaluate the performance of the steering mechanism on the craft under course-changing manoeuvring conditions [69]. The steady turning radius *R* for rudder angle of a minimum of 15 degrees was investigated to obtain a turning circle as shown in Figure 2-6.

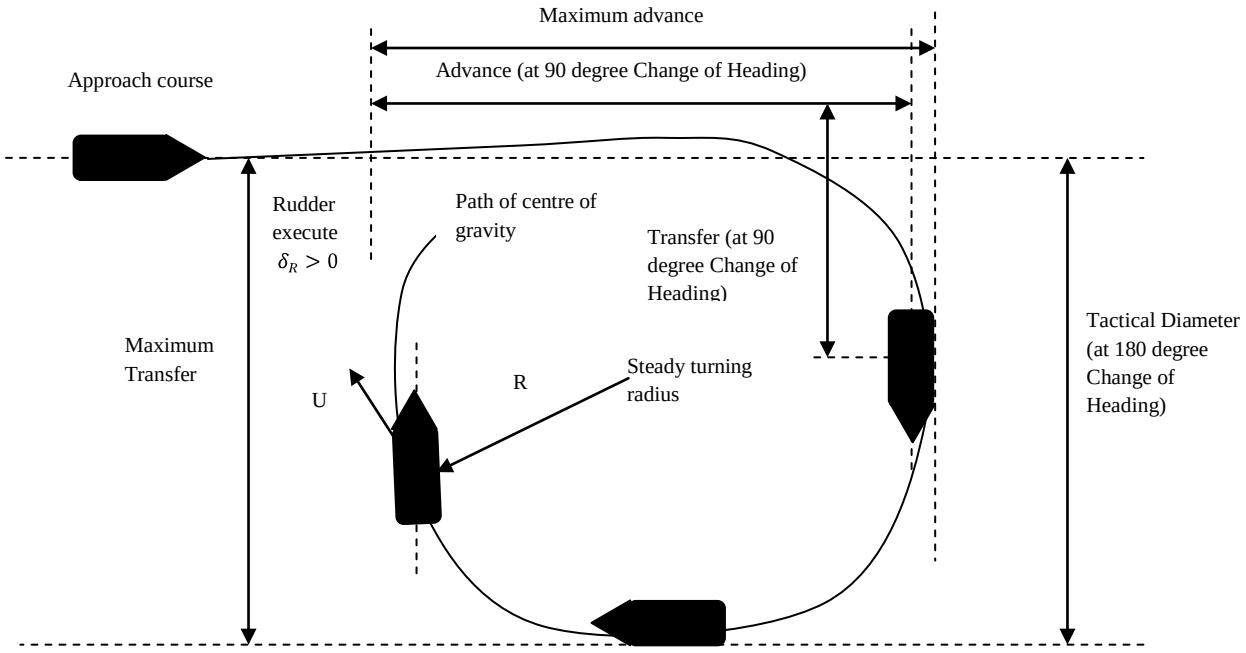

Figure 2-6: Turning Circle for Constant Rudder Angle [4]

For the turning circle trial, the marine craft move with constant radius in steady state. This led to r and v being constant and hence $\dot{v} = \dot{r} = 0$. The solution to the steady state equation for Davidson and Schiff [59] yields,

$$r = -\frac{(Y_\upsilon N_\delta - N_\upsilon Y_\delta)}{Y_\upsilon(N_r - mx_G u_0) - N_\upsilon(Y_r - mu_0)}\delta_R \tag{2.86}$$

with the marine craft turning radius defined as:

$$R \triangleq \frac{U}{r} \quad where\ U = \sqrt{u^2 + v^2} \tag{2.87}$$

2.15.2 Pull-Out Manoeuvre

This was used to check the straight line stability of the craft. The trial revealed, among other things, the degree of stability for the craft. The pull-out manoeuvre as shown in Figure 2-7 required a pair of manoeuvres in which a 20 degrees rudder angle is applied to the marine craft and returned to mid-craft after steady state turning has been achieved [70]. A difference in the turning rate from the starboard and port indicated that the stability of the marine craft has been compromised. In addition to the aforementioned characteristics of this trial, it also provided information about the degree of stability of the marine craft. Figure 2-8 demonstrated characteristics, where the straight line portion of the logarithmic curve indicated the degree of stability of the marine craft.

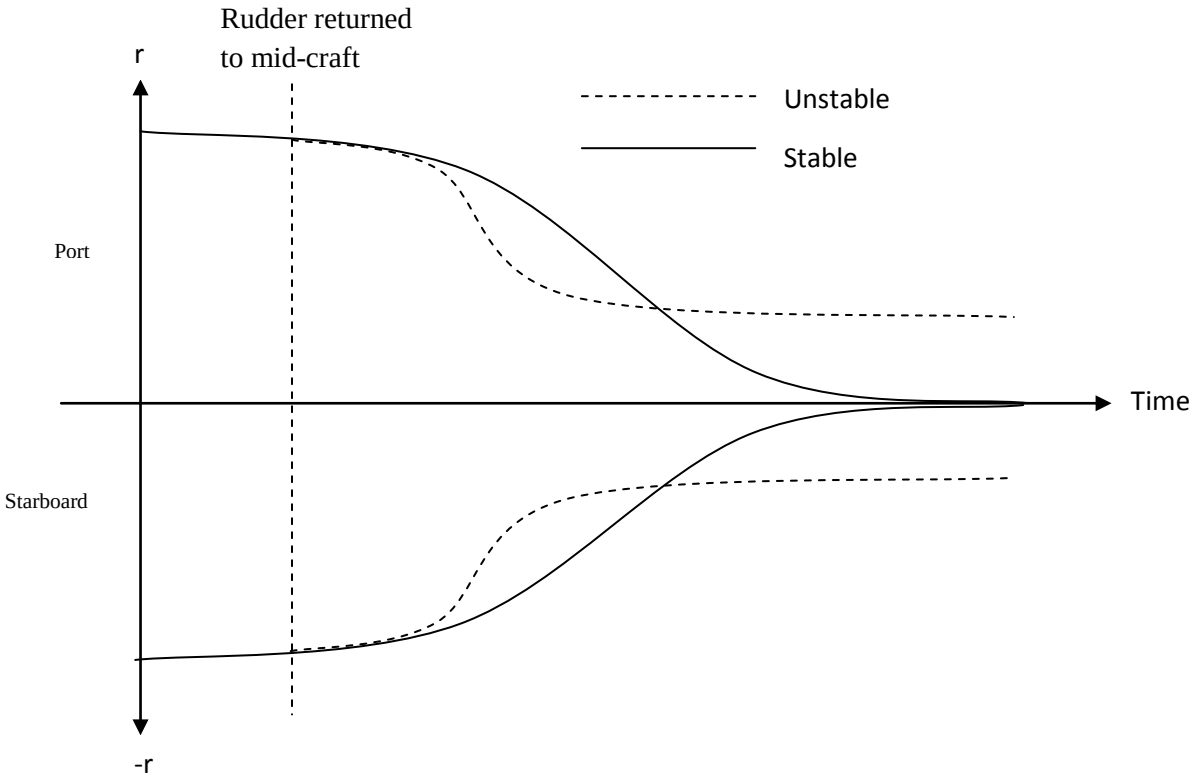

Figure 2-7: The Pull-Out Manoeuvre [4]

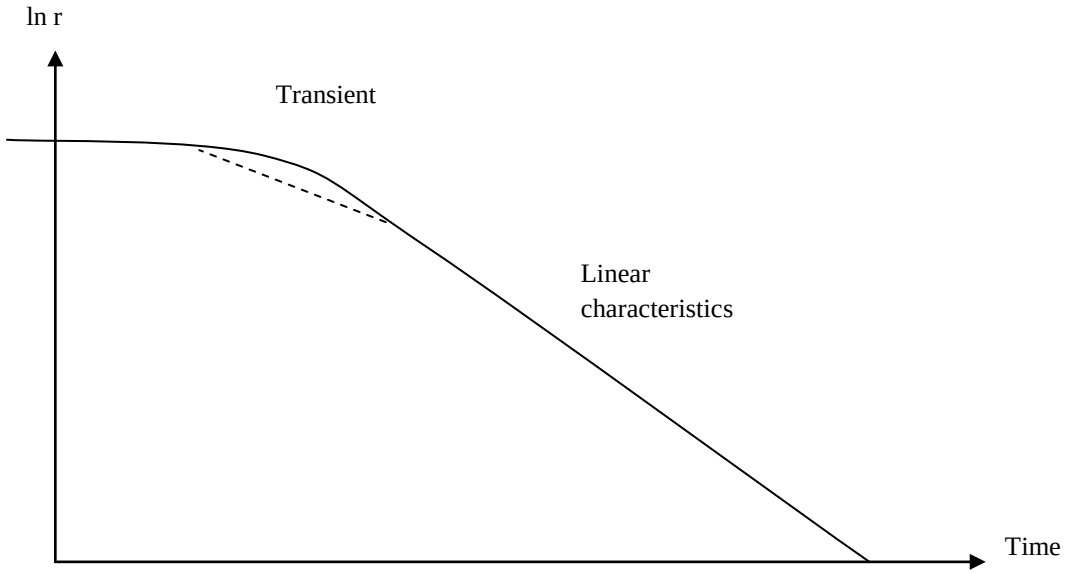

Figure 2-8: The Logarithmic Representation of the Pull-Out Manoeuvre [4]

2.15.3 Stopping Trials

This was used to determine the ability of the marine craft to undertake crash stops and low speed stopping activities required to compute the marine's craft head reach and manoeuvrability in emergency situations. The crash stop trial involved moving the marine craft at full ahead speed and reversing the propeller at full speed. Due to navigational requirements, low speed stopping trial was performed and investigated at full reverse propeller speed [71].

2.16 Forward Speed Control of Marine Craft

The automatic control of the marine craft involved modelling and designing systems that will control the forward speed motion, steering tracking and positioning of the marine craft. The difficulties associated with implementing and using the right propeller for speed and direction while meeting the high demands of thrust command was put into consideration. The models used are different as each marine vehicle system on its own have certain attributes which are particular to that system. The forward speed control of the autonomous marine craft was integrated into the system using a propeller for the propulsion system. The propeller has a fixed blade with fixed pitch to provide the necessary thrust for autonomous motion. The first order approximation for the propeller thrust, T and torque Q, was derived from lift force computations [56]. The model for positive thrust and torque are written as:

$$T = \underbrace{\rho D^4(\alpha_1}_{K_T} + \alpha_2 J_0)|n|n \quad ; \quad Q = \underbrace{\rho D^5(\beta_1}_{K_Q} + \beta_2 J_0)|n|n \tag{2.88}$$

where $\alpha_1, \alpha_2, \beta_1,$ and β_2 are constants.

The first order transfer function approximation and the second order transfer function were discussed in [72-73] , with the second order transfer function having a time delay incorporated into it. The motion of the autonomous craft occurs at variable speed inputs from the controller and as such the performance of the propeller becomes a function of the speed of water in the wake of the hull or advance speed $V_a(m/s)$, propeller revolutions per second $n\ (rps)$ and propeller diameter $D\ (m)$. The non-dimensional open water characteristics for the propeller were defined in terms of the open water advance coefficient, $J_{0,}$ and modeled as:

$$J_0 = \frac{V_a}{nD} \tag{2.89}$$

with the spectrum of J_0 values being narrow. The non-dimensional propeller thrust and propeller torque coefficients, K_T and $K_{Q,}$ and the thrust open water efficiency, η_0 in undistributed water were modelled as [74]:

$$K_T = \frac{T}{\rho|n|nD^4} \quad K_Q = \frac{Q}{\rho|n|nD^5} \quad \eta_0 = \frac{J_0}{2\pi} \cdot \frac{K_T}{K_Q} \tag{2.90}$$

where $\rho\ (kg/m^3)$ depicts water density and $T\ (N)$ and $Q\ (Nm)$ represent the propeller thrust and torque respectively. The term wake defines the relative speed reduction by introducing advance speed at propeller and it is the difference between the autonomous marine craft speed and the average flow velocity over the propeller [75-76].

$$V_a = (1 - w)U \tag{2.91}$$

where w represents the wake fraction number which ranges between 0.1 to 0.4 and $U\ (m/s)$ represents the forward speed of the autonomous marine craft. The thrust deduction t indicates the increase in the flow velocity in the boundary layer behind the autonomous marine craft and as a result, the propeller has an effect on the pressure balance between the bow and stern of the marine craft. This increases the resistance experienced by the hull of the marine craft. The thrust deduction characteristic range between 0.05 and 0.2 and the marine craft hull efficiency, $\eta_{H,}$ describes its influenced [67].

$$\eta_H = \frac{1-t}{1-w} \tag{2.92}$$

Equation (2.93) shows the ratio between the propeller thrust and torque

$$\eta_B = \frac{J_0}{2\pi}\frac{K_T}{K_{QB}} = \frac{K_Q}{K_{QB}} \tag{2.93}$$

where K_{QB} represents the torque coefficient for the propeller with the relative rotative propeller efficiency modelled as:

$$\eta_R = \frac{\eta_B}{\eta_0} \tag{2.94}$$

with the total propeller thrust efficiency given as

$$\eta_{Total} = \eta_0 \cdot \eta_M \cdot \eta_H \cdot \eta_B \tag{2.95}$$

with η_M, representing the mechanical efficiency which ranges between 0.7 – 0.8.

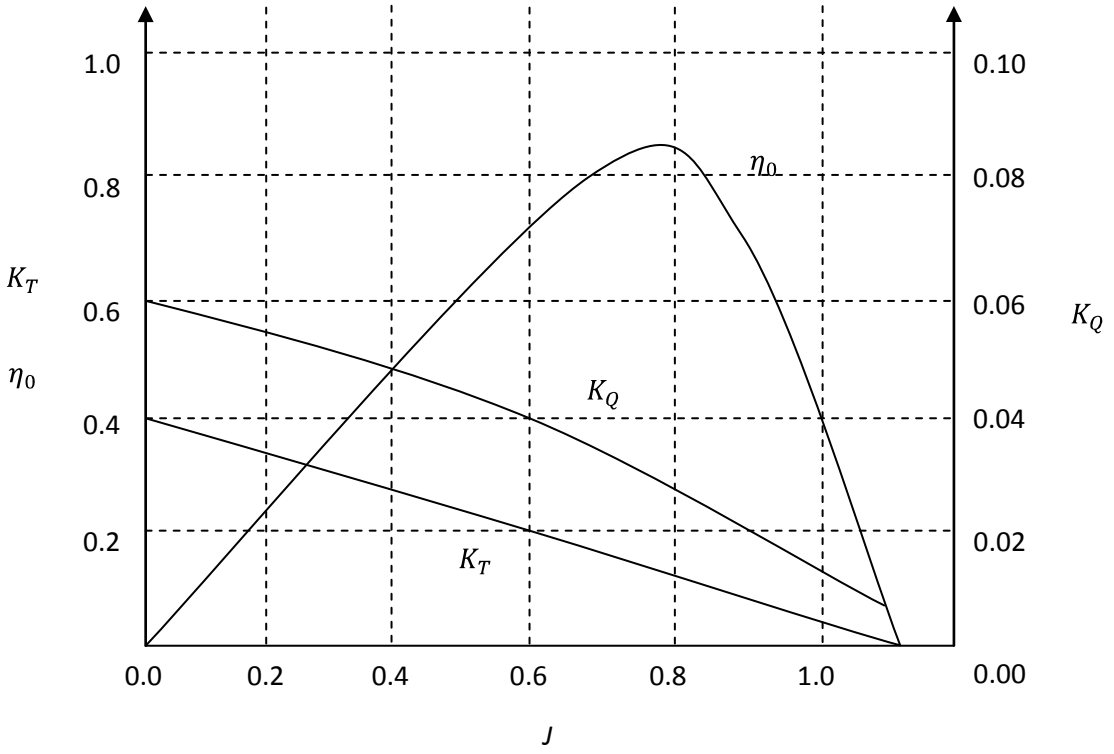

Figure 2-9: Typical Thrust and Torque Coefficients [62]

Thrust from the autonomous marine can be varied by adjusting inputs to motor driver controlling the propeller. The autonomous marine craft speed will increase or decrease until an equilibrium speed satisfying equation (2.96) is obtained

$$(m - X_{\dot{u}})\dot{u} = X_{|u|u}|u|u + (1-t)T + T_{loss} + T_{ext} \quad (2.96)$$

$$T = T_{|n|n}|n|n + T_{|n|V_a}|n|V_a \quad (2.97)$$

The braking of the marine was done by reducing the speed of the propeller. In situations where rapid deceleration was required, this was done by reversing the direction of rotation of the propeller. This implies the n in the above equation becomes negative. Equation (2.98) shows the steady state autonomous marine craft speed for positive n and u

$$u = n\frac{1}{-2X_{|u|u}}\left[T_{|n|V_a}(1-w)(1-t) + \sqrt{\left[T_{|n|V_a}(1-w)(1-t)\right]^2 - 4(1-t)T_{|n|n}X_{|u|u} - 4\frac{T_{ext}+T_{loss}}{n^2}X_{|u|u}}\right] \quad (2.98)$$

Manual speed control for the autonomous marine craft was achieved by setting the desired speed from a remote control module. This was achieved by adjusting the joystick on the remote control module to the require level. At higher speeds, the stochastic values of external thrust from winds and hull resistance may cause the variation in the speed of the marine craft to about 10% -30%.

2.17 Propeller Losses

Axial water inflow into the propeller and several other sources causes a reduction in propeller thrust and torque. The losses are experienced in cross coupling drag situations and it occurs when water inflow perpendicular to the propeller axis, caused by water current which causes marine craft speed to introduce a force in the direction of the inflow due to the deflection of the propeller race [77-78]. When loading on the propeller becomes intense, air suction caused by the decreasing pressure on the propeller blades may occur, especially when the submergence of the propeller decreases due to wave motion. Coanda effect may cause thrust reduction and change in thrust direction as a result of thruster-hull interaction induced by frictional losses and pressure effects, when the thruster race sweeps along the hull [79]. The thrust controller for the propeller required no optimization, due to the simple reason that the propeller has a fixed pitch [80].

2.18 Summary

The analytical and mathematical models of the USV were reviewed and modelled to enable the development of the autonomous marine craft. The importance of the dynamics and kinetic of the autonomous marine craft was demonstrated analytically within the subject of discussion. The autopilot system was also reviewed, discussed and modelled within the required physical specification of the marine craft.

Chapter 3

Mechanical Design

Introduction

This chapter discusses the mechanical modifications which were implemented in the design and development of the autonomous marine vehicle. The chapter sections include steering modification, marine vehicle body modification and stability. The chapter ends with a summary on the choice of modifications made in the design process.

3.1 Craft Design Material and Size

The marine vehicle was made from a combination of different materials which included wood for supporting the onboard electronics, fibre glass body, stainless steel and aluminium support structures. The craft was designed to be cost effective and was predominantly dependent on the power to displacement ratio. The hull form, waterline length and the long centre of gravity (LCG) of the marine vehicle have significant impact on the speed of the vehicle. The length of the craft was designed to be 2.5m and 1.5m in breadth.

3.2 USV Designs

The design and the development of the USVs were aimed at achieving an efficient USV which would be fast enough to be used in search and rescue activities. These designs featured the use of double fixed blade propellers and high speed water jet engines to power the USV. These are shown in Figures 3-1 and 3-2. The CAD designs were done using Autodesk Inventor professional to design and draw the models. The designs of these USVs were aimed at incorporating efficient propulsion systems that will enable the USVs to be fast in executing their mechanical obligations.

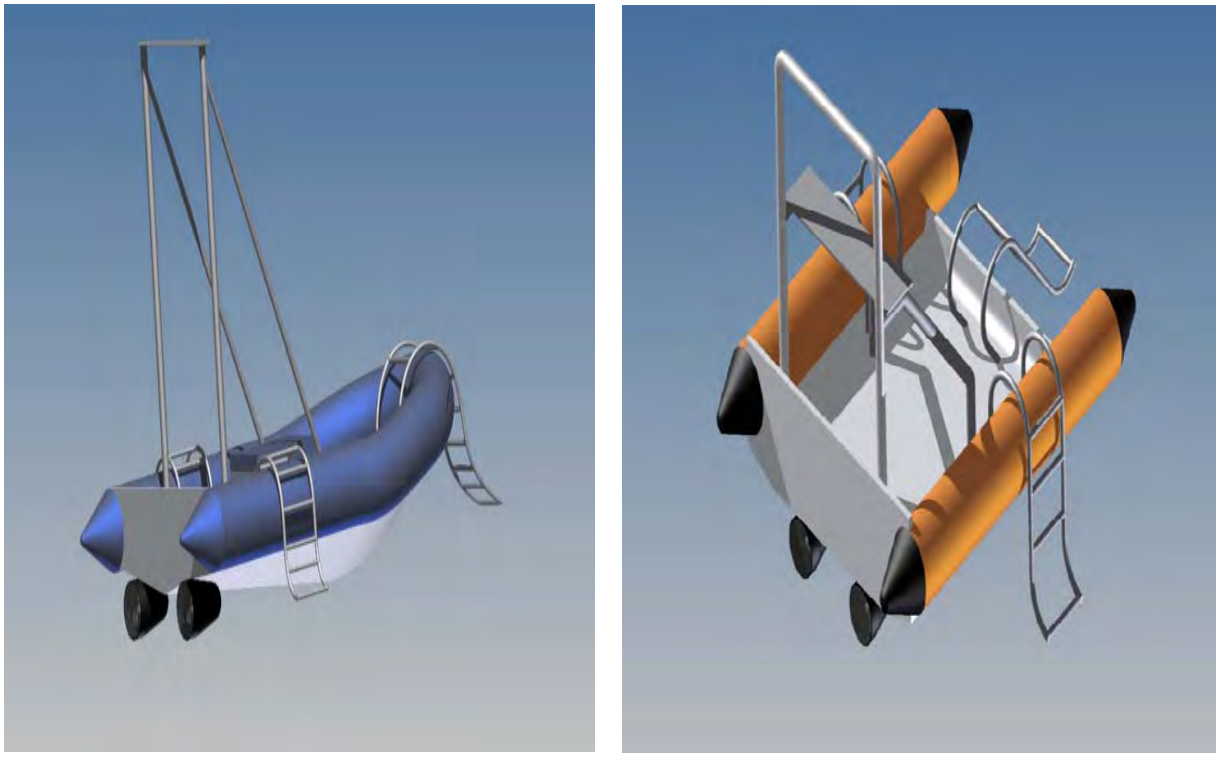

Figure 3-1: CAD Drawing of the USV Featuring Double Fixed Blade Propellers

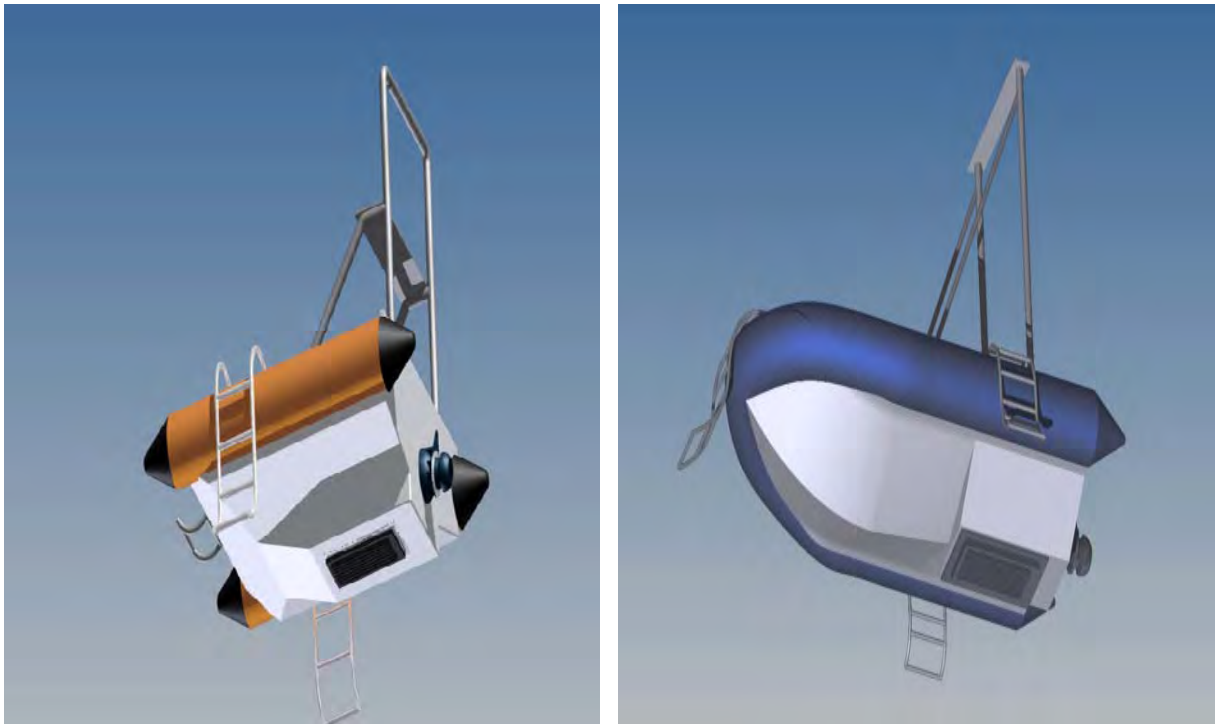

Figure 3-2: CAD Drawing of the USV Featuring Water Jet Engine

3.3 The Propulsion System

The propulsion system was chosen such that it was able to provide adequate power supply and propulsion requirement needed by the marine vehicle. The primary calculations and analysis of the design constraints are shown in appendices B and E. The different considerations which were put in place in selecting a suitable propulsion system for testing the craft are as follows:

- Power from the propeller to weight ratio
- The ability of the marine vehicle to stay in plane while turning
- Achieving a specified speed of 2*m/s* at full throttle in rough weather
- Providing additional thrust at low boat speed for more responsive control when manoeuvring

3.4 Steering Design

The steering of the marine vehicle was designed in such a way that allowed for smooth integration between the mechanical hardware, electronic control and software component of the steering system. The design was done using Autodesk Inventor. The steering modification featured two steering control systems. The first system shown in Figure 3-3 was a design that featured four DC servo motors arranged within a geared system to drive the pulley-type arrangement. The second system shown in Figure 3-4, featured a chain and sprocket arrangement and driven by a single high torque DC servo motor. Each of the designs has their advantages and disadvantages for the control of the USV. The chain and sprocket arrangement as shown in Figure 3-5, was chosen amongst the two steering setups. This provided a simpler method to implement and integrate a low cost mechatronic solution to the smooth control of the marine vehicle rudder system. The high torque DC servo motor shown in Figure 3-5 receives manoeuvring signals from the Arduino microcontroller board and turns the rudder in the required direction. The chain and sprocket system transmits the torque generated from the servo to the rudder.

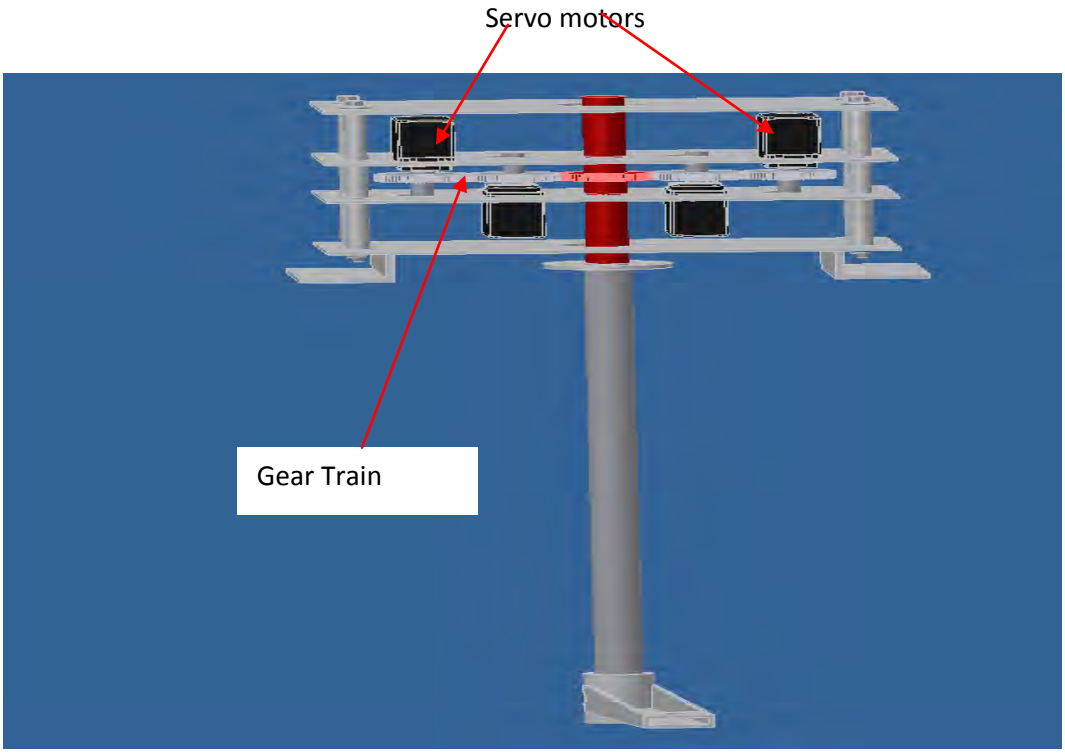

Figure 3-3: CAD Drawing of the Pulley System for the Steering Mechanism

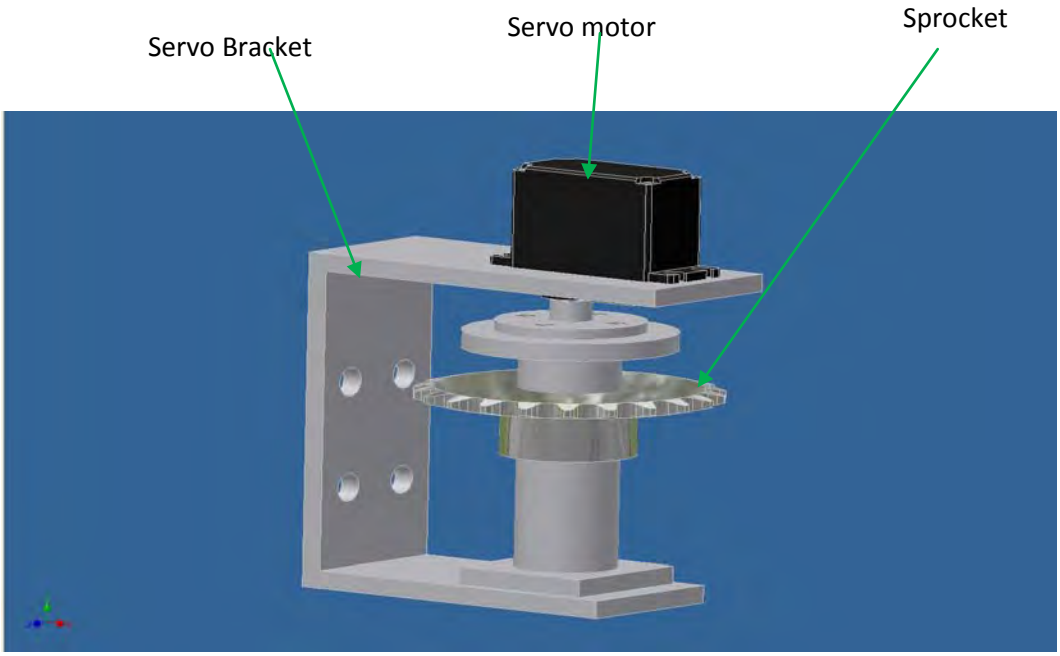

Figure 3-4: CAD Drawing of the Chain and Sprocket System for the Steering Mechanism

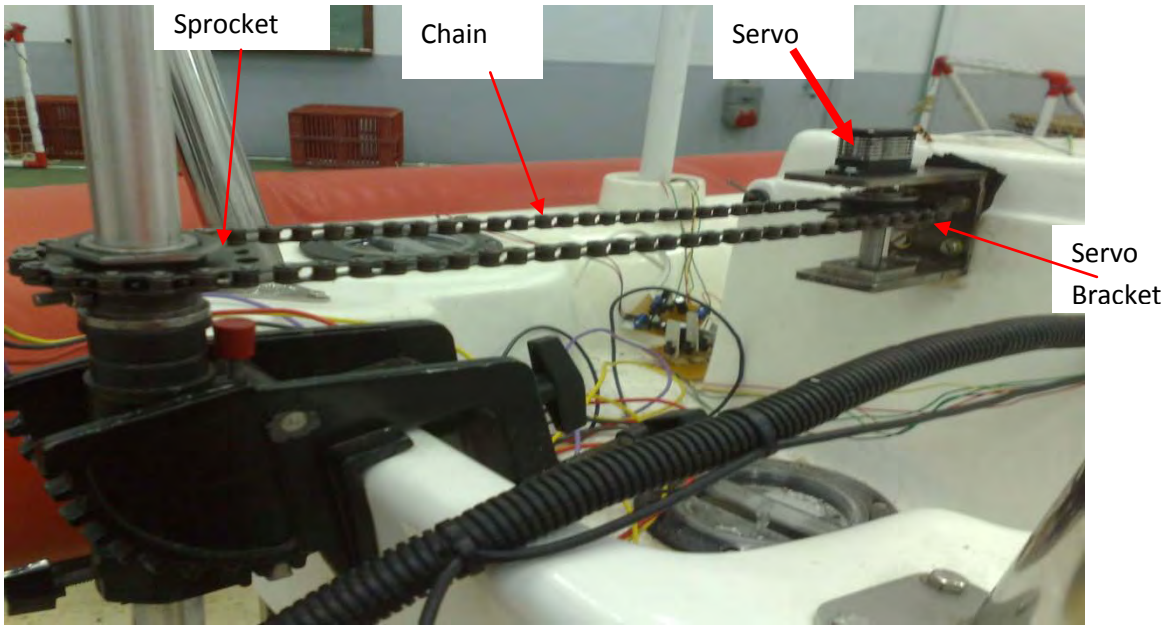

Figure 3-5: A Photo of the Complete Steering Assembly

3.5 Marine Vehicle Modification and Stability

Stands for the ultrasonic sensors were designed using PVC pipes and plastic base to provide support for the pipes. Plastic casings were used to provide protection for the ultrasonic sensors. The setup consisting of the PVC pipes shown in Figure 3-6 and ultrasonic sensors shown in Figure 3-6 and Figure 3-7 were mounted on the sides of the marine vehicle. A stainless steel bar shown in Figure 3-7 was designed and used to provide a mounting platform for the radar system. A rectangular wooden base shown in Figure 3-7 on which the radar and the screen was fixed to, was designed and mounted on the steel bar. The arrangement consisting of the radar, wooden base and stainless steel bar were mounted at the back of the marine vehicle. Also, at the front of the marine vehicle, is another wooden base shown in Figure 3-6 was mounted on a stainless steel frame and was used as a mounting for the surveillance cameras and other electronics. Each of these setups was positioned in such a way that the stability of the marine vehicle was not compromised.

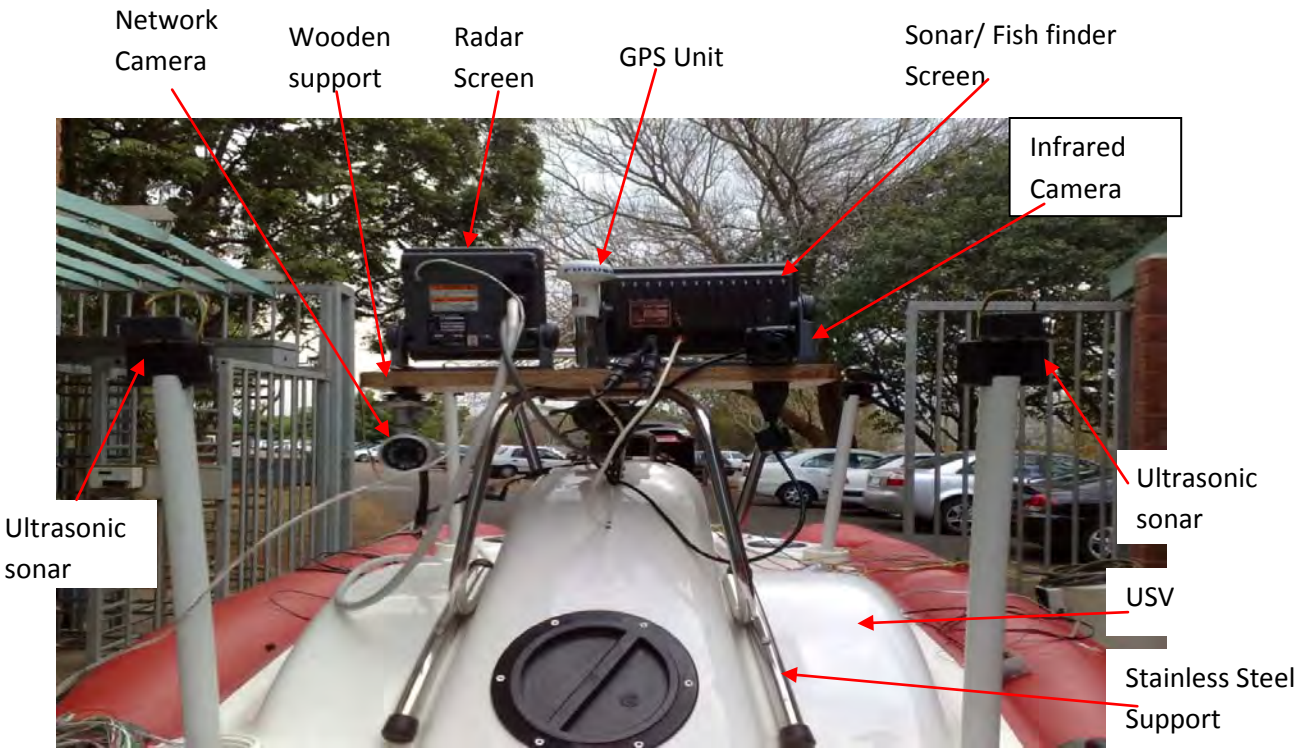

Figure 3-6: A Picture of the Front Section of the Marine Vehicle

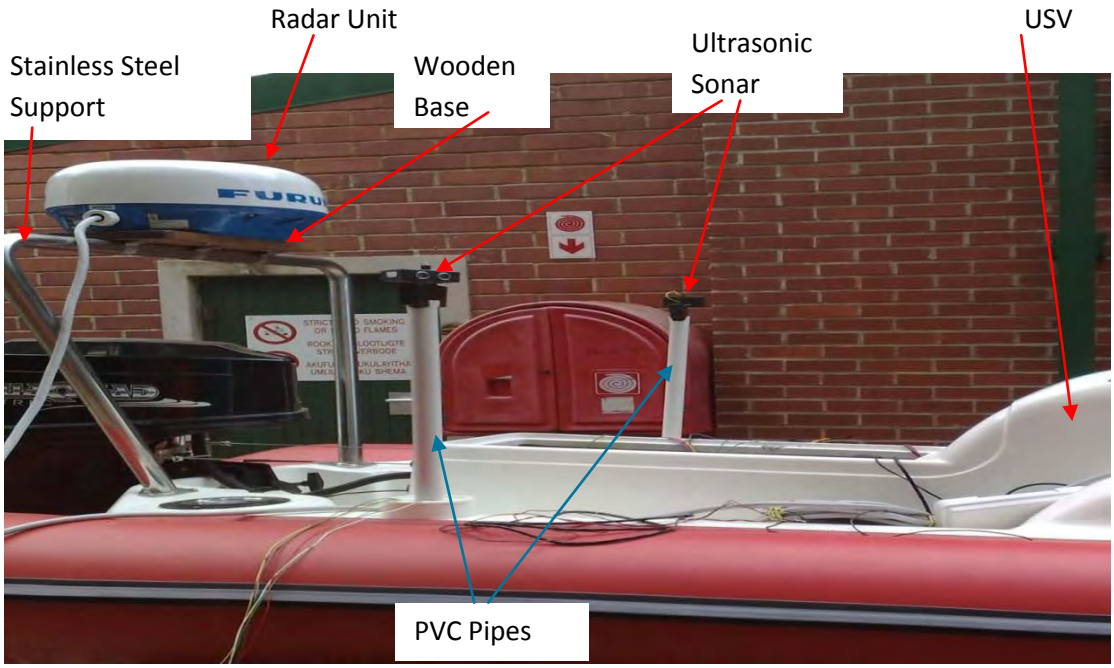

Figure 3-7: A Picture of the Rear Section of the Marine Vehicle.

3.6 Marine Vehicle Layout and Stability

To maintain the stability of the marine vehicle in pitch and roll, the layouts of the components on and inside the USV had to be carefully positioned. Two heavy duty DC batteries were placed at the center of the vehicle just beneath the seat of the craft. The radar unit was positioned at the rear of the craft as shown in Figure 3-8 while the surveillance cameras were positioned at the front of the craft as shown in Figure 3-8.

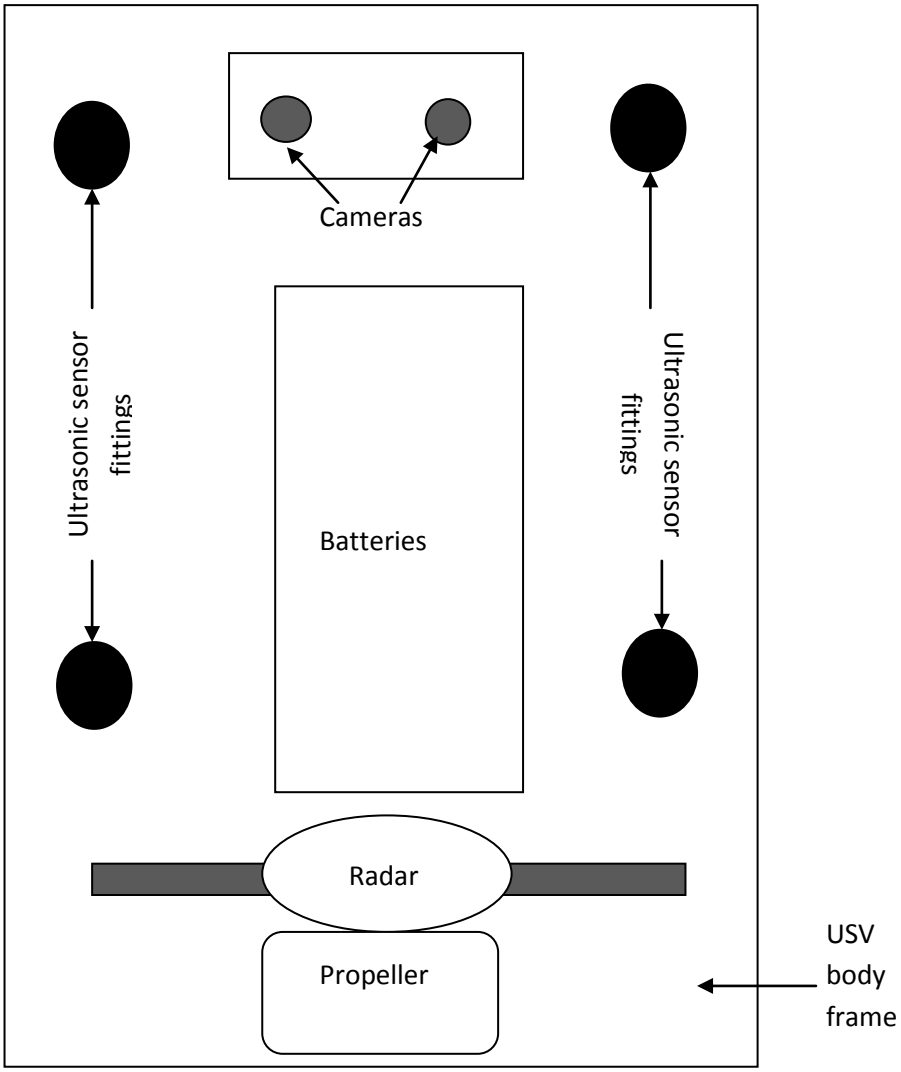

Figure 3-8: Component Layout of the USV

3.7 USV Manoeuvrability and Controllability

The USV utilizes a single propeller powered by two DC 12 Volts 90 Amps batteries. The propeller blade has a fixed pitch as shown in Figure 3-9. This allowed the output torque from the propeller to be a function of the rotational speed of the propeller instead of propeller pitch. Reverse rotation of the propeller provided for reverse motion of the USV. The rudder action of the marine vehicle was provided through the rotation of the propeller along the yaw axis. This rotation was controlled with the use of the steering mechanism [81].

Figure 3-9: Fixed Blade Propeller for the USV

3.8 Summary

The chapter discussed the mechanical modifications which were made and the design implementations made to ensure that the marine vehicle becomes a functional USV. It showed the modifications made to steering mechanism, component layouts and the choice of steering mechanism. The chapter also showed the designs of USVs intended for use in search and rescue activities.

Chapter 4

Sensory Architecture

4.0 Introduction

This chapter starts with an enumeration on the sensor technologies used in the integration and implementation of the different sensors used during the development of the marine craft. The sensory infrastructures used in this research are the sonar, GPS, digital compass, ArduIMU and servo motor. The servo was used for steering and rudder control of the marine craft. The radar was used for validation of targets detected by the sonar during autonomous navigation simulation and tests, as this would enable the validation of the rate at which the main processor and controller for craft process information. Digital compass and GPS were used to provide a sense of direction on the marine vehicle.

4.1 Component Selection

The components and the electronics that were used in the project were selected in such a way that facilitated the transformation of the marine vehicle into an autonomous marine robot. The selection of the components also took into consideration the compatibility of the Arduino microcontroller board with communication protocol and baud rate of these sensors and electronics.

4.2 Sonar

The sonar used for testing obstacle detection and avoidance algorithm was the SRF05 Daventech sonic range finders shown in Figure 4-1. The SRF05 sonic range finders are low-cost sonic modules that use two ultrasonic transducers and a PIC microcontroller for onboard processing capabilities. These range finders send out sonic pulses which allow obstacles to be detected from three centimetres away from the craft to about four meters. The distance of an object from the sonar was computed as a function the time of flight of the sound pulse sent out by the sonar as indicated in equation (4.1). Also included in the computation was an estimation of speed of sound in air. The time of flight was computed as the time it took the emitted sound waves to reflect back to the sonar.

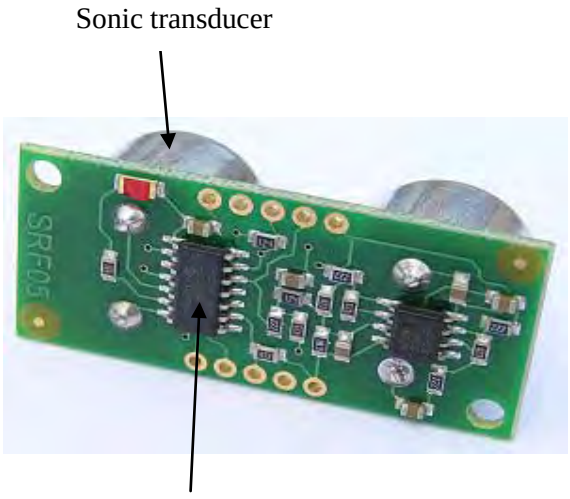

Figure 4-1: SRF05 Ultrasonic Module [82]

$$object\ distance\ from\ sonar = \frac{speed\ of\ sound\ \times time\ of\ flight}{2} \quad (4.1)$$

The timing range as shown in appendix G-4, Figure G-3 for SRF05 requires a 10*uS* pulse to trigger an input and to initiate ranging. It then sends out an eight cycle of ultrasound at a frequency of 40 *kHz* while keeping the echo pin high. The echo line listens and measures pulses whose width is proportional to the object distance. The echo pin remains high until an echo is detected. If nothing is detected after 30*mS*, the SRF05 will set the echo pin low [82].

4.2 Servo Motor

A high torque digital servo motor shown, in Figure 4-2, was used in the control and determination of the position of the marine craft steering. The implementation of this was achieved as a result of the in-built feedback control system in the servo. The servo motor was equipped with Titanium gears and this enabled the servo to deliver a maximum torque of 34*kg/cm* at 7.4 volts [83].

Figure 4-2: HS-7950TH [83]

4.3 HM55B Digital Compass

A Hitachi HM55B digital compass module made from Parallax Inc. shown in Figure 4-3(b) was used in determining the direction in which the marine craft was facing. The HM55B has a dual-axis magnetic field sensor which adds a sense of direction to the motion of the marine craft. It has an onboard regulator and resistor protection which allows the 3 volt HM55B chip to be compatible with 5 volt power supply and signal levels from the Arduino board. The configurations shown in the Figure 4-3(a) and (b) below was used to configure and setup the digital compass.

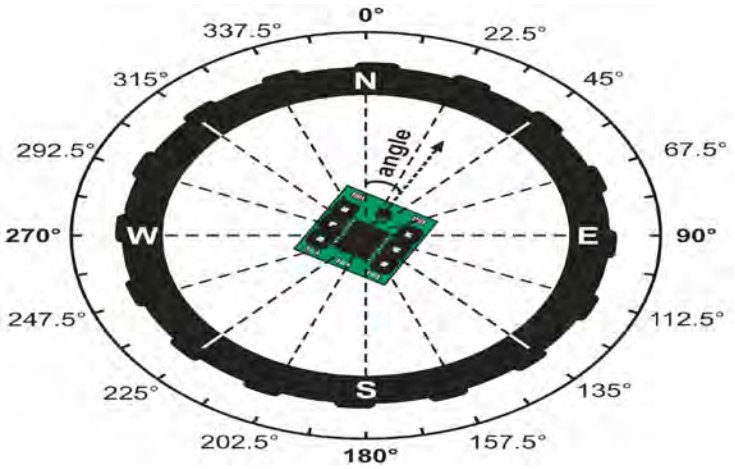

Figure 4-3 (a) : HM55B Calibration Setup [84]

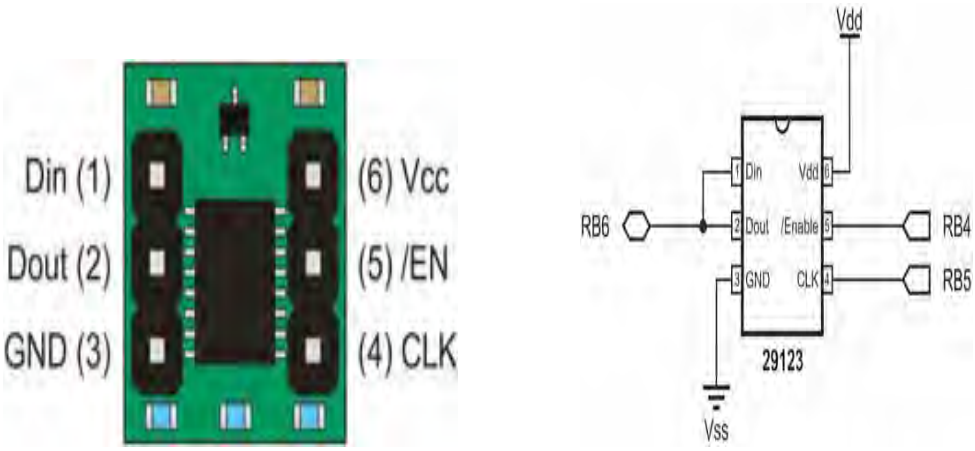

Figure 4-3 (b): HM55B Pin Configuration Setup [84]

4.3.1 HM55B Pin Configuration

Din	-	Serial data input
Dout	-	Serial data output
GND	-	Ground (0V)
CLK	-	Synchronous clock input
/EN	-	Active-low device enable
Vcc	-	+5V power supply
Baud rate	-	9600 bps

4.3.2 Hitachi HM55B Model

The *x* and *y* axes are the basic axes represented in the Hitachi HM55B compass module. The strengths of the magnetic field components parallel to the digital compass module are reported by each axis. The *x*-axis reports the field strength multiplied by the cosine of the angle to digital North and the *y*-axis reports the field strength multiplied by the sine of the angle to digital North. The angle to digital North is resolved by taking the negative Arctangent of *y*-axis divided by *x*-axis [84].

$$angle\ \theta = \arctan\frac{-y}{x} \tag{4.2}$$

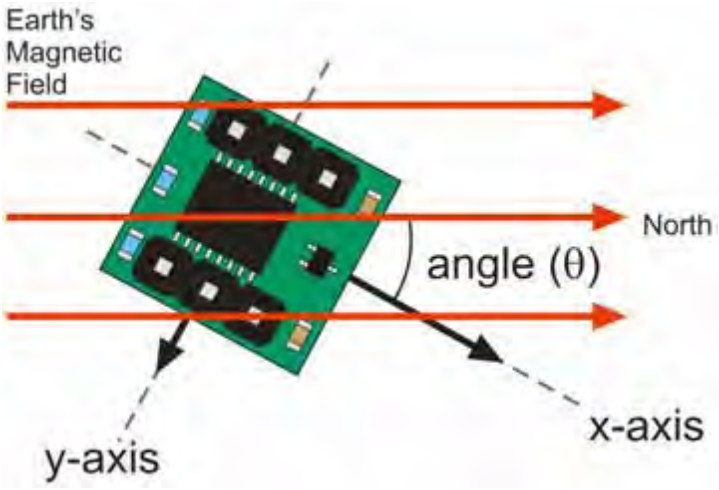

Figure 4-3 (c) : HM55B Magnetic Field And Axis [84]

4.4 Attitude Heading and Reference System (AHRS)

The low cost Inertia Measuring Unit (IMU) known as ArduIMU was used for the Attitude Heading and Reference System. The IMU shown in Figure 4-4 was based on an Arduino compatible Atmel chip that runs an open source firmware based on Bill Premerlani's DCM algorithm [85]. The IMU hardware comprised of three gyro sensors, 3-axis accelerometer, an I2C port for magnetometer input, a GPS port and has a dual power regulator that regulates 3.3V and 5V. Figure C-1 in appendix C shows the Ardu-IMU board schematic.

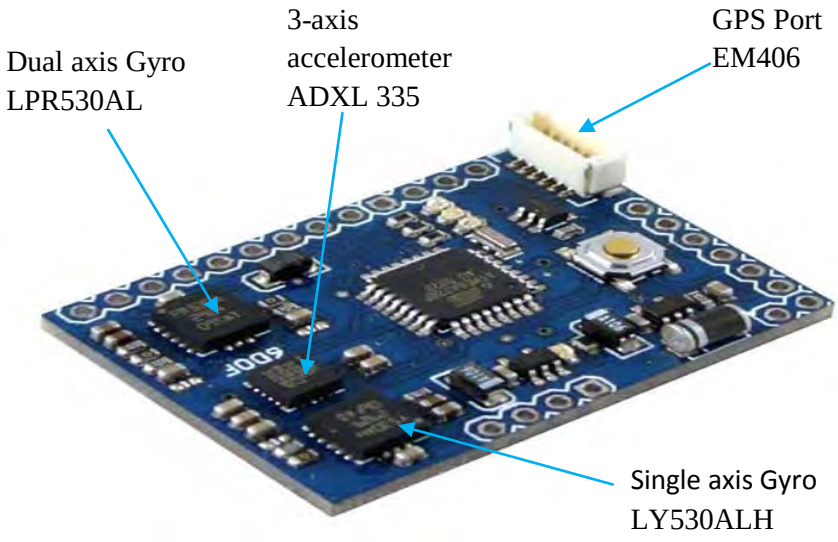

Figure 4-4: 6-DOF IMU (Ardu-IMU) [86]

The IMU uses the accelerometers, gyros and GPS to maintain a model of the marine craft orientation in space. The data from the accelerometers and gyros were used by the Direction Cosine Matrix (DCM), a mathematical algorithm for attitude heading computation. Gyro data were used in real time step integration to update the DCM matrix which was basically a 3 by 3 numerical matrix (array). Drift from gyros results in errors and quantization of gyro signals results in numerical errors as well as rounding off errors as a result of mathematical computations. These errors were corrected using data from the accelerometers and GPS. For debugging purposes, the IMU firmware can be configured to output streams of data which includes raw sensor data, GPS data, pitch, roll, and yaw data and any other computed data.

4.5 ADXL335 3-Axis Accelerometer

The low power 3 axis accelerometer shown in Figure 4-5 (a) and Figure 4-5 (b) with signal conditioned voltage output made by Analog Devices was used in the design of the IMU. The ADXL335 3-axis accelerometer measured acceleration with a minimum full scale range of $\pm$ 3*g*. It has the capacity of measuring dynamic acceleration which results from motion, vibration or shock applications as well as static acceleration due to gravity in tilt sensing. The ADXL335 has bandwidths which can be selected to suit the intended application. The *X* and *Y* axes has a bandwidth range of 0.5 Hz to 1600Hz and the *Z* axis has a bandwidth range of 0.5 Hz to 550Hz.

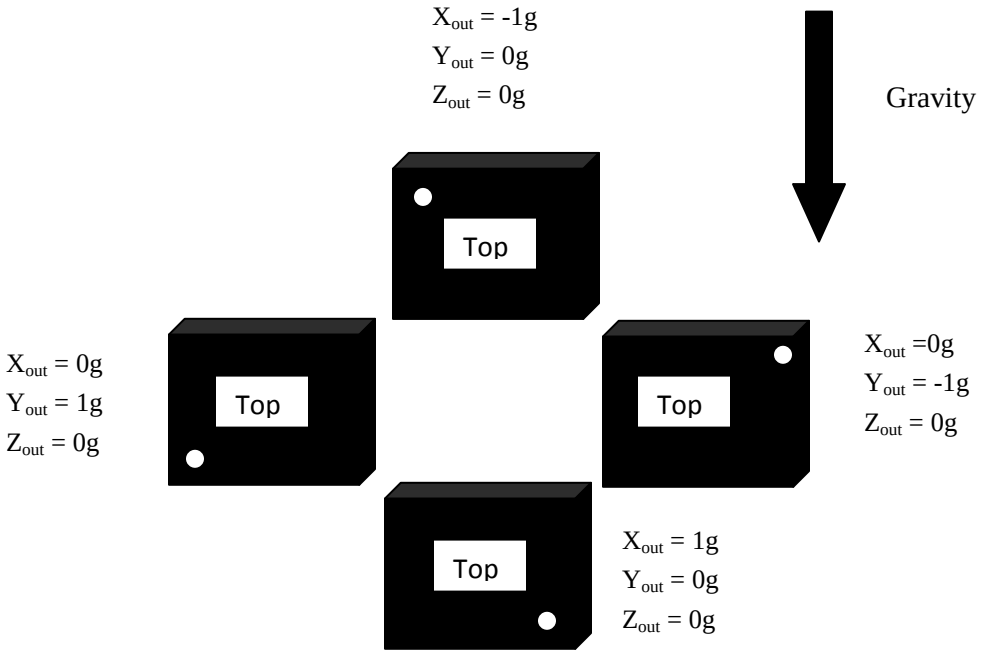

Figure 4-5(a): Output Response of ADXL335 with Respect to Orientation and Gravity [87]

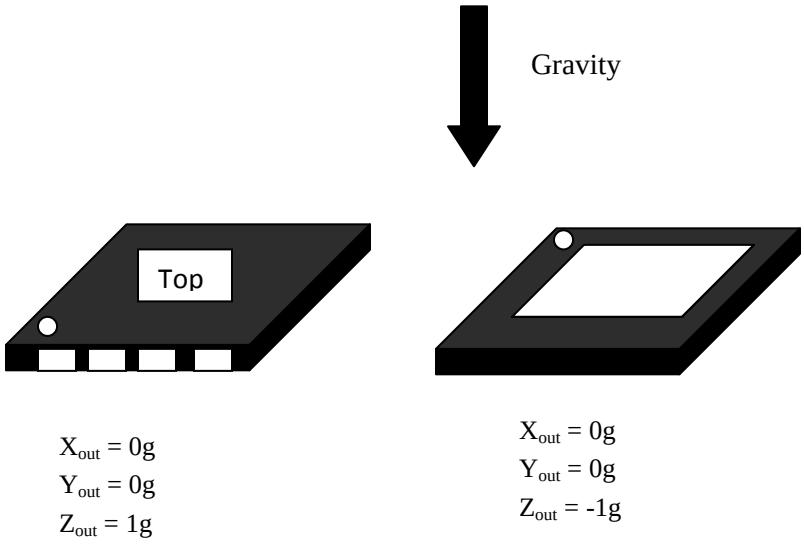

Figure 4-5 (b): Output Response of ADXL335 with Respect to Orientation and Gravity [87]

The ADXL335 with a complete 3- axis acceleration measurement system has a polysilicon surface-micro machined sensor and signal conditioning circuitry, used for open loop acceleration measurement. The output signals from the accelerometer are analog voltages which are proportional to acceleration. Polysilicon springs are used to suspend the polysilicon surface micro machined structure. The springs were put in place to provide resistance against acceleration forces. A differential capacitor consisting of independent fixed plates and plates attached to moving mass, measures the deflection in the micro machined structure. An unbalance in the differential capacitor results in an output signal from the sensor, whose amplitude is proportional to acceleration. Demodulation techniques which are phase sensitive were used to determine the magnitude and direction of acceleration. Amplification of demodulated outputs was done through a 32 kΩ resistor and the bandwidth set by including a capacitor. This sort of filtering improved the measurement resolution and prevented aliasing. The ADXL335 made use of a single structure for sensing acceleration in the *X*, *Y*, and *Z* axes [87]. The consequence of this procedure resulted in the three axes' sense of direction being highly orthogonal with little cross axis sensitivity. The innovative design implemented in the making of ADXL335 circuitry ensured that high performance becomes a built design specification, which resulted in no quantization error or non-monotonic behaviour with temperature hysteresis being very low to a range of -25^{o}C to +70^{o}C [87].

4.5.1 LPR530AL

The low powered LPR530AL dual axis micro-machined gyscope shown in Figure 4-6 and made by ST Microelectronics was used in measuring the angular rate along the *X* and *Y* axes. Having a high resolution and a stable extended temperature range of -40^{o}C to +85 ^{o}C. The LPR530AL has a full scale of $\pm$ 300^{o}/s and has the capacity of detecting rates within the bandwidth of -3dB to 140 Hz. A combination of one actuator and one accelerometer integrated into one micro machined structure forms the principal components of LPR530AL. This micro machined structure has a sensing component composed of a single driving mass kept in continous oscillatory movement, which reacts at the application of an angular rate based on Coriolis principle [88]. The LPR530AL has the following properties:

- Sensitivity: A positive output voltage from the LRP530AL defined a clockwise rotation around the sensitive axis that was considered. The sensitivity of LPR530AL defined the gain of the sensor and can be determined by applying a known angular velocity to it. The value of the gain changes very little over time and temperature.
- Zero rate level: This was the condition in which the actual output signal described the absence of angular rate. The zero rate level value changes very little with time and temperature.

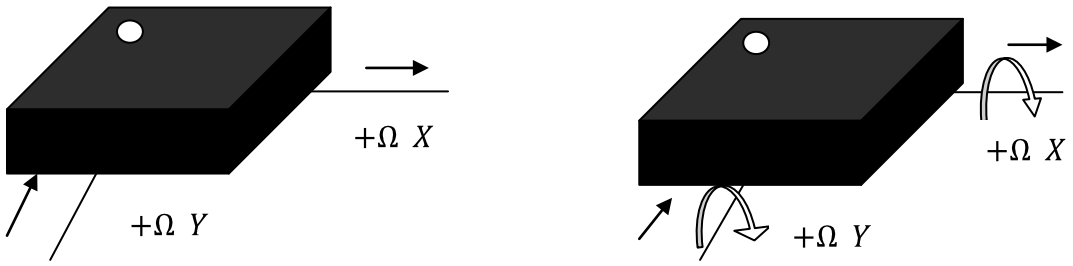

Figure 4-6 : Output Response of LPR530AL Against Rotation [88]

4.5.2 LY530ALH

To measure angular rate along yaw axis, a low power single axis LY530ALH gyroscope shown in Figure 4-7 and made by ST Microelectronics was used. The LY530ALH has good temperature stability of about -40^{o}C to +85^{o}C. It has a full scale of $\pm$ 300^{o}/s and has the capacity of detecting yaw rates within the bandwidth of -3dB up to 140 Hz. With a combination of a single accelerometer and one actuator integrated into a single micro machined structure, the LY530ALH has a sensing component made up of a single driving mass. The driving mass kept on continuous oscillation, reacts to the application of angular rate which has its basis on Coriolis principle. The measured angular rate is read off as an analog output voltage from a CMOS IC [89].

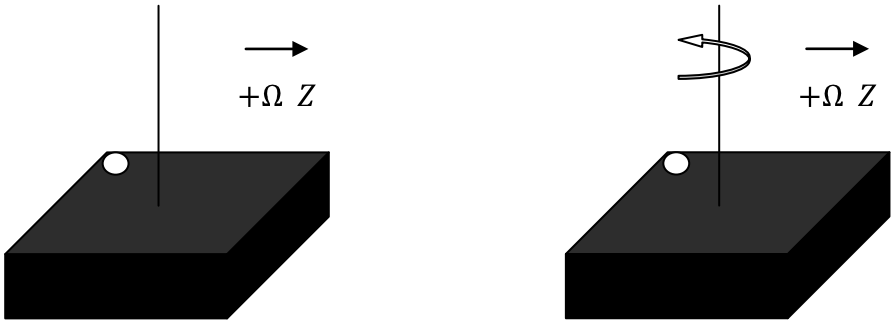

Figure 4-7: Output Response of LY530ALH against Rotation [89]

4.6 GPS Receiver

The U-Blox LEA-5H-0-007 GPS module shown in Figure 4-8 (a) was used to receive GPS data and position fixes from GPS satellites. This was used in the marine vehicle waypoint navigation algorithm. The module has functionalities for cold starting. The EM406 GlobeSat GPS receiver shown in Figure 4-8 (b) was used in the IMU setup and error correction algorithm.

U-Blox GPS Receiver @ 38400 bps (Left)

Figure 4-8 (a): U-Blox

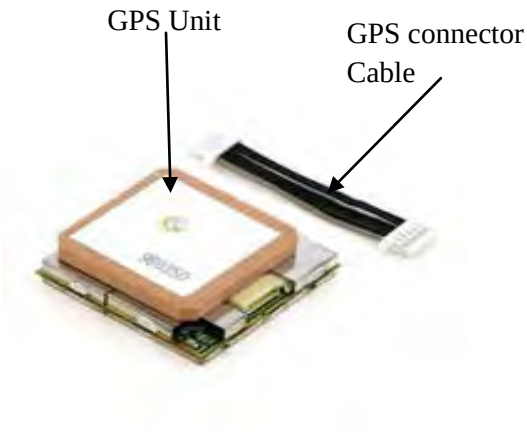

EM406 GPS Receiver @ 57600 bps [90] (Right)

Figure 4-8 (b): EM406

4.7 Xbee Module

For wireless transmission of data to the controller on ground, an Xbee 900 Pro DigiMesh wirelees RF module shown in Figure 4-9 was used. The wireless RF module required some sort of minimal power and provided reliable data transfer between remote devices for a setup which required low cost, low power wireless sensor networks. The Xbee wireless module was used to provide an extended wireless

communication and connectivity with Arduino micro controller board. The module used a DigiMesh peer- to-peer networking protocol which featured dense network operation and sleeping for routers. The Xbee wireless modules operated at a frequency of 900 MHz with data transfer rate of 156 Kbps. This capacity allowed the Xbee module to transmit data up to 6 miles or 10 Km line of sight communication with the installation of gaining antennas. To its credits, the Xbee module has self healing capabilities and discovery for network stability [91]. The specifications for the Xbee module are shown in appendix G-3.

Figure 4-9 : Xbee 900 Pro DigiMesh Module [91]

4.8 Magnetometer

The magnetometer shown in Figure 4-10 was a CMPS03 compass module used for drift correction in the IMU. The drift arose from the gyros incorporated in the IMU. The compass used Philips KMZ51 magnetic field sensor which detected earth's magnetic field. Outputs from two Philips KMZ51 magnetic field sensor mounted at right angles to each other were used to compute the direction of the horizontal component of the earth's magnetic field. The pin configuration and the calibration setup procedures are shown in appendix G-2.

Figure 4-10: CMPS03 Compass Module [92]

4.9 Network Camera

The VIVOTEK IP7330 network camera shown in Figure 4-11 was used for visuals in the marine craft sensor integration. The camera was specifically designed for outdoor applications and as such it has a weather proof housing, which shields the camera from harsh conditions such as dust and rain. The camera has integrated properties such as day and night functionalities, with dual-band lens incorporated alongside with infra-red illuminators, enabling the camera to have an effective range of up to 10 meters. Images from the camera are transmitted wirelessly to the operator of the marine vehicle. The transmitted image is received on the computer via the Ethernet port [93].

Figure 4-11 : VIVOTEK Network Camera [93]

4.10 Path Finding IR Camera

The FLIR system PathFindIR shown in Figure 4-12, is an IR camera integrated on the marine craft. The PathfinderIR is a thermal imaging camera for the ground station controller vision enhancement. The thermal imaging camera significantly reduces the dangers of operating the marine craft in low light and night periods. It enhances the marine craft operator's vision to detect and recognise potential obstacles in total darkness, smoke or rain [94].

Figure 4-12 : FLIR Systems PathFindIR [94]

4.11 Power Distribution Architecture

The power distribution for the marine vehicle shown in Figure 4-13 was accomplished through a custom made power distribution circuitry. The power inputs are from two 12 volts, 90A DC batteries, connected in series for input to the propeller and one of the 12 volts battery used as input for other power requirements. The power to the microcontroller boards, IMU, GPS, H-bridges, remote control receiver, and sonar were from 5 volts, voltage regulators which stepped down the 12 volts from the main supply to 5 volts. The high torque DC servo motor had a separate 7.4 volts regulated DC power supply.

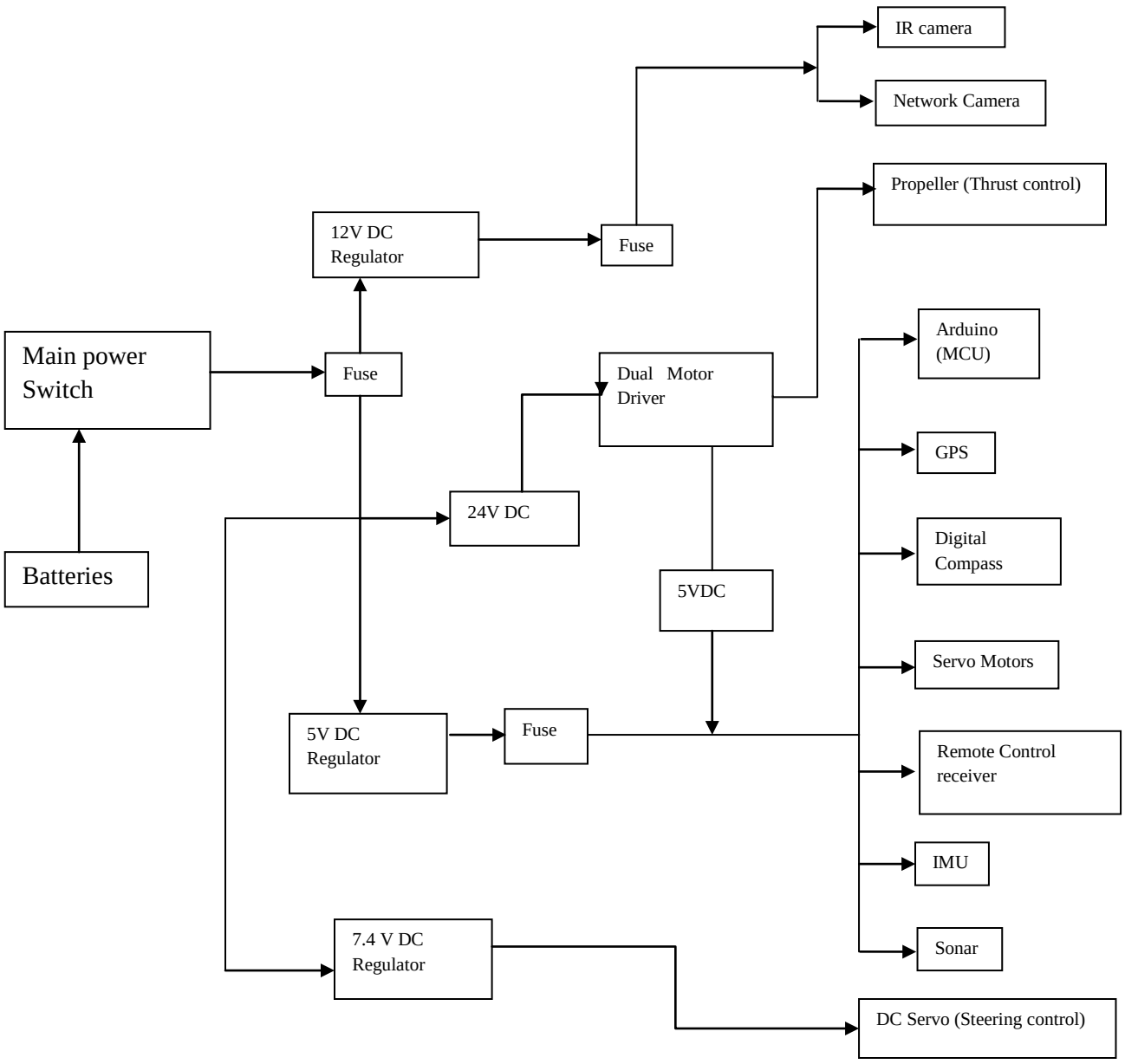

Figure 4-13: Power Supply Distribution Schematics

4.12 Summary

The chapter demonstrated the integration of different sensory architecture in the unmanned surface vehicle. It also showed the power, communication architecture and networks which used in the development of the USV. The chapter also provided the functional importance of each sensor in the overall functioning of the autonomous marine craft.

Chapter 5

Marine Craft Autonomous Motion and Uncertainty

5.0 Introduction

This chapter discusses the contributions made using mathematical deductions and reasoning in programming the Arduino microcontroller board in the Arduino programming environment. It also discusses probabilistic reasoning in an autonomous marine craft. The chapter starts with uncertainty in autonomous motion, decision making algorithms, identifies the probabilistic nature of marine vehicle autonomous motion and ends with a Bayesian postulation for autonomous marine craft motion.

5.1 Uncertainty in Autonomous Systems

The realistic domains and environments in which marine robots operate and function requires that some simplifications be made to accommodate deterministic and un-deterministic variables within the realistic domain and this formed the reasoning about any realistic operational autonomous motion environment. The preparatory procedures of information for use in the marine vehicle autonomous systems to support the realistic reasoning required that significant amount of information is left as unknown facts, indeterminate and inadequately summarised. The conditions under which decisions for autonomous navigation algorithms were formulated were usually ambiguously defined, and may be difficult to meet the requirements of real life decision making scenarios. Reasoning with exceptions depicts a scenario of path finding within an autonomous motion. Most steps taken are safe while some may prove to be fatal. Summarising the reasoning behind marine vehicle autonomous navigation algorithm provided an alternative to enumerating exceptions or extremely ignoring exceptions associated with autonomous navigation. Summarisation of decision making algorithm provided a reasonable compromise between speed of navigation and safety of movement [95-96].

5.2 Reasons for Uncertainty in Guidance and Control

The realisation that exceptions exist in algorithm formulation provided a way to summarize exceptions. The summarization of exception involved that each proposition be assigned a numerical measure of uncertainty and these measures were combined according to uniform syntactic principles in a similar

fashion in which truth tables are combined in logic. A comparison of truth table principles revealed that truth table characterised formulas under investigation while uncertainty measures characterised invisible facts, as they represented things which were totally different from truth table values. These uncertainty measures have proven to have significant effect on autonomous navigation algorithm. Arguably, the syntax of formula formed a perfect guide for combining visible or measured variables, in that it seems useless when it comes to joining invisible variables which affect autonomous navigation formulation.

The interaction of exception were intricate and occurred in clandestine ways which do not provide the opportunity to make use of the modularity and monotonicity that are available in classical logic computation. Interactions were visible in the sense that their effects on the autonomous system can be felt even though the interaction occurred in intricate ways within the frame work of logic. The visualisation of interactions allowed for computation of the effects of new data in stages through the process of derivation similar to propagation of waves. The computation of new data from sensors was done on a set of synthetically related lines of code identified as S_1, the results were stored, then the impact from S_1 were propagated to another set of lines of code identified as S_2 without having to come to S_1. This computational algorithm, so basic to logic deduction cannot be fully justified within the concept of uncertainty unless some restrictive assumptions of independence of data are made and conjoined. The uncertainty associated with measured incrementality of information tends to be lost as restrictive assumptions of independence appeared to force the computational algorithm to compute the effects of past observations from sensors in one global step.

5.3 The Methodology to Uncertainty

Different researchers in robotics and marine autonomous systems have their various ways of dealing with uncertainty within the frame work of the available approaches that can be applied to uncertainty. The approaches are viewed from three different perspectives. The first being the neo-probabilist, the second being the neo-calculist and the third being the logicist. Within the frame work of the logicist perspective, numerical methods are used to handle uncertainty primarily using non-monotonic logic algorithms. In the neo-calculist view, numerical representations of uncertainty are used while regarding probability calculus as unsuitable for the task hence entirely new calculus are invented for the task such as fuzzy logic, Dempster-Shafer calculus and certainty factors. The neo-probabilistic approach remains within the framework of probability theory while trying to expand the theory with computational capabilities needed to perform autonomous tasks [97]. An informal approach can also be applied to uncertainty. This heuristic approach embeds uncertainties within the specific domain procedures and data structures rather than giving explicit notation to uncertainty [98-100].

5.4 Bi-Directional Inferences in Marine Autonomous Systems

The capacity to use both predictive and diagnostic data in the marine autonomous system formed an integral part of plausible reasoning in the control of the autonomous systems. Inadequate use of such data led to results that were undesirable and was most probably strange to the intended application. The usual way of reasoning using bi-directional inferences involved an abductive reasoning which can also be regarded as an induction pattern. This was illustrated using two sensors; sensor *A* and sensor *B*. Abductive reasoning required that if data from sensor *A* implied data from sensor *B* for example, then the truth value of *B* made A more plausible [101]. The creation of a cycle of information in favour of sensor *A* amplified through sensor *B* and fed back to sensor *A* brought about a system where predictive inference and diagnostic inference were used with no factual justification of the data being used. The stoppage of such cycles created a system which allowed only diagnostic reasoning and no predictive inferences. For the autonomous system to be able to use bi-directional inference effectively without compromising the system circular reasoning, the principles of modularity which involved locality and detachment of data were sacrificed.

5.4.1 The Limitation of Modularity

The inference rules of Classical logic provided a platform that allowed the full realisation of the principle of locality. The rule " If input from sensor *A* then input from sensor *B*" implied that the truth value of *A* can allow the assertion of *B* with no further analysis, even if the streams of data coming in from the sensors contain some other information *P*. In credible reasoning, the luxury of ignoring the rest of information contained in streams of data from the sensors cannot be maintained at all times. The system of imposing a connection to unrelated data as an explicit exception defeated the purpose of modularity thereby forcing the autonomous systems' programmer to join and pack together information from sensors that are only remotely related to each other and this leads to an unmanageable large number of exceptions surfacing in the algorithm [97].

5.4.2 Incompleteness and Uncertainty in Marine Autonomous Systems

Human beings involved with search and rescue activities at sea are usually faced with the fundamental problem of incompleteness and its direct consequence of uncertainty. This has formed a major challenge for marine autonomous systems which are mainly made up of motors and sensory systems. The challenge came as a result of the idea of incompleteness in the models used for modelling their behaviours. The mathematical models at various stages of modelling have some form of hidden variables which may not be considered properly in the model and may also have a considerable effect on the phenomenon. The influences of these hidden variables in autonomous systems were verified through the inconsistencies that

exist between the model and the phenomenon. Abstract data were often used to program the marine craft in the sense that the programmer has imposed his own view of the environment in which the marine craft has to operate and function in. Irreducible incompleteness in models formed the main starting point of these difficulties as hidden variables which have an effect on inputs from sensors or bias motor outputs were not represented properly in the software program that drove the marine craft. This prevented the marine craft from relating properly the abstract data to raw sensory and motor data reliably [102-103].

5.4.3 The Probabilistic Method to Marine Autonomous Systems

The imposition of the programmer's concept of the environment depicted a symbolic approach to marine autonomous systems whereas a more agreeable concept of autonomous systems involved a model built and developed conjointly by the programmer and the marine craft. Preliminary data provided by the programmer provided certain clues to the autonomous marine craft as to what it may expect to observe through its sensors. The preliminary information acted as a gauge with free parameters that were modified through observed data from sensors. The raw data obtained from sensing the environment as measured by the sensors and used for driving the actuators showed the various levels of complexities of the interaction between the autonomous marine craft and the environment and also reflected the hidden variables effects on the autonomous system which were not taken into consideration by the preliminary data. The probabilistic method for the autonomous system followed two steps as shown in Figure 5-1. The variables X_1 and X_2 in Figure 5-1 can be inputs from two similar sensors or different sensors.

5.4.4 The Relevance of Probability in Marine Autonomous Systems

The objective of the autonomous system in the marine craft application required the provision of a computational model that described the autonomous and intelligent behaviour of the marine craft, most importantly within the premise of commonsense reasoning. The use of probability theory provided a coherent view of how intelligent decisions should change in the light of partial or uncertain information. Most importantly, probability revealed not only the use of numbers in decision making rather it involved and revealed the structure of decision making in the autonomous marine craft system. The uniqueness of probability theory expressed the ability to process and analyse context-sensitive views and factors required to make computations feasible while specifying the context dependencies that were manipulated by local propagation [97].

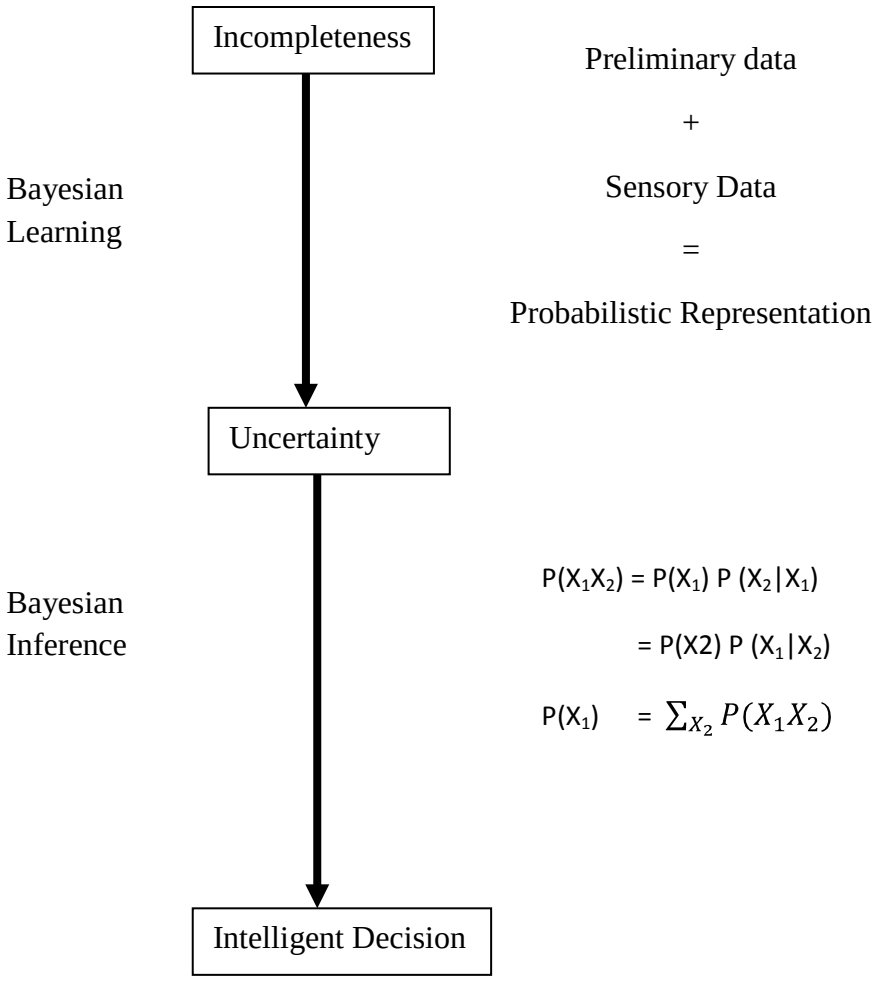

Figure 5-1: The Probabilistic Approach to Autonomous Decision Making [104].

5.5 Data Identification, Classification and Estimation.

The development of the autonomous marine craft was an attempt to create a product which can be used in serving humanity more especially in search and rescue activities. The system design and control of the marine craft involved ways of manipulating data from the environment to move the marine craft and stabilize the craft and carry out other functions. Such actuations were possible as a result of information in terms of physical values which described the environment surrounding the craft. This information was usually prior knowledge of the environment or empirical data generated from sensorial observations. A merger of empirical data and prior data led to posterior data or knowledge. The information given by the posterior data represented accurate and more complete information that described what was observed by the sensory system. Hence data signals were analysed in conjunction with prior knowledge of the craft environment [50].

5.5.1 Data Classification

Data classification involved the assignment of labels to obstacles which are within detectable distance from the marine craft. Assigning labels to data required the conversion of sensed signals to specific binary data or image which can be differentiated. It also involved retrieval of information from a digital data base such as finding a matching binary image through specified image features.

5.5.2 Data Estimation

This involved the derivation of the parametric description for an ongoing physical process such as detecting an object using ultrasonic waves. Usually measurements were taken from known positions for example, the current position and location of the marine craft to the object. The process involved solving for certain unknowns which were in the mathematical formulation. This also included the uncertainty which was associated which the measuring device. As such data estimation required not only estimation of parameters but also an assessment of the uncertainties associated with the estimate. The use of prior information was helpful in the reduction of uncertainty of the final estimate. Accuracy was improved to a certain degree by increasing the number of independent measurements to more than one measurement and the cost and time on the sensory system were improved by decreasing the number of measurements leading to fewer measurements than parameters to estimate.

Since the nature of problems addressed in this dissertation was within the frame work of statistical inference, the strategy used was to formulate posterior data in relation to a conditional probability density function [50]:

$$P(\text{data of interest} \mid \text{available data (measured)}) \tag{5.1}$$

The posterior probability combined empirical data with prior data using Bayes' theorem for conditional probability. This was done under the assumption that the physical events such as measurements from sensors, marine craft motion were captured in the mathematical model. With appropriate generalization level selected, the empirical data formed the basis for the set of possible measurements which were given with adequate weights added to the data. The right balance between the mathematical model depended on noise or accidental peculiarities and the one which depended heavily on prior knowledge was dependent on the statistical importance of the data. Dimensionality of the measured data has an important relation to the statistical significance of the data. The difficulties associated with classical logic do not originate from its non-numeric, binary character. The difficulties arose when truth or plausible data and certainty are measured on grey scale through interval bounds, point values or by linguistic quantifiers such as "likely" and "credible" which seemed to portray a conflict between procedural modularity and semantic coherence; independent of the classification used.

5.5.3 Statistical Inference in the Marine Vehicle Design

In the development of the autonomous craft, the first process in the developmental process was to identify the primary need of the craft in relation to the global view of the functional requirements of the craft with the actual need for the craft known at a high and abstract level. At every developmental stage, a more detailed requirement became available and design decisions were made based on explicitly defined evaluation procedure. The evaluation steps consisted of collecting and organising data at each developmental stage and it was followed by an explicit mathematical formulation of the task being described. Figure 5-2 shows an iterative process used at different developmental stage for the different systems and subsystems in the marine craft. The process starts by identifying the specific requirement of the marine craft. This is followed by identifying the method or protocol that is necessary to acquire data. The data is analyzed and evaluated in the autopilot control program. The result that emerges from the analysis enables the autopilot to make strategic decision which would lead and facilitate the autonomous motion of the marine vehicle. The process is repeated and evaluated to facilitate the development of other requirements which are necessary for autonomous decision making.

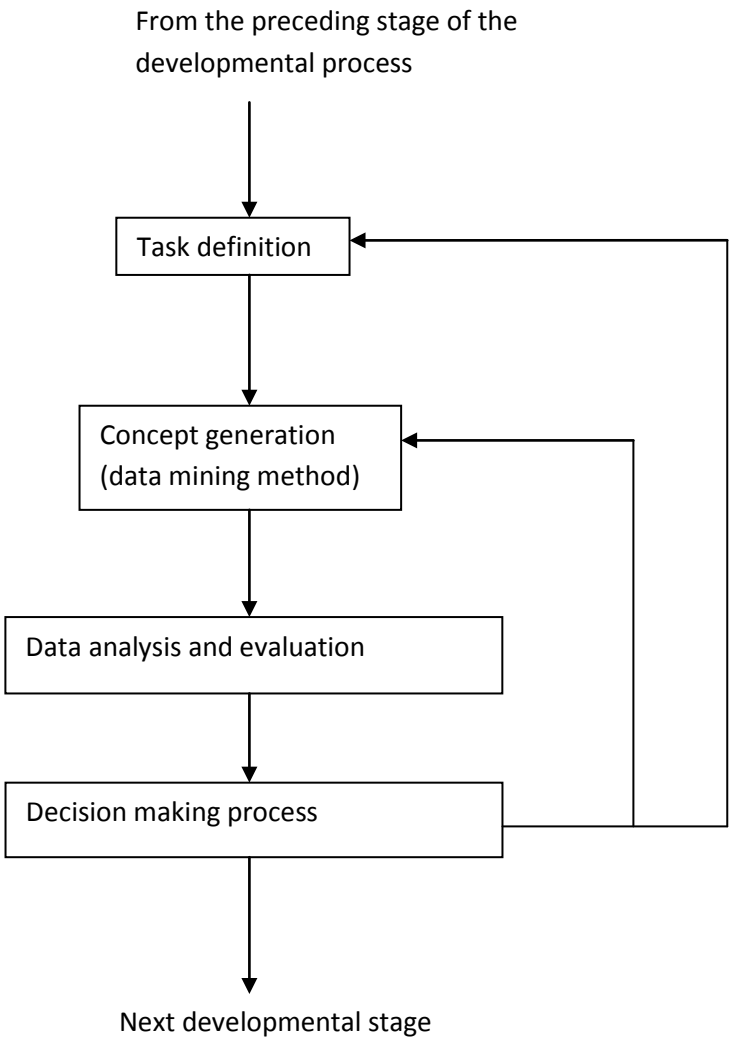

Figure 5-2 : The Elementary Step in Algorithm Formulation Process [105]

5.6 Sensory Data Detection and Classification.

The autonomous motion of the marine craft dealt with ability of the navigation algorithm to identify reliable data from the sonar whose integrity was not compromised and used in making navigational decisions. Decision making in guidance and control of the marine craft was a consequence of proper data identification and classification. The decision making model from a primary perspective was introduced into the system using Bayesian classification.

5.6.1 Bayesian Classification for Sensors

Bayesian theorem of data classification thrived on the platform of probability theory as its solid base for data and pattern classification model. Within this method of classifying data, the pattern generating mechanism, which in this case was the sensory network, was represented with the probabilistic framework in one way or the other. In classifying the data from the sensory network, classification was done on the assumption that the information streaming in from the different sensors was mutually exclusive. A set of $\Omega = \{\omega_1 \dots \dots \omega_T\}$ shown in Figure 5-3 described the classes of data from the sensors and was used to analyse the probability of classifying streams of data coming in from the sensors.

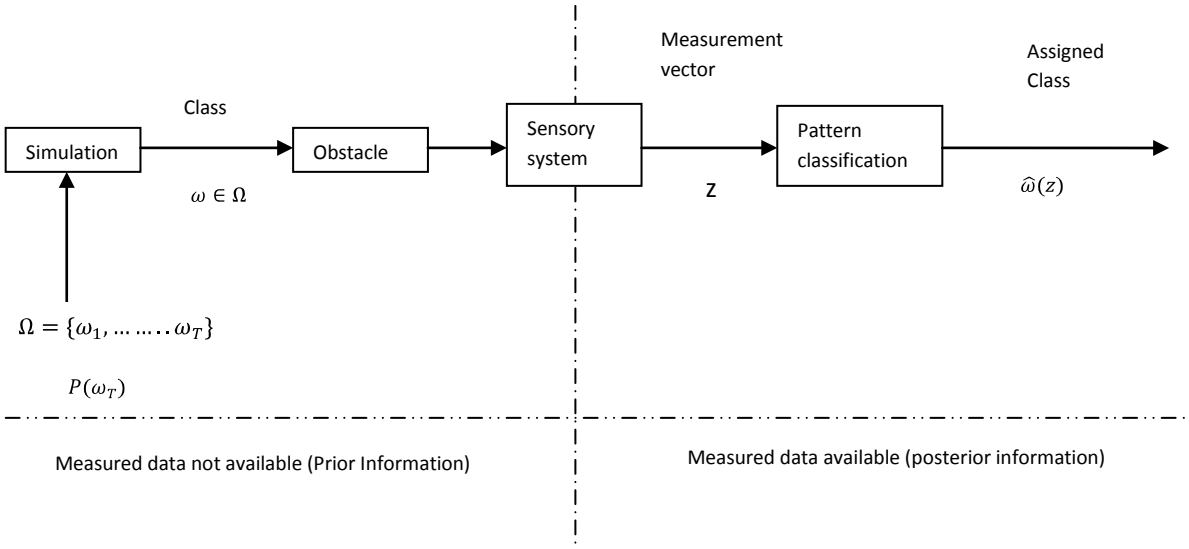

Figure 5-3: Statistical Sensory Data Pattern Classification [50]

The probability $P(\omega_T)$ of having a data classification of (ω_T) known as prior probability represented the known or prior information about the capacity of the sensors. Given that *T* represented the number of possible classes that can be derived from the data we have:

$$\sum_{T=1}^{T} P(\omega_T) = 1 \tag{5.2}$$

The sonar produced a measurement vector *X* with dimension *M*. Different obstacles were grouped into different classes as a result of the intensity of reflected sonic waves having different measurement vectors. Variations occurred in the measurements as a result of randomness associated with some degree of unpredictability of the sensory system. These variations and randomness were accounted for within the probability density function *Z*. The conditional probability of *Z* denoted by $P(z|\omega_T)$ represented the density of *Z* from an obstacle with a known classification or class ω_T and the unconditional probability of *Z* denoted by $P(z)$ represented the density from an unknown classification or class. The unconditional

densities were derived from the conditional density by using appropriate weights from prior probabilities to weigh the densities.

$$P(z) = \sum_{T=1}^{T} P(z|\omega_T)P(\omega_T) \tag{5.3}$$

5.6.2 Probabilistic Formulation Using Bayesian Inversion

The partial concepts and ideas in the marine autonomous system under uncertainty conditions were proposed using Bayesian methods as a platform for the models. The formulation attributed numerical parameters to the proposition which indicated the degree of certainty accorded to the proposition within the framework of available information in the operational environment and these were manipulated according to the rules of probability theory. For instance, if A stands for the condition or statement that "the wind has an eastwards direction", then P (*A* | *D*) represented the subjective reasoning in *A* given that the information *D* was available. In The Bayesian approach, the reasoning obeyed three basic axioms of probability theory:

$$0 \leq P(A) \leq 1 \tag{5.4}$$

$$P(\,certain\,proposition) = 1 \tag{5.5}$$

$$P(\,A\,or\,B) = P(A) + P(B)\;if\;A\;and\;B\;mutually\;exclusive \tag{5.6}$$

The third axiom stated that the sum total of the reasoning assigned to the non-intersecting components of the algorithm came from the reasoning assigned to any set of events in the autonomous motion of the craft. This implied that any event *A* can be written as the union of joint events (*A* and *B*) and (*A* and –*B*) with their associative property written as:

$$P(A) = P(A,B) + P(A,-B) \tag{5.7}$$

$$P(A) = \sum_i P(A,B_i) \tag{5.8}$$

for *i = 1, 2 ...n.*

The Bayesian reasoning for conditional probability specified the reasoning that any event in *A* under the assumption that activity *B* has information occurs with absolute certainty. Hence the expression:

$$P(A \mid B) = P(A) \tag{5.9}$$

This implied that and *B* were independent activities and

$$P(A\,|B,C) = P(A\,|C) \tag{5.10}$$

This indicated that *A* and *B* were conditionally independent given *C*. The axioms and the associated utility theories are discussed further in appendix D.

The probabilistic approach discussed so far, has provided the platform required for coherent prescriptions in choosing adequate motion actions and meaningful reliability on the quality of the choices made by the autonomous marine craft. The prescriptions were based on the paradigm of normative information. This implied that decisions about values, preferences and desirability represented the valuable abstraction of the actual human experience and like its factual data counterpart, were encoded in the firmware for controlling the marine craft and manipulated to yield useful results. The set of motion actions available to the autonomous marine craft in any given situation were represented by a variable or groups of variables that were under full control of the autonomous marine craft. Choosing an action led to the selection of a set of decision making variables within the Bayesian formulation and also amended their values unambiguously to yield the desired results. This type of choice usually altered the probability distribution of other set variables determining the autonomous motion of the craft. These were regarded to be the consequence of the decision components. Given the configuration c as a result of a consequence set C with a utility measure $U(c)$ representing the degree of desirability, the overall expected utility associated with an autonomous motion a has the following model:

$$U(a) = \sum_c U(c)P(c|a,e) \tag{5.11}$$

Where $P(c|a,e)$ represented the probability distribution of the consequence c, conditioned as a result of the autonomous motion a with sensor data or observed data e.

The Bayesian approach to autonomous motion regarded the expected utility $U(a)$ as a gauge for validating the autonomous motion a and treated it as a prescription for choosing among motion command alternatives. For the situation where autonomous motion a_1 or autonomous motion a_2 were the available motion choices, $U(a_1)$ and $U(a_2)$ were computed with the motion choice that yielded the highest value selected. The value of $U(a)$ depended on sensor data e observed until the time of decision. This made the outcome of the Maximum-Expected-Utility (MEU) criterion to be a sensor data dependent decision rule and had the form "if observed sensor data e_1, choose autonomous motion a_1; if observed sensor data e_2 choose autonomous motion a_2....." The maximum-expected-utility rule was used on the basis of

pervasive psychological attitudes towards choice, likelihood and risk associated with autonomous motion [106].

5.6.3 Consequences, Payoffs and Lotteries of Marine Autonomous Motion

The consequences of autonomous motion were not usually associated with numerical payoffs or justifications but rather, they involved and integrated the complex descriptions of the actual environment surrounding the autonomous marine craft. Rationales in choosing between two autonomous motion actions required the evaluation of the benefits, desirability, and risk of each of the various consequences and the benefits weighed with the probability that the consequences will occur. The autonomous motion consequences associated with expected results or benefits were regarded as desirables, expected results or payoffs. This suggested that the components of rationale theory of choice were pairs of the form:

$$L = (C, P) \tag{5.12}$$

Where $C = \{C_1, C_2, \ldots . . C_n$ represented finite set of desired results or consequences and P represented the probability distribution over C which satisfied:

$$\sum_i P(C_i) = 1 \tag{5.13}$$

Each pair of $L = (C, P)$ represented a lottery and are shown by a list of pairs

$$L = [C_1, P(C_1);\ C_2, P(C_2); \ldots . ; C_n, P(C_n)]\ , \tag{5.14}$$

or by a treelike diagram where each probability $P(C_i)$ labelled an arc directed from L to the corresponded to consequence node C_i. In Figure 5-4 the consequences shown indicated the situations created during an autonomous motion of turning right, moving forward, turning left, and these had probabilities 0.20, 0.60, 0.20 respectively as test cases. The weights of the turning right and turning left probabilities had to be equal to allow for a better control in the event of the USV making a turning movement. The weight on moving forward had to be different from turning right or left so as to differentiate the command line in the autonomous motion program. The consequences not represented in the diagram were presumed to have zero probability.

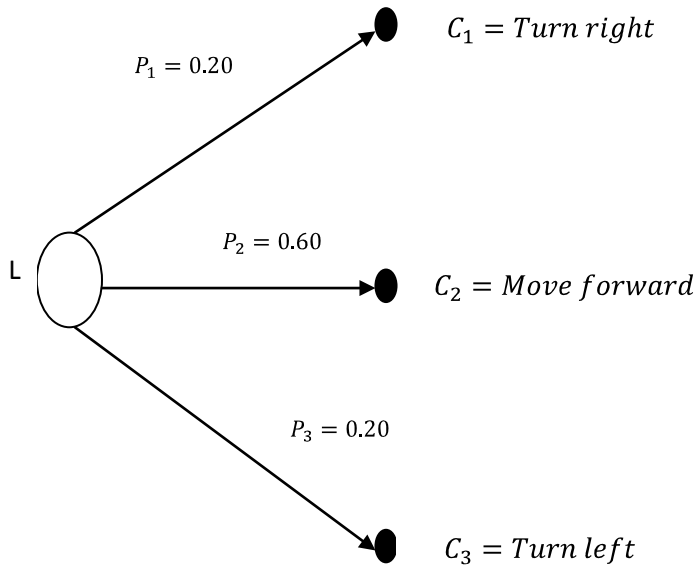

Figure 5-4: The Lottery Representation of Uncertainty in Autonomous Motion [97]

5.7 Bayesian Programming for Autonomous Marine Craft

Bayesian programming involved the use of propositions, variables and probability to determine the actions and movement of the autonomous marine craft. Having identified the uncertainty that exist in autonomous motion, data from the sensors are classified and weighted for use in the propositions, variable classification and probabilistic inference that are used for autonomous decision, guidance and control of the marine vehicle. The lotteries of each of the probabilistic inferences that are in the control algorithm are used to formulate the Bayesian program for the autonomous marine craft.

5.7.1 Logical Proposition

Logical Propositions were used in the Bayesian programming and can either be true or false. They were poised to obtain a new proposition using logical operators such as conjunctions, disjunctions and negations to the initial proposition. The Propositions were denoted using lower-case letters or names. For instance, $x \wedge y$ represented the conjunction of proposition x and y, $x \vee y$ represented their disjunction and $-x$ denoted the negation of proposition a [104].

5.7.2 Discrete Variable

The discrete variable refers to the set of logical propositions which are mutually exclusive and exhaustive (at least one of the propositions a_i is true). $\langle A \rangle$ represented the cardinality of the set A. This implied that the number of propositions a_i or number of values the variable A can accommodate. The set of $\langle A \rangle \times \langle B \rangle$ propositions of $a_i \wedge b_j$, defined the conjunction of the variable A and B was denoted as $A \wedge B$. The set $A \wedge B$ had the characteristic of being mutually exclusive and exhaustive logical proposition and as such it became a new variable. The conjunctions of n variables were variables that were renamed at any instance and were considered as a unique variable in the development [104, 107].

5.7.3 Probability in Proposition

In order to manage the issue of uncertainty in real world applications, probabilities were attached to propositions. In order to assign a probability to proposition x, some form of preliminary information expressed in a proposition λ became a requirement. As a consequence, the probability of proposition x had to be conditioned at least by λ. For each different λ, $P(\cdot \mid \lambda)$ has to be assigned to each proposition x, as an application, with a unique real value $P(x \mid \lambda)$ in the interval $[0,1]$. The formulation showed a clearer picture in the probabilities of conjunction, disjunctions and negation propositions represented as $(x \wedge y \mid \lambda)$, $P(x \vee y \mid \lambda)$ and $P(-x \mid \lambda)$ respectively. $P(x \mid y \wedge \lambda)$ represented the probability of proposition x conditioned by both the preliminary information λ and some other proposition y [104, 107].

5.7.4 Inference Formulation and Rules

The conjunction and normalization formulation for each proposition were embodied in the probabilistic reasoning. The probabilistic reasoning for the autonomous system required two basic rules [108-109]

- The conjunction rule: This generated the probability of a conjunction of propositions

$$P(x \wedge y \mid \lambda) = P(x \mid \lambda) \times P(y \mid x \wedge \lambda) \tag{5.15}$$

$$P(x \wedge y \mid \lambda) = P(y \mid \lambda) \times P(x \mid y \wedge \lambda) \tag{5.16}$$

- The normalization rule: This stated that the sum of the probabilities of a and $-a$ is one.

$$P(x \mid \lambda) + P(-x \mid \lambda) = 1 \tag{5.17}$$

Equation (5.18) represented the conjunction rule for the variables

$$P(A \wedge B \mid \lambda) = P(A \mid \lambda) \times P(B \mid A \wedge \lambda) \tag{5.18}$$

$$P(A \wedge B \mid \lambda) = P(B \mid \lambda) \times P(A \mid B \wedge \lambda) \tag{5.19}$$

Equation (5.20) denoted the normalization rule for the variables

$$\sum_X P(A \mid \lambda) = 1 \tag{5.20}$$

Equation (5.21) represented the marginalization rule for the variables

$$\sum_X P(A \wedge B \mid \lambda) = P(B \mid \lambda) \tag{5.21}$$

5.8 The Bayesian Program for Autonomous Marine Craft

The Bayesian program formed part of the generic formalisation used in developing the probabilistic model required for solving decision and inference model for the autonomous marine craft model. The Bayes formalisation was divided into two parts namely the description and the question parts. The description was the actual probabilistic model of the marine vehicle autonomous movement while the question part of the program specified an inference problem required to solve the autonomous motion model. The description was further divided in two parts namely, specification and identification. Specification formalized the data from the programmer or controller and identification used raw or experimental data to teach or adapt them to free parameters. The specification section of the program was then developed from three sections which were the relevant variables section, decomposition and parametric forms. The relevant variable section was basically the selection of adequate variable which was necessary to program the marine vehicle. The decomposition took joint distribution on the significant variables and expressed them as a product of simpler distributions. The parametric form used mathematical functions or a question or query to a different section in the program and associated it with each of the distributions appearing in the decomposition as shown in Figure 5-5[104, 107].

$$Program \begin{cases} Description \begin{cases} Specification \begin{cases} Relevant\ variables: \\ Dir,\quad Prox,\quad Vrot \\ Decomposition: \\ P(Dir \wedge Prox \wedge Vrot \mid \delta_{avoid} \wedge \pi_{reactive}) \\ = P(Dir \mid \delta_{avoid} \wedge \pi_{reactive}) \times P(Prox \mid \delta_{avoid} \wedge \pi_{reactive}) \\ \times P(Vrot \mid Prox \wedge Dir \wedge \delta_{avoid} \wedge \pi_{reactive}) \\ Parametric\ Forms: \\ P(Dir \mid \pi_{reactive}) \equiv Uniform \\ P(Prox \mid \pi_{reactive}) \equiv Uniform \\ P(Vrot \mid Prox \wedge Dir \wedge \delta_{avoid} \wedge \pi_{reactive}) \\ \equiv G\left(\mu(Prox, Dir), \sigma(Prox, Dir)\right) \end{cases} \\ Identification: \\ Remote\ control\ mode \end{cases} \\ Question: \\ P(Vrot \mid prox^t \wedge dir^t \wedge \delta_{avoid} \wedge \pi_{reactive}) \end{cases}$$

Figure 5-5: Generic Bayesian Program

The complexity of the Generic Bayesian Program (GBP) was reduced into the following procedures used in modelling the motion of the marine vehicle. The marine vehicle was equipped with five ultrasonic sensors for obstacle detection. The ultrasonic sensors returned values from 3cm to 400cm in relation to the distance from obstacles. These values were stored in variables $P_1, \ldots\ldots\ldots P_5$. The marine vehicle was controlled through the rotation of a servo motor attached to the rudder and the forward motion of the craft was controlled through the propeller. Their values were stored in variables M_{servo} and $M_{propeller}$ as shown in Figure 5-6 respectively. From these basic sensory and motor variables, two new variables (Dir,$Prox$) and one new motor variable ($Vrot$) were derived [107]. Dir represented an approximate bearing of the closest obstacle with values ranging from -40 to +40. These values were treated as angles of rotation in degrees. This was defined as:

$$Dir = ocean\ surface\ \left(\frac{(90 \times (P_4 - P_5) + 45(P_3 - P_1) + P_2}{8 \times (1 + P_1 + P_2 + P_3 + P_4 + P_5)}\right) \tag{5.22}$$

Prox represented an approximate proximity of the closest obstacle taking values between 3cm and 400cm and was defined as:

$$Prox = ocean\ surface\ \left(\frac{Max\ (P_1, P_2, P_3, P_4, P_5}{25}\right) \tag{5.23}$$

The variable "ocean surface" in equation (5.22) and equation (5.23) can be represented with a constant. The marine craft was controlled from the rotation of the rudder and the propeller. It received motion control command from $Vprop$ and $Vrot$ variables shown in Figure 5-6 and these took values between + 40 and – 40.

$$V_{prop} = M_{prop} \tag{5.24}$$

$$V_{rot} = M_{servo} \tag{5.25}$$

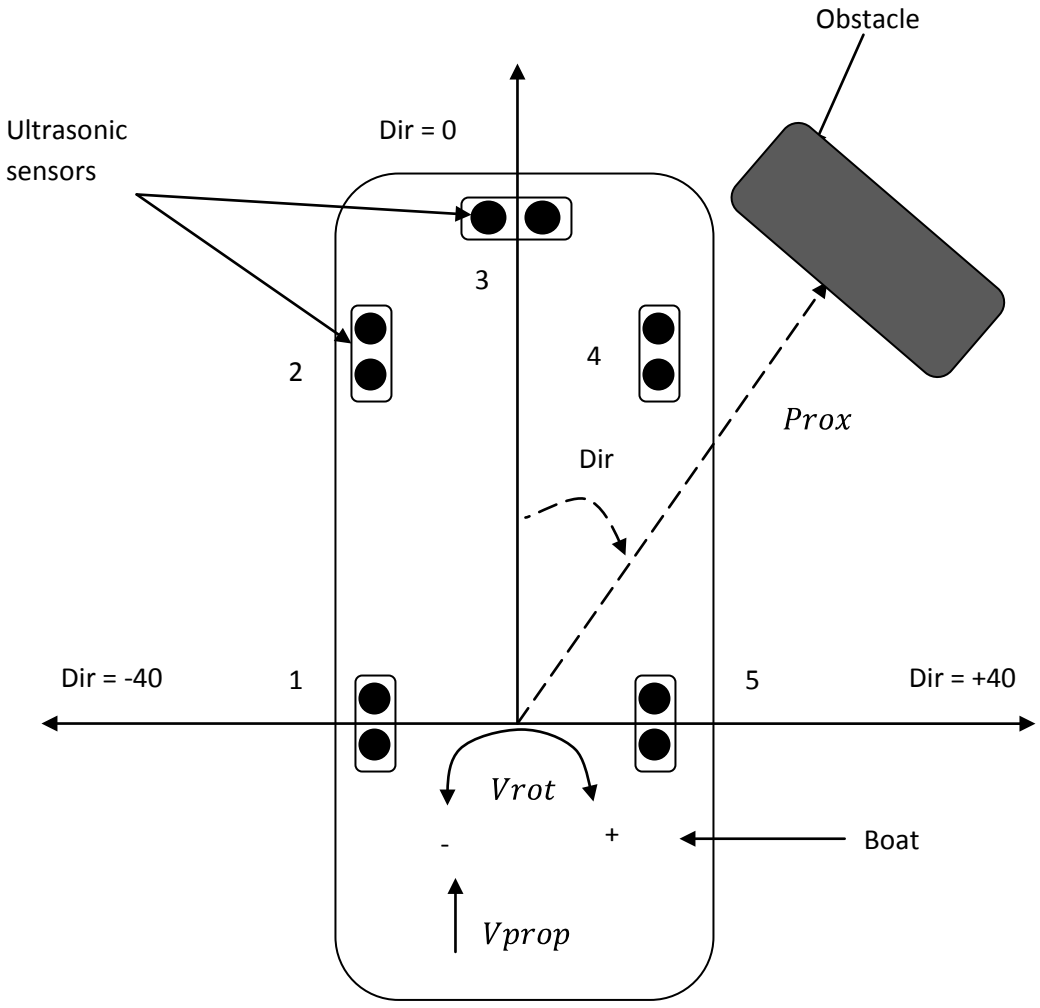

Figure 5-6: Diagram of the Marine Craft Indicating the Position of the Five Ultrasonic Sensors [104]

5.8.1 Reactive Behaviours

The objective of this modelling was to demonstrate some reactive behaviour such as following the planned waypoints and obstacle avoidance. The objective and program protocol was to drive the marine craft with a remote control and check if the navigational algorithm was able to collect navigation data from the GPS and obstacle avoidance data from the sonar.

5.8.2 Bayesian Model Construction

Variables which were relevant to enable the encoding of information were selected and named for identification purposes. The ultrasonic sensors provided data required for proximity determination and these were summarised in the two variables: Dir and Prox. These were assumed to be constant as a result of the maximum distances the sonar can detect an obstacle, as well as the settings on the remote control. This provided the flexibility of controlling the marine vehicle by its rudder $Vrot$. These three variables were the basic requirements for controlling the marine vehicle. Their definitions are summarised as:

$$Dir \in \{-40, \ldots\ldots\ldots, 40\} \langle Dir \rangle = 81 \tag{5.26}$$

$$Prox \in \{3, \ldots\ldots 400\} \langle Prox \rangle = 398 \tag{5.27}$$

$$Vrot \in \{-40, \ldots\ldots\ldots, 40\} \langle Vrot \rangle = 81 \tag{5.28}$$

5.8.3 Bayesian Decomposition

The decomposition of the Bayesian program involved expressing the joint distributions within the program as products of simpler terms. The conjunction rule in equation (5.16) was applied recursively to the joint distribution. This provided the platform used to derive the exact mathematical expression for the program.

$$P(Dir \wedge Prox \wedge Vrot \mid \delta_{avoid} \wedge \pi_{reactive})$$

$$= P(Dir \mid \delta_{avoid} \wedge \pi_{reactive}) \times P(Prox \mid Dir \wedge \delta_{avoid} \wedge \pi_{reactive})$$

$$\times P(Vrot \mid Dir \wedge Prox \wedge \delta_{avoid} \wedge \pi_{reactive}) \tag{5.29}$$

This was then followed by including some conditional independence conditions between the variables. The condition simply meant that direction of an obstacle in relation to the marine vehicle provided no information concerning the distance or how far the obstacle was from the marine vehicle. A further implication was that $Prox$ was independent of Dir.

$$P(Prox \mid Dir \wedge \delta_{avoid} \wedge \pi_{reactive}) = P(Prox \mid \delta_{avoid} \wedge \pi_{reactive}) \tag{5.30}$$

The final decomposition for the program became:

$$P(Dir \wedge Prox \wedge Vrot \mid \delta_{avoid} \wedge \pi_{reactive})$$

$$= P(Dir \mid \delta_{avoid} \wedge \pi_{reactive}) \times P(Prox \mid \delta_{avoid} \wedge \pi_{reactive})$$

$$\times\ P\left(Vrot \mid Prox\ \wedge\ Dir\ \wedge\ \delta_{avoid} \wedge \pi_{reactive}\right) \quad (5.31)$$

5.8.4 Bayesian Parametric Forms

Parametric forms were assigned to each term in the decomposition. This enabled the computation of the joint distribution.

$$P(Dir \mid \delta_{avoid} \wedge \pi_{reactive}) = P\left(Dir \mid \pi_{reactive}\right) \equiv Uniform \quad (5.32)$$

$$P\left(prox \mid \delta_{avoid} \wedge \pi_{reactive}\right) = P(prox \mid \pi_{reactive}) \equiv Uniform \quad (5.33)$$

$$P(Vrot \mid Prox \wedge Dir \wedge \delta_{avoid} \wedge \pi_{reactive}) \equiv G(\mu(Prox, Dir), \sigma(Prox, Dir)) \quad (5.34)$$

Equation (5.32) and equation (5.33) are uniform distributions because there was no prior data about the distance and direction of obstacles along the path of motion of the marine craft and they do not depend on the information δ_{avoid}. Hence all proximities and directions had the same probability. In each sensory analysis, only the propeller speed and rudder rotation was preferred. This made the distributions $P(Vrot \mid Prox \wedge Dir \wedge \delta_{avoid} \wedge \pi_{reactive})$ to be uni-modal. The Gaussian parametric form assigned to $P(Vrot \mid Prox \wedge Dir \wedge \delta_{avoid} \wedge \pi_{reactive})$ enabled $Vrot$ which was a discrete variable to be more or less certain. $P(Vrot \mid Prox \wedge Dir \wedge \delta_{avoid} \wedge \pi_{reactive})$ represented the family of Gaussian distributions, one for each possible position of an obstacle relative to the marine vehicle. The model construction yielded unspecified 81×398 means and 81×398 standard deviations which was dependent on data from δ_{avoid} [104].

5.8.5 Bayesian Model Identification

The objective of the model identification phase was to obtain free parameters. These free parameters were obtained by controlling the marine vehicle in the semi autonomous mode via the remote control module. The values of Dir and $Prox$ were obtained and the value of $Vrot$ was obtained from the position of the joystick on the remote control module. Data collected at time t was represented as $(vrot^t, dir^t, prox^t)$. The series of such representation gave an instance of δ_{avoid} data set. The free parameters were then identified from the computation of the means and standard deviations of $Vrot$ for each possible position of an obstacle.

5.8.6 Bayesian Model Utilization

The reactive behaviour of the marine vehicle controller was called into play when sensor values are read and the values of dir^t and $prox^t$ are computed. The Bayesian program then runs with the following problem to be solved.

$$P(Vrot \mid prox^t \wedge dir^t \wedge \delta_{avoid} \wedge \pi_{reactive}) \quad (5.35)$$

The variable $Vrot$ was given a value $vrot^t$ obtained from the distribution and $vrot^t$ was used as the rudder command [104].

5.9 Summary

This chapter has discussed the probabilistic model of an autonomous marine craft. The reasoning and ideology which were used in the programming of the Arduino microcontroller board were discussed. The uncertainty levels and probabilistic inferences that existed at various levels in autonomous marine craft model analysis were also identified and discussed. A proposed Bayesian model for autonomous marine craft programming was also analysed to showcase how an autonomous marine craft modelling and analysis was done using probability and Bayesian inferences implemented in the software formulation and code development in the Arduino-Mega board.

Chapter 6

Sensor Fusion and Software Design Implementation

6.0 Introduction

The chapter discusses sensor fusion within a multisensory architecture and the implementation of the software architecture in the Arduino microcontroller board. Research and development efforts in guidance of autonomous marine vehicle fits into two main categories: Unmanned Guided Marine Vehicles (UGMV) and Intelligent Marine Transport Systems (IMTS). UGMVs are primarily concerned with underwater and surface water navigation and coastal sea mappings whereas, IMTS research is much broader area of research concerned with safer and more efficient marine transport systems for different marine applications [110]. The vision system for the autonomous navigation of the craft was classified into the following roles:

- Detection and following of predefined path or route
- Detection of obstacles
- Detection and tracking of other marine vehicles as obstacles
- Detection and identification of coastal landmarks using GPS coordinates

Sensor fusion was the method used in integrating signals obtained from multiple sensors on-board the marine craft. The method provided means of extracting information from different sensor sources and integrated the information from the sensors to produce a single result. In several instances the perception of the environment around the marine vehicle was provided by these sensors. The data gathered from these different sensors was processed using data fusion or sensor fusion algorithm. The algorithm can either be sensor fusion based on least-squares methods, sensor fusion based on probabilistic models or sensor fusion based on intelligent reasoning. The least-squares technique made use of Kalman filtering, optimal theory and regularization. The probabilistic models made use of Bayesian reasoning, evidence theory, robust statistics techniques and recursive operators. The intelligent reasoning are neural networks, genetic algorithms and fuzzy logic methods [111]. The process of sensor fusion was implemented in the

software design process. The software design process demonstrated the processes which were implemented in harnessing data from different sensors and how they were used and implemented.

6.1 Visual Sensors

Visual sensors can be active or passive. The difference between the two is that passive sensors rely upon ambient radiation whereas, active sensors illuminates the scene or environment with radiation and determines how these radiations are reflected by the surroundings. Distinguishing further the difference between active sensors and active vision is that, active vision refers to techniques in which passive cameras are moved so that they can focus on particular fixtures. Active sensors have a clear advantage for outdoor application as they are not affected by changes in ambient conditions. The sonar, network camera and the radar form the visual system of the autonomous marine craft [112].

6.2 Active Sensors

Active sensors such as the radar use radio waves, microwaves or electromagnetic waves to identify and detect the direction, speed and range of obstacles. A radio wave scanned within a certain region in the operational environment of the marine vehicle and reflected back to the sensor and off an obstacle; the time of flight of the wave can be measured. The sonar uses ultrasonic pulses to perform the same function.

6.3 Sensor and Data Fusion

The most important task for a Visual Guidance System (VGS) was to provide accurate description of the coastal terrain for the path planner. The quality of the coastal terrain map was assessed by miss rate and false alarm. Miss rate refers to the occurrence frequency of missing a true obstacle and a false alarm refers to a situation when the VGS classifies a transferable region as an obstacle region. The objective of sensor fusion was to combine results and signals from multiple sensors at raw data level or obstacle map level, to produce a more reliable description of the environment than any of the sensors individually [110].

The data fusion process provided the platform of fusing different data from multiple sensors in order to generate useful information that is of tactical value for the intended use and can also be regarded as the combination of information from different sensors and the representation of that information into one data format that is meaningful for the intended purpose. Various types of sensors were used as sources of information for data fusion. Data coming from one or different sensors such as a GPS receiver or radars and sonars, were used for navigation purposes and the development of navigation and guidance algorithms. Data fusion algorithms were intended to have the ability to produce results and handle

conflicting data types. The advancement in sensor technologies provided a vast range of data at different frequencies; some of which were more valuable than others [113-114]. The characteristics of the sensors, the algorithms and processes that were used to select and determine the most valuable data from the sensors, as well as techniques that were used for data fusion in real time, were carried out in such a way that it enabled the system as a whole to provide timely and meaningful information to autonomous system. These sensors provided information about the specific areas of interest in the system and its environments. This was done and achieved with different signal quality and frequency of data transmission and redundant information may be supplied by sensors. The fusion of data from different sensors enabled the overall system to reduce sensor noise. This gave an understanding of the received information and the information which can be observed and cannot be directly sensed. The importance of data fusion was observed in the area in which sensors were complementary to each other. This enabled the system to gather information and perform functions that none of the sensors could perform independently. An evolving technology in data fusion and accurate estimation was in the application of multi-sensory data fusion to autonomous marine vehicles. Data fusion for autonomous marine vehicle included the gathering of environmental information. Accurate estimation of these environmental information and marine vehicle state vector played an important role in enabling the autonomous marine vehicle to perform complex missions. Successful mission planning, guidance and control of autonomous marine vehicle were dependent on accurate estimation of the marine vehicle state and its dynamics. Sensor measurements, vehicle dynamics, vehicle state and the relations that existed between these variables were accurately estimated using Kalman Filter (KF) and Extended Kalman Filter (EKF) while fusing sensor data in an accurate state estimate. The Kalman filter and Extended Kalman Filter were implemented in the Simulink model used during the simulation process in marine systems simulator [112]

.

Multi-sensory data fusion provided the integration and extraction of useful information from data obtained from two or more sensors [115]. Measured data has some form of noise contamination and interference. The necessary definitions and concepts required to formulate a multi-sensory network and data fusion was viewed as a problem of inference transformation of data, to bring about integration and extraction of information data that provided a platform for multi-sensory fusion [115]. For the past few decades, a sizeable interest has been shown in the area of multi-sensory data fusion in non-military applications. Data fusion procedures put together data from multiple sensors and similar information to achieve specific deductions that could not be achieved by using single independent sensor. Recent advancements in artificial intelligence, improvements in computing and sensing have provided the competence to emulate, in hardware and software the natural data fusion abilities of human and animals.

Presently, data fusion systems are extensively used for automated identification of objects, target tracking and restricted automated reasoning applications in the engineering world. Data fusion technology has advanced with such a speed from unrestricting collection of similar techniques to an up-and-coming true engineering discipline with standardized terminology, collection of mathematical methods which are robust and system design principles which are well established. Multi-sensory data fusion applications are widespread in the area of marine robots. Non-military applications include search and rescue marine robots, condition based maintenance of complex machinery, manufacturing process monitoring, environmental observations, different aspects of robotics and medical applications. Military applications comprises of smart weapons or automated target recognition, remote sensing, guidance of autonomous vehicles, battle field surveillance and automated threat recognition to mention a few among the numerous applications that exist. Methods used to merge or fuse data are taken from a wide set of more traditional disciplines. These consist of digital signal processing, control theory and application, statistical estimation, artificial intelligence and classical numerical methods [116].

6.4 The Importance of Multi-Sensory System

Fused data from multiple sensors offer a number of advantages over data from a single sensor. First, if a number of identical sensors are used, say identical radars tracking a moving target, a mix of the observations would cause an improved estimate of the object position and velocity. A statistical advantage was achieved by adding N independent observations which was the estimate of the object location or velocity improved by a factor proportional to $N^{1/2}$ given that the data were fused in an optimal manner. Similarly, the same information could be achieved by joining N observations from an individual sensor. The second advantage came from the use of relative placement or motion of multiple sensors to improve the observation process. Consider two sensors that measure angular directions to a target, by triangulation technique, the position of the object can be determined from the coordination of the two sensors [117]. This technique was widely used in commercial navigation and surveying. In the same way or method, a sensor moving in a known direction relative to another sensor can be used to measure instantaneously a target's position and velocity with respect to the observing sensors. Improved environmental cognisance has been the third advantage that was achieved with the use of multiple sensors. Widening the baseline of physical observables resulted in major improvements [52]. Figure 6-1 showed the multi-sensory communication architecture which has indicated the importance of sensor fusion in autonomous marine craft motion. In the presence of a moving target such as the marine vehicle that as observed by radar and the network camera; the radar unit has the ability to determine the boat's range except that it has limited ability to determine the angular direction of the boat. On the contrary, the forward looking infrared imaging sensor embedded in the network camera can determine the angular

direction of the boat accurately but cannot measure the range. If these two findings are adequately associated, the joining of the two sensors provided a more improved determination of track and location than could not have been achieved by either of the two independent sensors. The consequence of this was a reduced error region as indicated in the fused or combined location estimate. An identical effect may also be achieved in determining the identity of the target on the basis of observations of the target's attributes and properties.

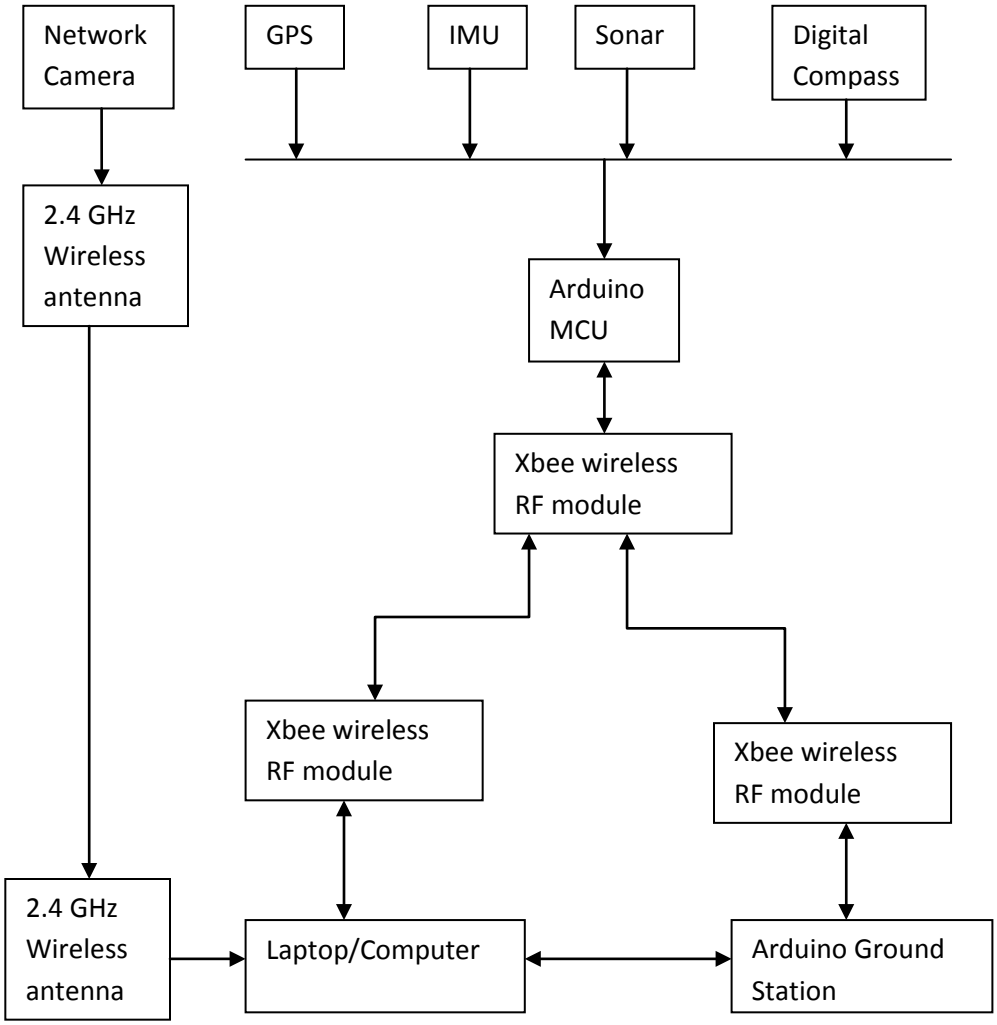

Figure 6-1: Multi-Sensory Fusion Communication Architecture

Explicit external and internal measurements of the physical environments may not be the only resource requirement for marine robots to function. The use of various landmarks such as islands, watch towers, beaches may also be forms of providing information to marine robots in order for them to get a practical

knowledge of where they are. Triangulation approaches can be used in landmark recognition through visual sensors and the associations of these landmarks with an internal map can provide position estimates for the robot. Intelligent and meaningful interactions with other marine vessels were one of the characteristics that marine robots needed to participate in, with the aid of different sensing and perception technologies. The sensing capabilities of marine robots portrayed their ability to perceive things in their environment, without which information collected by the sensors will be a collection of meaningless data. The crucial importance of sensors functioning on autonomous marine robots cannot be over emphasized. These sensors enable marine robots to operate in unknown and dynamic environment where full prior knowledge of the environment might not be accessible to marine robots. With vast amount of information that was provided from various sensors, sensor fusion and data fusion techniques are very important in the exploitation of the various available data that improve the capabilities of marine robots [114].

6.5 Dynamic Environment Modelling Using Ultrasonic Sonar

The dynamic environment in which the marine vehicle operated was modelled briefly in this section using ultrasonic range sensors. The setup for the model is shown in Figure 6-2.The model was implemented for the test marine craft equipped with five SRF05 ultrasonic range sensors. There are two ultrasonic range sensors on each side of the marine vehicle and one ultrasonic range sensor placed at the front of the marine vehicle. Range data from all the five sensors were acquired continuously and plotted on radar-like screen as small circles in global coordinates accompanied by an uncertainty covariance. The raw range data from the sensors formed the starting point for reactive obstacle detection and avoidance for the marine vehicle when considering short ranges. The position and orientation of the sensors with respect to the origin of the boat are defined as follows [118]:

r: The distance from the marine vehicle origin to the ultrasonic sensor,

γ: The angle from the marine vehicle axis to the ultrasonic sensor,

β: The orientation of the ultrasonic sensor with respect to the marine vehicle.

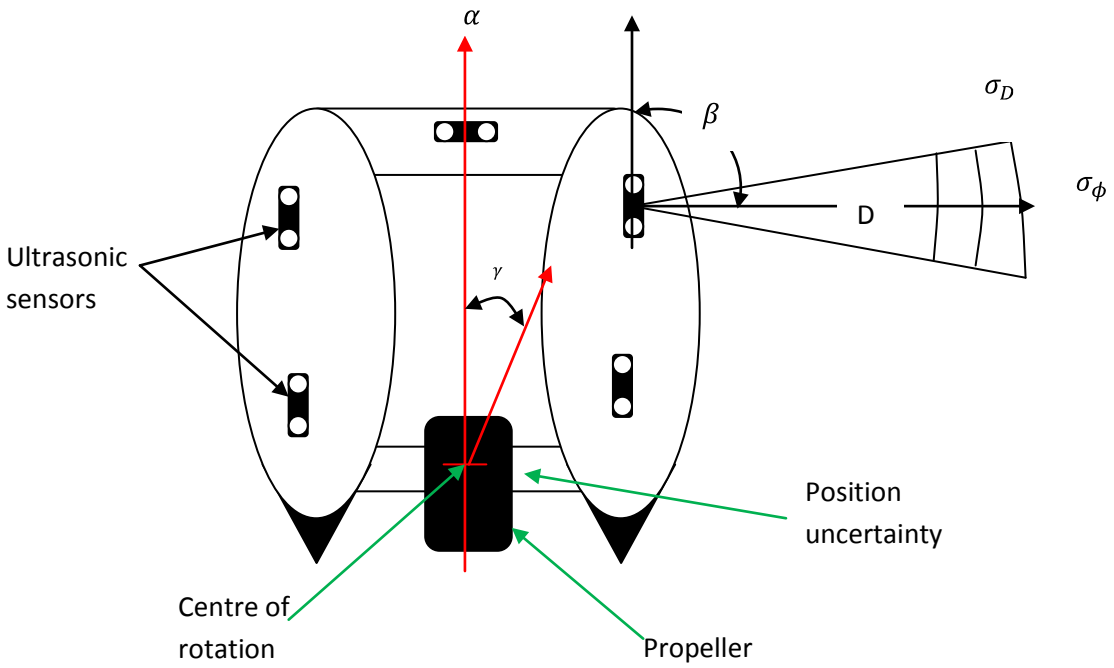

Figure 6-2: The Projection of Ultrasonic Range Data to External Frame of Reference [119].

Ultrasonic sensor data description process acquired data from range measurements and also from estimated position data from the marine vehicle control algorithm. With this data, the distance *D*, for each of the ultrasonic sensors were projected to the external frame of reference, (x_s, y_s) using the position of the marine craft, (x, y, α) as shown in Figure 6-2.

$$x_s = x + r\cos(\gamma + \alpha) + Dcos(\beta + \alpha) \tag{6.1}$$

$$y_s = y + r\sin(\gamma + \alpha) + Dsin(\beta + \alpha) \tag{6.2}$$

The angles α, β, γ were not precise, hence an absolute angle ϕ for the sensors are defined as:

$$\phi = \alpha + \beta + \gamma \tag{6.3}$$

To combine the data coming in from the different sides of the craft, the precision of the incoming data was estimated. This was achieved by using a model that predicted echoes coming from an ultrasonic range sensor in an arc shaped region defined by an uncertainty orientation, σ_ϕ and an uncertainty distance, σ_D [120] .The uncertainty region may be approximated using a covariance that approximated σ_ϕ and σ_D in Cartesian coordinates and was represented by:

$$X = \begin{bmatrix} x \\ y \end{bmatrix} = \begin{bmatrix} D\cos(\alpha+\beta) \\ D\sin(\alpha+\beta) \end{bmatrix} \tag{6.4}$$

The transformation of the covariance from circular to Cartesian coordinates was given by:

$$\left| {}^{X}_{D\phi}J \right| \triangleq \frac{\partial \begin{bmatrix} x \\ y \end{bmatrix}}{\partial(D,\phi)} = \begin{bmatrix} cos\phi & -Dsin\phi \\ sin\phi & Dcos\phi \end{bmatrix} \tag{6.5}$$

The transformation of the uncertainty region having an elliptical profile to Cartesian coordinates was given by:

$$C_s = \begin{bmatrix} \sigma_x^2 & \sigma_{xy} \\ \sigma_{xy} & \sigma_y^2 \end{bmatrix} = {}^{X}_{D\alpha}J^T \begin{bmatrix} \sigma_D & 0 \\ 0 & \sigma_\phi \end{bmatrix} {}^{X}_{D\alpha}J \tag{6.6}$$

The most important requirement criterion for sensor uncertainty in local modelling was that the uncertainty be larger than any true errors that may be associated with the data. Hence each measurement from the ultrasonic sensor horizon was represented by x_s, y_s, C_s expressed in an external frame of reference. The modelling process constructed a description of the raw data coming in from the sensors, as shown in Figure 6-3. The function of the description was to filter the sensor noise by detecting range measurements that were mutually consistent. The description also formed a representation for which the estimated position and orientation of the marine vehicle may be constrained to. It also provided "obstacle constancy" at the level that fits the geometric description of the environment. The obstacle constancy enabled the marine vehicle to react to events without requesting a symbolic interpretation of the model [119].

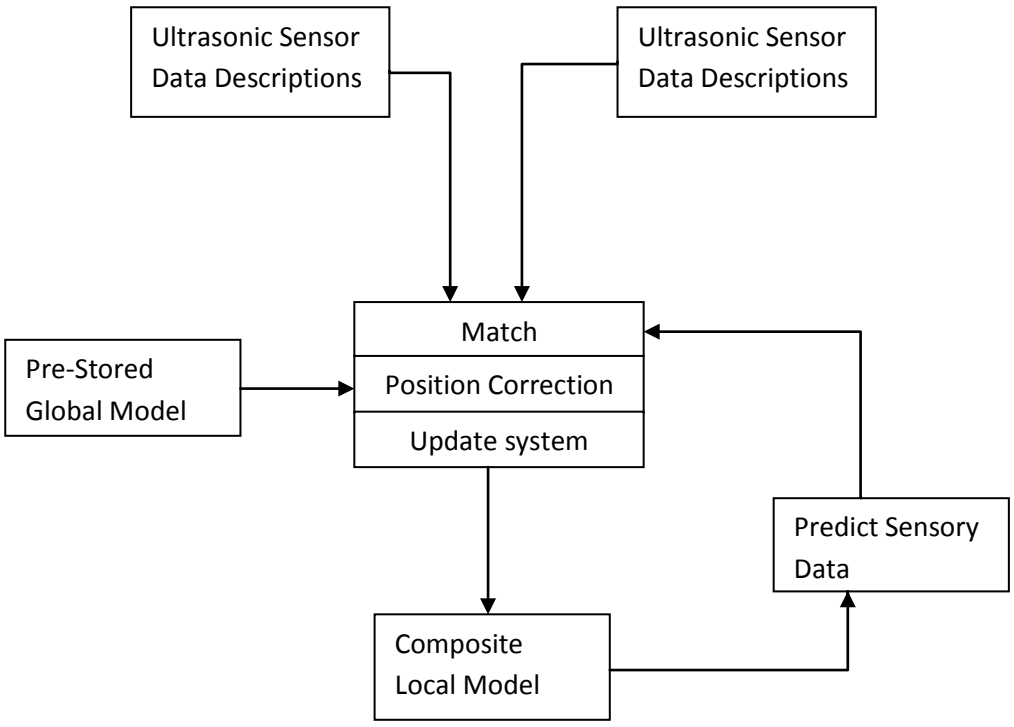

Figure 6-3: Dynamic World Modelling by Fusing Ultrasonic Sensor Data and Prior Information

6.6 Sensor Fusion Using Kalman Filter

The fusion of sensory data in the autonomous marine craft formed a crucial part of the development of the USV. This was because data fused from the IMU; GPS and INS system formed the essential navigational system for the marine vehicle. Kalman Filter was integrated in the navigation system so as to improve the overall performance of the navigational algorithm as well as to improve the attitude estimation of the marine craft. The Kalman Filter used a recursive algorithm to improve the trajectory estimates. The Kalman Filter algorithm used four computational steps to improve the performance of the navigational algorithm. The steps were gain computation, trajectory estimate update, covariance update and the prediction step [52, 121]. The integrated system is shown in Figure 6-4. The GPS provided Course-On-Ground (COG) information and this was joined with data from the INS as indicated in Figure 6-4.

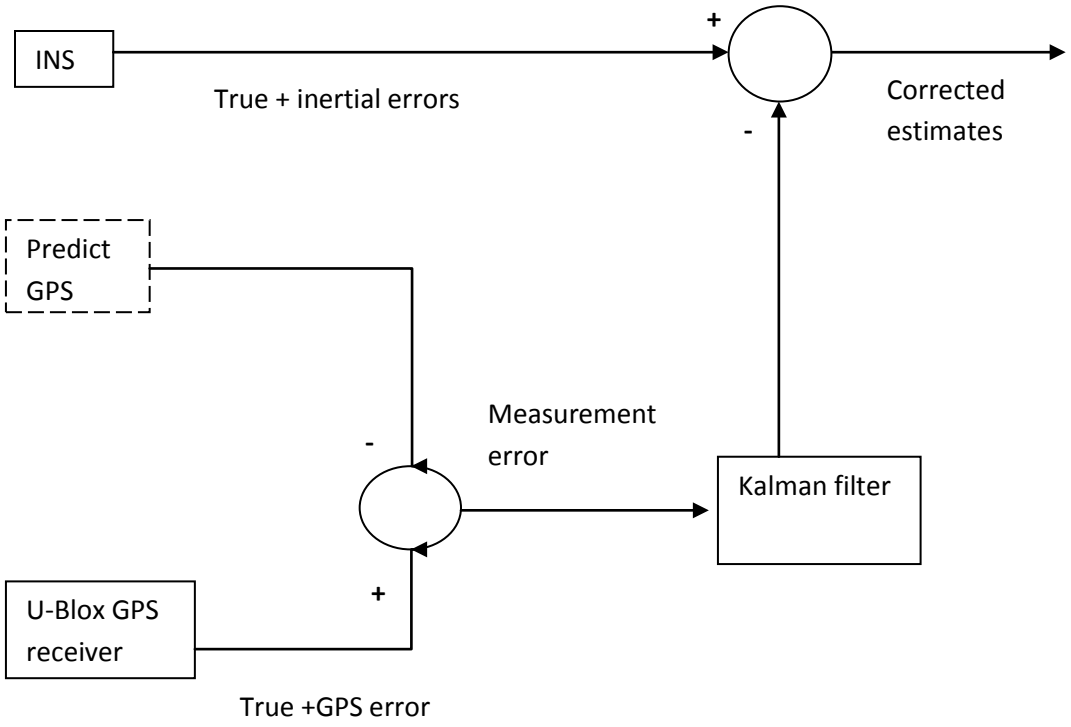

Figure 6-4: Fusion of Data From INS and a GPS Receiver [122].

Since an autonomous system such the USV system was made of various nonlinear systems such as the navigation algorithm of the USV, an improvement of the trajectory estimates in nonlinear environments became paramount. This system shown in Figure 6-4 was changed slightly by the inclusion of Extended Kalman Filter (EKF) instead of using the normal Kalman Filter. The EKF allowed the integration of sensory data to be adaptive within nonlinear environments. Since the algorithm used a recursive linear filter, at each cycle the trajectory estimate was updated by joining new data with predicted data from previous measurements. The improved system is shown in Figure 6-5.

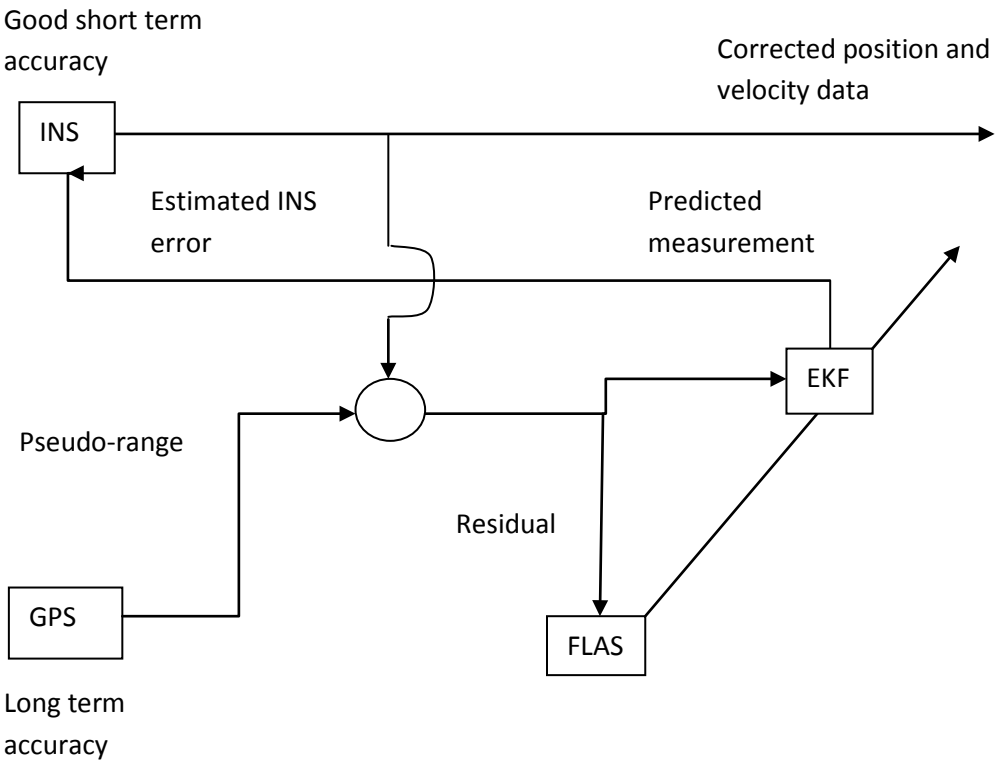

Figure 6-5: Adaptive Extended Kalman Filter Integrated with GPS and INS [122].

6.7 Software Design

This section discusses the software implementation and development of the autonomous marine craft. The section shows the procedures that were followed in the software design and then discusses the software implementation for this particular application as well as software monitoring system and the implementation of the control board as shown in Figure 6-6. The section will start with a discussion on the firmware used for IO board. The IO board provided the required low level-interfaces for the sensors and actuators. The sections that follow thereafter discuss the Arduino and Processing programming environment implementation.

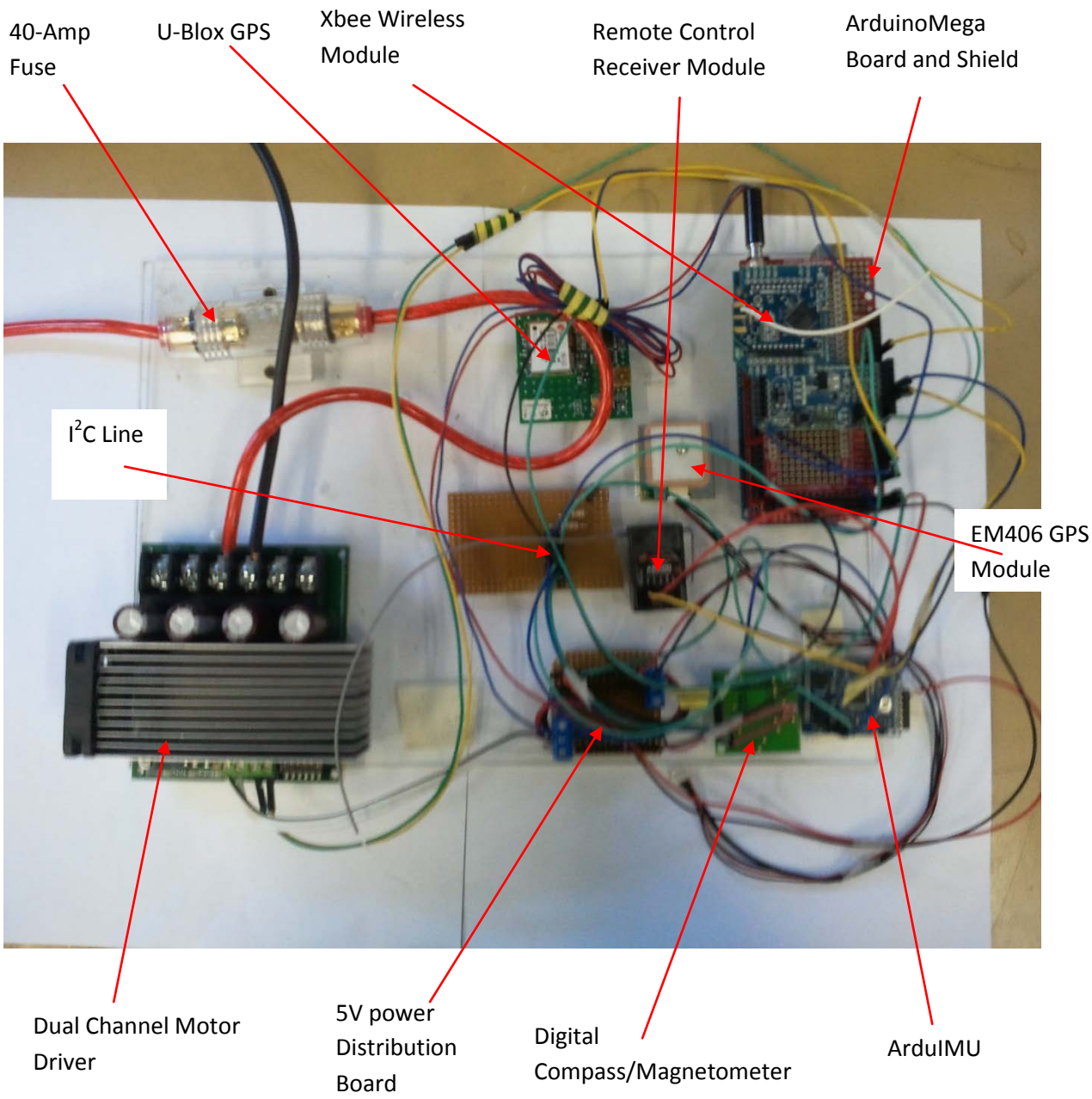

Figure 6-6: Seacat Autopilot Control Board

6.8 The IO Board Firmware

The IO boards were used to provide the necessary low-level interfaces to the ultrasonic sensors, GPS, IMU and actuators. The Arduino-Mega IO board was used to provide interface for the GPS, remote control module, ultrasonic sensors and the digital compass. The ArduIMU IO board was used to provide interface for the accelerometers, gyro and GPS module. Figure C-2 in appendix C shows the schematic for the Arduino-Mega board and the pin configuration shown in appendix C3. The IO board software was based on the Ardunio/Wiring language. This language provided for interrupt applications, digital input and output application as well as analog input and output applications. The different sensor modules used in this project communicates to the IO board using different communication protocols. The GPS send information to IO board using a serial communication protocol, the digital compass uses an I^2C or Two Wire Interface (TWI) protocol, and the ultrasonic sensors send information in a digital format to the board while the accelerometers and gyros communicate with the board using analog protocols. The main commands implemented in the IO board software the sequence of operations shown in Figures 6-7 and 6-8. At the start of the program, the software initializes the IO pins which have been designated as inputs and outputs for data flow. The setup section of the program also initializes the serial ports on the Arduino-Mega Board for serial communication at specified baud rates within the software. The software control loop shown in Figure 6-7 generally searches for data inputs and compares them to the conditional statements and control algorithms in the software code. When conditions specified in the algorithms are satisfied an output command is initiated and data is sent to the output pins. The interrupt subroutines shown in Figure 6-8 were put in place to enable data acquisition using the ADC function in the Arduino-Mega board. Data obtained from the sensors are converted to the required format using the ADC function in the Arduino-Mega board. After the execution of the subroutines, data obtained from the routines are used in the main control loop to control the marine vehicle. The software architecture shown in Figure 6-7 and the interrupt routines shown in Figure 6-8 can be summarized as follows:

- The software programme starts and IO pins are initialized.
- The serial ports are initialized with the required baud rate and ADC subroutines are also initialised.
- The main loop calls for UART subroutines to receive GPS data and ADC subroutines to receive IMU data.
- The main loop calls for digital data from the sonar.
- Conditional statements are evaluated and control commands executed.
- The loop repeats again.

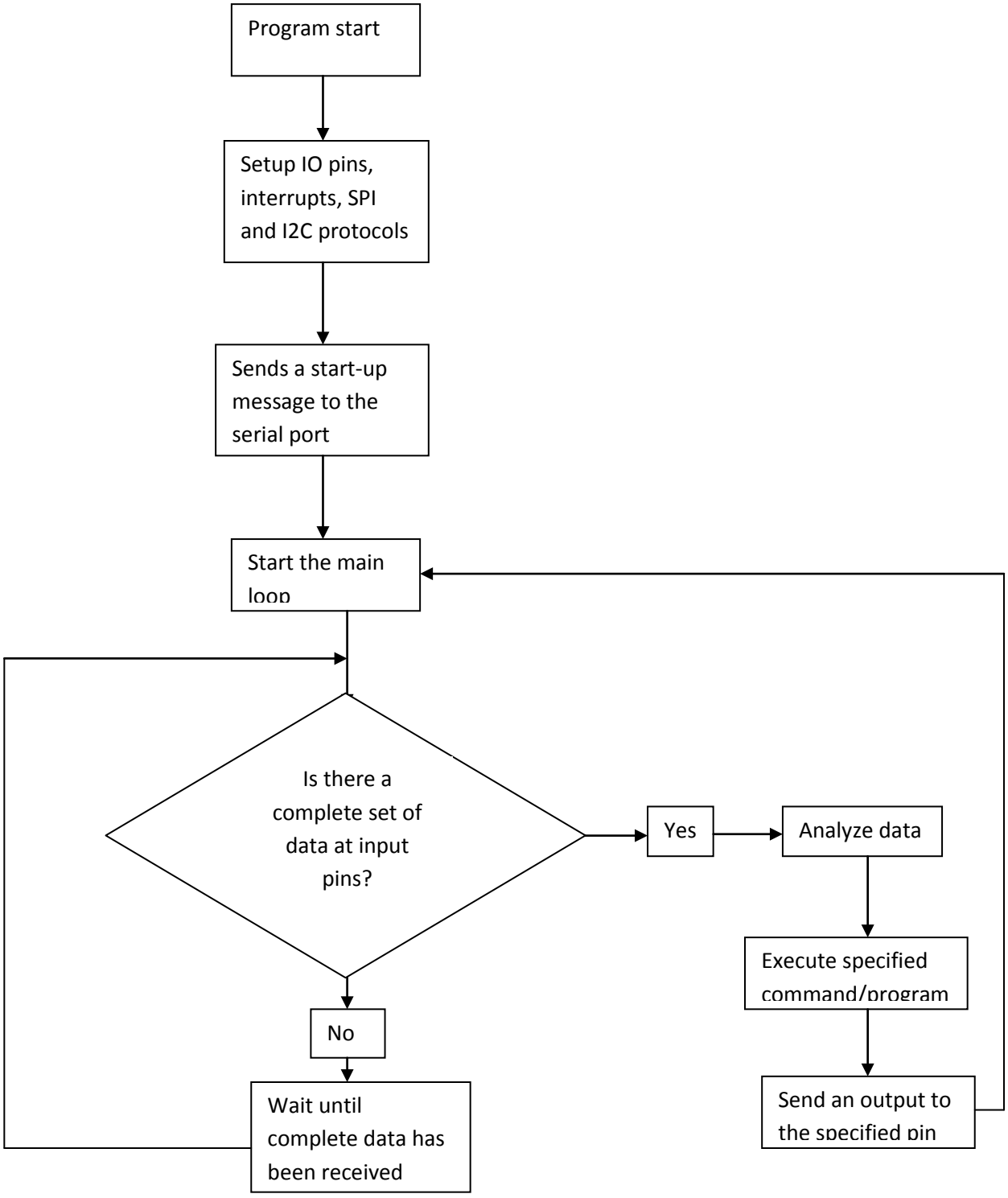

Figure 6-7: IO Software Architecture

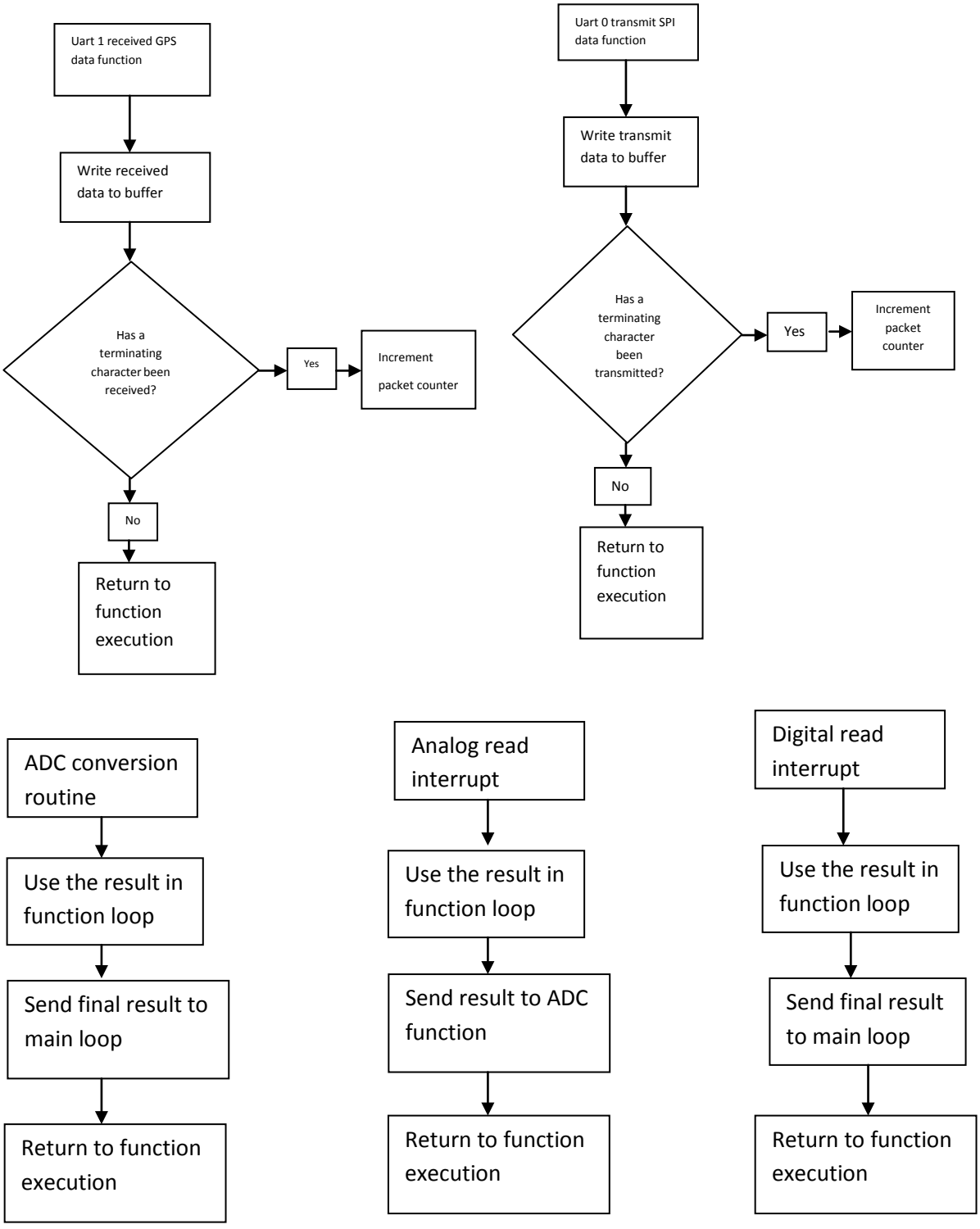

Figure 6-8: IO Software Implementation Indicating Interrupt Routines

6.9 Ground Station and Control Software

The ground station monitoring software was used to configure and select the marine vehicle navigation path. The Navigation configuration software that was implemented was an open source Ardupilot configuration toolbox. The tool box allowed for path planning and selection, waypoint selection and input of selected waypoints into the microcontroller. A display of selected waypoints is shown in Figure 6-9.

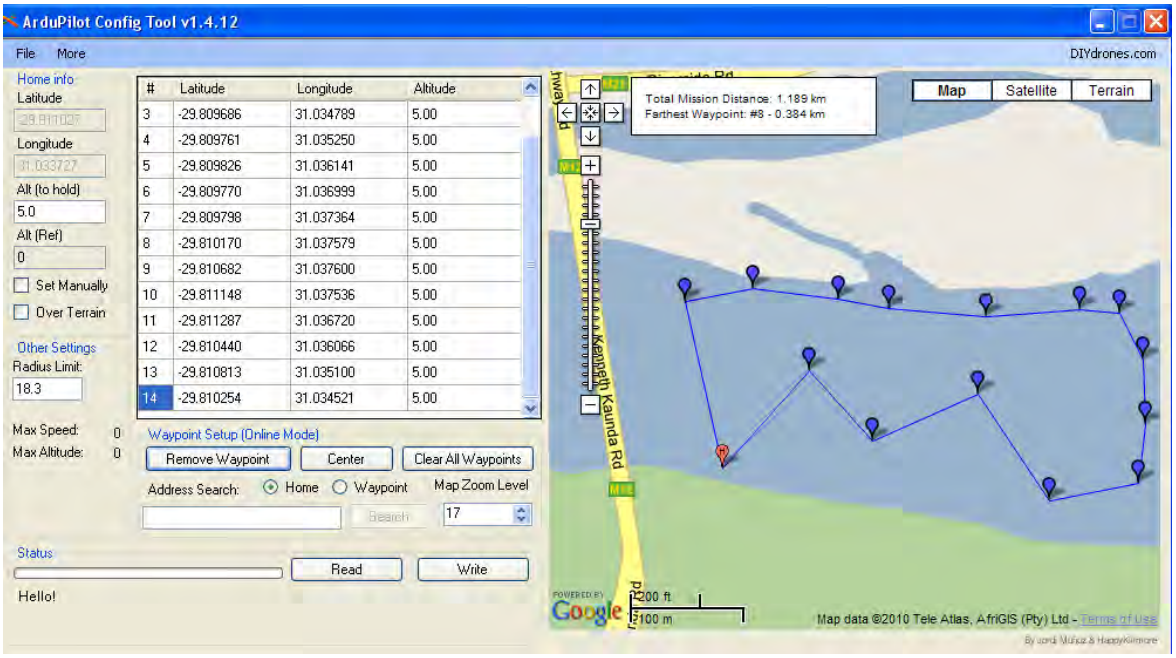

Figure 6-9: ArduPilot Configuration Tool [123]

The monitoring of obstacles along the path of motion of the marine craft was done using modified radar screen software. This is shown in Figure 6-10. The radar screen software scans the environment around the marine vehicle, takes obstacle distance values as input from the ultrasonic sensors placed around the marine vehicle and displays the actual distances in real time. With this radar screen an operator of the marine vehicle was able to monitor the performance of the obstacle detection and avoidance algorithm.

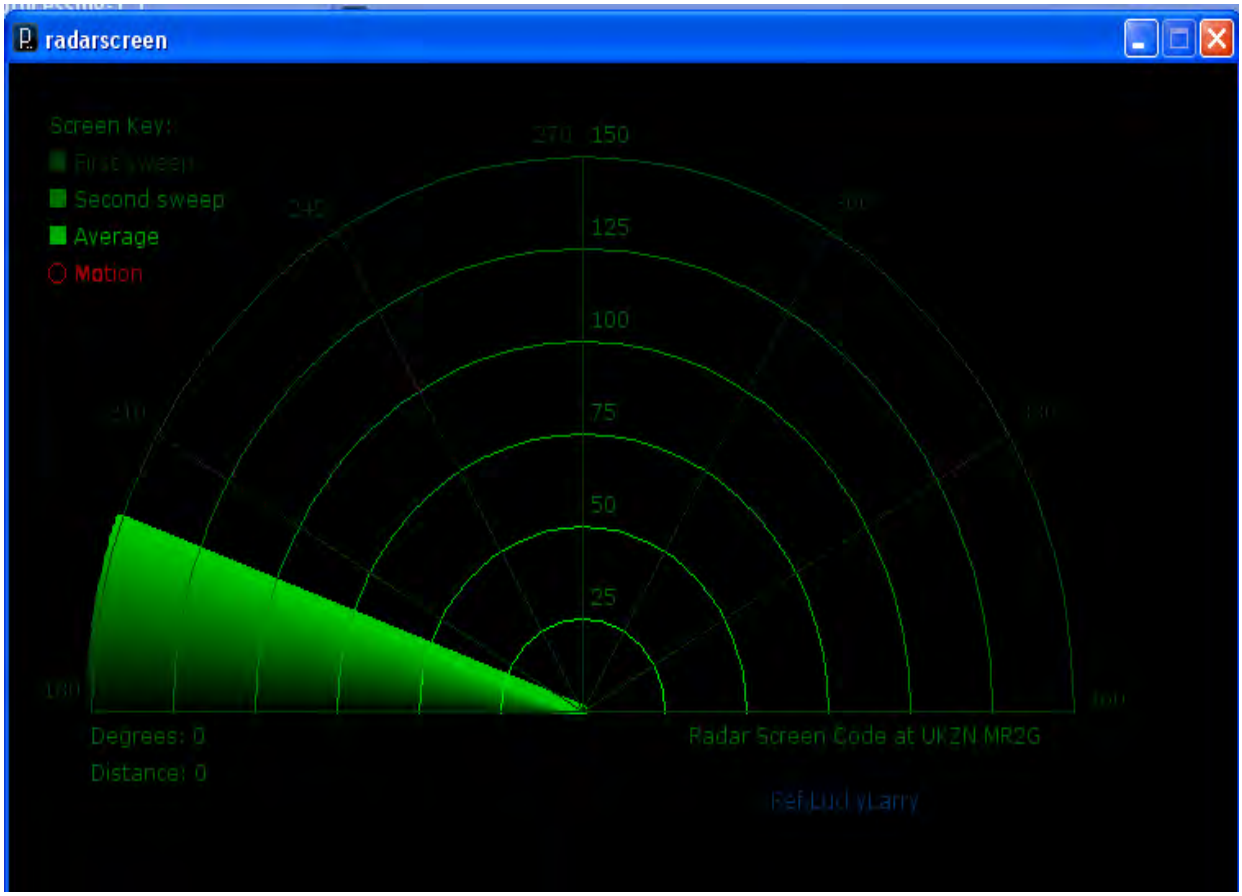

Figure 6-10: Obstacle Detection Radar Screen [124]

The attitude of the marine craft was monitored using a modified graph plotting software developed using Processing programming environment. The software displays the roll, pitch and yaw values of the marine vehicle in real time and also has modified options which can be toggled to display corrected roll, pitch and yaw. This software can also be used to display values from the accelerometer. The marine vehicle attitude monitoring software is shown in Figure 6-11. The upper section of the screen shown in Figure 6-11 displays data from the gyro. The lower section of the screen displays data from the accelerometer. The half-full circle indicates the rotation from the marine vehicle as movements in a horizon.

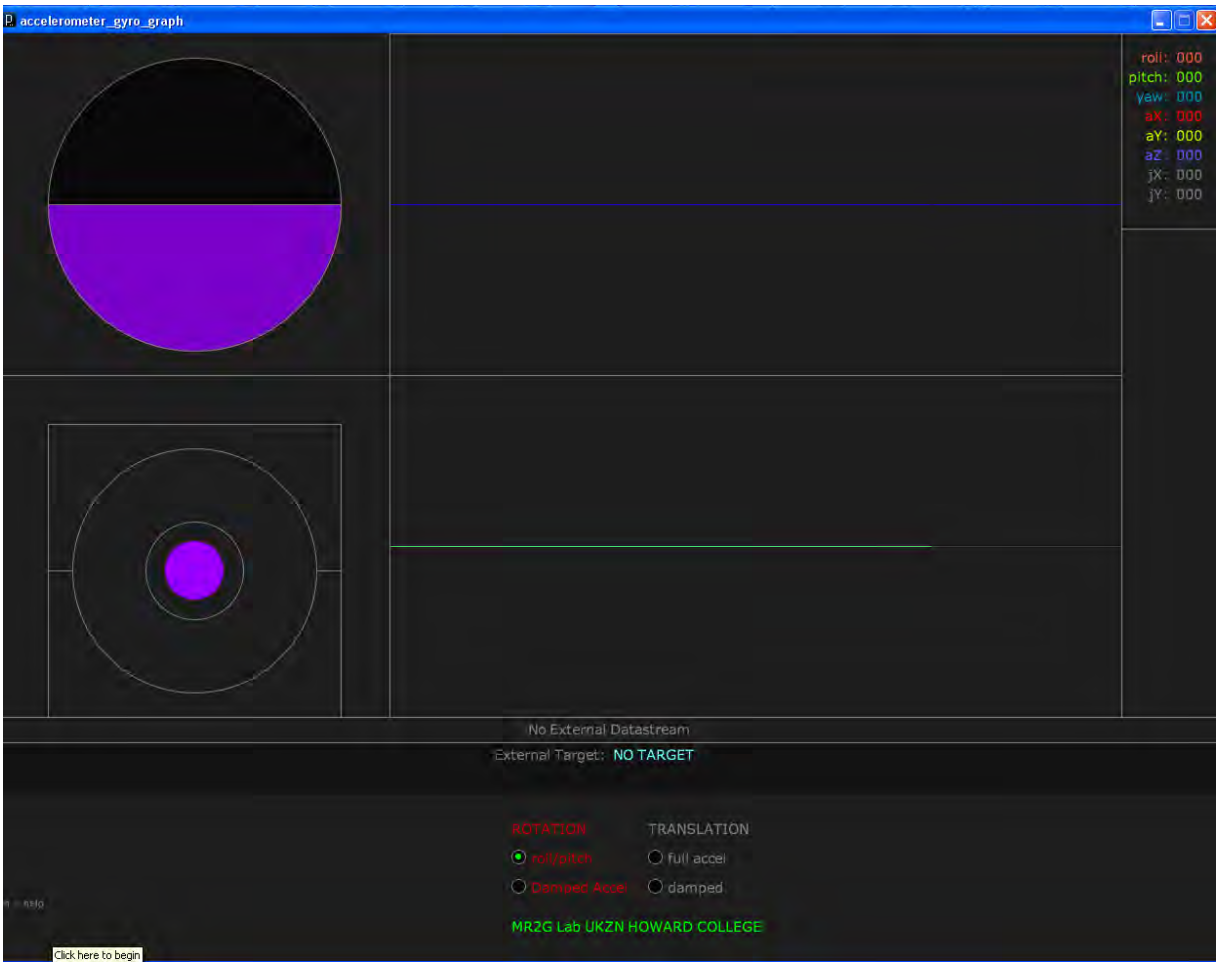

Figure 6-11: Marine Vehicle Attitude Monitoring Screen [125]

6.10 Summary

This chapter discussed the sensor and data fusion modelling implemented in the autonomous marine craft and also discussed the use of a multi-sensory system in improving the autonomous navigation functionality of the marine vehicle. The data gathered from the sensors were used according to their hierarchy of relevance in the guidance and navigation algorithm of the marine craft. The chapter also demonstrated the fusion of data from INS, GPS using Kalman Filter and EKF algorithm. The identification of the relevant sensors, the fusion method was discussed and the chapter ended with the modelling of the sensors in a dynamic environment. This chapter also discussed the integration and implementation of software architecture of the autonomous marine craft. These included the navigation configuration tool box, attitude monitoring software and obstacle detection monitoring radar screen. These programs enabled the controller at the ground station to have full knowledge of the marine craft autonomous navigation.

Chapter 7

Results and Discussion

7.0 Introduction

This chapter discussed the various software integrations, simulation and implementation of the different marine vehicle modelling discussed in previous chapters. The autonomous marine craft model discussed in chapter 2 was investigated, analyzed and implemented in MATLAB [126] using Marine Systems Simulator (MSS). The simulator allowed for adaptation and modification of the various inputs to the marine craft system model. This allowed for qualitative analysis of the various results derived from the simulations. The chapter also discussed the validation of software integration, electronic integration, in a functional mechanical infrastructure, such as the autonomous marine vehicle. The programmings of the Arduino microcontroller boards were done using the Wiring programming language within the Arduino programming environment. The real time data outputs were captured and visualized with an adapted Processing GUI programmed using the Processing programming language within the Processing programming environment. The testing of the craft took place at the controlled section of a river as shown in Figure 7-1. The focus in the discussion and analysis of autopilot system was in the sway motion and yaw analysis as this was important for the autonomous control, guidance and navigation of the marine craft. All the programs that were used for analysis, simulation and visualization of results were adapted from open source programs under the general public license.

Figure 7-1: Seacat during Testing Exercise

7.1 Discussion and Validation

This subsection looked at the analytical functions of the marine craft and the research questions implied and posed at the introduction of this dissertation. This section also demonstrated and indicated the type of solutions that were provided in relation to the results and simulations that were achieved during the course of the research.

7.2 System Kinematics and Dynamics Results

In chapter two, the system dynamic model of the autonomous marine craft was discussed. The validation of the presented model was done using the rotation matrix represented in equations (2.5) through to (2.10). Equation (2.4) through to equation (2.11) were implemented in the MSS to achieve the results shown in Figure 7-2 and Figure 7-3.In the Figure 7-2 (a) showed the derivation of quaternion from ordinary differential equations. Figure 7-2 (b) showed the derivation of quaternion from Euler angles. In Figure 7-3 (a), it showed the derivation of Euler angles from quaternion and Figure 7-3 (b) showed the derivation of Euler angles from ordinary differential equation. The initial parameters for the Euler angles were set at 5 degrees for roll and pitch motion and 10 degrees for yaw motion. These parameters were varied in the MSS to investigate the kinematic behaviour of the marine craft model. The implication of these results was that the use of Euler angles or quaternion to represent and model marine vehicle kinematics was efficient in the kinematic model representation and each one of these models as discussed in chapter 2 can be effectively used in analyzing and representing marine vehicle kinematics.

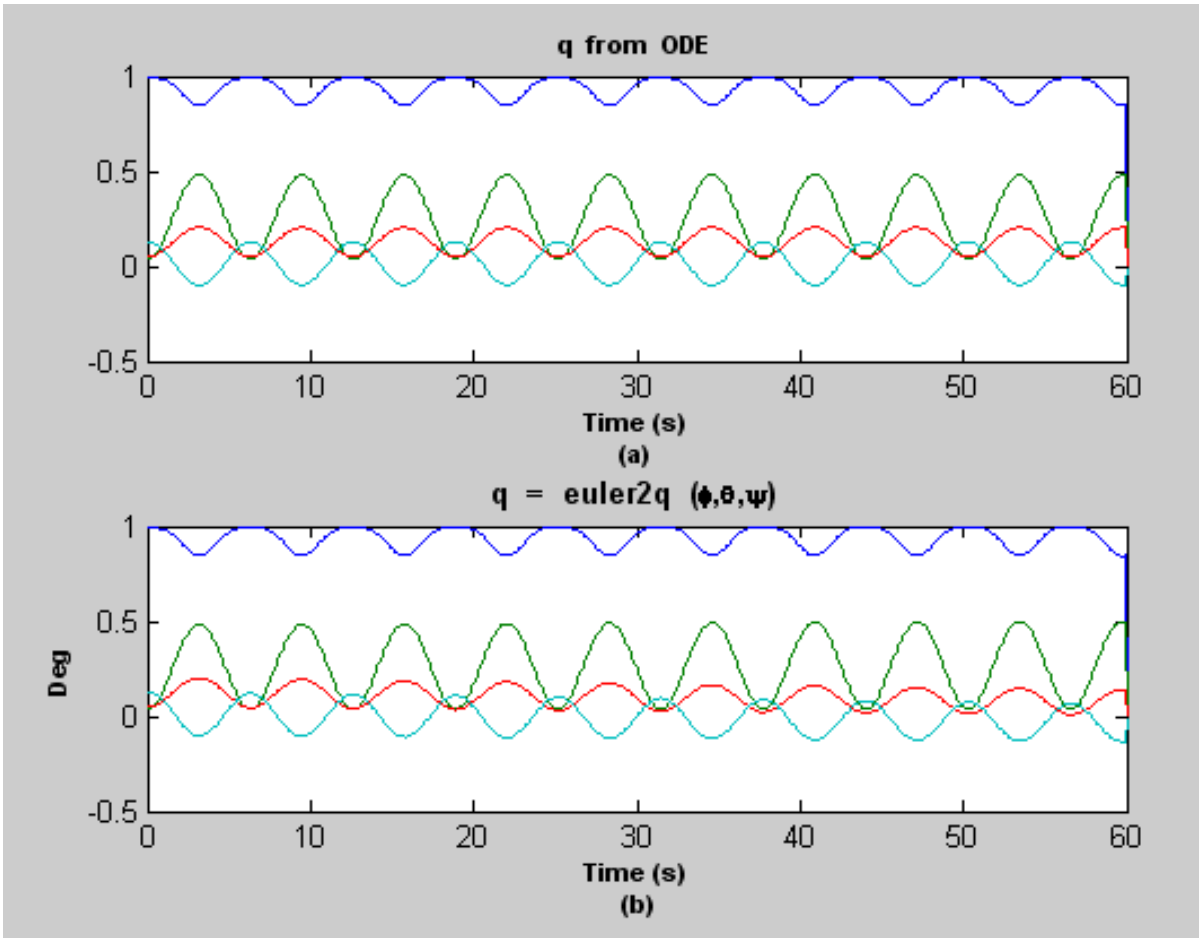

(a) Quaternion Derivation from Ordinary Differential Equation (b) Quaternion Derivation from Euler

Figure 7-2: Quaternion Model Investigation and Analysis Results

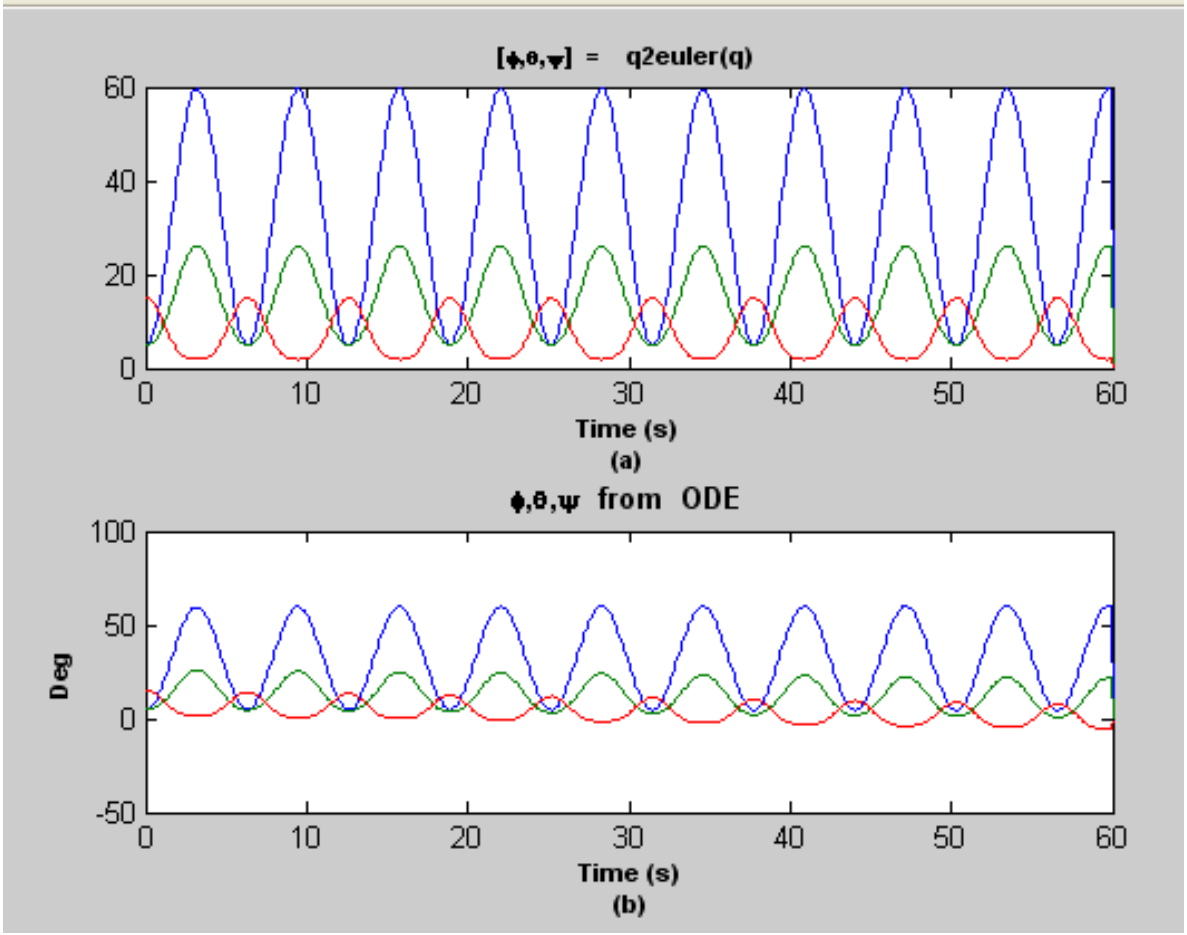

(a) Euler Derivation from Quaternion (b) Euler Derivation from Ordinary Differential Equation

Figure 7-3: Euler Model Investigation and Analysis Results

In Figure 7-4, the turning circle performance evaluation simulation and trial was used to test the rudder characteristic of the marine craft in both autonomous and semi-autonomous mode. The investigation was implemented in the MSS using equation (2.86) and equation (2.87). The red star in the figure indicated the start of the turning exercise and the red small circle in the figure indicated the start of the 90 degrees turn. The evaluation investigated the ability of the autonomous marine vehicle in making a full 90 degree turn. The performance trial was done at an initial constant speed of 3m/s. It followed that below this initial speed, the marine vehicle was not able to complete the turning circle performance test. Also above this speed, the marine craft completed the turning circle test; however it continued spinning for some time. After 10 seconds the rudder of the marine craft was executed at an angle of 15 degrees to achieve the turning circle performance test.

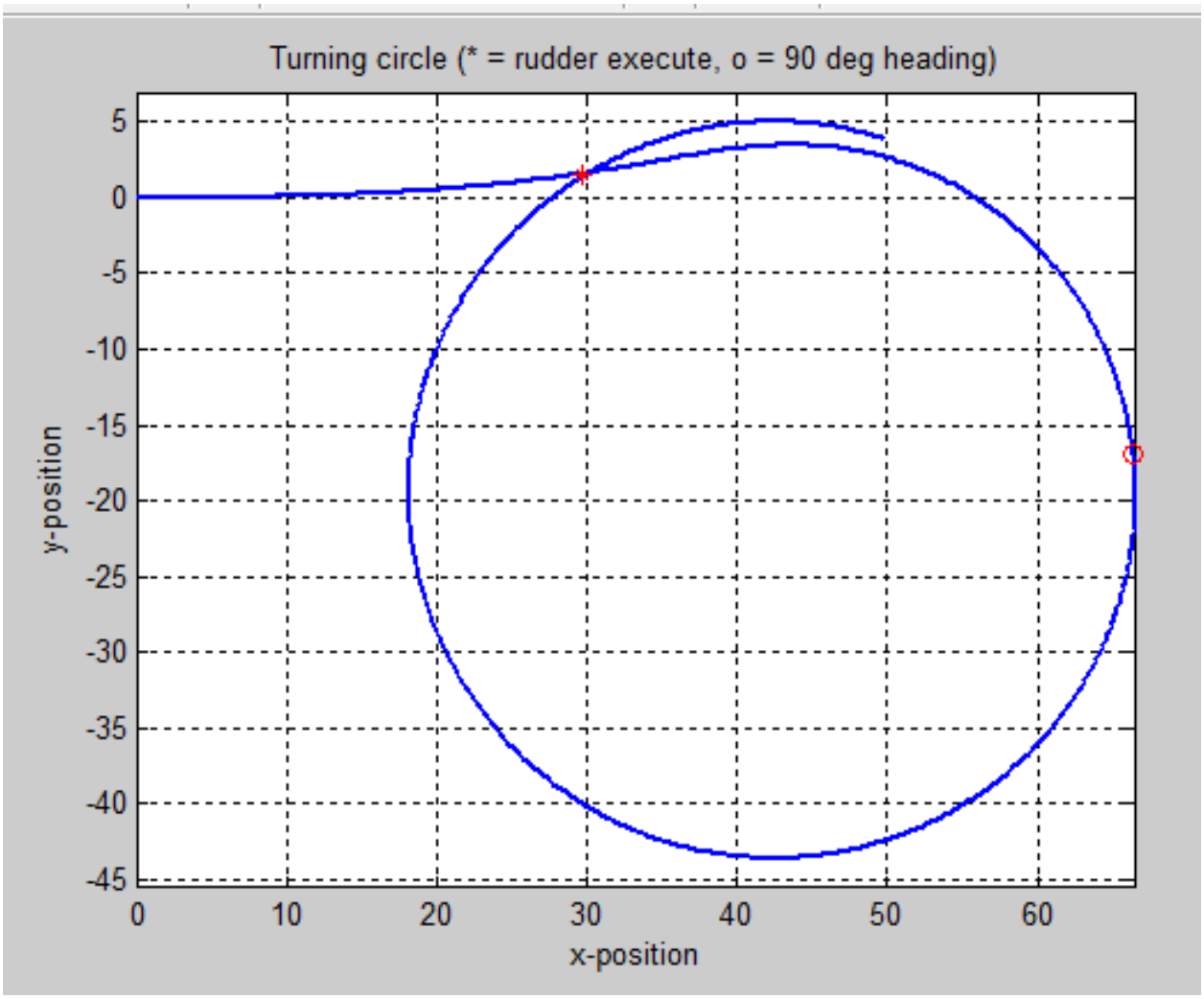

Figure 7-4: The Turning Circle Test

In Figure 7-5, the marine vehicle started the turning circle test at a speed of 2.5m/s and cruises off at a speed of 2.1 m/s after the test. The yaw rate for the test levels was positive at the beginning of the turning and remained fairly constantly negative during the test. The turning circle test was performed in semi-autonomous mode and autonomous mode of operation of the marine craft. The waypoint were selected and encoded into the autopilot software controlling the marine craft.

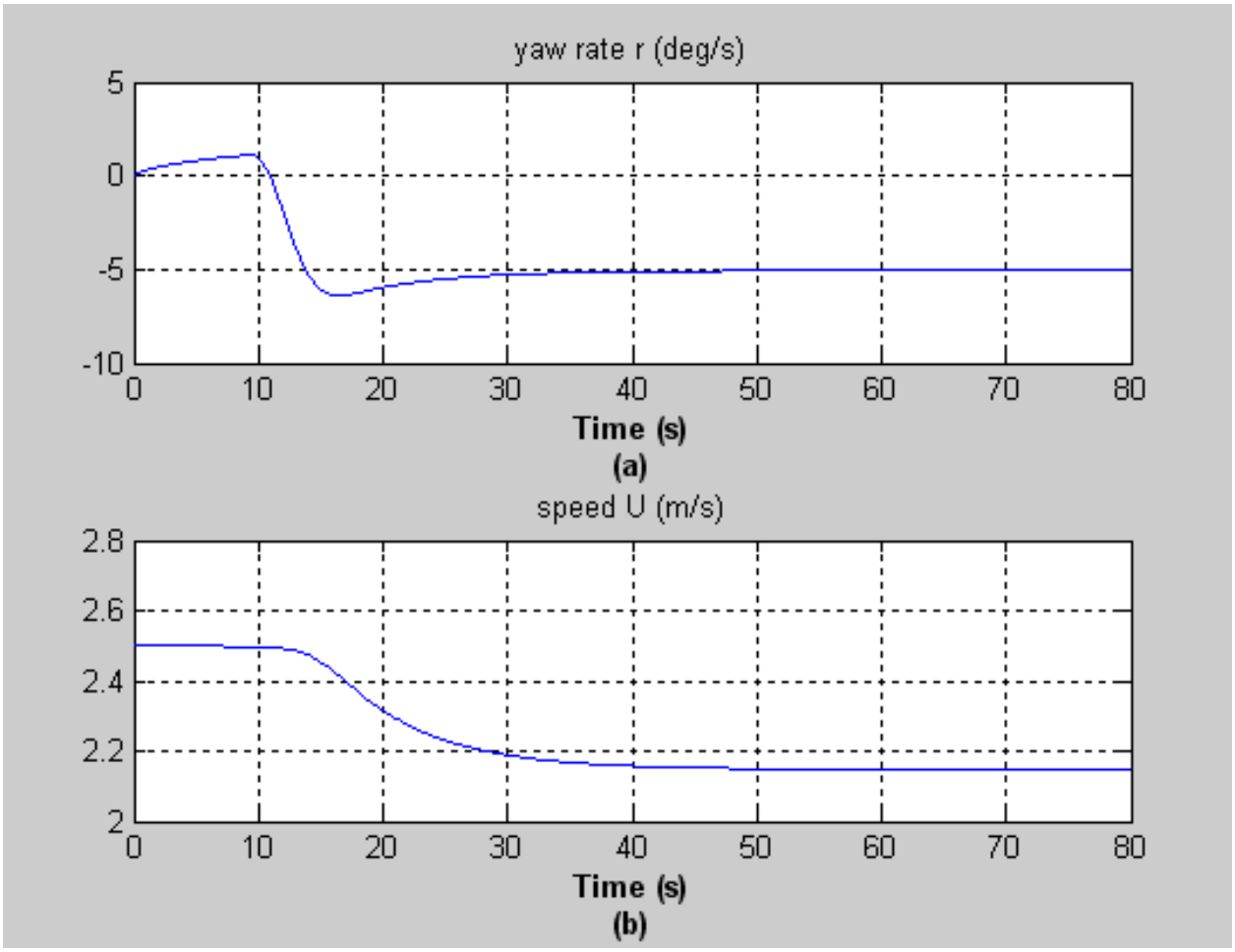

Figure 7-5: The Yaw and Speed Response during Turning Circle Test

In Figure 7-6, the pull-out manoeuvre was executed at 10 degrees. This was done to check the straight line stability of the craft. After 300 seconds the marine craft regained its straight line motion with the yaw rate levelling off at 2deg/s. The pull-out manoeuvre was performed in the remote control mode of operation of the marine craft. The speed of the craft was selected by adjusting the joystick on the remote control module.

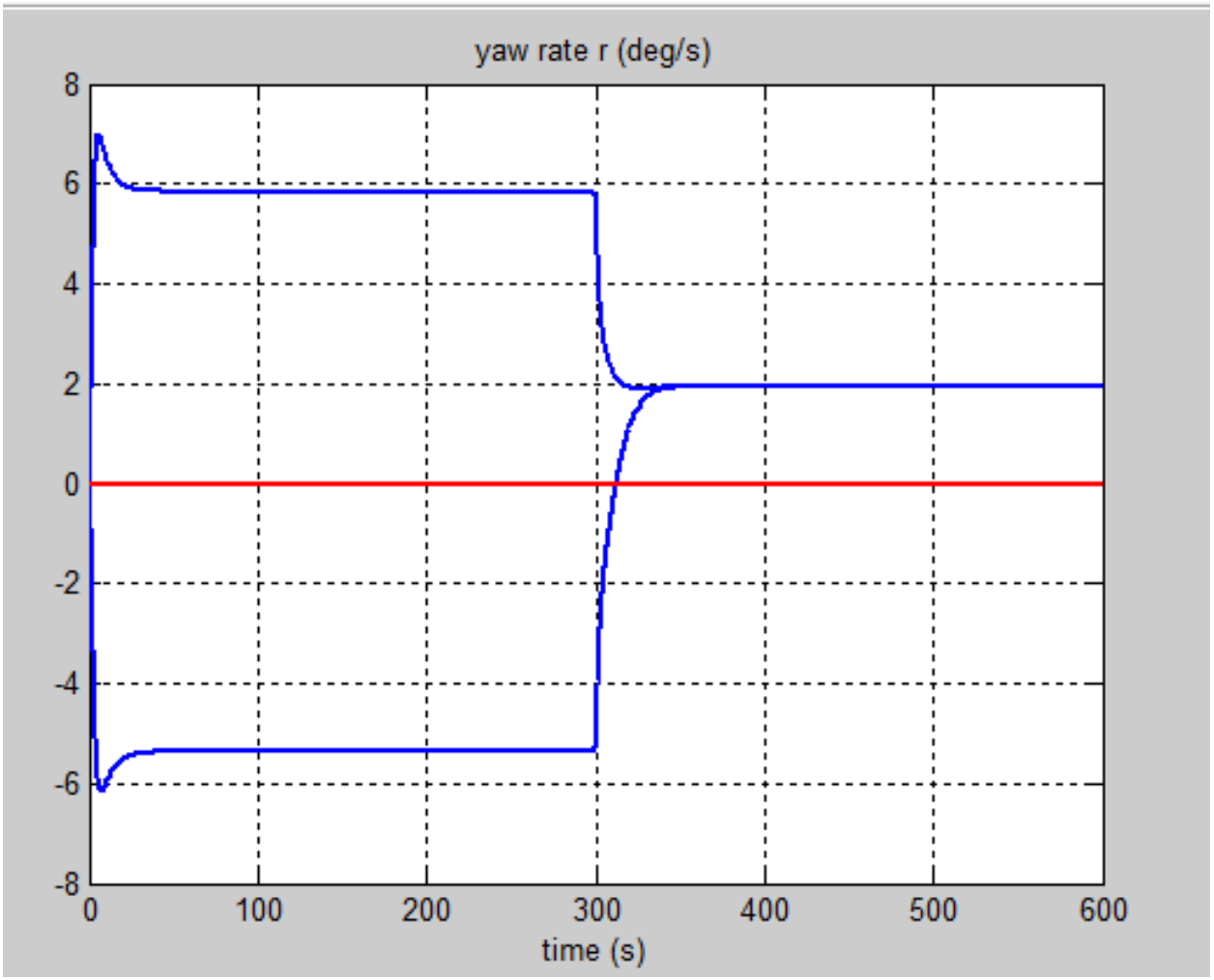

Figure 7-6: The Pull-Out Manoeuvre Test [3]

In Figure 7-7, the computation of the navigation path of the autonomous marine vehicle was investigated using cubic splines algorithm in the MSS and in Figure 7-8 the navigation path was computed using a 5^{th} order polynomial algorithm in the MSS. Both algorithms used navigation waypoints as inputs in their computations. The algorithms were developed using equation (2.83) equation (2.84) and equation (2.85). In Figure 7-9, the actual navigation path displayed was a function of the waypoints encoded in the autopilot programme using the Arduino programming language.

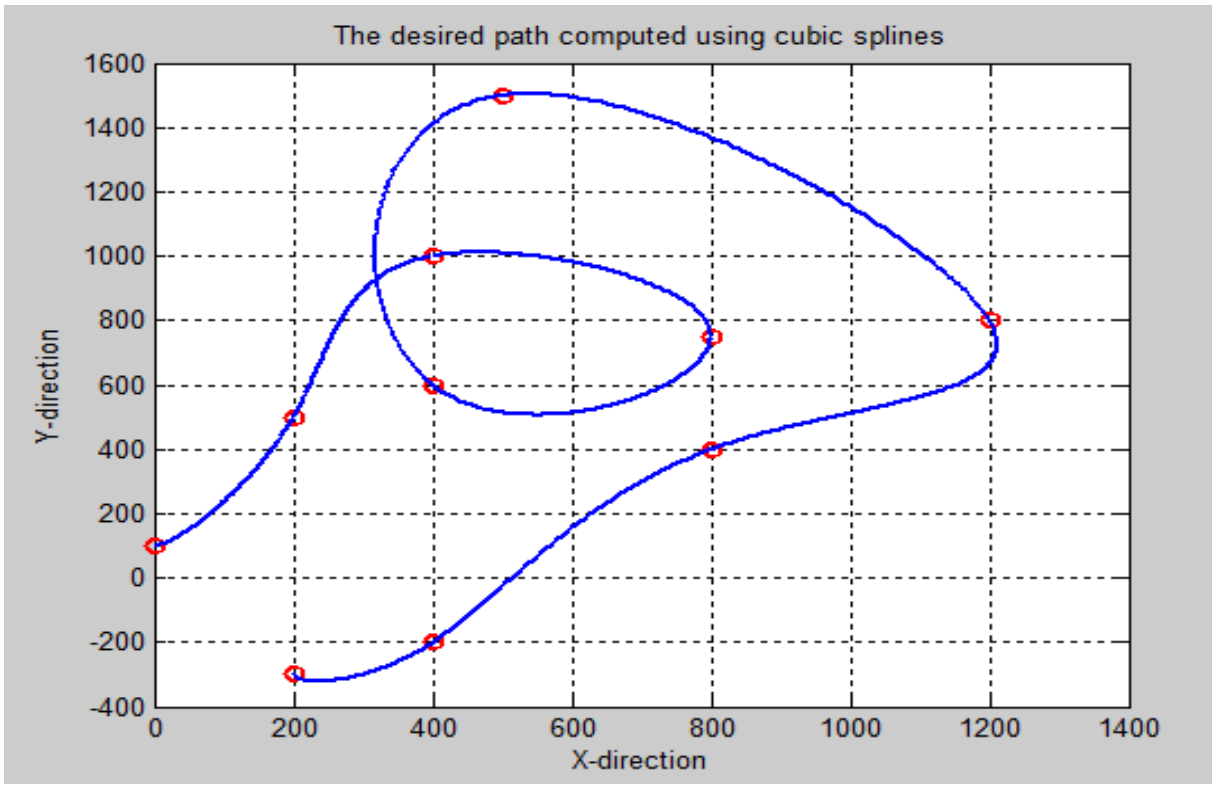

Figure 7-7: Waypoint Navigation Computation using Cubic Splines Algorithm

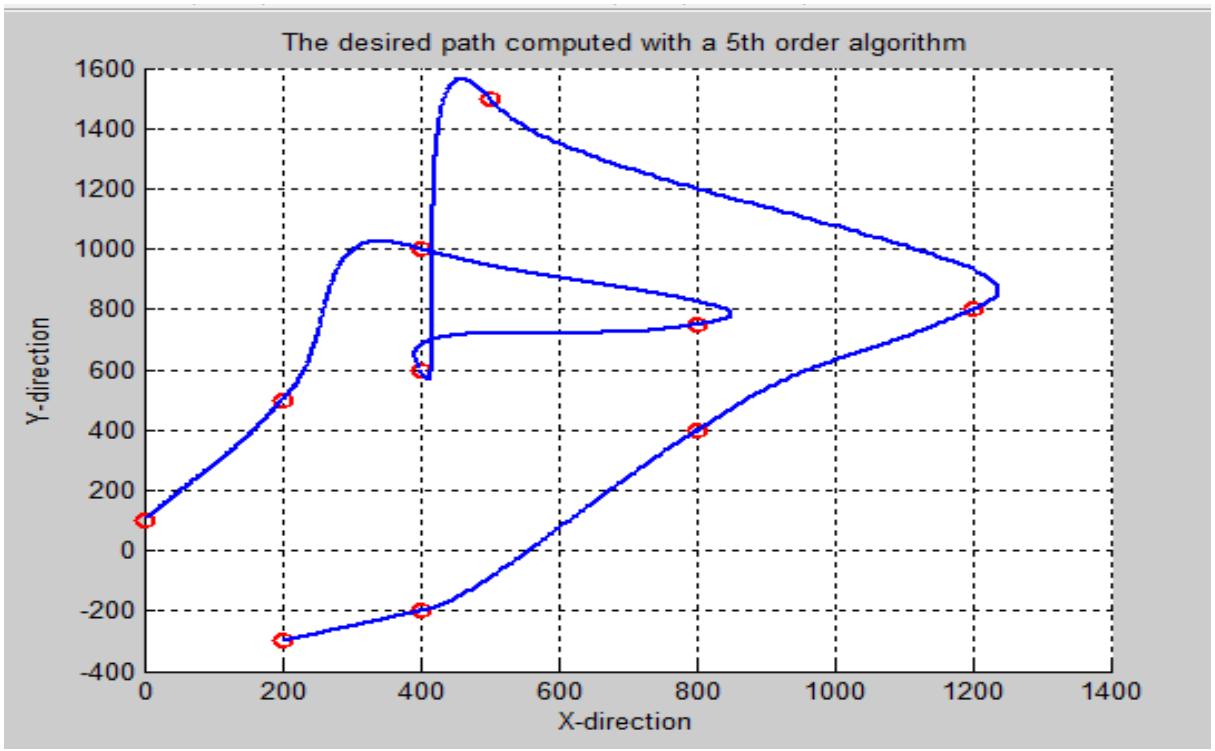

Figure 7-8: Waypoint Navigation Computation using 5th Order Polynomial Algorithm

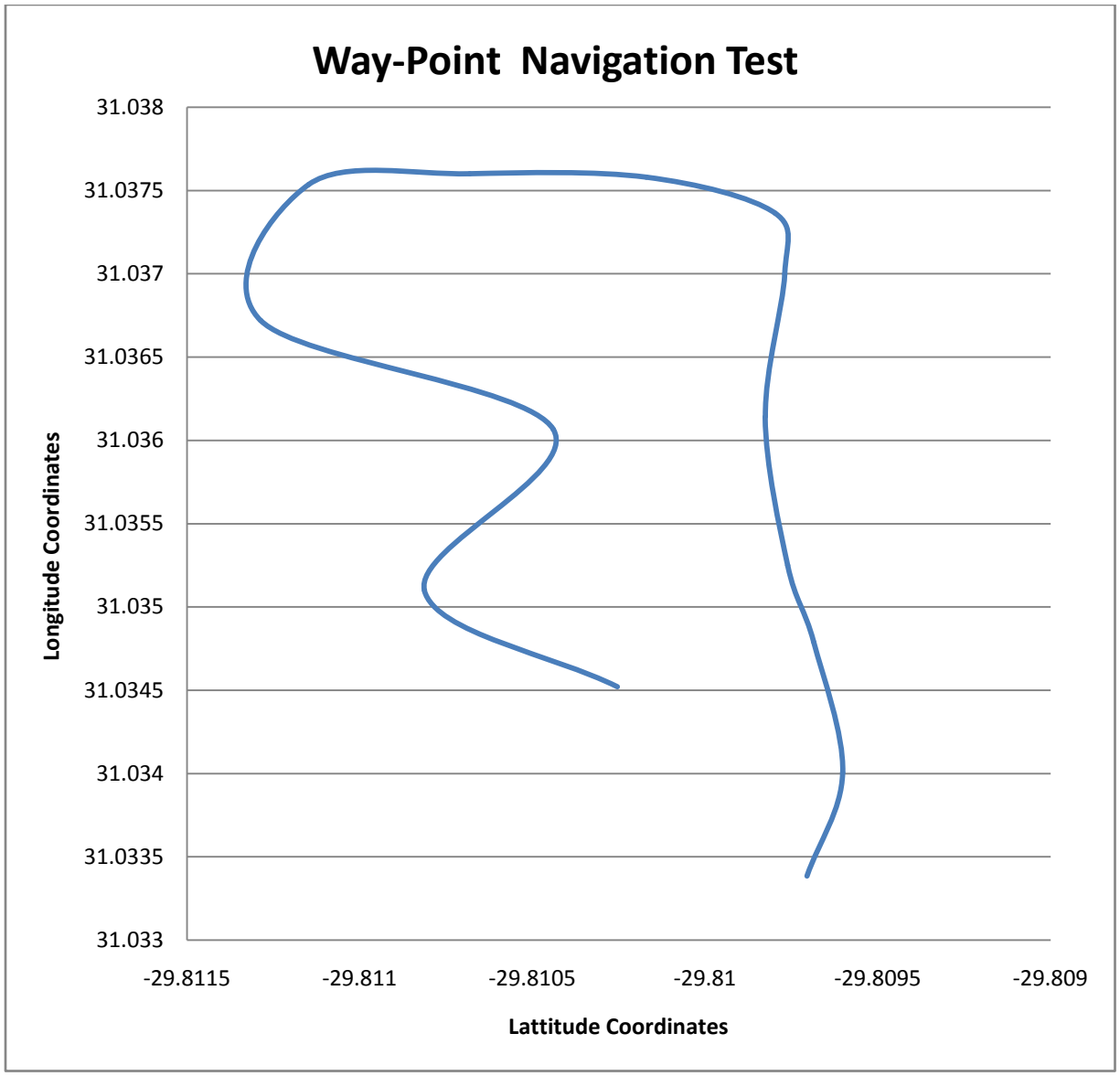

Figure 7-9: Actual Waypoint Navigation

7.3 Attitude and Heading Reference System Results

The onboard IMU system was used to monitor the marine craft attitude. The results shown in this section were from the IMU and were viewed and monitored in real time using an adapted GUI developed in Processing programming environment. The IMU data were streamed from the Ardu-IMU through to the serial ports and from the serial ports the data was sent to the IMU monitoring screen shown in Figure 7-1.1. The results derived from the IMU were used to stabilize the marine craft and the control algorithm was implemented effectively by adjusting the marine vehicle rudder for stability and control. Figure 7-10 indicated no marine craft motion or the marine craft can be said to be steady while Figure 7-11 showed the marine craft attitude in 6-DOF while in motion.

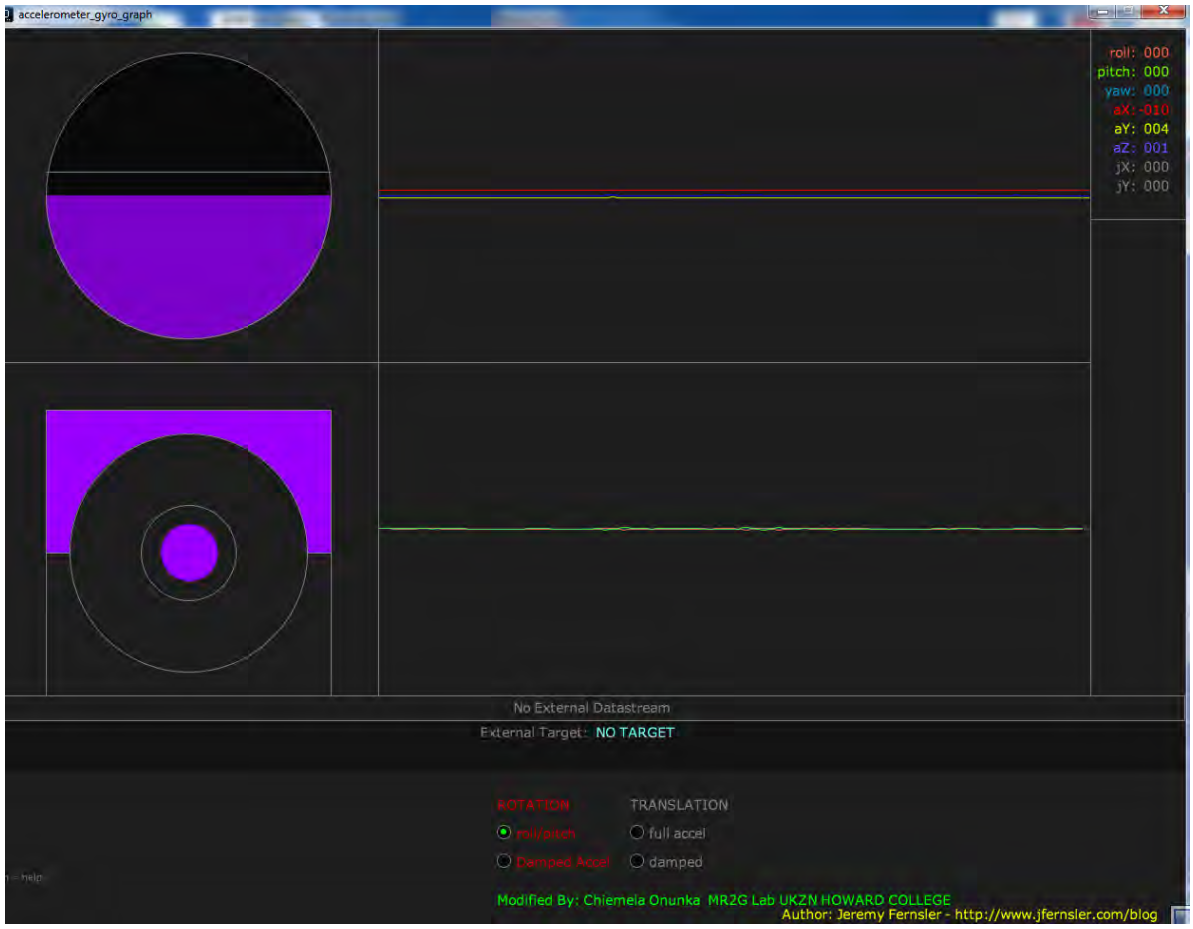

Figure 7-10: IMU Monitoring Screen Indicating Zero Marine Craft Attitude

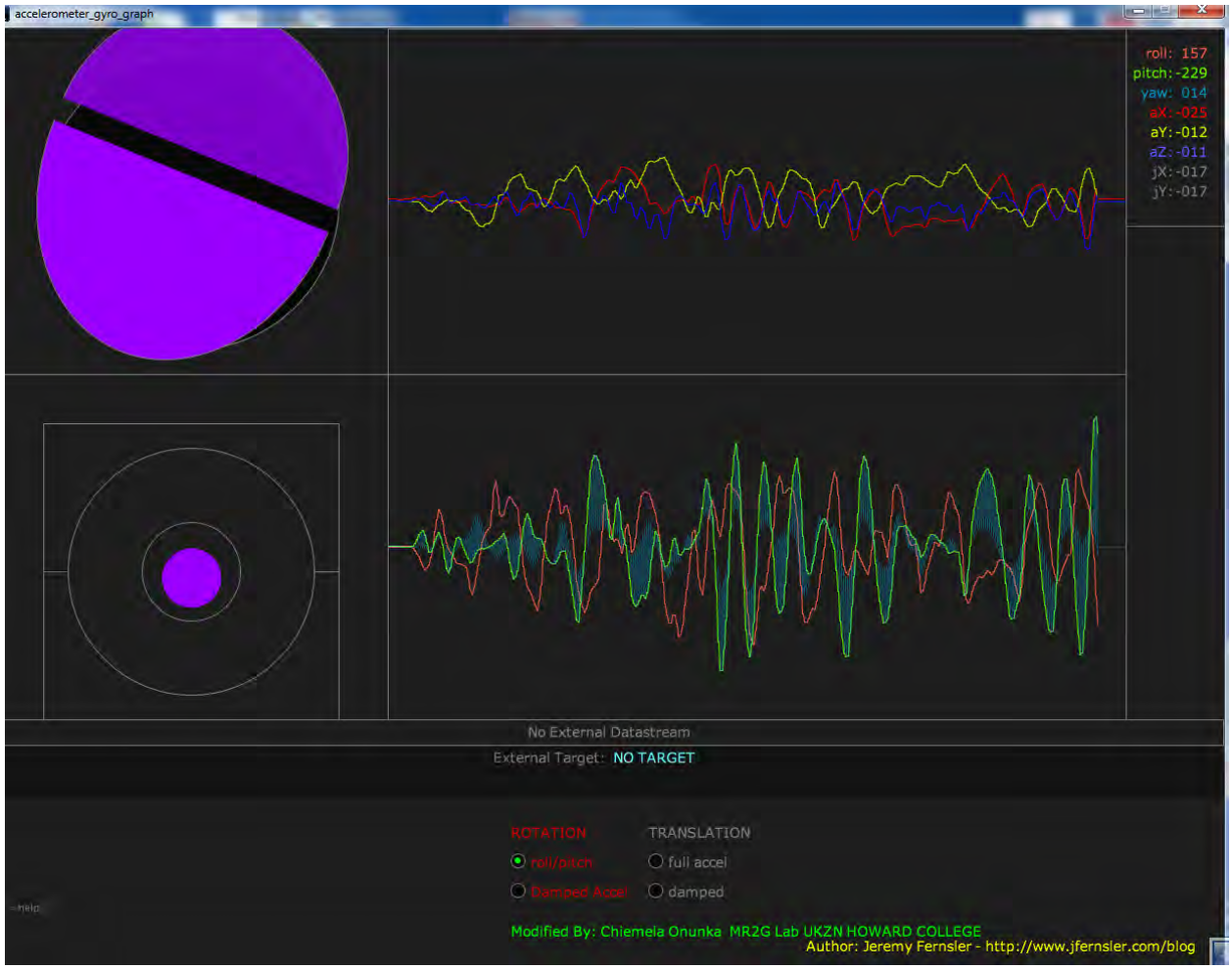

Figure 7-11: IMU Monitoring Screen Indicating Marine Craft Attitude

7.4 Obstacle Detection Results

In Figure 7-12 and Figure 7-13, data from the ultrasonic sensors are displayed. These results displayed how far an obstacle was from the marine craft. The red circles in the Figures 7-12 and 7-13 indicated the exact obstacle position. They are also indicated using the green shades in figures. The actual values representing actual obstacle distances are also displayed on the screen.

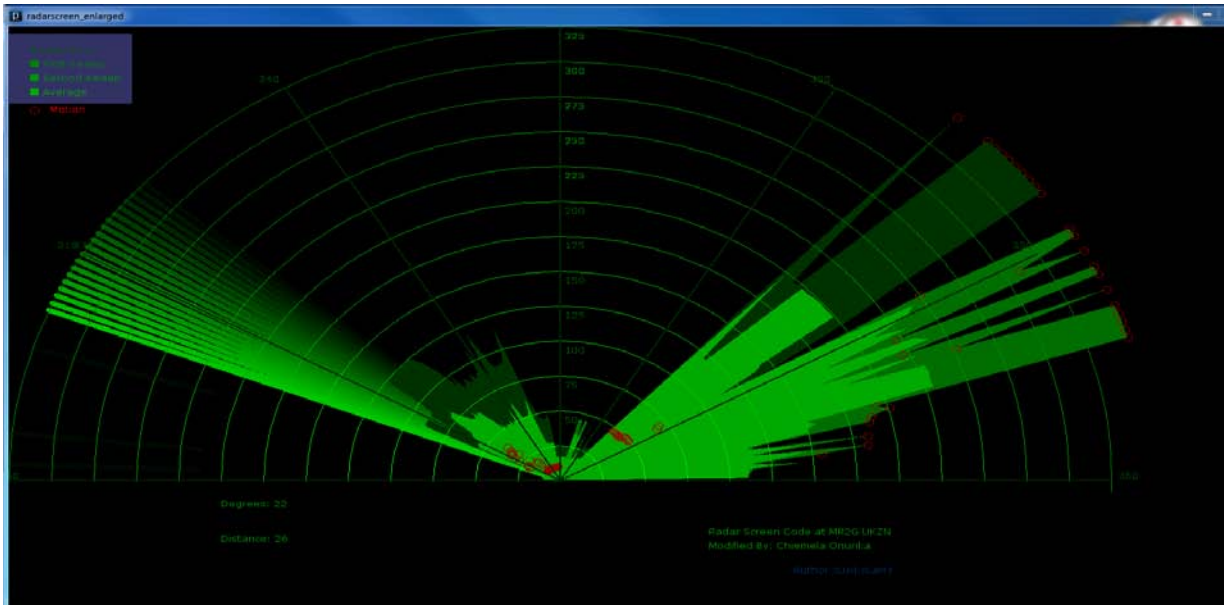

Figure 7-12: Radar Sweep from Left to Right

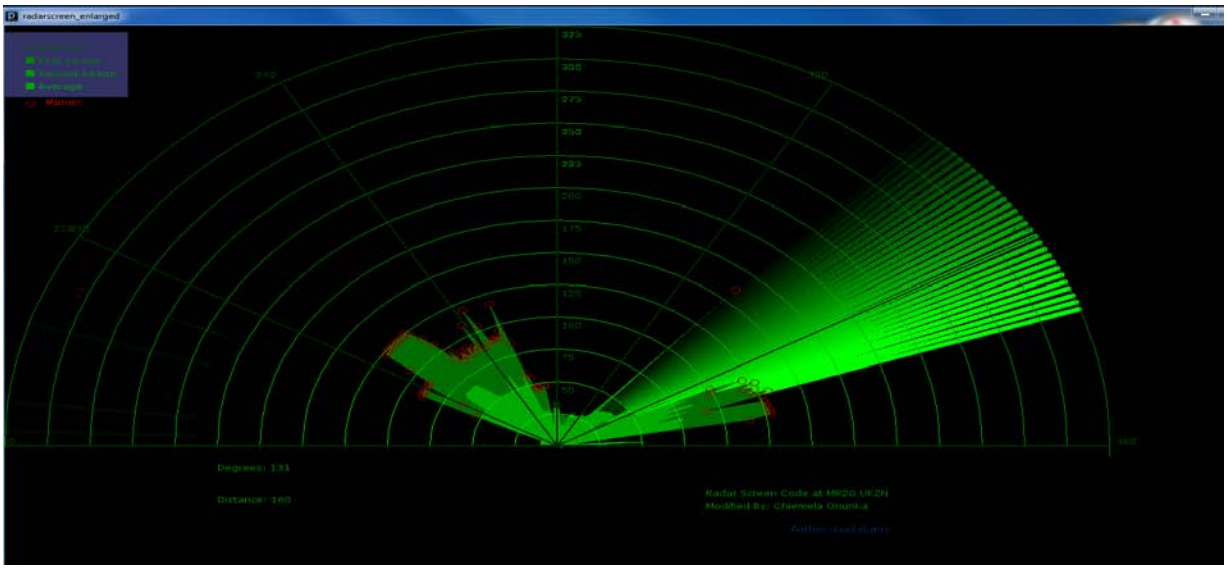

Figure 7-13: Radar Sweep from Right to Left

7.5 Autopilot System Analysis and Results

The results from the autopilot system were investigated under three conditions using the MSS. The first condition was investigating the performance of the autopilot using feedbacks from the digital compass and the IMU fitted on the marine craft. The autopilot used a passive wave filter to filter wave inputs in the investigation setup. The Simulink setups shown in appendix A, Figure A-1, Figure A-2 and Figure A-3 were used for the analysis. A sine wave generator with bias was used to model the ocean wave input to system. Increasing the bias in the wave model rendered the autopilot system less effective as the disturbance into the system was prevalent. This allowed for a zero bias input into the wave model so as to allow the autopilot to effectively control the marine craft in the desired navigation track. Improving the limiting differentiator in the model which has the yaw angle as the input to a second order model resulted in a smoother output from the angular rates and low frequency angular rates as shown in Figure 7-14 and also kept the sway motion of the craft as close as possible to low frequency output shown in Figure 7-15. The increase of the damping ratio within the autopilot system eliminated the effects of wave disturbances with the performance of the autopilot changing slightly in the negative as shown in Figure 7-15. To make full use of the feedbacks from the digital compass and gyro, the wave inputs were filtered as much as possible in order to achieve the desired performance from the autopilot system In Figure 7-16, an increase in the amplitude of the wave resulted in an erratic type of response from the craft and was kept close to the low frequency response by the autopilot.

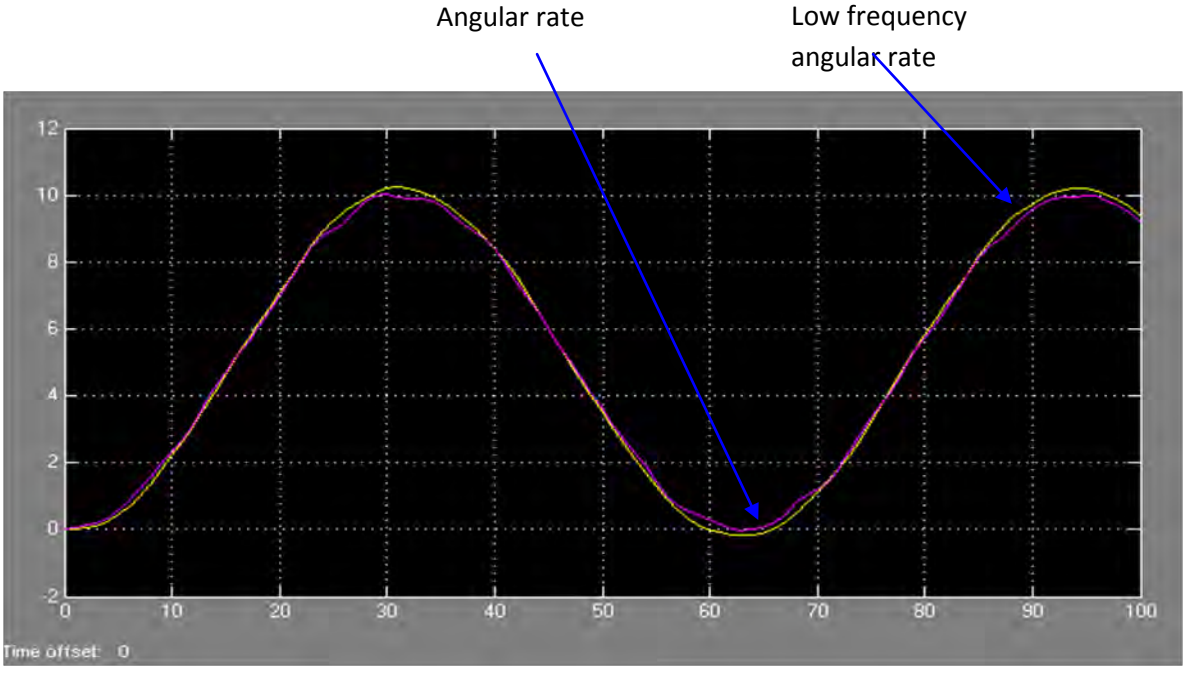

Figure 7-14: Angular Rate Comparison

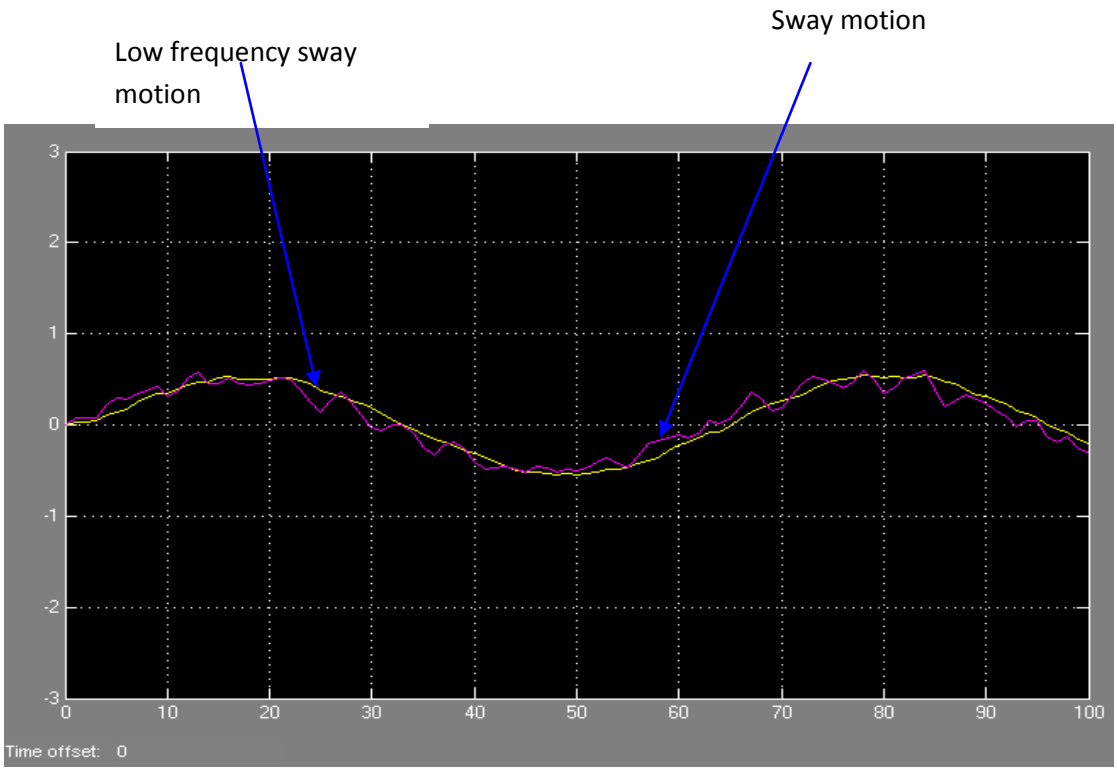

Figure 7-15: Sway Motion Comparison

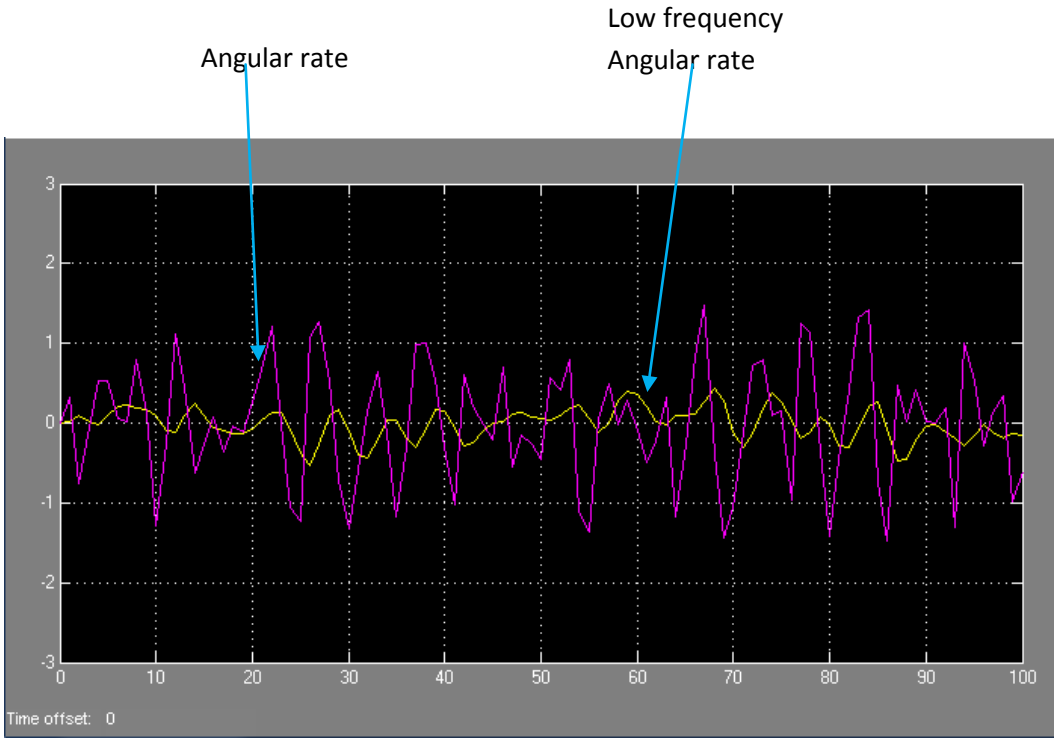

Figure 7-16: The Effect of Increased Wave Amplitude on Angular Rate

From the results shown in Figure 7-14, Figure 7-15 and Figure 7-16, the autopilot was able to keep the marine craft on the desired course using feedback signals from the digital compass and IMU and filtering off disturbances from wave inputs as much as possible.

The second scenario that was investigated was a case in which the autopilot used only the digital compass for feedback control. The performance of the autopilot was smoother at smaller rudder angles of about 10 to 15 degrees as shown in Figure 7-17 and started to deviate from the desired course from rudder angles of about 30 degrees and above. In Figure 7-18, the rudder input angle was at 40 degrees and the autopilot was able to bring the marine vehicle to turn at 25 degrees. This demonstrated that the response of the marine vehicle autopilot having only the digital compass for feedback control was very slow as it took long before the vehicle could turn at the reference angle. In Figure 7-19, the low frequency speed and the actual speed of the marine vehicle are shown. In Figure 7-19, the undulating response shown in the result was a consequence of the wave input as a disturbance into the system. The disturbance lingered for sometime as the autopilot took considerable amount of time to control the marine craft. In Figure 7-20 the low frequency angular rate and the actual angular rates as a function of wave disturbance are shown.

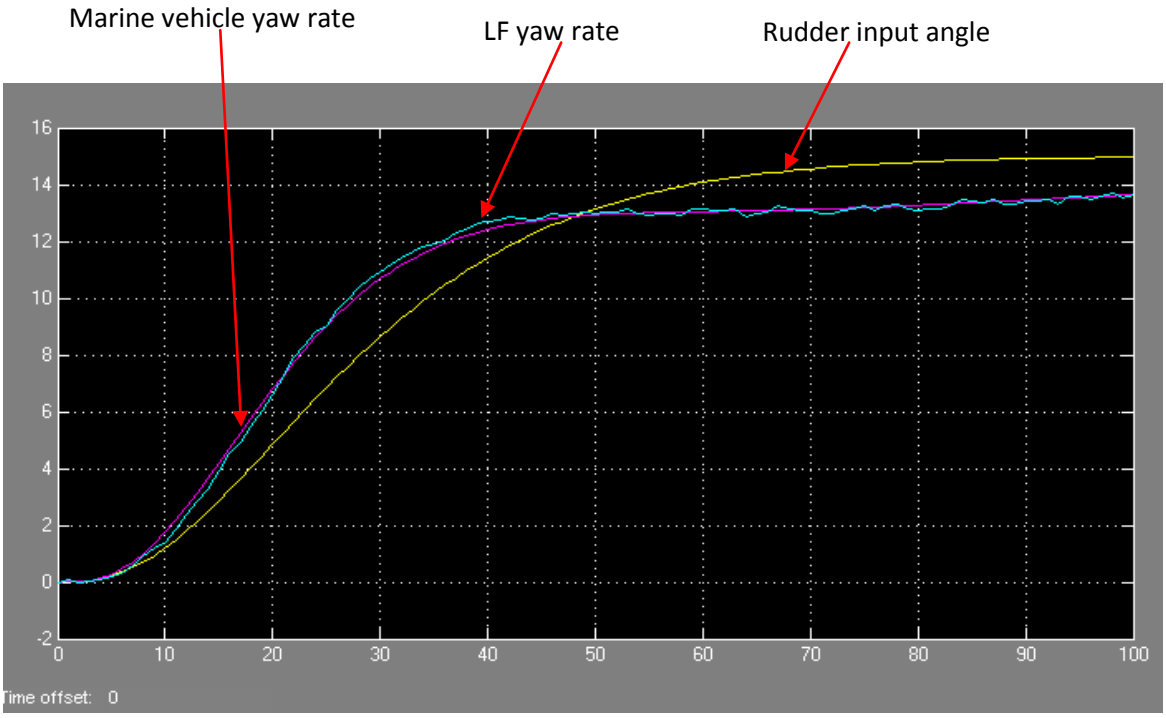

Figure 7-17: Rudder Response at 15 Degrees using only Digital Compass

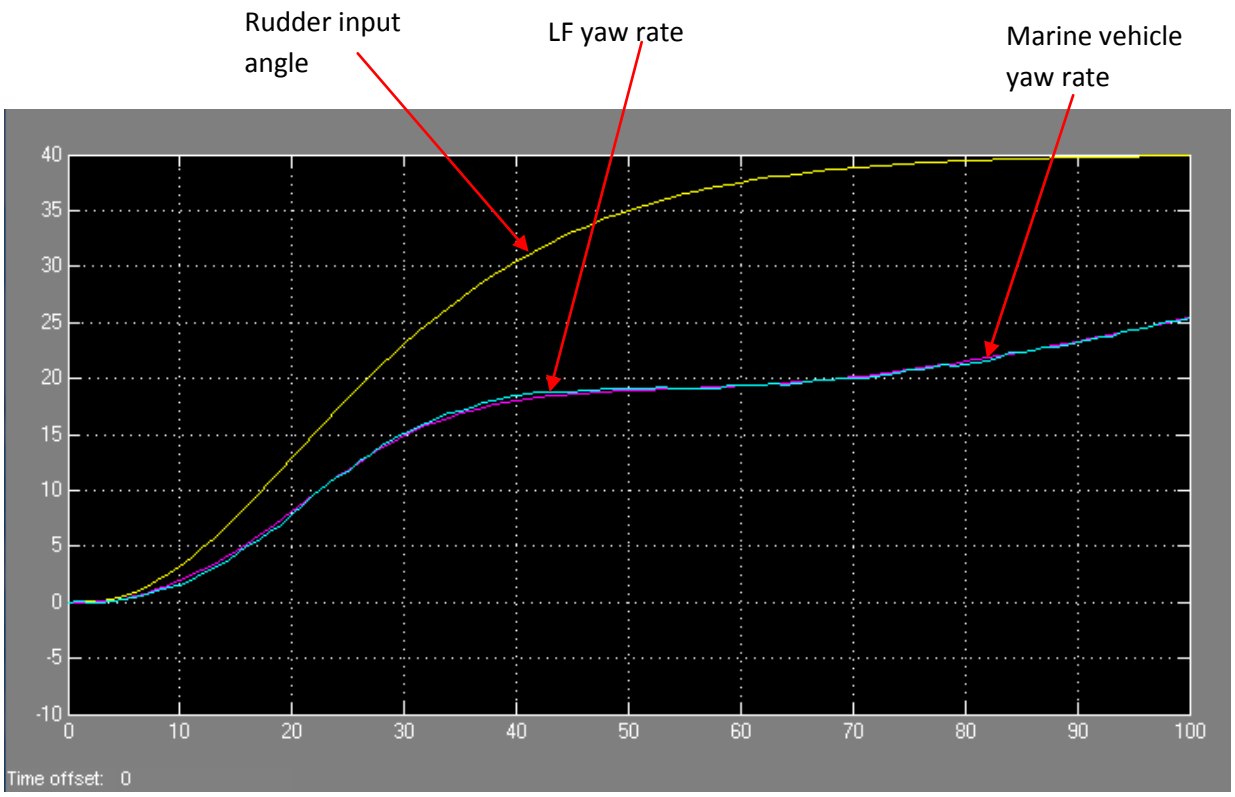

Figure 7-18: Rudder Response at 40 Degrees using only Digital Compass

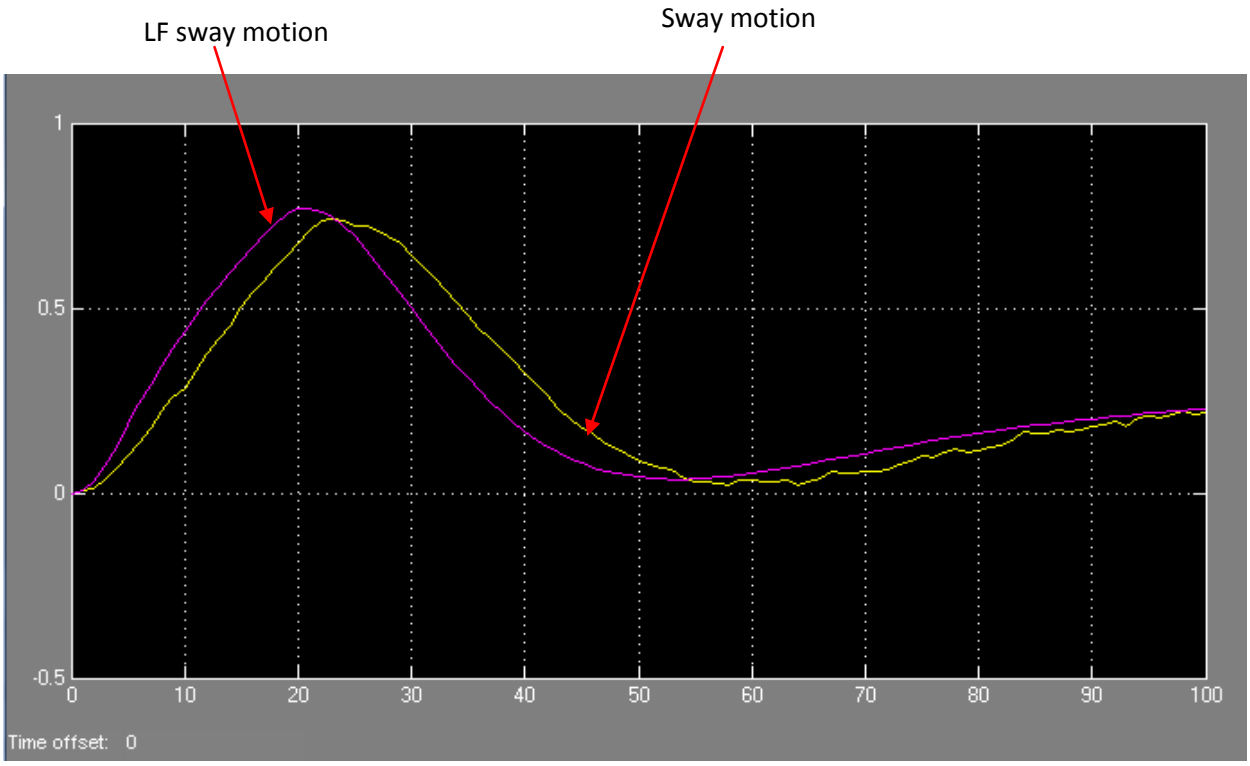

Figure 7-19: Sway Motion in Autopilot System with only Digital Compass

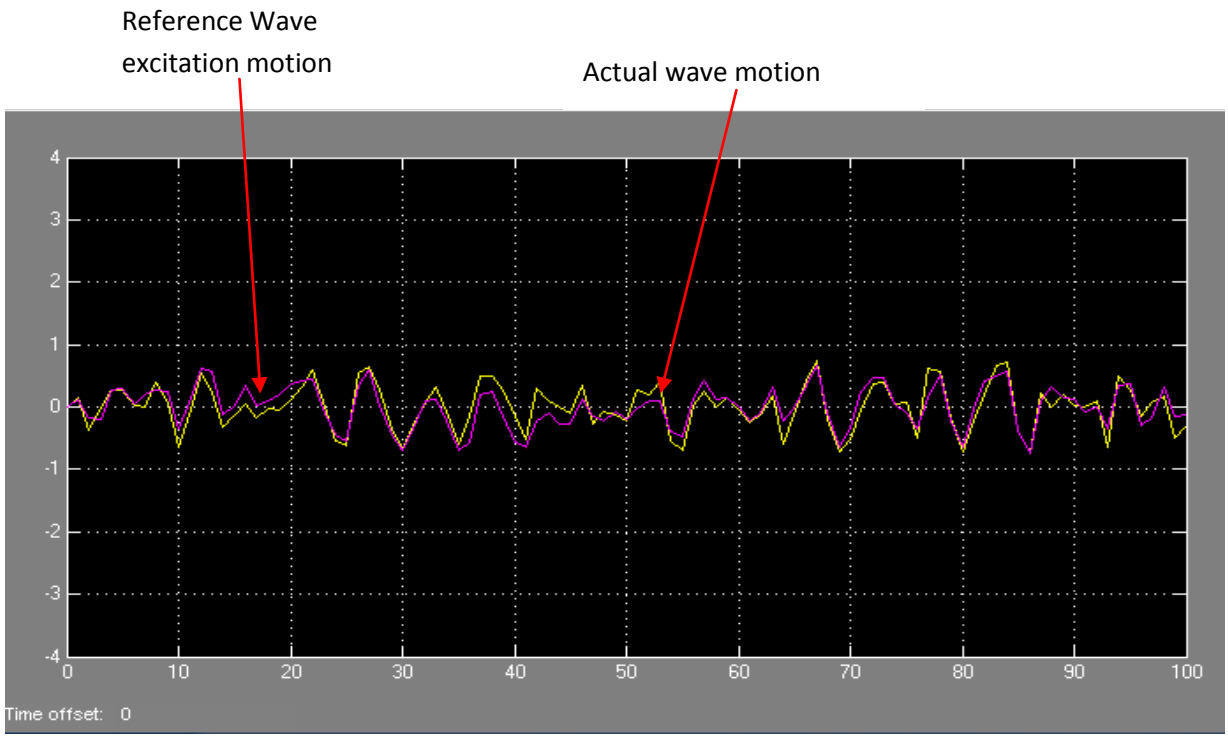

Figure 7-20: Angular Rates of the Marine Vehicle Autopilot System with only Digital Compass

The third investigation featured the use of the Kalman filter and the digital compass in the control system of the autonomous marine craft guidance, control and navigation. The Kalman filter was used to predict marine vehicle state estimates and was also used to filter wave inputs into the system. The rudder response shown in Figure 7-21 showed an improved performance of the autopilot system equipped with Kalman filter and digital compass when compared to the result shown in Figure 7-17. The results from Figure 7-21 showed that the autopilot was able to reach the reference data in 120 seconds while the results from Figure 7-17 showed that there is still a difference in the reference data and actual data. The autopilot in Figure 7-17 will continue to adjust the error in the system until the error is approximately zero or actual data is equal to the reference data and this takes longer than 120 seconds. The speed response shown in Figure 7-22 had a faster response of 18 seconds when compared to the result shown in Figure 7-19 having a response of about 25 seconds. 95% of the wave disturbance input in the system shown in Figure 7-22 was filtered off within 120 seconds as opposed to the undulating response indicated in Figure 7-19. In Figure 7-22, the response from the wave excitation motion and the actual wave motion were very similar. These investigations reveal among other things that the inclusion of Kalman filter into the autopilot system increased the robustness of the control, guidance and navigation system of the autonomous marine craft by 20%. The Kalman filter enabled the autopilot to have more control and performance in situations where disturbances to the control system were eminent.

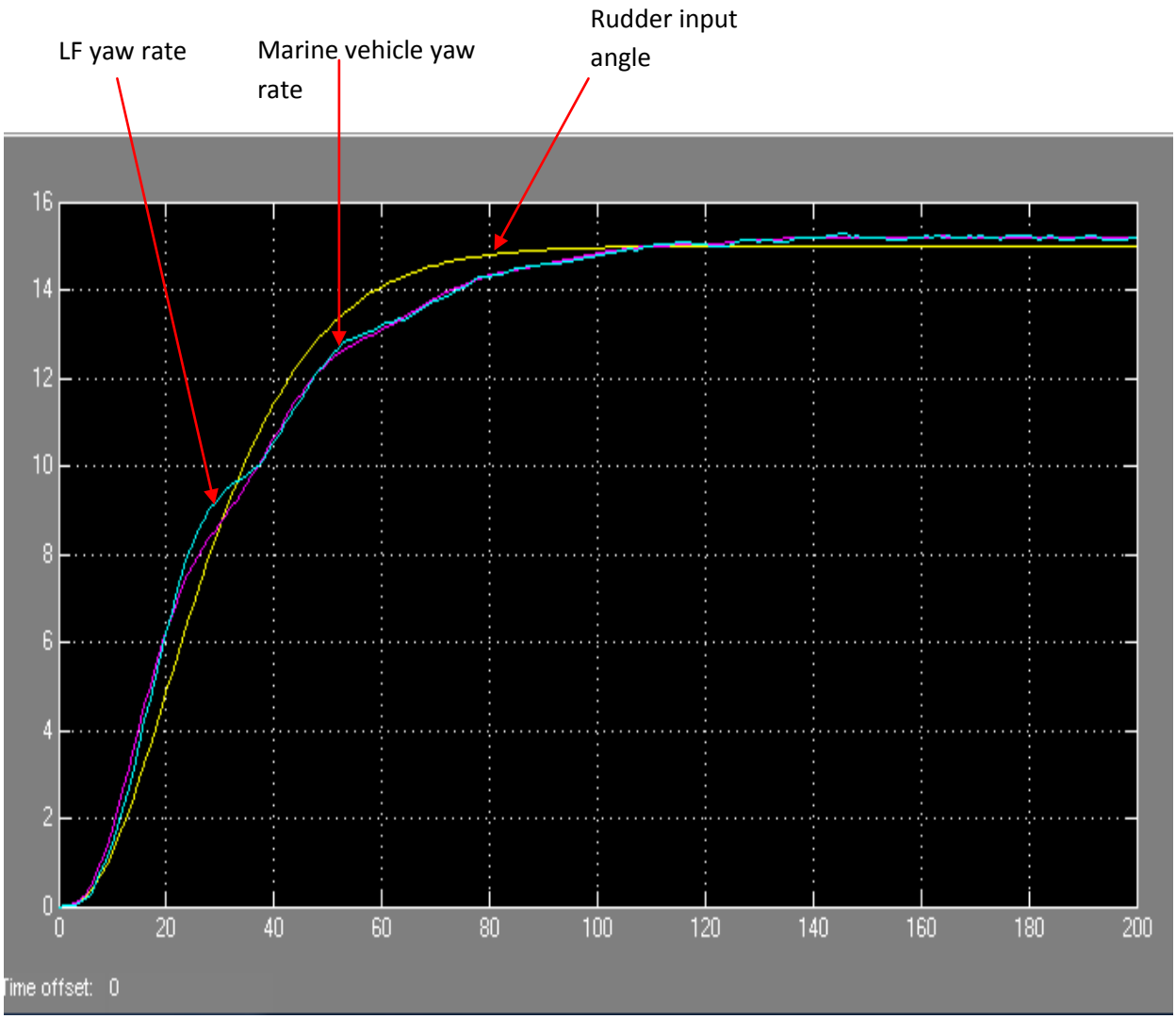

Figure 7-21: Rudder Response at 15 Degrees using Kalman Filter and Digital Compass

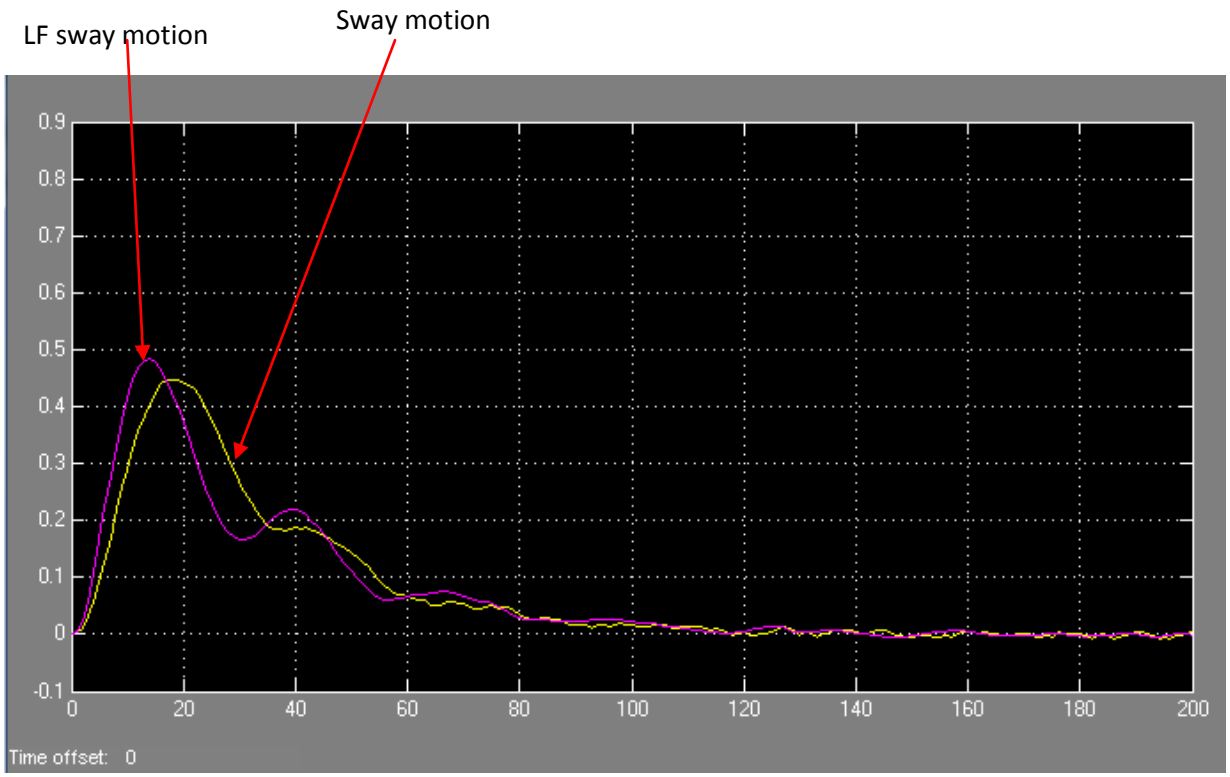

Figure 7-22: Sway in Autopilot System with Kalman Filter and Digital Compass

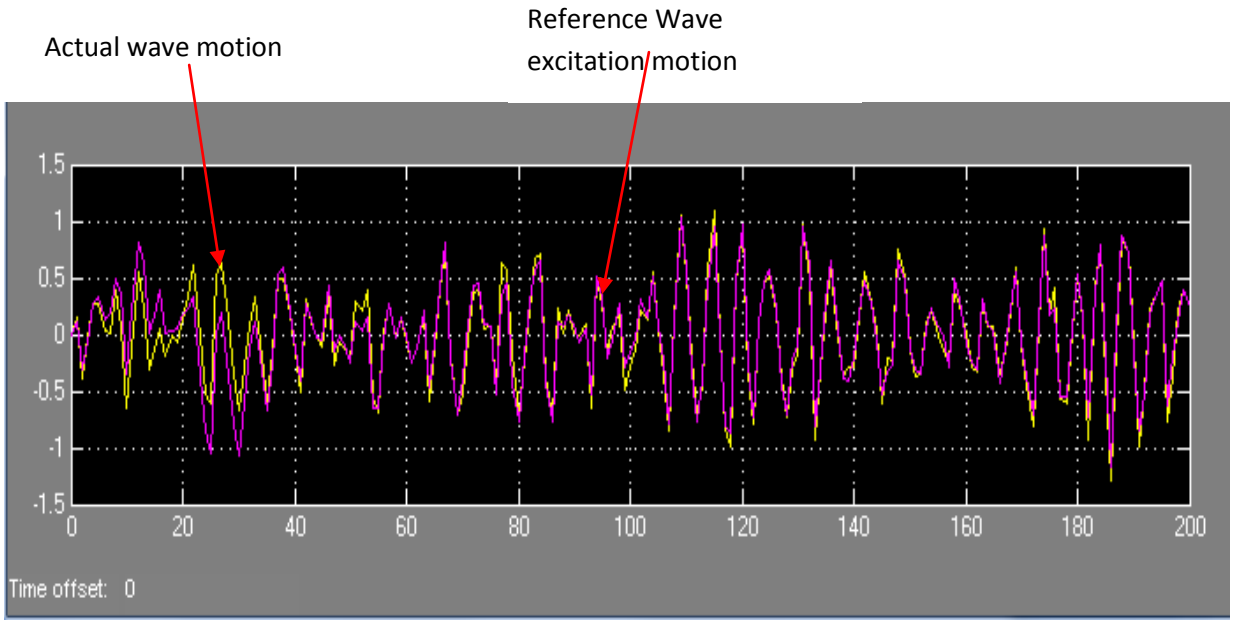

Figure 7-23: Angular Rates of the USV Autopilot System with Kalman Filter and Digital Compass

7.6 Control System Results

The control system design of the autopilot system featured the use of a proportional derivative (PD) control system to control the motion of the marine craft as well as the rudder action and motion. The PD control of the autopilot system demonstrated and showed the rudder response and yaw response of the marine vehicle. At low speeds of about 5.567 m/s, the autopilot PD controller took about 170 seconds to stabilize the marine craft and keep it in the intended navigation track. A small change in rudder angle per second made the rudder response output to fluctuate and behave in an unsettled manner before stabilizing. On the other hand, an increase in the rudder angle derivative per second made the rudder response to stabilize within a very short time of about 200 seconds. Figure 7-24 (a) showed the yaw rate, Figure 7-24 (b) showed the marine vehicle speed, Figure 7-24 (c) yaw angle response and Figure 7-24 (d) showed the rudder angle at a maximum rudder input angle of 35 degrees and a maximum change in rudder angle per second of 5 degrees per second. Figure 7-25 showed the motion of the marine vehicle as it moved at approximately a speed of 5.567 m/s. In Figure 7-25 the reference rudder angle was at 10 degrees which was scaled in radians on the graph and was also indicated in Figure7-24 (c).

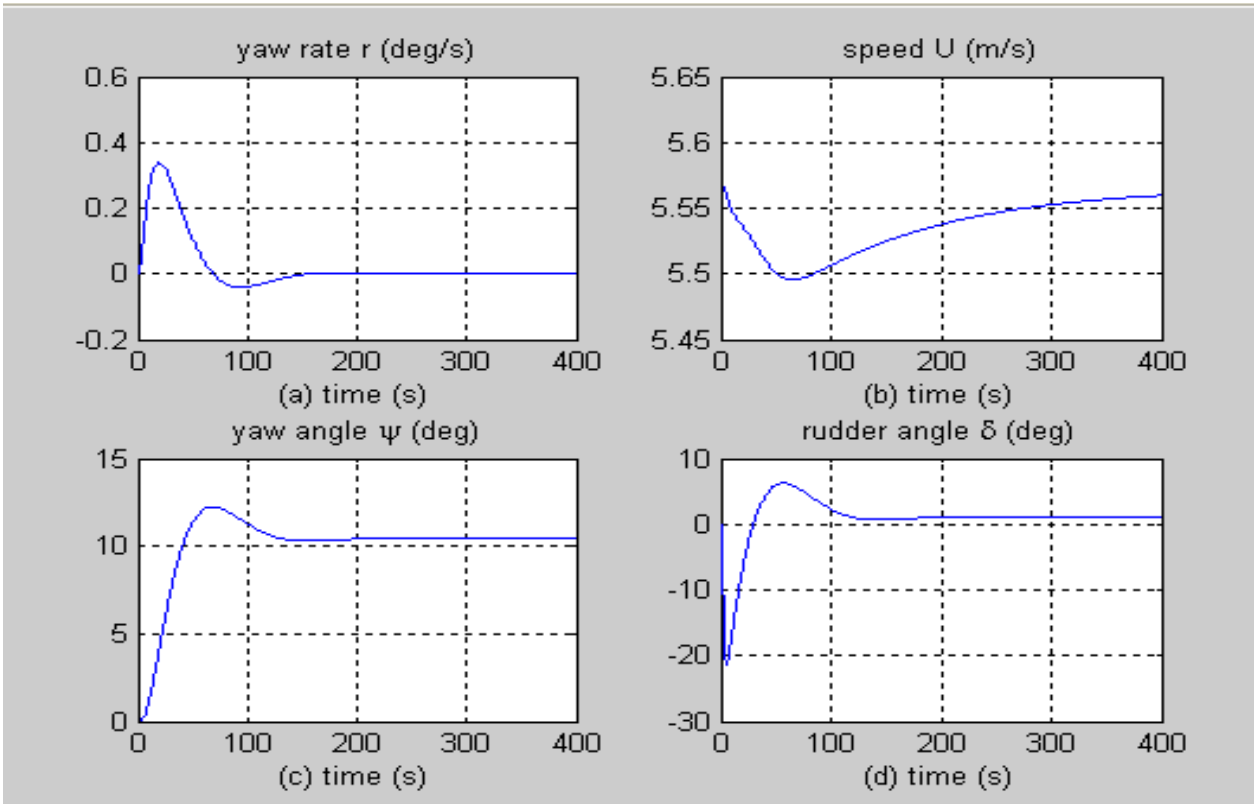

(a) Yaw Rate (b) Speed (c) Yaw Angle (d) Rudder Angle

Figure 7-24: Autopilot PD Control at 10 Degrees Rudder Input Angle

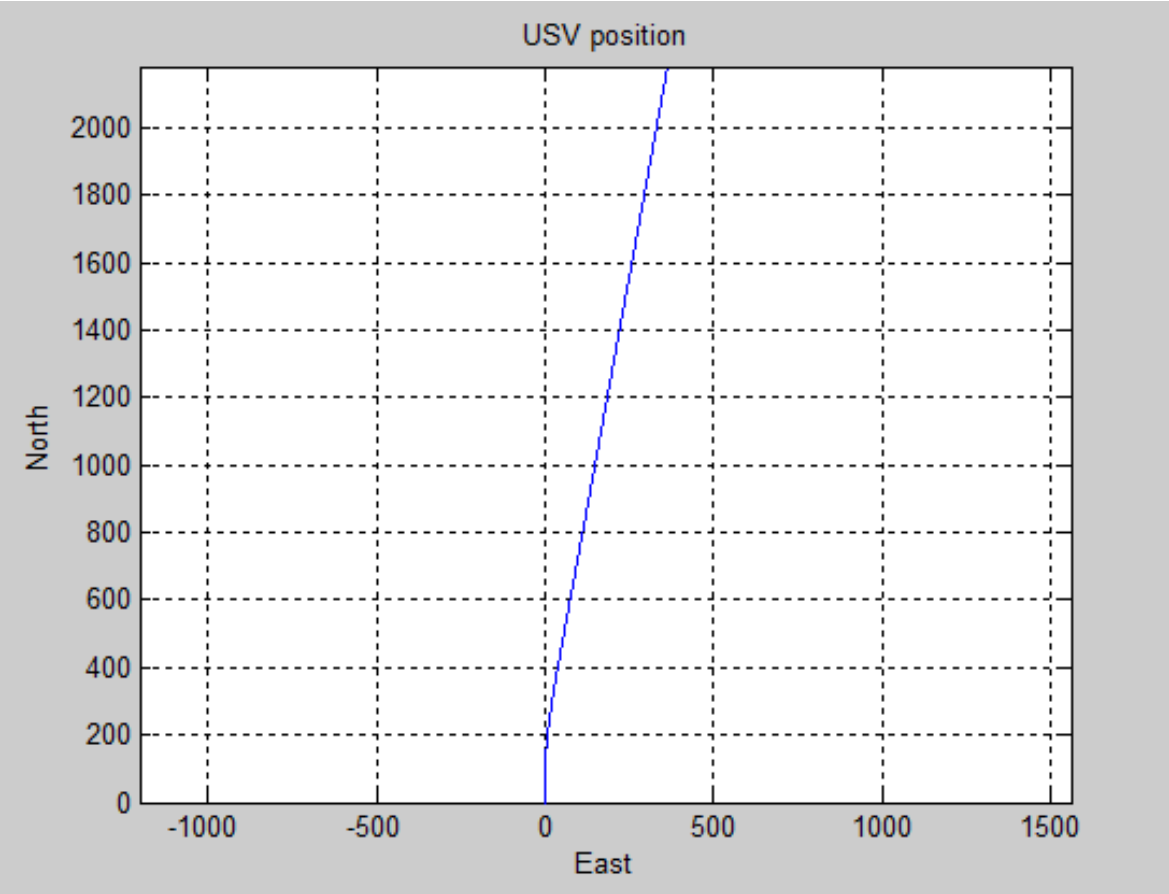

Figure 7-25: USV Motion under Autopilot PD Control at 10 Degrees Rudder Reference Angle

Figure 7-26 and Figure 7-27 showed the rudder response of the marine craft using the autopilot PD control system at a rudder input angle of 35 degrees. It was noted that the time it took the controller to get the marine vehicle on the desired navigation path was approximately 200 seconds. This demonstrated that with adequate tuning of the autopilot system that the marine vehicle was able to manoeuvre at different input angles. This allowed for proper control of the marine vehicle.

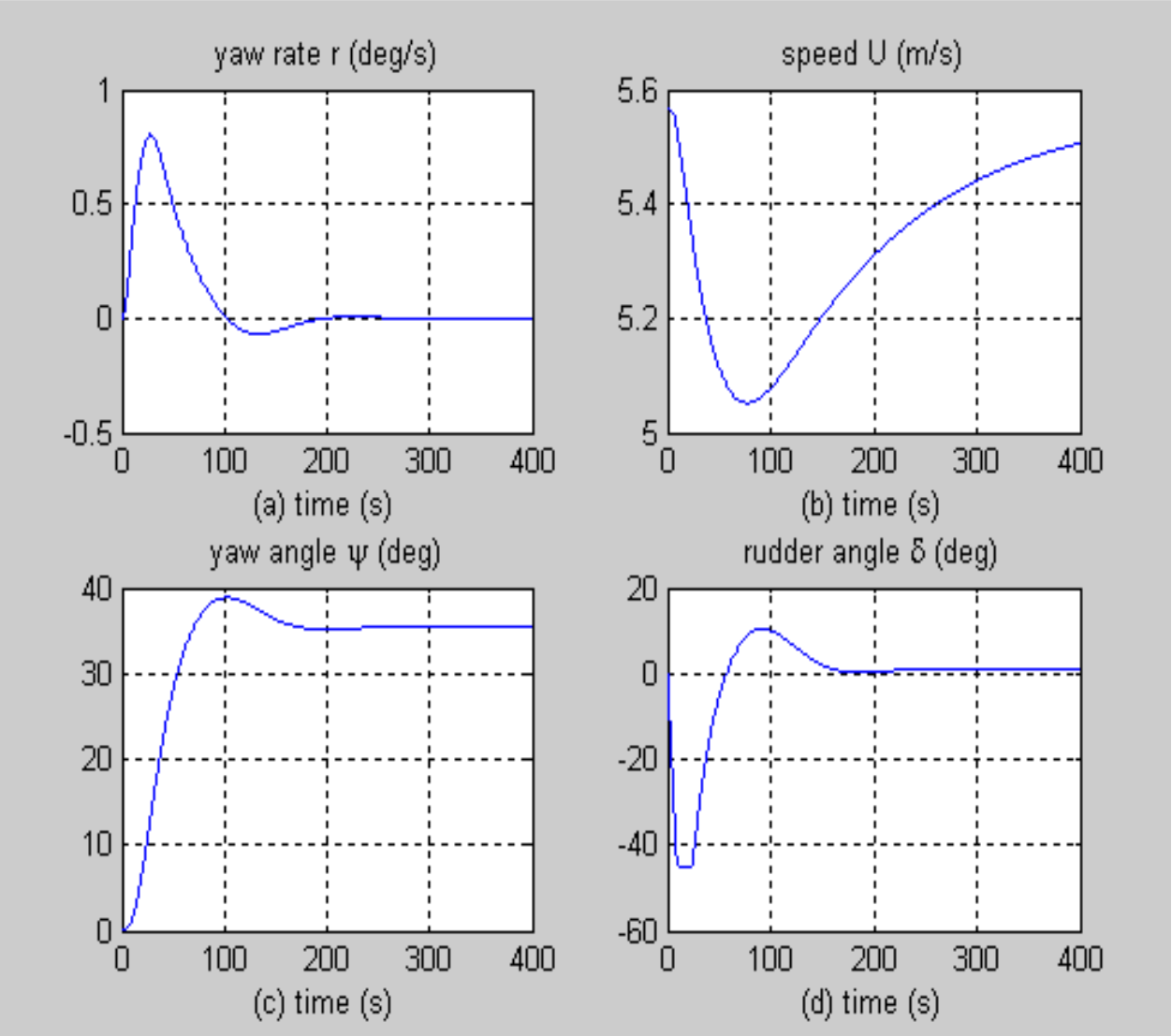

(a) Yaw rate (b) Speed (c) Yaw Angle (d) Rudder Angle

Figure 7-26: Autopilot PD Control at 35 Degrees Rudder Input Angle

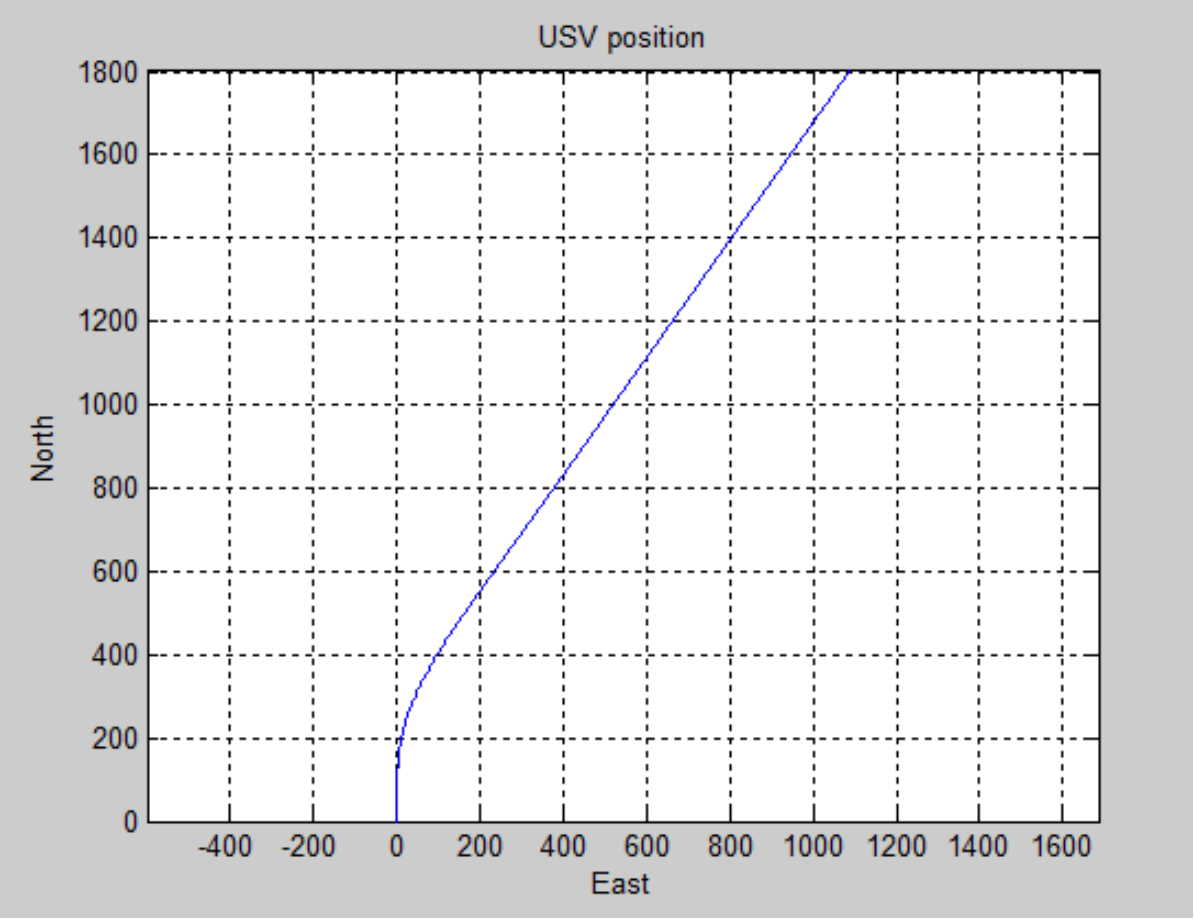

Figure 7-27: USV Motion under Autopilot PD Control at 35 Degrees Rudder Reference Angle

The results discussed so far on the autopilot control system can be said to be acceptable as the response of the control system algorithm were not erratic to input angles of 10 and 35 degrees respectively. The control system algorithm gradually controlled the marine vehicle according to the rudder reference angles.

7.7 Course Keeping and Stability Results

The course keeping specification of the autonomous marine craft was investigated and validated using the stability tests or criterion. This was used to check the performance of the autopilot course controller. Appendix A Figure A-4 shows the selection menu for the stability test analysis. The input to the system was based on Nomoto's [60] low frequency first order steering model discussed in chapter two subsections 2.7.2. At an initial surge speed of 3m/s the results are shown in Figure 7-28. In Figure 7-28 subfigure B indicated the yaw rate and subfigure C indicated the yaw angle. Figure 7-29 showed the directional stability of the marine vehicle. This investigation was necessary so as to determine the stability of the marine craft as it turns under the action of wind and water current. The result showed in Figure 7-29 especially in subfigure B was a system that was critically damped in order to achieve the expected

results. Figure 7-30 showed the behaviour of the same system at the same speed with an under damped autopilot course keeping controller.

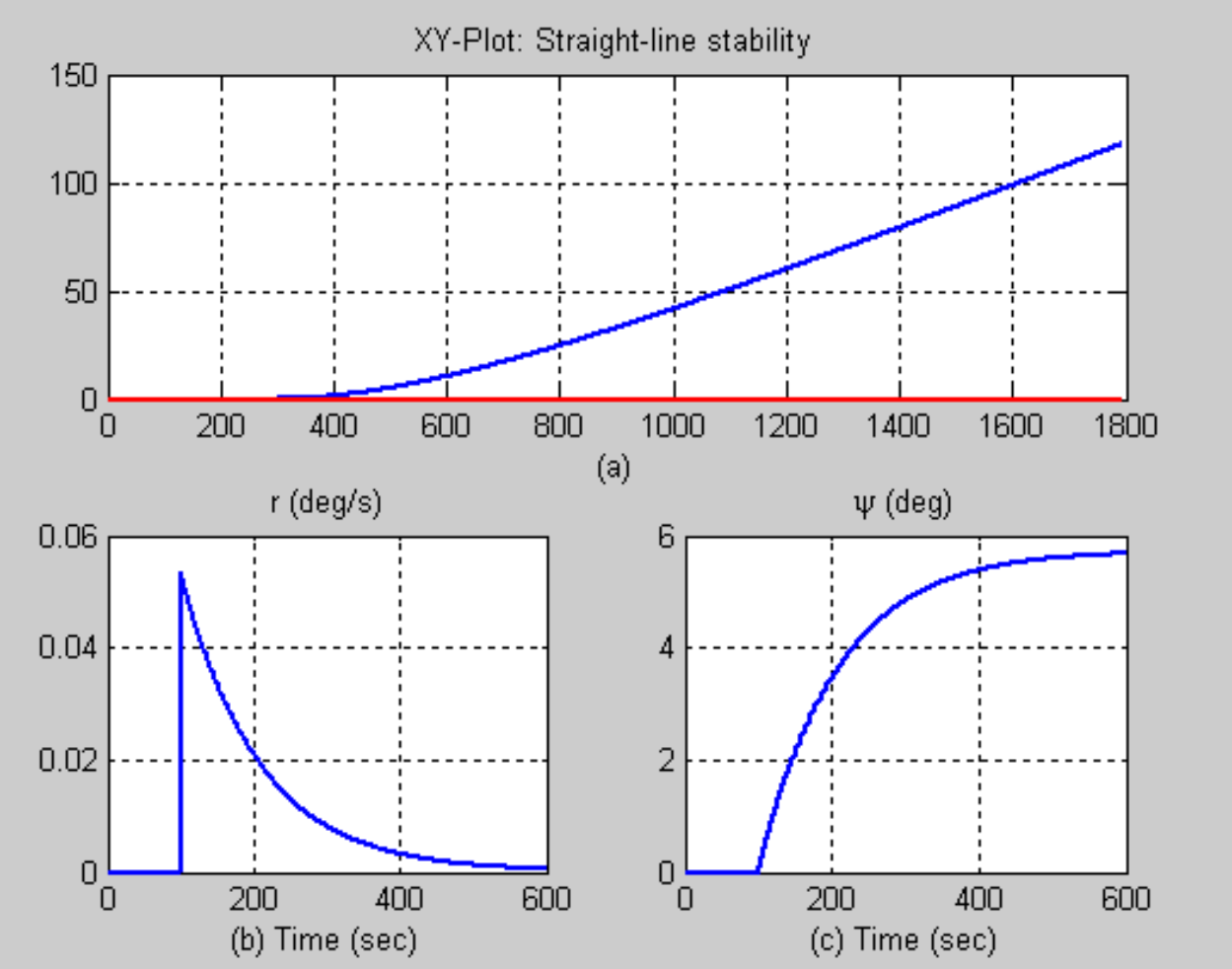

(a) Straight-Line Stability (b) Yaw rate (c) Yaw

Figure 7-28: Straight Line Stability at 3m/s Surge Speed

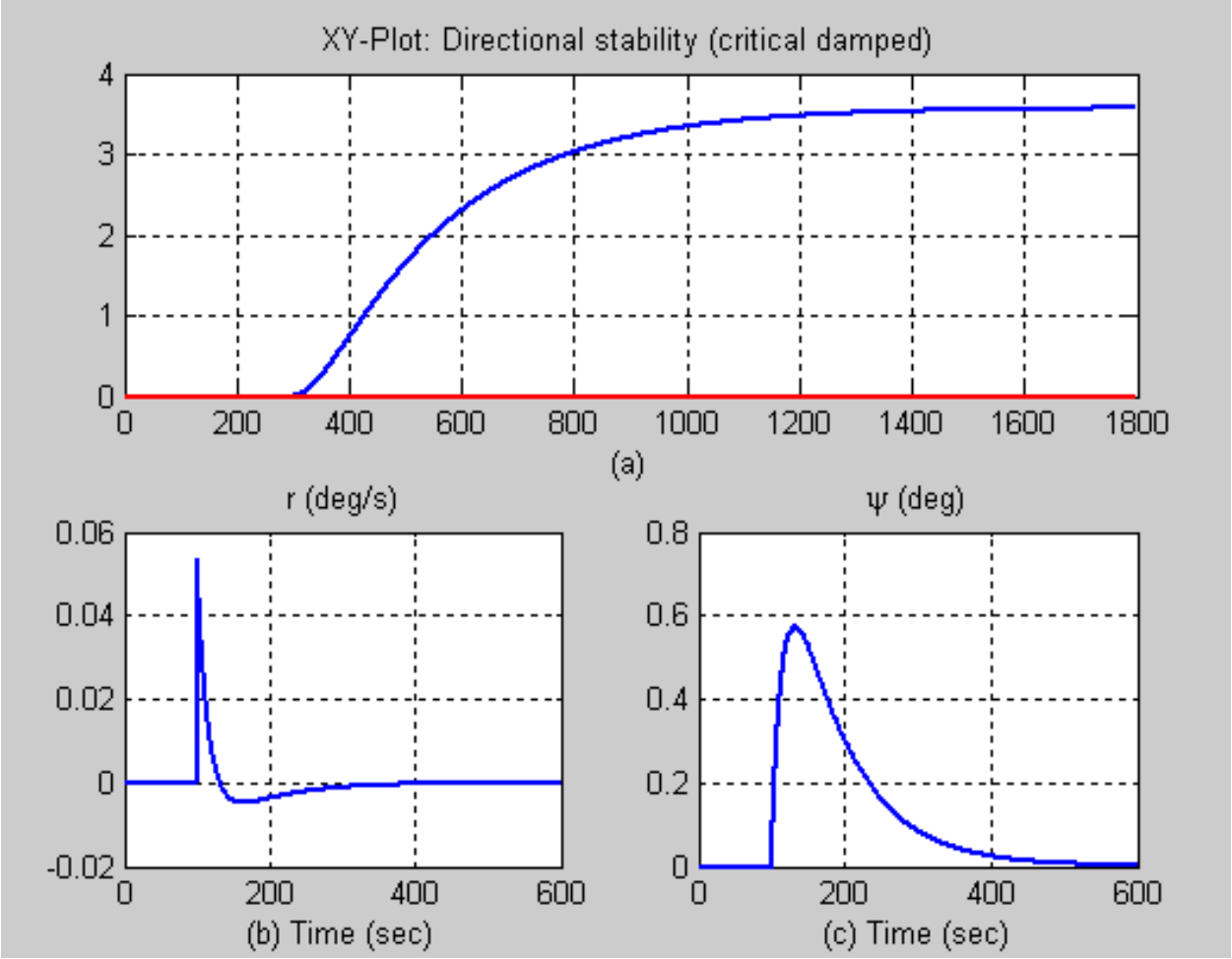

(a) Directional-Line Stability (b) Yaw rate (c) Yaw

Figure 7-29: Stability Test of Critically Damped Autopilot System.

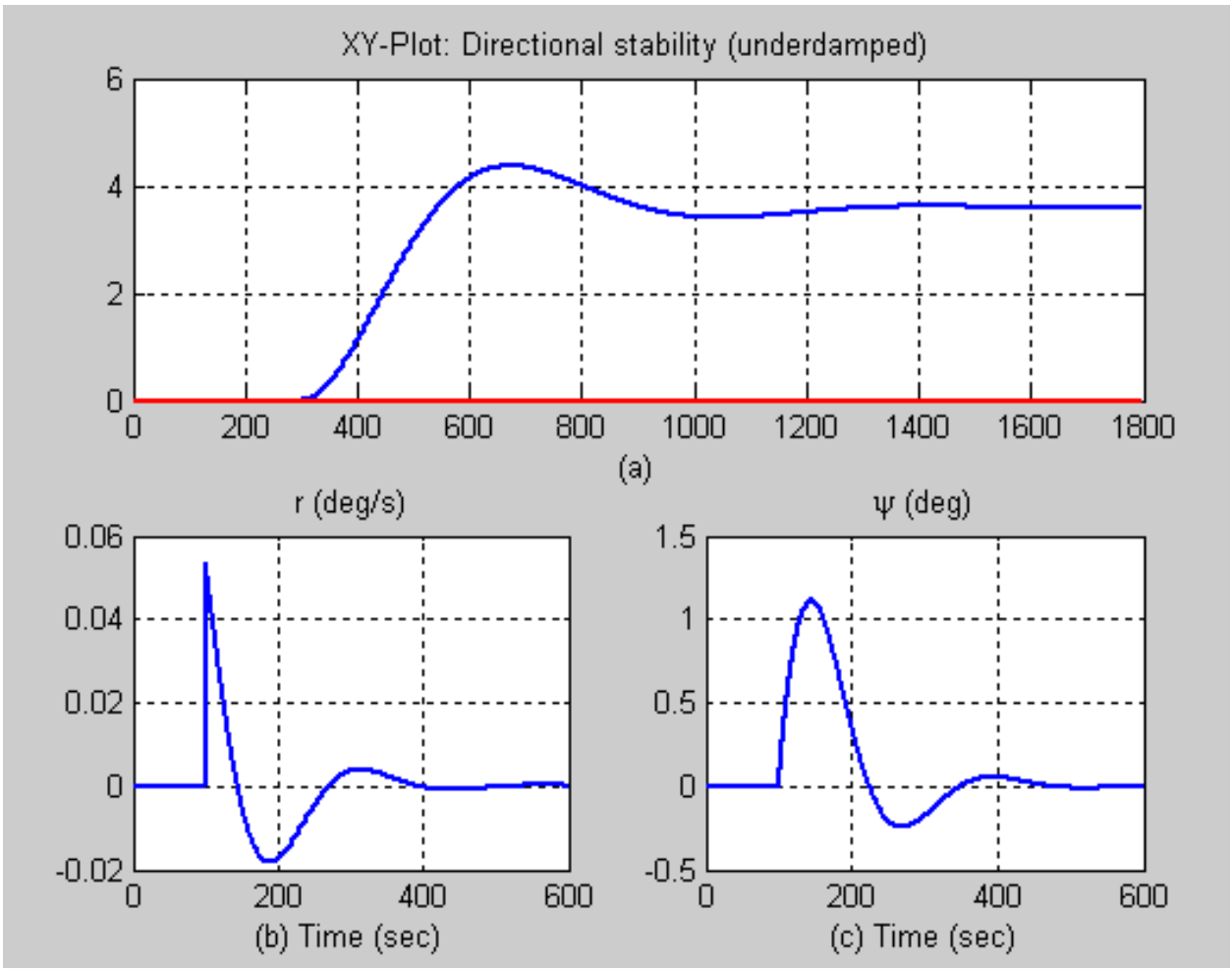

(a) Directional Stability (b) Yaw rate (c) Yaw

Figure 7-30: Stability Test of an Under-Damped Autopilot System

7.8 Implication of Test Results

The results discussed so far have the following implications:

- The system kinematic and dynamic results implied that the use of Euler angles were suitable for small rudder angle input and quaternion provides a more robust application for all angles.
- The turning performance revealed that the marine vehicle can make full circle turning at relatively low speeds.
- The pull-out manoeuvre provided data on the stability the marine craft while tracking its course.
- The attitude and heading reference results provided data on the performance of the of the IMU system. This data allows for further analysis on the stability of the marine vehicle.
- The stability tests also provided data on the performance of the course-keeping algorithm.
- The results from the obstacle avoidance system and the autopilot system were used to complement each other for the autonomous navigation of the marine vehicle. The results also gave an indication of course-keeping of the marine vehicle. It can be used as a means of monitoring the performance of the course tracking algorithm.

7.9 Summary

The chapter showcased the various results and simulations which were achieved from the autonomous marine craft system which were analysed and implemented on the MSS and tested on the autonomous marine craft. The analyses of the various models were presented and discussed in the chapter. The findings and results were shown graphically.

Chapter 8

Conclusions

Introduction

The system specifications and functionalities given in chapter one which were expected of the autonomous search and rescue marine craft were investigated and tested to validate the different aspects of modelling, programming, sensor and electronic integration which were measures and benchmarks for this research. The results were as follows:

- The search of an area such as a river bank was conducted with the aid of a network camera onboard the craft. This enabled the controller to have a clear picture of the search environment.
- Reconnaissance and mapping of search was done using GPS coordinates. These were used as inputs in the navigation algorithm and implemented in the form of navigational waypoints.
- The marine craft was able to transmit information from the craft such as marine craft attitude information with the aid of the Xbee wireless module onboard the craft. Also the video from the network camera was also transmitted wireless to the controller on the shore. This validated the mobile beacon and repeater functionality of the marine craft.
- The marine craft was able to be controlled using three control modes. The first mode was a remote-control mode which allowed the controller to control the craft fully with the aid of a remote control module. The second mode was the semi autonomous mode which featured waypoints or pre-programmed route and also allowed for remote control mode. The last mode was autonomous mode. In this mode the marine craft only used GPS coordinates as waypoints to navigate. It returns to a lunch point or the starting point of the navigation sequence after completion of navigation routine.
- The steering of the marine craft rudder was modified and was controlled using the closed loop control system of a DC servo motor.
- Obstacles were detected with aid of ultrasonic sensors and viewed with the aid of the radar-like screen.
- The attitude of the marine craft was also determined using low cost IMU and was also monitored.
- Through the PD controller embedded into the autopilot system, the marine craft was able to turn the rudder in the right direction.

- Adequate investigation, simulation and analysis were carried out to determine the guidance, control and navigation of the USV.

This research has indicated that an autonomous marine craft for search and rescue operations can be designed and developed using relatively low cost components which are readily available at the market. The navigation of such USV was successfully done using GPS waypoints. The development of such a craft showed that with low-cost sensors, a search and rescue craft or coast line monitoring craft can be developed and utilized to the benefit of humankind. Path planning and obstacle avoidance algorithms were achieved using low-cost ultrasonic sensors. The attitude of the craft was monitored and observed using a low-cost IMU. These low-cost sensors and instruments were generally used to investigate the control and navigation principles which were associated with the development of an autonomous marine craft. The semi-autonomous control of the marine craft was achieved using a remote control module.

8.1 Summary of Contributions

This research study has made contributions in the development of search and rescue marine vehicles. It has also demonstrated the importance of USV in marine search and rescue operations. The study made contributions to marine vehicle guidance and control, mechanical design, electronic and software integration into USV. The study also made contributions to the analytical development and investigation of a search and rescue marine craft. The mechanical contributions included the adaptation of a commercial or pleasure marine vehicle into unmanned surface vehicle.

The electronic contribution includes the type of sensor integration coupled with sensor fusion emanating from different electronic components and how to effectively communicate with these components. The integration of these sensors involved certain level of signal processing and power supply to IO boards. The software contributions were in the radar monitoring screen used for obstacle avoidance, IMU monitoring screen, sensor integration and communication software and the autopilot software for the autonomous marine craft. The contributions also included providing three modes of controlling an unmanned surface vehicle. These control modes include remote control mode, semi-autonomous mode and autonomous mode.

The results obtained from the research provide insights on the importance of using multi-sensory system for practical applications leading to USV development. It shows that the integration of multisensory system in marine vehicle can be used as the necessary platform for the development of an autonomous marine craft. System kinematics and dynamics results, autopilot system, course tracking and keeping algorithms provide the integral frame work for practical analysis in USV development.

8.2 Suggestions for Further Research

The research into USVs has been gaining adequate attention every day as there are more areas in which USVs are proving to be useful in our everyday applications. The commercialization of USV has called for an improved technological advancement in these following areas. The first improvement area is the development of robust marine craft attitude estimation, using low-cost components to maintain the stability of the marine craft. More research is also required in the effect of hydrodynamic forces to the autonomous control USVs.

The obstacle avoidance algorithms also require improvements and more research is also required in the integration of marine radar system into the navigation algorithm. This will involve methods of fusing the video signals from the radar into the navigation and control algorithm.

More research is required in developing a robust H-bridge circuit to drive the propeller for longer periods. There are different propulsion systems that are available for use in marine craft development. More research is required in the area of modifying existing marine vehicles to be able to use a jet propulsion system. Jet propulsion system has some advantages which can be implemented in an autonomous marine craft so as to make it an efficient search and rescue craft. Effective torque, power and manoeuvrability are some of functional requirements of a search and rescue marine craft that needs adequate attention.

The visual system of the autonomous marine vehicle also requires further research especially in the areas of image processing, object identification and integration of camera images in the navigation and control of the marine vehicle.

The efficiency of the control and navigation algorithm can be improved by using high quality control and navigation sensors as these will reduce computational and latency errors.

References

[1] Schoerling, D., Van Kleeck, C., Fahimi, F., Koch, C. R., Ams, A. and Lober, P., "*Experimental Test of a Robust Formation Controller for Marine Unmanned Surface Vessels," Autonomous Robots*, vol. 28, pp. 213-230, 2010.

[2] Siciliano, B. and Khatib, O., *"Springer Handbook of Robotics,"* Springer, Springer-Verlag, Berlin Heidelberg, 2008.

[3] Fossen, T. I. and Perez, T., *"Marine Systems Simulator,"* 2010. Available: http://www.marinecontrol.org. Accessed: February 2010.

[4] Fossen, T. I., *"Guidance and Control of Ocean Vehicles"*, John Wiley & Sons Ltd. Baffins Lane, Chichester, West Sussex PO19, 1UD, England, 1994.

[5] Bertram, V., *"Unmanned Surface Vehicles- A Survey,"* 2008. Available: http://www.skibstekniskselskab.dk/public/dokumenter/Skibsteknisk/Download%20materiale/2008/10%20marts%2008/USVsurvey_DTU.pdf. Accessed: June 2009.

[6] Brizzolara, R., *"ONR Unmanned Sea Surface Vehicle (USSV),"* 2010. Available: http://www.onr.navy.mil/~/media/Files/Fact%20Sheets/Unmanned%20Sea%20Surface%20Vehicle.ashx . Accessed: December 2010.

[7] Veers, J. and Bertram, V., *"Development of the USV Multi-Mission Surface Vehicle III,"* 5th Int. Conf. Computer and IT Application in the Maritime Industries (COMPIT), Leiden, pp.345-355, 2006.

[8] Radix Marine. *"The Growing US Market for Unmanned Surface Vehicles (USVs),"* 2003. Available: http://www.radixmarine.com/PDFs/USV%20Market%\20Study.pdf. Accessed: June 2009.

[9] Taggart, R., *"Anomalous Behaviour of Merchant Ship Steering Systems," Marine Technology* pp. 205-215, 1970.

[10] Van Gunsteren, F. F., "*Analysis of Roll Stabilizer Performance," Trans of the society of Naval Architect and Marine Engineers*, vol. 21, pp. 125-146, 1974.

[11] Cowley, W. E. and Lambert, T. H., *"The Use of a Rudder as a Roll Stabilizer," In 3rd Ship control system symposium-SCSS*, Bath, UK, 1972.

[12] Carley, J. B. and Duberley, A., *"Design Considerations for Optimum Ship Motion," In 3rd Ship Control system Symposium-SCSS*, Bath, UK, 1972.

[13] Carley, J. B., *"Feasibility Study of Steering and Stabilizing by Rudder," In 4th Ship Control system Symposium-SCSS*, Netherland, 1975.

[14] Fossen, T. I., *"A Nonlinear Unified State-Space model for Ship Maneuvering and Control in a Seaway," International Journal of Bifurcation and Chaos (IJBC)*, vol. 15, pp. 2717-2746, 2005.

[15] Perez, T., *"Previous Research in Control of Rudder Roll Stabilisation and Fin Stabilisers," In Ship Motion Control*, ed: Springer London, 2005, pp. 193-205.

[16] Lloryd, A. R. J. M., *"Roll Stabilization by Rudder,"* in *4th Ship Control system Symposium-SCSS*, Netherland, 1975.

[17] Van der Klugt, P. G. M, *"Rudder Roll Stabilization,"* PhD, Delft University of Technology, Netherland, 1987.

[18] Van Amerongen, J., Van der Klugt P. and van Nauta L. H., *"Rudder Roll Stabilization for Ships," Automatica*, vol. 26, pp. 679-690, 1990.

[19] Blanke, M. and Yang, C., *"Rudder Roll Damping Controller Design Using μ-Synthesis," In Proceeding of IFAC CAMS'98*, 1998, pp. 127-132.

[20] Haals, P., Blanke, M. and Andreasen, K. K., , "*Rudder roll damping experience in Denmark," In Proc. Of IFAC workshop CAMS'89*, Lyngby, Denmark, 1989.

[21] Adrian, J., Blanke, M., Larsen, K. and Bentsen, J., *"Rudder Roll Damping in Coastal Region Sea Conditions," In Proc of 5th IFAC Conference on Maneuvering and Control of Marine Craft, MCMC'2000*, 2000.

[22] Kallstrom, C.G., Wessel, P. and Sjolander, S., "*Roll Reduction By Rudder Control," In Spring Meeting-STAR Symposium 3rd IMSDC*, 1988.

[23] Christensen, A. and Blanke, M., *"Rudder Roll Damping Autopilot Robustness to Sway-Yaw-Roll Couplings," In Proc. 10th SCSS*, Ottawa, Canada, 1993, pp. 93-119.

[24] Blanke, M. and Hearns, G., *"Quantitative Analysis and Design of Rudder Roll Damping Controllers," In Proc. Of CAMS'98*, 1988.

[25] Zhou, W.-W., Cherchas, D. B. and Calisal, S., *"Identification of rudder—yaw and rudder—roll steering models by using recursive prediction error techniques," Optimal Control Applications and Methods,* vol. 15, pp. 101-114, 1994.

[26] Zhou, W.-W., Chercas, D., Calisal, S. and Tiano, A., "*A New Approach for Adaptive Rudder Roll Stabilization Control," In Proc. Of the 9th Ship Control System Symposium*, 1990, pp. 115-127.

[27] Katebi, M. R., Wong, D. D. K. and Grimble, M. J., "*LQG Autopilot and Rudder Roll Stabilization Control System Design," In Proc of the 8th Ship Control System Symposium*, 1987.

[28] Hearns, G. and Blank, M., *"Quantitative Analysis and Design of Rudder Roll Damping Controller,"* In Technical Report R-1998-4243, Department of Control Engineering, Aalborg University, Denmark, 1997.

[29] Stroustrup, J., Niemann, H. H. and Blanke, M., *"A Multi Objective H_∞ Solution to The Rudder Roll Damping Problem," In Proc. Of CAMS'95*, 1995.

[30] Sharif, M. T., Roberts, G. N. and Sutton, R., *"Robust Fin/Rudder Roll Stabilization," In Proc. IEEE 3rd Conference on Control Applications* 1994, pp. 1107-1112.

[31] Blanke, M., *"Uncertainty Models for Rudder Roll Damping Control," In Proc. Of IFAC World Congress*, 1996.

[32] Fossen, T. I. and Laudval, T., *"Nonlinear Rudder-Roll Damping of Non-Minimum Phase Ships Using Slide Mode Control," In Proc. Of the European Control Conference* Brussels, Belgium, 1997.

[33] Oda, H., Ohtsu, K. and Hotta, T., *"Statistical Analysis and Design of a Rudder Roll Stabilization System," Control Engineering Practice,* vol. 4, pp. 351-358, 1996.

[34] Sasaki, M., Oda, H., Seki, Y., Ohtsu, K. and Hotta, T., *"Actual Experiences in Designing Rudder Roll Control Systems," In Proc. of IFAC Conference on Control Applications of Marine Systems-CAMS*, 1992.

[35] Oda, H., Ohtsu, K. and Hotta, T., "*A Study on Roll Stabilization by Rudder Control," Journal of Japan Institute of Navigation* 1995.

[36] Oda, H., Sasaki, M., Seki, Y. and Hotta, T., *"Rudder Roll Stabilization Control System Through Multivariable Autoregressive Model," In Proc. of IFAC Conference on Control Applications of Marine Systems –CAMS*, 1992.

[37] Bitmead, R., Gevers, M. and Wertz, V., *"Adaptive Optimal Control: The thinking Man's GPC,"* Prentice Hall, New York, 1990.

[38] Perez, T. and Goodwin, G. C., *"On Constrained Control of Fin, Rudder or Combined Fin Rudder Stabilizers: A Quasi-Adaptive Control Strategy," In IFAC Conference on Control Applications of Marine Systems –CAMS*, 2004, pp. 113-118.

[39] Perez, T., Goodwin, G. C. and Tzeng, C. Y., *"Model Predictive Rudder Roll Stabilization Control for Ships," In 5th IFAC Conference on Manoeuvring and Control of Marine Crafts. (MCMC2000)*, Aalborg, Denmark, 2000.

[40] Perez, T. and Goodwin, G. C., *"Constrained Predictive Control of Ship Fin Stabilizers to Prevent Dynamic Stall," Control Engineering Practice,* vol. 16, pp. 482-494, 2008.

[41] Goodwin, G. C., Graebe, S. and Salgado, M., *"Control Systems Design,"* Prentice Hall, Inc. New York. 2001.

[42] Tzeng, C. Y., Wu, C. Y. and Chu, Y. L.,*"A Sensitive Function Approach to the Design of Rudder Roll Stabilization Controller," Journal of Marine Science and Technology,* vol. 9, pp. 100-112, 2001.

[43] Moreira, L., Fossen, T. I. and Guedes, S. C., *"Path following control system for a tanker ship model," Ocean Engineering*, vol. 34, pp. 2074-2085, 2007.

[44] Çimen, T., *"Development and validation of a mathematical model for control of constrained non-linear oil tanker motion,"* Mathematical and Computer Modelling of Dynamical Systems: Methods, Tools and Applications in Engineering and Related Sciences, vol. 15, pp. 17 - 49, 2009.

[45] Omerdic, E. and Roberts, G., "*Thruster fault diagnosis and accommodation for open-frame underwater vehicles," Control Engineering Practice,* vol. 12, pp. 1575-1598, 2004.

[46] Hegrenses, O., Hallingstad, O. and Jalving, B., "*Comparison of Mathematical Models for the HUGIN 4500 AUV Based on Experimental Data,*" *In Underwater Technology and Workshop on Scientific Use of Submarine Cables and Related Technologies Symposium , 2007*, pp. 558-567.

[47] Velasco, F. J., Revestido, E., Moyano, E. and López, E., *"Remote laboratory for marine vehicles experimentation," Computer Applications in Engineering Education*, 2010.

[48] SNAME, *"The Society of Naval Architects and Marine Engineers,"* In Nomenclature for Treating the Motion of a Submerged Body through a Fluid, Technical and Research Bulletin, No.1-5, 1950.

[49] Kyu, H., Sun, Y. N., Gyeong, S. and Lee, J., *"Estimation of the Roll Hydrodynamic Moment Model of a Ship by Using the System Identification Method and the Free Running Model Test," Oceanic Engineering, IEEE Journal of,* vol. 32, pp. 798-806, 2007.

[50] Van der Heijden, F., Duin, R. P. W., De Ridder, D. and Tax, D. M. J., "*Classification, Parameter Estimation and State Estimation :An Engineering Approach using MATLAB,"* John Wiley & Sons Ltd, The Atrium, Southern Gate, Chichester, West Sussex, London, 2004.

[51] Hongwei, B. and Weifeng, J. Z. T., "IAE-Adaptive Kalman Filter for INS/GPS Integrated Navigation System," *Journal of Systems Engineering and Electronics*, vol. 17, pp. 502-508, 2006.

[52] Francois, D. E. C., Denis, P. and Philippe,V., "*GPS/IMU Data Fusion Using Multisensor Kalman Filtering: Introduction of Contextual Aspects," Information Fusion*, vol. 7, pp. 221-230, 2006.

[53] Bijker J. and Steyn, W.,*"Kalman Filter Configurations for a Low-Cost Loosely Integrated Inertial Navigation System on an Airship," Control Engineering Practice,* vol. 16, pp. 1509-1518, 2008.

[54] Loebis, D., Sutton, R., Chudley, J. and Naeem, W., *"Adaptive Tuning of a Kalman Filter via Fuzzy Logic for an Intelligent AUV Navigation System," Control Engineering Practice,* vol. 12, pp. 1531-1539, 2004.

[55] Zirilli, A., Roberts, G. N., Tiano, A. and Sutton, R., "Adaptive Steering of a Containership Based on Neural Networks," *International Journal of Adaptive Control and Signal Processing,* vol. 14, pp. 849-873, 2000.

[56] Blanke, M., "*Ship Propulsion Losses Related to Automated Steering and Prime Mover Control,"* PhD Thesis, The Technical University of Denmark, Lyngby, 1981.

[57] Gianluca, A., Fossen, T. I. and Yoerger, D. R., "*Underwater Robotics," In Springer Handbook of Robotics*, B. Siciliano and O. Khatib, Eds., ed: Springer Berlin Heidelberg, 2008, pp. 987-1008.

[58] Van Berlekom, W. B., *"Effects of Propeller Loading on Rudder Efficiency*," *In Proceedings of the 4th International Ship Control Systems Symposium (SCSS'75)*, Haag, Netherland, 1975, pp.5.83-5.98.

[59] Davidson, K. S. M. and Schiff, L. I., "*Turning and Course Keeping Qualities," Transactions of SNAME,* vol. 54, 1946.

[60] Nomoto, K., Tauguchi, T., Honda, K. and Hirano, S., *"On the Steering Qualities of Ships,"* Technical Report , International Shipbuilding Progress, Vol 4.," 1957.

[61] Tomera, M., "*Nonlinear Controller Design of a Ship Autopilot," International Journal of Applied Mathematics and Computer Science*, vol. 20, pp. 271-280, 2010.

[62] Triantafyllou, M. S. and Hover, F. S., *"Maneuvering and Control of Marine Vehicles,"* Cambridge Press, Massachusetts, USA, 2003.

[63] Fossen, T. I. and Blanke, M., *"Nonlinear Output Feedback Control of Underwater Vehicle Propellers using Feedback from Estimated Axial Flow Velocity," IEEE Journal of Oceanic Engineering,* vol. 25, 2000.

[64] Whitecomb, L. L. and Yoerger, D. R., *"Preliminary Experiments in Model-Based Thruster Control for Underwater Vehicle Positioning," IEEE Journal of Oceanic Engineering*, vol. 24, pp. 495-506, 1999.

[65] El-Hawary, F., *"The Ocean Engineering Handbook,"* The Electrical Engineering Handbook Series. Boca Raton, Florida: CRC Press LLC, 2001.

[66] Sørensen, A. J., *"Structural Issues in the Design and Operation of Marine Control Systems," Annual Reviews in Control,* vol. 29, pp. 125-149, 2005.

[67] Newman, J. N., *"Marine Hydrodynamics,"* MIT Press, Cambridge, MA, 1977.

[68] Ohtsu, K., *"Tracking Problem,"* 2006. Available: http://asari.soi.wide.ad.jp/class/20050026/slides/04/29.html. Accessed: August, 2009.

[69] Gertler, M. and Hagen, G. R., "*Handling Criteria for Surface Ships"*, Technical Report DTMB-1461, Naval Ship research and Development Center,Washinton D.C1960.

[70] 12thITTC, *"A Review of Methods Defining and Measuring the Maneuverability of Ships," In Proceedings of the 12th International Towing Tank Conference*, Rome, 1969a, pp. 1-19.

[71] 14thITTC, "*Discussions and Recommendations for an ITTC 1975 Maneuver Trial Code," In Proceedings of the 14th International Towing Tank Conference*, Ottawa, 1975, pp. 348-365.

[72] Ohtsu, K. and Ishizuka, M., *"Statistical Identification and Optimal Control of Marine Engine," In Proc. of 2nd IFAC Workshop on Control Applications in Marine Systems*, Genova, Italy, 1992.

[73] Horigome, M., Hara, M., Hotta, T. and Ohtsu,K., *"Computer Control of Main Diesel Engine Speed for Merchant Ships," In Proc. of ISME Kobe90*, Kobe, Japan, 1990.

[74] Oosterveld, M. W. C. and Van Oossanen, P., *"Further computer-analyzed data of the Wageningen B-screw series," Int. Shipbuilding Progress*, vol. 22, pp. 251-262, 1975.

[75] Hearly, A. J., Rock, S. M., Cody, S., Miles, D. and Brown, J. P., *"Toward an Improved Understanding of Thrust Dynamics for Underwater Vehicles," IEEE Journal of Oceanic Engineering*, vol. 20,4, pp. 354-360, 1992.

[76] Blanke, M., Lindegaard, K. P. and Fossen, T. I., *"Dynamic Model for Thrust Generation of Marine Propellers," In Proceedings of IFAC Conference on Maneuvering and Control of Marine Craft (MCMC'2000)*, Aalborg,Denmark, 2000.

[77] Smogeli, Ø. N., Sørensen, A. J. and Minsaas, K. J., *"The Concept of Anti-Spin Thruster Control," Control Engineering Practice*, vol. 16, pp. 465-481, 2008.

[78] Blanke, M. and Fossen, T. I., *"Nonlinear Output Feedback Control of Underwater Vehicle propellers using feedback form estimated axial flow velocity," Oceanic Engineering, IEEE Journal of*, vol. 25, pp. 241-255, 2000.

[79] Minsaas, K. J., Thon, H. J. and Kauczynski, W., *"Influence of Ocean Environment on Thruster Performance,"* In Proc. Int. Symposium, Propeller and Cavitation,Supplementary volume, Shanghai:The Editorial Office of Shipbuilding of China, 1986.

[80] Sørensen, A. J. and Smogeli, Ø. N., *"Torque and Power Control of Electrically Driven Marine propellers," Control Engineering Practice*, vol. 17, pp. 1053-1064, 2009.

[81] van Zwieten, J. H. and Driscoll, F. R., *"A Comprehensive General Simulation of Small Twin Screw Displacement Hull Boats with Validation," Mathematical and Computer Modelling of Dynamical Systems: Methods, Tools and Applications in Engineering and Related Sciences*, vol. 14, pp. 269 - 301, 2008.

[82] Robot-Electronics, *"SRF05-Ultra-Sonic Ranger," Technical Specification,* 2005.Available: http://www.robot-electronics.co.uk/htm/srf05tech.htm. Accessed: July 2009.

[83] Hitec, *"HS-7950TH Ultra Torque HV Coreless Titanium Gear Servo,"* 2010. Available: http://www.hitecrcd.com/products/servos/digital/hv-ultra-premium-digital/hs-7950th.html. Accessed: March 2010.

[84] Parallax Inc., *"Hitachi HM55B Compass Module,"* 2005. Available: http://www.parallax.com/dl/docs/prod/compshop/HM55BModDocs.pdf. Accessed: September 2009.

[85] Premerlani, W. and Bizard, P., *"Direction Cosine Matrix: Theory,"* 2009. Available: http://gentlenav.googlecode.com/files/DCMDraft2.pdf. Accessed: September 2009.

[86] Drones, D. I. Y., *"DIY Drones-The Amateur UAV SuperStore,"* 2010. Available: http://store.diydrones.com/ArduIMU_V2_Flat_p/kt-arduimu-20.htm. Accessed: February 2010.

[87] Analog Devices, *"Small, Low Power 3-Axis ±3g Accelerometer ADXL335,"* 2009. Available: http://api.ning.com/files/vuLVL7FAtL5UFAb8JcPW*Y2072K8FbqRFcjGsQm-YrsxNL*NLqdModEjPLbOTqa0rB-JwP7YG3splBtAxt5CEq7Z37tlnEM4/adxl335.pdf

[88] ST-Microelectronics, *"LPR530AL MEMS Motion Sensor: Dual Axis Pitch and Roll ± 300 °/s Analog Gyroscope,"* 2009. Available: http://api.ning.com/files/PP1zbrJcnJxWPnI1bg1aFLzvBQ0pxMxos8uAyHCT0Xstr-eeAI5P-mzFAib4pJR*c1fDbwIoIrLB2ih0 le8b4jWOtyYcYuN/lpr530al.pdf. Accessed: March 2010.

[89] ST-Microelectronics, *"LY530ALH MEMS Motion Sensor: High Performance ±300 °/s Ananlog Yaw-rate Gyroscope,"* 2009. Available: http://api.ning.com/files/btvkW9HA84tfowJHxvQcBmYJzWkOKWz8zWKm2Hg-fox*WYxPRqT6N12xEWhdckGi*12CrhBziVs1zw-iZgNcXwmA*h0g-5ki/LY530ALH.pdf Accessed: March 2010.

[90] DRONES, D. I. Y., *"DIY Drones- The Amateur UAV SuperStore,"* 2010. Available: http://store.diydrones.com/category_s/10.htm. Accessed: February 2010.

[91] Digi, *"XBee-PRO DigiMesh 900-Mesh Networking Embedded Rf Modules for OEMs,"* Available: http://www.digi.com/pdf/ds_xbeeprodigimesh900.pdf. Accessed: March 2010.

[92] Robot-Electronics, *"CMPS03 - Compass Module,"* 2008. Availabe: http://www.robot-electronics.co.uk/htm/cmps3tech.htm. Acccessed: February, 2010.

[93] VIVOTEK, *"VIVOTEK IP7330 Network Bullet Camera,"* 2010. Available: http://www.vivotek.com/products/model.php?network_camera=ip7330. Accsessed: August 2009.

[94] FLIR Systems Inc. *"PathFindIR," 2008*. Available: http://www.flir.com/uploadedFiles/Brochure_PathFindIROEM.pdf. Accessed: June 2010.

[95] O'Kane, J. M., Tovar, B., Cheng, P. and LaValle, S. M., *"Algorithms for Planning under Uncertainty in Prediction and Sensing,"* Taylor & Francis Group, LLC, 2006.

[96] Milisavljevic, I. R. N., *"Sensor and Data Fusion,"* In-Tech, Croatia, 2009.

[97] Pearl, J., *"Probabilistic Reasoning in Intelligent Systems," 2nd ed.* Elsevier, 1988.

[98] Clancey, W. J., *"Heuristic classification,"* In proc. *Artificial intelligence,* vol. 27, pp. 289-350, 1985. Also in: Knowledge Based Problem Solving, (Ed.) Janusz, S. K., Prentice-Hall, 1986.

[99] Cohen, P. R., *"Heusristic reasoning about uncertainty: An artificial intelligence approach,"* TR-STAN-CS-83-986, Dept. of Computer Science, Stanford University, 1985. Also in press by Pitman Publishing, Inc. Marshfield, MA, USA.

[100] Chandrasekaran, B., and Mittal, S., *"Conceptual Representation of Medical Knowledge for diagnosis by Ccomputer: MDX and related systems," In Advances in Computers. ed. M.C. Yovits. 22.,217-93*. 1983.

[101] Polya, G., *" Patterns of Plausible Inference,"* Princeton University Press, Princeton. 1954.

[102] Harnad, S., *"Mind, Machines and Searle," Physica D 42*, pp. 335–346, 1989.

[103] Harnad, S., *"The Symbol Grounding Problem," Journal of theoretical and experimental artificial intelligence,* vol. 1, pp. 5–25, 1990.

[104] Christian, L., Bessière, P. and Siegwart, R., *"Probabilistic Reasoning and Decision Making in Sensory-Motor Systems," Springer Tracts in Advanced Robotics,* vol. 46, 2008.

[105] Finkelstein, L. and Finkelstein, A. C. W., *"Design Principles for Instrument Systems in Measurement and Instrumentation," Finkelstein,L., and Grattan K. T. V., Eds.*, Pergamon Press, Oxford, UK, 1994.

[106] Von Newman, J. and Morgenstenstern, O., *"Theory of Games and Economic Behaviour," 2nd ed.* Princeton University Press, Princeton, 1947.

[107] Bessière, P. and Lebeltel, O., *"Basic Concepts of Bayesian Programming,"* in *Probabilistic Reasoning and Decision Making in Sensory-Motor Systems*. vol. 46, P. Bessière, *et al.*, Eds., Springer Berlin / Heidelberg, 2008, pp. 19-48.

[108] Robinson, J. A., *"A Machine-Oriented Logic Based on the Resolution Principle," Journal of the ACM*, vol. 12, pp. 23-41, 1965.

[109] Robinson, J. A.,*"Logic: Form and Function"*. North-Holland, Amsterdam, 1979.

[110] Sam Ge, S. and Lewis, F. L., *"Autonomous Mobile Robots: Sensing, Control, Decision Making and Applications,"* Control Engineering Series. Boca Raton: CRC Taylor & Francis Group, 2006.

[111] Sasiadek, J. Z.,*"Sensor Fusion," Annual Reviews in Control*, vol. 26, pp. 203-228, 2002.

[112] Shacklock, A., Xu, J. and Wang, H., *"Visual Guidance for Autonomous Vehicles: Capabilities and Challenges,"* Taylor & Francis Group, LLC, 2006.

[113] Lee, S., Hanseok, K. and Hernsoo, H., *"Multisensor Fusion and Integration for Intelligent Systems," Lecture Notes in Electrical Engineering*, vol. 35, 2008.

[114] Martin, E., Hall, D. L. and Llinas, J., *"Handbook of Multisensor Data Fusion- Theory and Practice," The Electrical Engineering and Applied Signal Processing Series*, 2009.

[115] Smith, R. C., and Erickson, G. J., *"Multisensor Data Fusion: Concepts and Principles,"* In Proc. IEEE Pacific Rim Conference on Communication, Computers and Signal Processing 1991.

[116] Llinas, J. and Hall, D. L., *"An Iintroduction to Multi-sensor Data Fusion, in Circuits and Systems," 1998. ISCAS '98. Proceedings of the 1998 IEEE International Symposium on*, 1998, pp. 537-540 vol.6.

[117] Hall, D. L. and Llinas, J., *"Handbook of Multisensor Data Fusion," The Electrical Engineering and Applied Signal Processing Series*, 2001.

[118] Crowley, J. L., *"Dynamic modeling of Free-Space for a Mobile Robot,"* In Proc. at the IEEE Conference on Robotics and Automation, Scottsdale, 1989.

[119] Crowley, J. L. and Demazeau, Y., *"Principles and Techniques for Sensor Data Fusion," Signal Process.*, vol. 32, pp. 5-27, 1993.

[120] Crowley, J. L. and Ramparany, F.,*"Mathematical Tools for Manipulating Uncertainty in Perception," AAAI Workshop on Spatial Reasoning and Multi-Sensor Fusion*. Kaufmann Press, 1987.

[121] Cheng, Y. L. J., Thomas, E. R. and Farrell, J. A., *"Data Fusion via Kalman Filter: GPS and INS,"* Taylor and Francis Group, LLC, 2006.

[122] Welch, G. and Bishop, G., *"Integrated GPS and INS,"* 2006. Available: http://www.cs.unc.edu/~welch/kalman/Levy1997/fig6.htm Accessed: October 2009

[123] Drones, D. I. Y., *"Config Tool," 2009*. Available: http://code.google.com/p/ardupilot/wiki/ConfigTool. Accessed : May 2009.

[124] Larry, L., *"Arduino + Processing- Make a Radar Screen to Visualize Sensor Data From SRF05,"* Available: http://luckylarry.co.uk/arduino-projects/arduino-processing-make-a-radar-screen-to-visualise-sensor-data-from-srf-05-part-1-setting-up-the-circuit-and-outputting-values/. Accessed: February 2009.

[125] Fernsler, J.,*"Wii Nunchuck To Maya,"* 2010. Available: http://www.jfernsler.com/blog Accessed: May 2010.

[126] Mathworks, *"MATLAB and Simulink,"* 2010 . Available:http:// www.mathworks.com. Accessed: February 2010.

[127] Dimension Engineering, *"Sabertooth 2x50HV,"* 2009. Available: http://www.dimensionengineering.com/datasheets/sabertooth2x50hv.pdf. Accessed: April 2010.

Appendix A

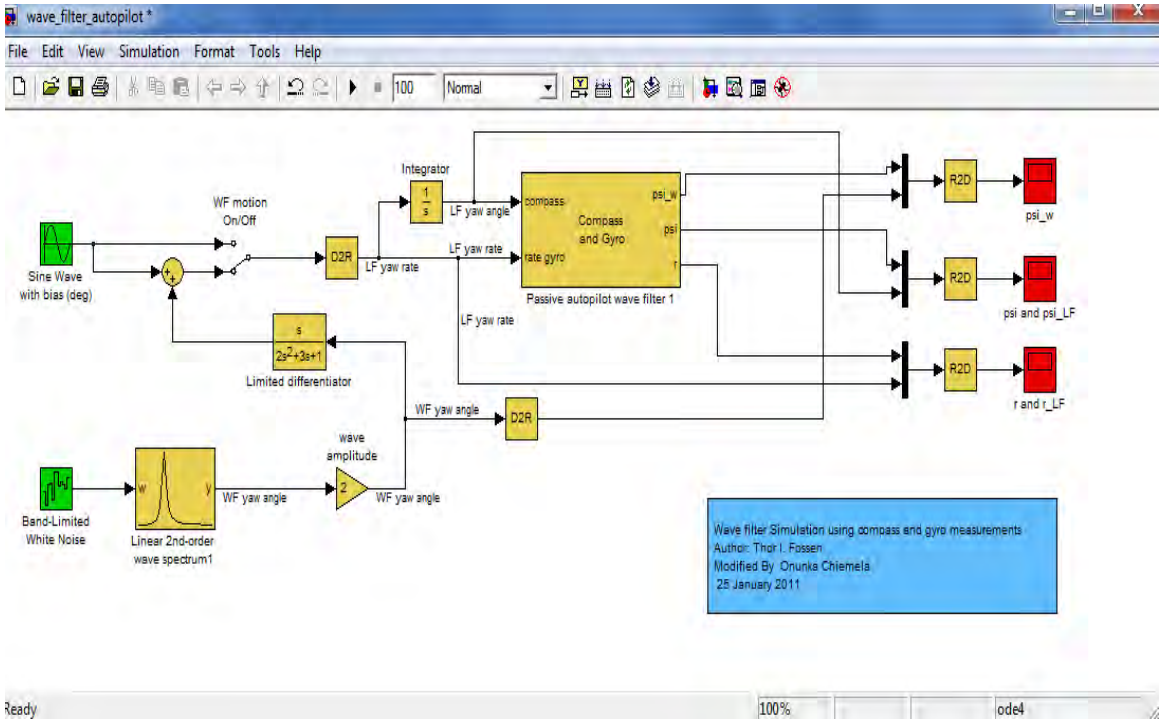

Figure A-1: The Simulink Setup of a Gyro-Compass Autopilot

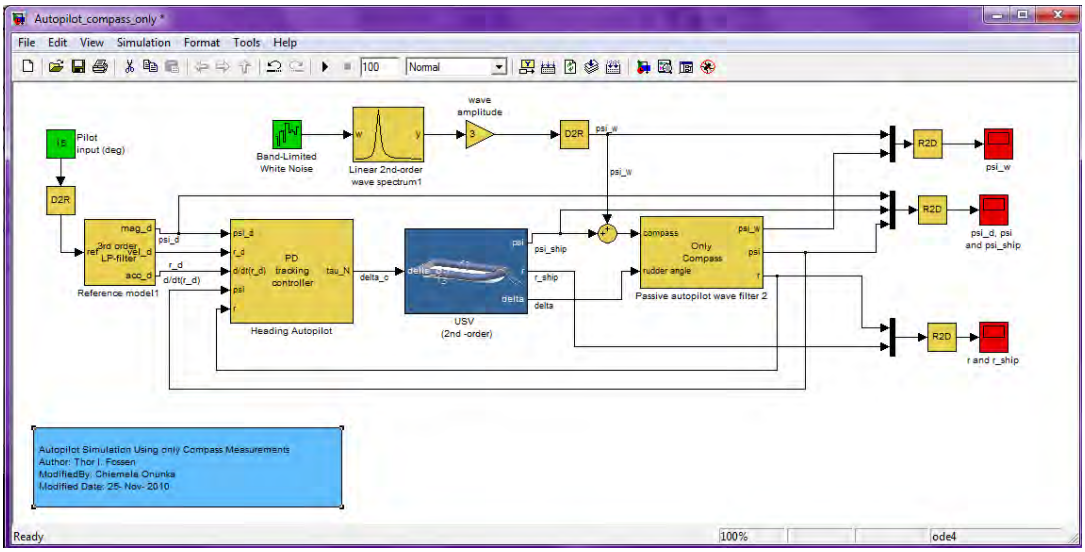

Figure A-2: The Simulink Setup of a Compass only Autopilot

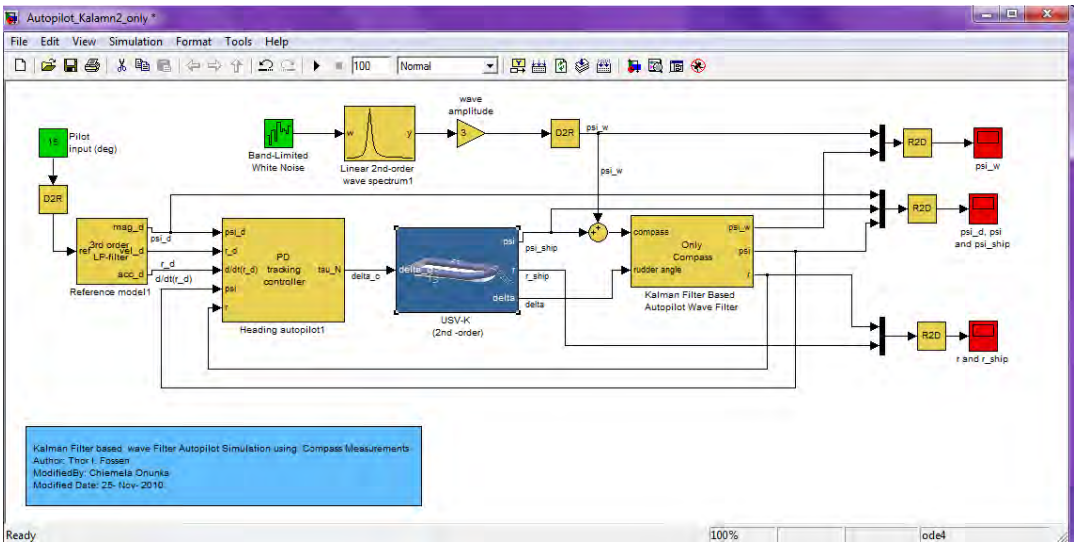

Figure A-3: The Simulink Setup a Kalman Filter Based Autopilot

Figure A-4: Straight Stability Selection Menu

Appendix B

B-1 Maximum Motor Power

The maximum motor power in Kilowatts was determined by the manufacturer. This was determined using the following procedure and shall exceed that which was calculated using the following formula:

$P_{max} = 10 \times F(d) - 33$

where

P_{max} is the maximum motor power rating in kilowatts, determined in accordance with ISO 8665;

F (d) is the dimensional factor = *l x b*

where

l is the overall length of the boat in meters from bow to the extremity of the rear float; *b* is the overall beam of the boat in meters."

The overall length of the marine craft was 2.5*m* and the breath was 1.5*m*

F(d) = 2.5 *x* 1.5

= 3.75 m^2

$$P_{max} = 10 \times F(d) - 33$$

$$P_{max} = 10 \times 37.5 - 33$$

P_{max} = 4.5 Kilowatts

B-2 Marine Vehicle Stability Calculations

The marine vehicle was equipped with the manufacturers maximum rated motor and it did not capsize when the maximum permissible number of persons recommended by the manufacturer moved to one side of the boat. The stability factor was determined using the following formula was not greater than the recommended threshold of 250 *kg-m*^{5} (i.e. F(s) > 250)

$$F(s) = \frac{m(l^2 \times b^3)}{1000}$$

where

F(s) is the stability factor

m is the total mass of the boat in kg

l is the overall length in meters

b is the overall beam of the boat in meters."

$$F(s) = \frac{100(2.5^2 \times 1.5^3)}{1000}$$

F(s) = 2.109 *kg-m*^{5}

Appendix C

C-1 The Ardu-IMU Board

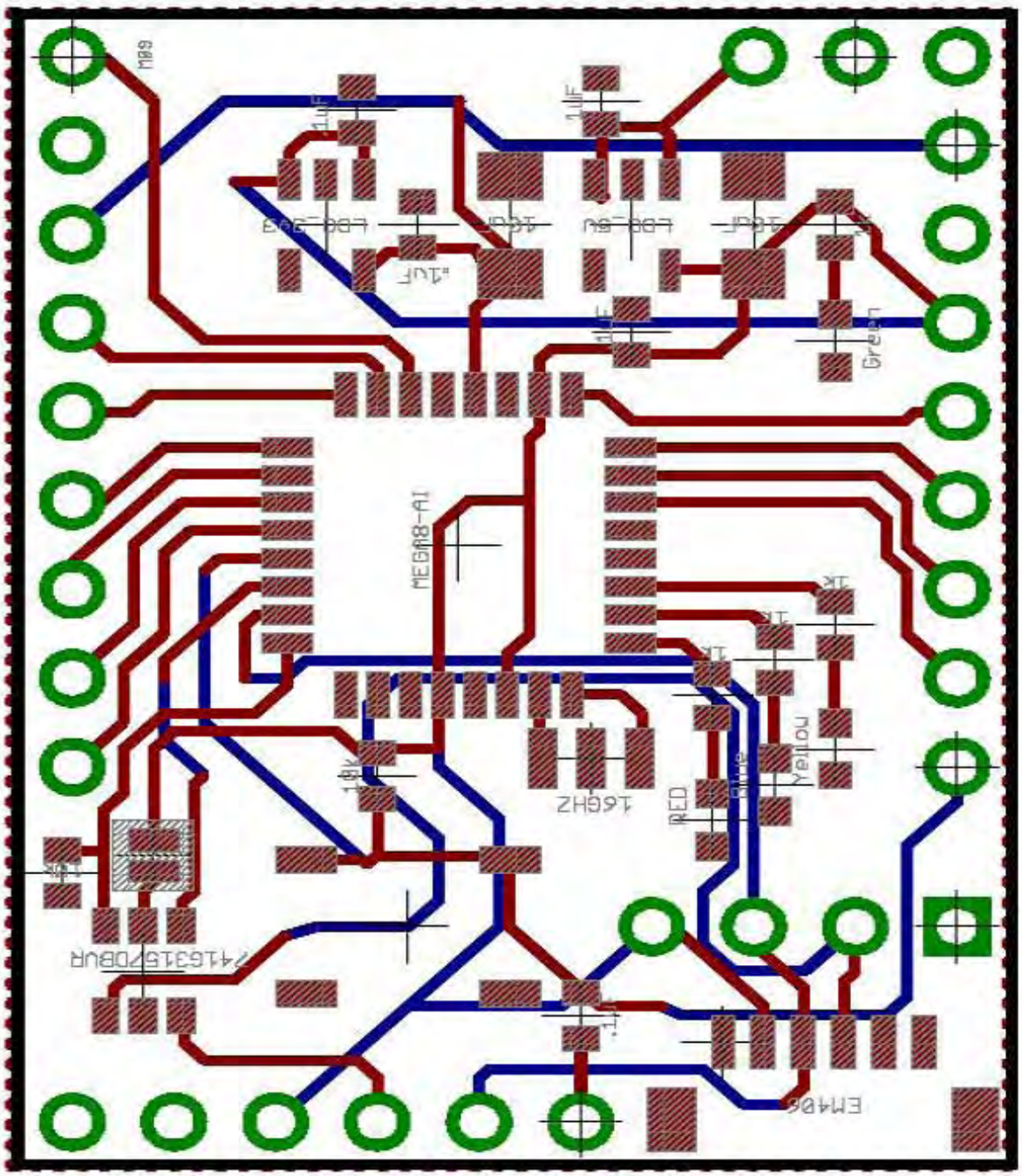

Figure C-1: Ardu-IMU Controller Board Schematic

C-2 Arduino Mega board

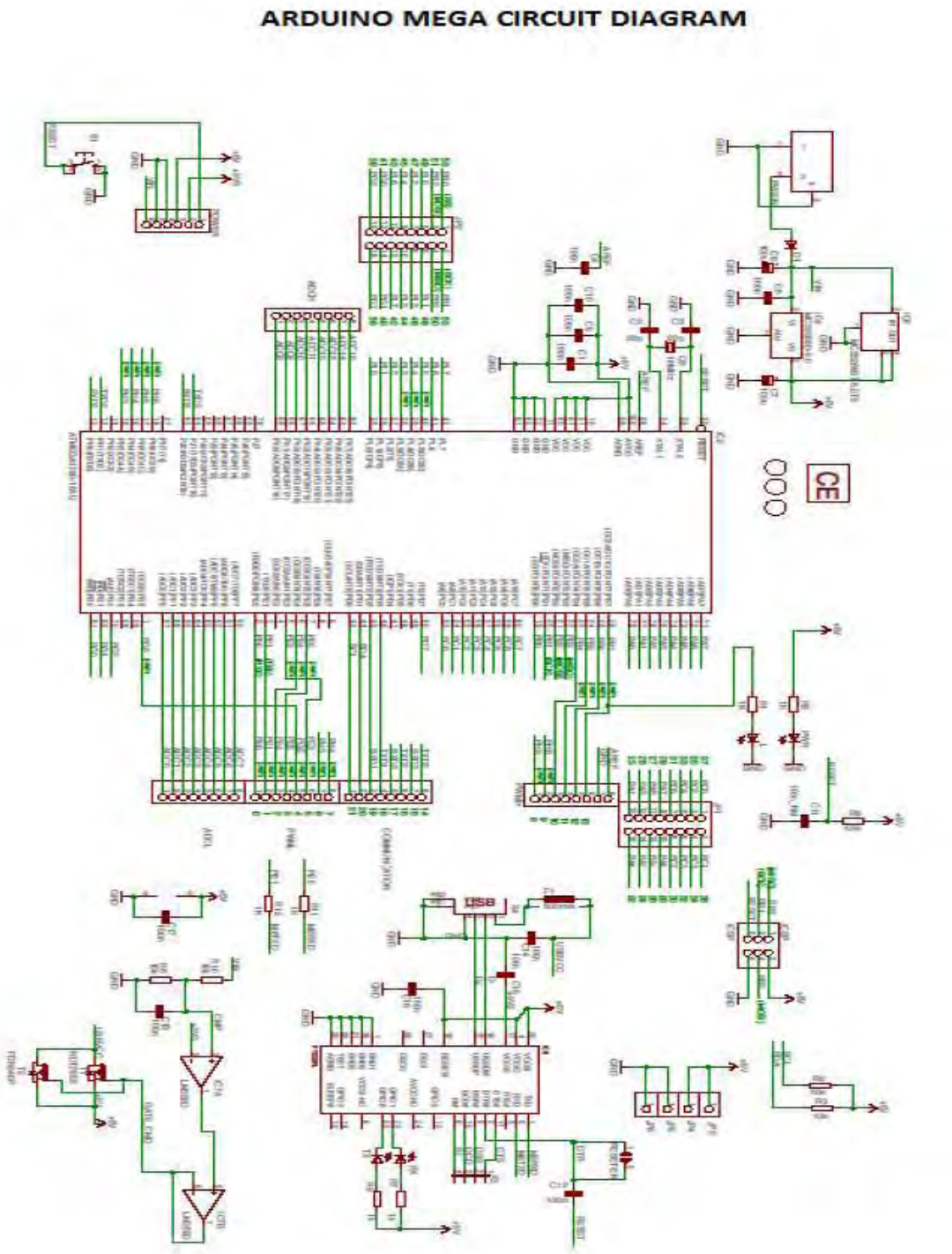

Figure C-2: Arduino Mega circuit Schematic

Digital Pin	**Arduino 328**	**Arduino Mega 1280**

C-3 ATMEGA 328 and ATMEGA 1280 Pin Configuration on Arduino

Table C-1: Arduino Board Pin Configuration

	Port	**Analog Pin**	**Usage**	**Port**	**Analog Pin**	**Usage**
0	PD 0		USART RX	PE 0		USART0 RX, pin Int 8
1	PD 1		USART TX	PE 1		USART0 TX
2	PD 2		Ext Int 0	PE 4		PWM T3B INT4
3	PD 3		PWM T2B, Ext Int 1	PE 5		PWM T3C, INT 5
4	PD 4			PG 5		PWM T0B
5	PD 5		PWM T0B	PE 3		PWM T3A
6	PD 6		PWM T0A	PH 3		PWM T4A
7	PD 7			PH 4		PWM T4B
8	PB 0		Input Capture	PH 5		PWM T4C
9	PB 1		PWM T1A	PH 6		PWM T2B
10	PB 2		PWM T1B	PB 4		PWM T2A, Pin Int 4
11	PB 3		PWM 2A, MOSI	PB 5		PWM T1A, Pin Int 5
12	PB 4		MISO	PB 6		PWM T1B, Pin Int 6
13	PB 5		SCK	PB 7		PWM T0A, Pin Int 7
14	PC 0	0		PJ 1		USART3 TX, Pin Int 10
15	PC 1	1		PJ 0		USART3 RX Pin Int 9
16	PC 2	2		PH 1		USART2 TX
17	PC 3	3		PH 0		USART2 RX
18	PC 4	4	I2C SDA	PD 3		USART1 TX, Ext Int 3

19	PC 5	5	I2C SCL	PD 2		USART1 RX, Ext Int 2
20				PD 1		I2C SDA, Ext Int 1
21				PD 0		I2C SCL, Ext Int 0
22				PA 0		Ext Memory addr bit 0
23				PA 1		Ext Memory addr bit 1
24				PA 2		Ext Memory addr bit 2
25				PA 3		Ext Memory addr bit 3
26				PA 4		Ext Memory addr bit 4
27				PA 5		Ext Memory addr bit 5
28				PA 6		Ext Memory addr bit 6
29				PA 7		Ext Memory addr bit 7
30				PC 7		Ext Memory addr bit 15
31				PC 6		Ext Memory addr bit 14
32				PC 5		Ext Memory addr bit 13
33				PC 4		Ext Memory addr bit 12
34				PC 3		Ext Memory addr bit 11
35				PC 2		Ext Memory addr bit 10
36				PC 1		Ext Memory addr bit 9
37				PC 0		Ext Memory addr bit 8
38				PD 7		
39				PG 2		ALE Ext Mem

						RD Ext Mem
40				PG 1		Wr Ext Mem
41				PG 0		ALE Ext Mem RD Ext Mem
42				PL 7		
43				PL 6		
44				PL 5		*PWM 5C
45				PL 4		*PWM 5B
46				PL 3		*PWM 5A
47				PL 2		T5 External Counter
48				PL 1		ICP T5
49				PL 0		ICP T4
50				PB 3		SPI MISO
51				PB 2		SPI MOSI
52				PB 1		SPI SCK
53				PB 0		SPI SS
54				PF 0	0	
55				PF 1	1	
56				PF 2	2	
57				PF 3	3	
58				PF 4	4	

59				PF 5	5	
60				PF 6	6	
61				PF 7	7	
62				PK 0	8	
63				PK 1	9	
64				PK 2	10	
65				PK 3	11	
66				PK 4	12	
67				PK 5	13	
68				PK 6	14	
69				PK 7	15	
FUNCTIONS NOT AVAILABLE ON ARDUINO MEGA						
				PD 6 T1(External Counter)		
				PE 6 T3, Int 6		
				PE 7 Int 7, ICP 3		
				PH 7 T4 (External		

				Counter)		
				PJ 2 Pin Int 11		

C-4 Arduino Programming Language Key words

pinMode: This command was used to assign a digital pin as input or output. This also toggles the digital pins between 0 and 5V.

digitalRead: This command was used to read the values of the digital pins. It will read any digital pin that has been configured for input.

digitalWrite: This command was used to write digital values to the digital pins. It will write to any digital pin that has been configured as an output pin.

Servo.attach: This command was used to attach an already created servo object to a digital pin.

Serial.begin: This command was used to initialize serial communication on the board.

Serial.available: This command was used to check if there are serial bytes on the serial receive pin.

Serial.read: This command was used to read serial bytes on the serial receive pin.

pulseIn: This command was used to read pulses from the RC remote control module receiver.

map: This command was used to map the values received from the RC receiver module to the actual servo pulses or PWM values.

Millis: This command was used to provide internal board timer to software architecture and to reset the board timer. It returns the number of milliseconds since the board started running.

Delay: This command was used to provide some sort of timing stamp or function within the software architecture. It pause the program to the specified number of milliseconds.

Wire.begin: This command initialized the I^2C communication protocol.

Wire.beginTransmission: This command was used to initiate I^2C communication on the I^2C bus.

Wire.send: This command was used to send information to the register we wish read on the I^2C bus.

Wire.endTransmission: This command was used to end I^2C communication on the I^2C bus.

Wire.requestFrom: This command was used to request information from an address on the I2C bus.

Wire.available: This command was used to check for information on the I^2C bus.

Wire.receive: This command was used to read or receive information on the I^2C bus.

attachInterrupt: This command was used to attach an interrupt functionality to a digital pin that is capable of handling an interrupt routine function.

analogWrite: This commands wrote PWM waves or analog values to specified digital pins. The duty cycle of the PWM can also be specified using this command.

Analog_Init: This function was used to activate ADC interrupts on the board.

ISR (ADC_vect): This function was used to initiate the interrupt service routine. It was executed each time analog values from the gyro and the accelerometer are converted to digital signals.

The software routines and implementation process are indicated in Figure 6-7 and Figure 6-8.

Appendix D

D-1 Utility Theory Axioms

The theory of utility makes use of five axioms that constrains the patterns of preference an autonomous marine craft might exhibit towards the set of possible lotteries. These lotteries are regarded as a set of general rules that the autonomous marine craft can use a basis for decision making process or the type of motion action it wants to execute. Prizes in this context are autonomous decision outcomes.

Axiom 1- Orderability: "A linear and transitive preference relation must exist between prizes of any lottery".

Using the symbol $A \geq * B$ to represent the statement that "*A* preferred or equivalent to *B*". Axiom 1 states that if C_1, C_2, and C_3 are any three prizes of some lottery then

(a) Linearity condition : either $C_1 \geq * C_2$ or $C_2 \geq * C_1$ or both and
(b) Transitivity condition : if $C_1 \geq * C_2$ and $C_2 \geq * C_3$ then $C_1 \geq * C_3$

If $A \geq * B$ and not B $\geq * A$ then it said that *A* is preferred to *B* and written as $A \geq * B$. If $A \geq * B$ and $B \geq * A$ then it is said that *A* and *B* are equivalent and written as $A - B$

Axiom 2- Continuity: "if $C_1 \geq * C_2 \geq C_3$ then there exists a lottery *L* with only two prizes, C_1 and C_3, which is equivalent to receiving C_2 for sure". i.e.,

$$L = [p, C_1; (1-p), C_3] \sim C_2$$

The probability p at which equivalence occurs will be used to calibrate the advantage of C_2 relative to the prizes C_1 and C_3.

Axiom 3 – Substitutability: "For any $0 < p \leq 1$ and any three lotteries L_1, L_2 and L_3",

$$L_1 \sim L_2 \quad iff \quad [p, L_1; (1-p), L_3] - [p, L_2; (1-p), L_3]$$

Axiom 3 alludes that adding the same prize (L_3) with the same probability (*1-p*) to two equivalent lotteries will not change the preference between the two. Hence things equivalent when considered alone remain equivalent as part of the larger context.

Axiom 4 – Monotonicity: "In comparing two lotteries each one with the same two prizes, the lottery producing the better prize with higher probability is preferred, i.e. if $C_1 > * C_2$ then

$$[p, C_1; (1-p), C_2] \geq * [p', C_1; (1-p'), C_2] \quad iff \quad p \geq p'$$

Axiom 5 – Reduction of compound lotteries: "Preferences are determined solely on the basis of the final outcomes and their associated probabilities, not on the way these outcomes are presented, i.e. for any two lotteries L_1 and L_2 = *[q, C_1 ;(1-q), C2],*

$$[p, L_1; (1-p), L_2] \sim [p, L_1; (1-p)q, C_1; (1-p)(1-q), C_2]$$

This means that the compound lottery [p, L_1 ;(1-p), L_2] with L_2 as a prize can be reduced to an equivalent lottery that lists explicitly L_2's prizes C_1 and C_2 and their associated probabilities. This axiom places no importance on the number of steps taken to achieve the required outcome.

D-2 Bayesian Inference

The probability of *A* was represented as *p (A)* while the probability of *A* and *B* was represented as *p (A, B)*. The joint distribution of the robotic motion of the marine vehicle was represented as:

p(A,B) = p(A) p(B) if the robotic motions are independent.

$$p(A|B) = \frac{p(A,B)}{p(B)}$$

The provided the platform to formulate the total probability of the robotic motion having discrete characteristics.

$$p(A) = \sum_{B} p(A|B)p(B)$$

The Bayes rule for the robotic motions then states that:

$$p(A|B) = \frac{p(B|A)p(A)}{p(B)} = \frac{p(B|A)p(A)}{\sum_{A'} p(B|A')p(A')}$$

$$p(A|B) = p(B|A)p(A)$$

D-3 The Hypotheses of Multi-Valued Autonomous Decision System

The assumption of conditional independence in Bayes formulation is justified if both the failure of the autopilot system to react to an obstacle in the path of motion of the robot and the factors that can cause the autopilot system to be activated prematurely depend solely on the systems and mechanisms relevant to the individual obstacle detection systems such as low sensitivity and internal noise in the sensors. If false alarms are activated by external conditions affecting the sensors such as power failure to the sensors, then the two hypotheses *H = obstacle detection* and *–H = No obstacle detection* may be too large to allow for sensor independence. This would require additional modification of the hypothesis. This modification condition usually occurs when a proposition or its negation covers several possible robotic states, each linked to a distinct set of evidence. Each mode of detection has a distinct effect on the sensors and has to be spelled out separately. Similarly the negation condition of no obstacle detection, each has an influence in a unique way to the obstacle detection system. For this reason it is paramount that the hypothesis space

be refined beyond the binary propositions and the group hypothesis into multi-valued variables where each variable reflects a set of exhaustive and mutually exclusive hypotheses.

Appendix E

E-1 Marine Vehicle Hull Modelling

The hydrodynamic effects on the speed of the RIB were investigated briefly using MAXSURF. The figures and tables indicate findings which observed.

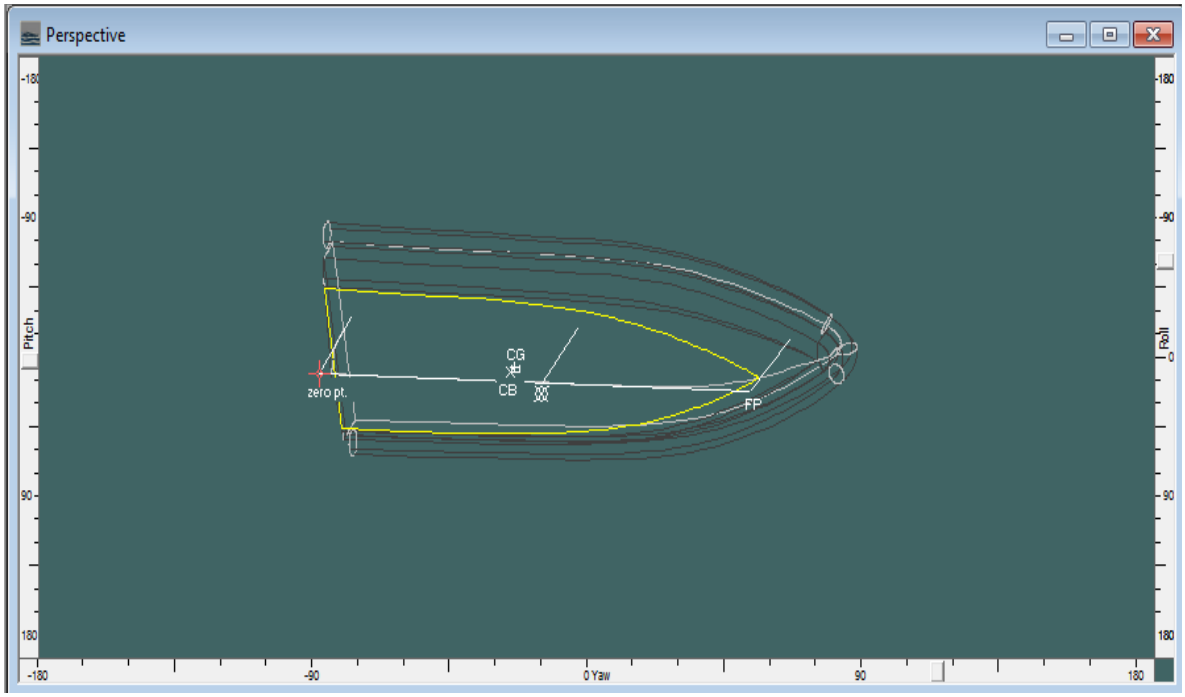

Figure E-1: RIB Model Analysis

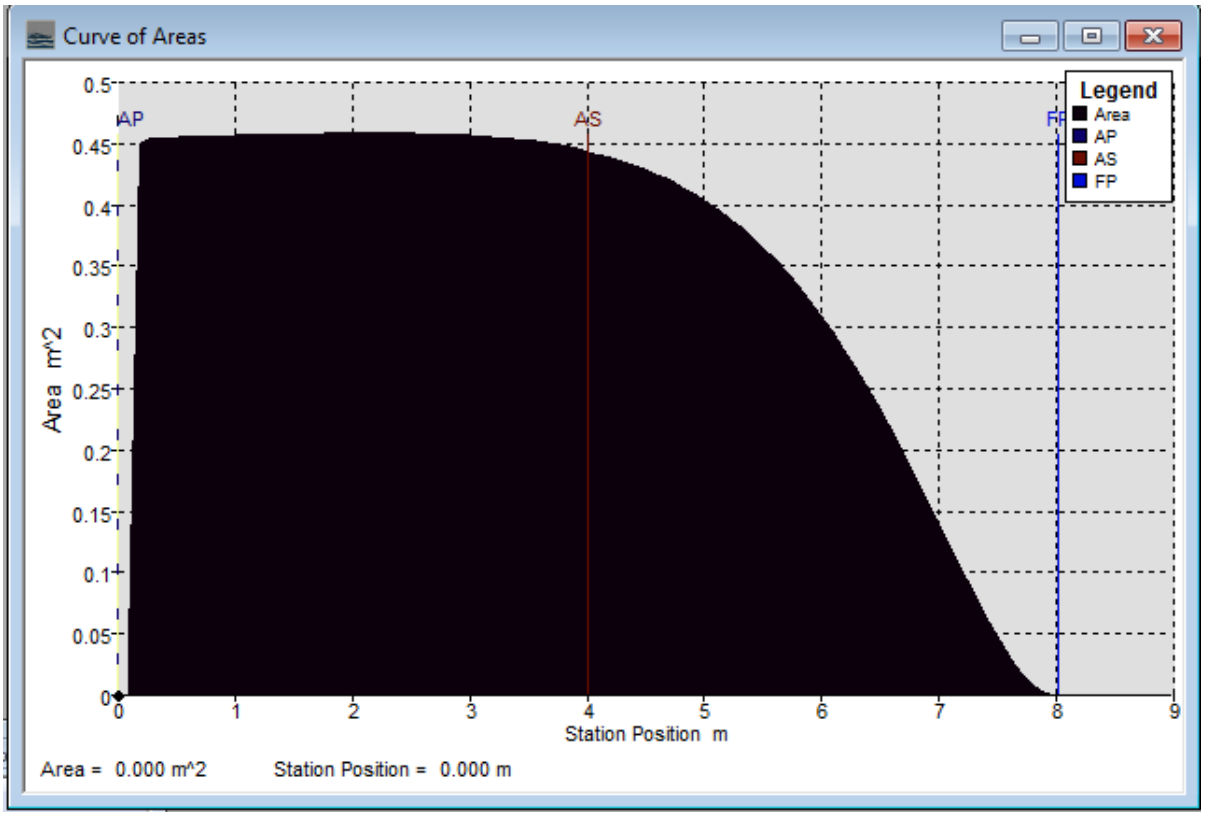

Figure E-2: RIB Curve Area

Table E-1: RIB Hull Form Data

Item	Value	Units
LWL	7.889	m
Beam	2.126	m
Draft	0.425	m
Displaced volume	2.832	m^3
Wetted Area	14.729	m^2
Prismatic Coefficient (Cp)	0.783	

Water plane area coefficient (Cwp)	0.795	
½ angle of entrance	21.77	Deg
LCG from mid-boat(+ve for d)	-0.681	m
Transform area	0.036	m^2
Transform water length beam	2.126	m
Transform draft	0.018	m
Max sectional area	0.459	m^2
Bulb transverse area	0.002	m^2
Bulb height from keel	0	m
Draft at FP	0.425	m
Deadrise at 50 % LWL	22.38	Deg
Hard chine or Round bilge	Hard chine	
Frontal area	0	m^2
Headwind	0	kts
Drag coefficient	0	
Air density	0.001	tonne/
Appendage area	0	m^2
Nominal Appendage	0	m

length		
Appendage factor	1	
Correlation allowance	0.00040	
Kinematic viscosity	0.0000011	m^2/s
Water density	1.026	tonnel/

Table E-2: Hull Speed Result

Speed (kts)	Froude No. LWL	Froude Vol.
0	0	0
0.5	0.029	0.069
1	0.058	0.138
1.5	0.088	0.207
2	0.117	0.276
2.5	0.146	0.345
3	0.175	0.414
3.5	0.205	0.483
4	0.234	0.552
4.5	0.263	0.622
5	0.292	0.691
5.5	0.322	0.76

6	0.351	0.829
6.5	0.38	0.898
7	0.409	0.967
7.5	0.439	1.036
8	0.468	1.105
8.5	0.497	1.174
9	0.526	1.243
9.5	0.556	1.312
10	0.585	1.381
10.5	0.614	1.45
11	0.643	1.519
11.5	0.673	1.588
12	0.702	1.657
12.5	0.731	1.726
13	0.76	1.795
13.5	0.79	1.865
14	0.819	1.934
14.5	0.848	2.003
15	0.877	2.072
15.5	0.907	2.141
16	0.936	2.21

16.5	0.965	2.279
17	0.994	2.348
17.5	1.024	2.417
18	1.053	2.486
18.5	1.082	2.555
19	1.111	2.624
19.5	1.141	2.693
20	1.17	2.762

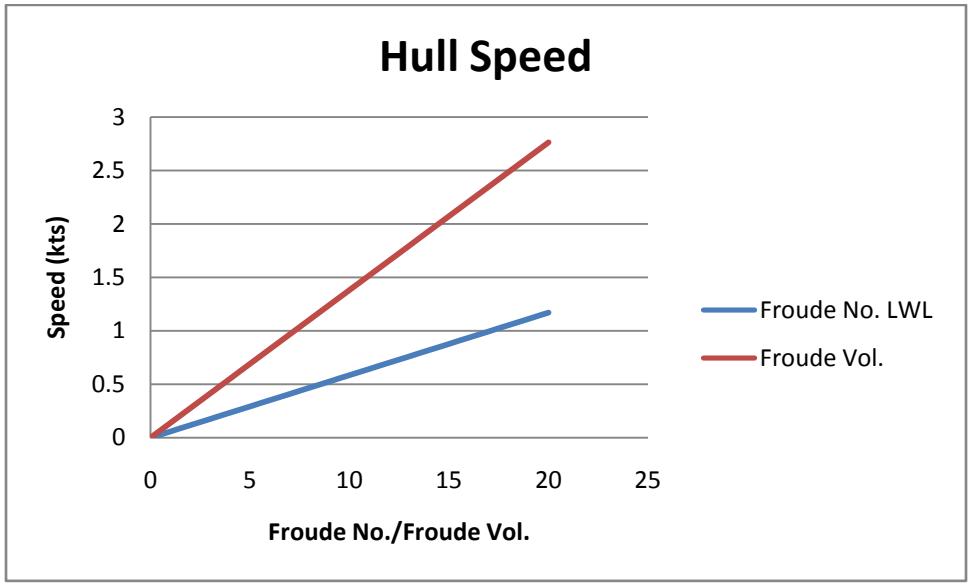

Figure E-3 : Hull Speed Analysis

Appendix F

F-1 Sabertooth Motor Driver

The Sabertooth motor driver was used to drive the USV propeller and the setup configurations are discussed in this section.

Figure F-1 :Sabertooth 2x50HV

F-2 Sabertooth Motor Driver Operating Modes and Dip Switch Setup

Mode 1: Analog Input

The analog input mode takes one or two analog inputs and uses the inputs to set the speed and direction of rotation of the propeller. The valid input range is 0v to 5v from the Arduino microcontroller board. This enables the Sabertooth to control the marine vehicle using a potentiometer, the PWM output of a microcontroller (with an RC filter) or an analog circuit.

The Analog input mode is selected by setting switches 1 and 2 to the UP position. Switch 3 should be either up or down, depending on the battery type being used. Inputs S1 and S2 are configured as analog inputs. The output impedance of the signals fed into the inputs should be less than 10k ohms for best results. In all cases, an analog voltage of 2.5V corresponds to no movement. Signals above 2.5V will command a forward motion and signals below 2.5V will command a backwards motion. There are three operating options for analog input. These are selected with switches 4, 5 and 6. All the options can be used independently or in any combination [127].

Switch 4: Mixing Mode

When switch 4 is in the UP position, the Sabertooth 2x25 is in mixed mode. This mode is designed for easy steering of differential-drive systems. The analog signal fed into S1 controls the forward/back motion of the vehicle, and the analog signal fed into S2 controls the turning motion of the vehicle. If Switch 4 is in the DOWN position, the Sabertooth 2x25 is in Independent mode. In Independent mode, the signal fed to S1 directly controls Motor 1 (outputs M1A and M1B) and the signal fed to S2 controls Motor 2 [127].

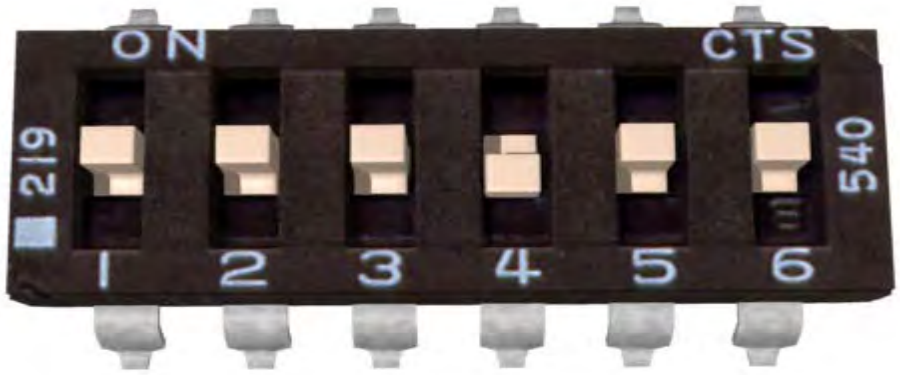

Figure F-2: Mixed or Independent Mode

Switch 5: Exponential response

When switch 5 is in the DOWN position, the response to input signals will be exponential. This softens control around the zero speed point, which is useful for control of the marine vehicle with fast top speeds or fast max turning rates. When switch 5 is in the UP position, the response is linear [127].

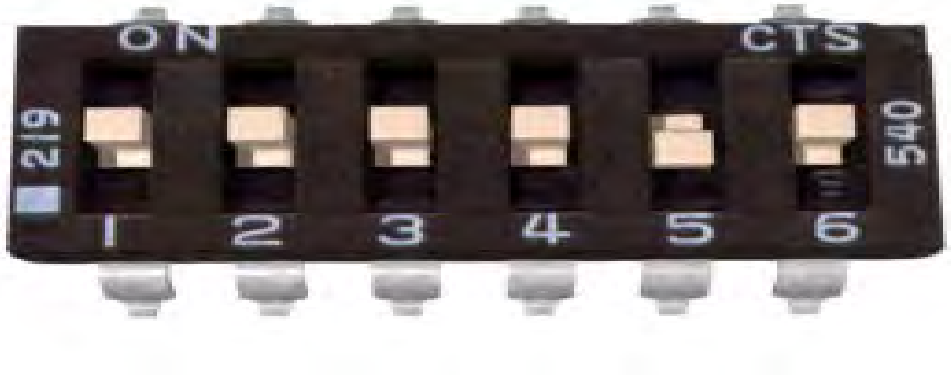

Figure F-3: Exponential Response

Mode 2: R/C Input

The R/C input mode takes two standard R/C channels and uses the inputs to set the speed and direction of the propeller. There is an optional timeout setting. When timeout is enabled, the motor driver will shut down on loss of signal. This is for safety and to prevent the marine vehicle from running away should it encounter interference this mode was used when a radio was being used to control the driver. If timeout is disabled, the motor driver will continue to drive at the commanded speed until another command is given. This enabled the Sabertooth to interface to low speed microcontrollers.

The R/C input mode is used with a standard hobby Radio control transmitter and receiver, or a microcontroller using the same protocol. The R/C mode is selected by setting switch 1 to the DOWN position and switch 2 to the UP position. When running from a receiver, it is necessary to obtain one or more servo pigtails and hook them up according to Figure 5.1 [127]**.**

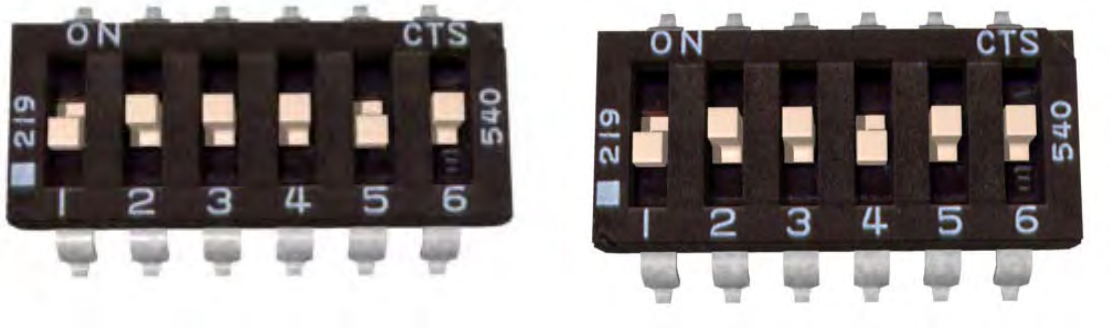

R/C Exponential mode R/C Mixed or Independent Mode

Figure F-4: R/C Input configuration

Switch 6: R/C Mode/Microcontroller Mode Select

When switch 6 is in the UP position, then the Sabertooth is in standard R/C mode. This mode is designed to be used with a hobby-style transmitter and receiver. It automatically calibrates the control center and endpoints to maximize stick usage. It also enables a Timeout Failsafe, which will shut down the propeller if the Sabertooth stops receiving correct signals from the receiver.

When switch 6 is set in the DOWN position, then Microcontroller mode is enabled. This disables the Timeout Failsafe and auto-calibration. This means that the Sabertooth will continue to drive the proppeller according to the last command until another command is given. If the control link is possible unreliable – like a radio - then this can be dangerous due to the marine vehicle not stopping. However, it is extremely convenient if you are controlling the Sabertooth from a microcontroller. In this case, commanding the controller can be done with as little as three lines of code.

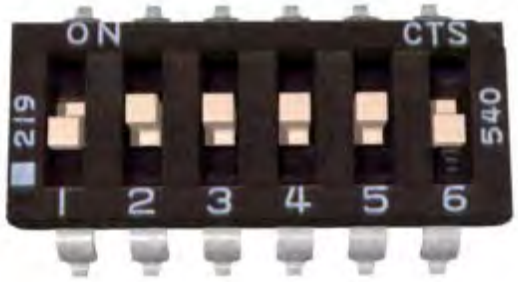

Figure F-5: Microcontroller mode

Mode 3: Simplified serial.

The simplified serial mode uses TTL level RS-232 serial data to set the speed and direction of the propeller. This is used to interface the Sabertooth to a PC or microcontroller. When using a PC, a level converter such as a MAX232 chip was used. The baud rate is set via DIP switches. Commands are single-byte. There is also a Slave Select mode which allows the use of multiple Sabertooth 2x25 from a single microcontroller serial port.

Simplified Serial operates with an 8N1 protocol – 8 data bytes, no parity bits and one stop bit.

The baud rate is selected by switches 4 and 5 from the following 4 options [127].

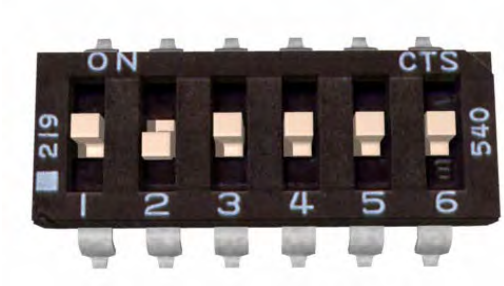

(a) Baud-rate: 2400 bps

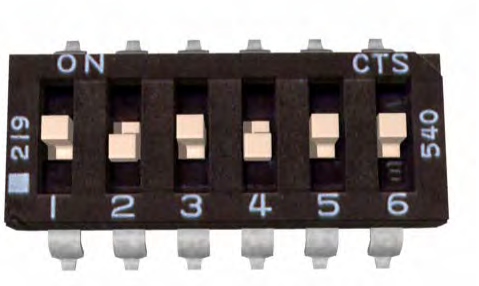

(b) Baud-rate 9600 bps

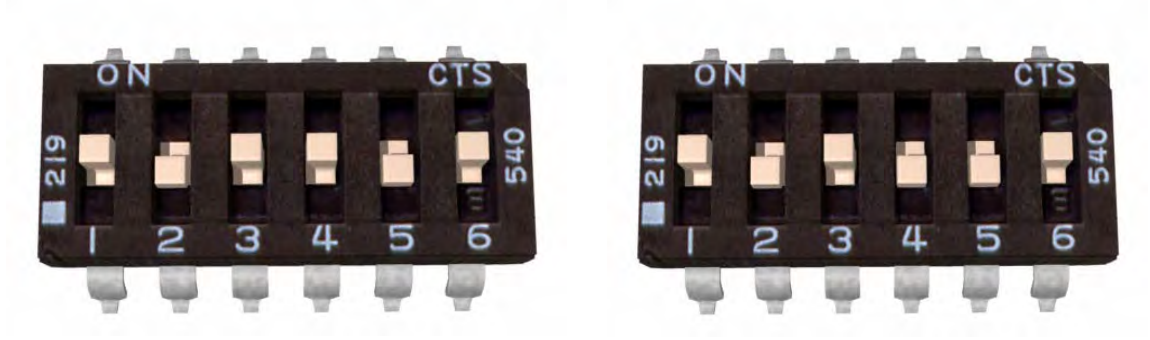

(c) Baud-rate: 19200 bps (d) Baud-rate : 38400 bps

Figure F-5: Simplified Serial Configuration

Mode 4: Packetized serial

The packetized serial mode uses TTL level RS-232 serial data to set the speed and direction of the propeller. There is a short packet format consisting of an address byte, a command byte, a data byte and a 7 bit checksum. Address bytes are set via dip switches. Up to 8 Sabertooth motor drivers may be ganged together on a single serial line. This makes packetized serial the preferred method to interface multiple Sabertooths to a PC or laptop

Serial data is sent to input S1. The baud rate is selected with switches 4 and 5. Commands are sent as single bytes. Sending a value of 1-127 will command motor 1 Sending a value of 128-255 will command motor 2. Sending a value of 0 will shut down both motors [127].

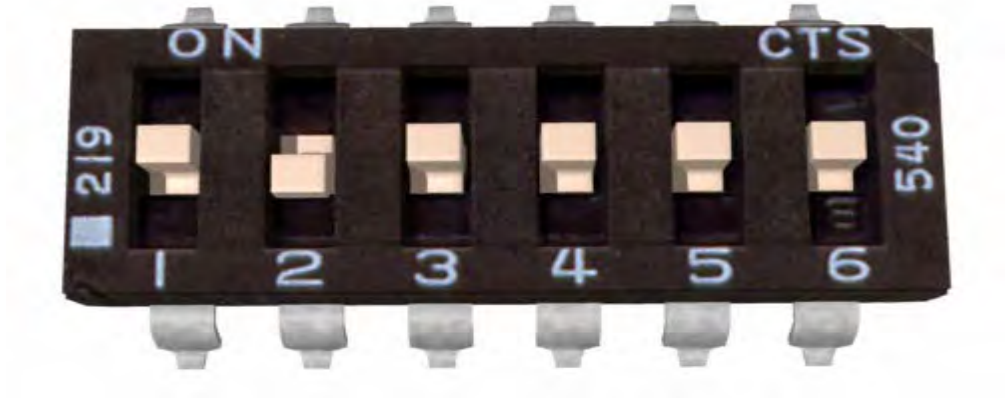

Figure F-6: Standard Simplified Serial communication

Lithium cut-off

Switch 3 of the DIP switch block selects lithium cut-off. If switch 3 is in the down position as shown the Sabertooth will automatically detect the number of series lithium cells at startup, and set a cut-off voltage of 3.0 volts per cell. The number of detected cells is flashed out on the Status LED. When 3.0V per cell is reached, the Sabertooth will shut down, preventing damage to the battery pack. This is necessary because a lithium battery pack discharged below 3.0v per cell will lose capacity and batteries discharged below 2.0v per cell may not ever recharge. Lithium cut-off mode may also be useful in increasing the number of battery cycles you can get when running from a lead acid battery in noncritical applications. When the Sabertooth is being run from NiCd or NiMH batteries, or from a power supply, switch 3 is in the up position [127].

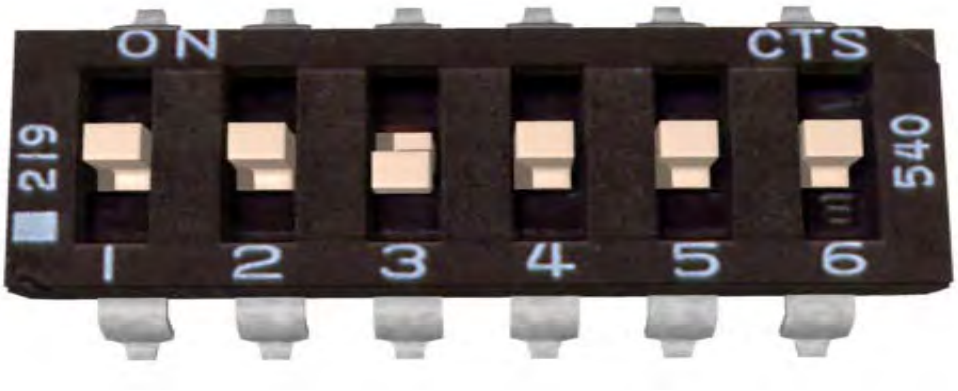

Figure F-7: Lithium Cut-Off Enabled.

Appendix G

G-1 Xbee Shield

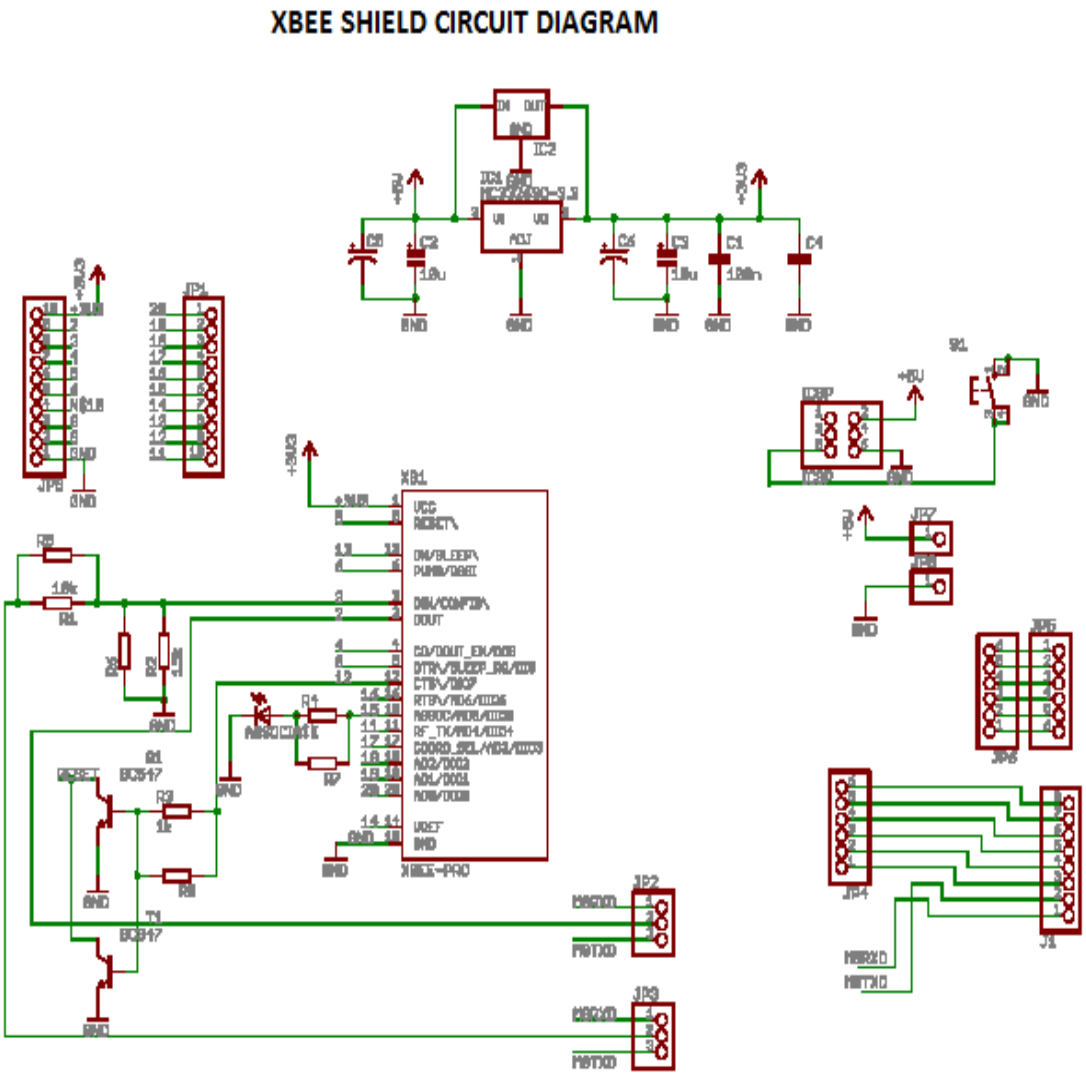

Figure G-1: Xbee Shield Circuit Schematic

G-2 CMPS03 Calibration

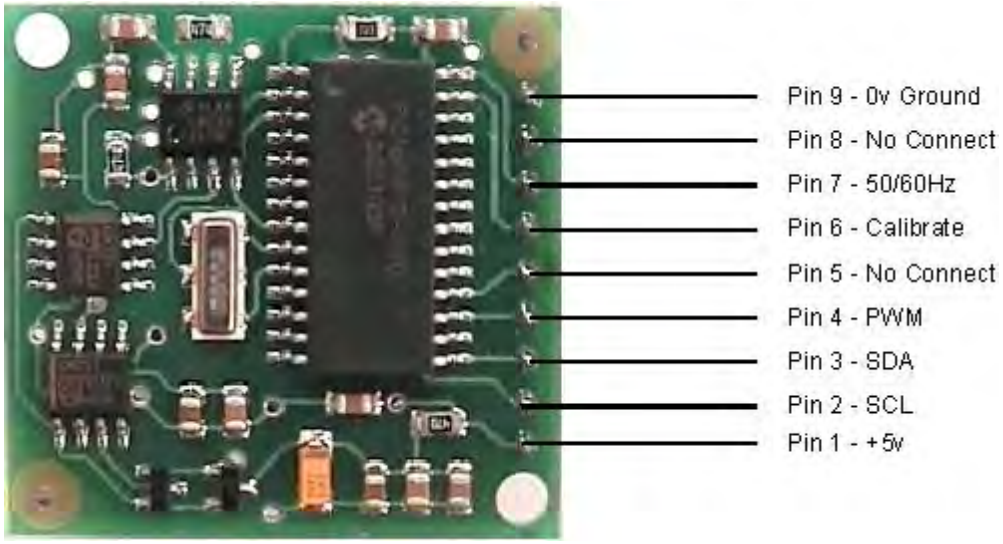

Figure G-2: The Connection Pins in CMPS03

I2C Method

To calibrate the CMPS03 digital compass using the I2C bus, 255 (0xff) is written to register 15, once for each of the four major compass points North, East, South and West. The 255 is cleared internally and automatically after each point is calibrated. The compass points are set in any order, but all four points must be calibrated. The calibration procedure is as follows:

1. the compass module is set flat, pointing North. 255 is written to register 15, the Calibrating pin (pin5) is set low.
2. The compass module is set flat, pointing East. 255 is written to register 15,
3. The compass module is set flat, pointing South. 255 is written to register 15,
4. The compass module is set flat, pointing West. 255 is written to register 15, the Calibrating pin (pin5) goes high.

Pin Method

Pin 6 is used to calibrate the compass. The calibration input (pin 6) has an on-board pull-up resistor and can be left unconnected after calibration. To calibrate the compass, the calibration pin is set low and then high again for each of the four major compass points North, East, South and West. A simple push switch wired from pin6 to 0v (Ground) is OK for this. The compass points can be set in any order, but all four points must be calibrated. The calibration procedure is as follows:

- The compass module is set flat, pointing North. The switch is pressed and released briefly the calibrating pin (pin5) is set low.
- The compass module is set flat, pointing East. The switch is pressed and released briefly
- The compass module is set flat, pointing South. The switch is pressed and released briefly
- The compass module is set flat, pointing West The switch is pressed and released briefly
- The calibrating pin (pin5) is set high.

G-3 Xbee Pro 900 DigiMesh Module Specifications

Table G-1: Xbee Specification

PERFORMANCE	
Indoor/ Urban Range	140 m
Outdoor RF line of sight Range	3km with w/2 1dB dipole antenna 10km with w/high gain antenna
Transmit power output	+17dBm (50mW)
RF Data Rate	156.25 kbps
Data throughput	Up to 87000 bps
Serial Data Interface	3.3 V CMOS Serial UART (5V tolerant UART)
Receiver Sensitivity	-100dBm
Serial Data Rate	230 kbps
Frequency Band	900 MHz ISM
POWER REQUIREMENTS	
Supply Voltage	3.3 – 3.6VDC
Transmit Current	210mA
Receive Current	80mA

Sleep/Power down Current	48µA @ 3.3V
NETWORKING AND SECURITY	
Network Topologies	Point-to-point, point-to-multipoint, peer-to-peer
Number of Channels	8 Hopping patterns on 12 Channels
Encryption	128 Bit AES
Addressing Options	PAN ID, Channel and 64 Bit Addresses
Reliable Packet Delivery	Retries /Acknowledgements

G-4 SRF05 Timing Diagram

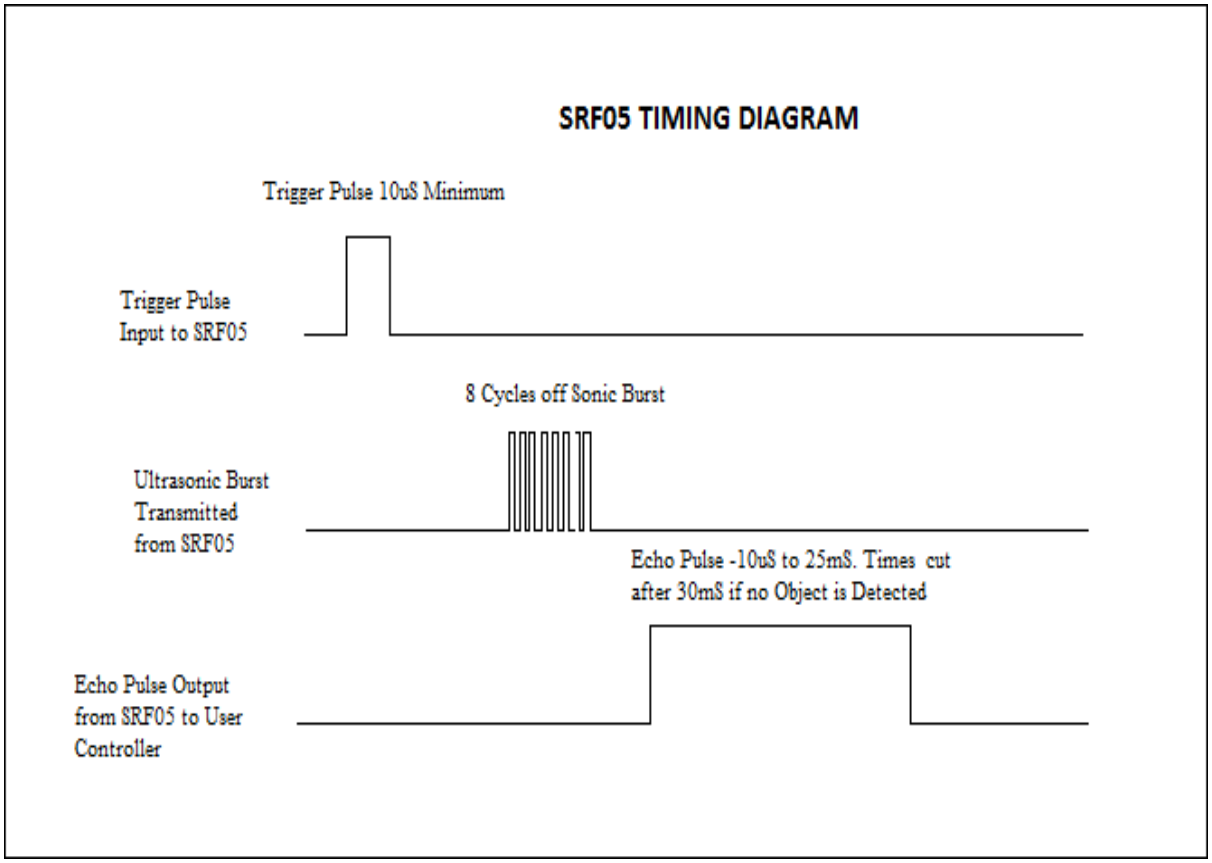

Figure G-3: SRF05 Timing Diagram

Appendix H

The autopilot code consists of eight sections. These are:

- ACME.pde
- ArduPilot.pde
- AutoPilot.pde
- GPS_Navigation.pde
- Init.pde
- Mission_Setup.pde
- PID_Control.pde
- Sevo_Control.pde

The Ardu-IMU code consists of six sections. These are:

- ADC.pde
- Ardu_IMU.pde
- DCM.pde
- GPS.pde
- Matrix.pde
- Vector.pde

The MATLAB code consists of nine sections. These are:

- Expullout.m
- Pullout.m
- ExTurncircle.m
- Turncircle.m
- KINDEMO.m
- euler2q.m
- eulerang.m
- q2euler.m
- euler2.m